## ABSTRACT

THEUERKAUF, SETH JOSEPH. A Geomorphological, Ecosystem Services, and Population Dynamics Approach to Oyster Restoration and Management. (Under the direction of Dr. David Eggleston).

Globally, estuaries support a diversity of habitat-producing ecosystem engineers and associated biotic assemblages that provide vital ecosystem services to coastal communities, such as support of viable fisheries, provision of nursery habitats, and water filtration. As a result of detrimental human activities within estuaries, many of these ecosystem engineers, and the associated habitat that they provide, have been degraded yielding concomitant reductions in the quantity and quality of provided ecosystem services. Estuarine habitat restoration has been the focus of many stakeholder groups to recover lost ecosystem services. In particular, the > 85% global loss of oyster reefs has prompted extensive, multi-scale restoration efforts. Despite considerable investment, the success of previous oyster restoration efforts is varied. To successfully restore oyster reefs to ensure sustainable enhancement of oyster population sizes and to maximize provision of ecosystem services, a comprehensive understanding of the factors that determine successful oyster restoration is required, including an understanding of the drivers of habitat quality, ecosystem service delivery, and metapopulation dynamics.

In Chapter 1, I identified an upper wave exposure limit above which natural intertidal oyster reefs cannot persist with implications for the siting and selection of materials for intertidal oyster reef restoration. In Chapter 2, I compared oyster density, demographic rates (growth and survival), and population estimates (1) across estuarine landscape settings (i.e., comparing natural intertidal reefs within adjacent water bodies that vary in tidal regimes and fetch distances) and (2) across natural habitats and human-made structures to assess variation in habitat quality between natural reefs and hardened shorelines to better inform future intertidal oyster reef

restoration and shoreline management scenarios. In Chapter 3, I developed novel ecosystem service spatial layers for integration within a geospatial decision support tool that integrates multiple biophysical, socioeconomic and ecosystem service variables to identify optimal locations that maximize water filtration ecosystem service provision and long-term persistence of restored oyster populations. In Chapter 4, I adapted a size-structured, discrete-time matrix metapopulation model to simulate the dynamics of an oyster metapopulation to understand overall metapopulation trends, the degree and relative importance of local larval retention and inter-reef connectivity on metapopulation dynamics, and spatiotemporal variation in source-sink structure within the metapopulation with implications for oyster restoration and fishery management. Through informing the maximization of restored habitat quality, ecosystem service delivery, and metapopulation persistence and connectivity, the four chapters of this dissertation contribute support needed for a science-based approach to oyster restoration and management.

# A Geomorphological, Ecosystem Services, and Population Dynamics Approach to Oyster Restoration and Management.

by
Seth Joseph Theuerkauf

A dissertation submitted to the Graduate Faculty of
North Carolina State University
in partial fulfillment of the
requirements for the degree of
Doctor of Philosophy

Marine, Earth and Atmospheric Sciences

Raleigh, North Carolina

2017

APPROVED BY:

| | |
|---|---|
| _____ | _____ |
| Dr. David Eggleston<br>Committee Chair | Dr. Patrick Halpin<br>Inter-Institutional Member |
| _____ | _____ |
| Dr. Craig Layman | Dr. Brandon Puckett |

## DEDICATION

This dissertation is dedicated to my wife, Katelyn Theuerkauf, in recognition of her endless support that made all of this possible. Thank you for keeping us all sane while we measured oysters in > 100°F heat while swatting horseflies and dodging rogue cows and horses on Brown's Island. Thank you also for helping me through struggles with mixed models and rejoicing in successes, like when we figured out after days of trial-and-error that ASCII sorting instead of natural sorting was the bug in the Python larval connectivity code. More seriously, thank you for pushing me to always reach higher and to follow my passion and dreams.

## BIOGRAPHY

Seth was born and raised in Gloucester, Virginia – a small town bordering Chesapeake Bay where he spent much of his childhood fishing and canoeing the Bay's waters. As a high school student at Chesapeake Bay Governor's School for Marine and Environmental Science (CBGS), he first learned of the severely degraded state of the Bay's ecosystem and the human actions that led it to that condition. At CBGS, a resounding message was instilled in Seth's mind early on: through science, restoration, and responsible management, we can recover the Bay. This hopeful message has been his personal call-to-action in the field of marine conservation.

Seth began working in the Marine Conservation Biology laboratory of Drs. Romuald Lipcius and Rochelle Seitz at the Virginia Institute of Marine Science (VIMS) the summer after his sophomore year at CBGS. At VIMS, he assisted with the field monitoring of large-scale, innovative oyster restoration efforts coordinated in the Bay by the U.S. Army Corps of Engineers and VIMS. The next summer, he conducted his own study at VIMS where he evaluated the efficacy of a novel form of three-dimensional reef material known as the "oyster castle." This novel material was found to be superior to oyster shell (the material traditionally used in restoration efforts), and the results of his high school study were cited that same year in a funded grant proposal by The Nature Conservancy (TNC) to use the material in an upcoming large-scale oyster restoration project. After this experience, he was hooked—he saw how applied scientific research he conducted could contribute to positive restoration outcomes.

As an undergraduate at the College of William and Mary (W&M), Seth grew interested and skilled in geospatial analysis (GIS)—he was fascinated by the spatial tools that were available to aggregate and distill vast amounts of data into usable maps and information that could guide decision-making and policy. During his sophomore year, he was accepted into the

selective, research-intensive Monroe Scholar Program at W&M through which he designed a study that applied large spatial scale GIS techniques to guide oyster restoration within a Chesapeake Bay tributary. His project focused on collaboratively developing a GIS-based biophysical model with the USACE and VIMS to identify locations where oyster restoration efforts would most likely succeed—allowing for the USACE Norfolk District to visually compare restoration options and to cost-effectively apply limited restoration funds. That experience taught him that in order for science to effectively inform management, it must be translated and delivered in a comprehensible format—a skillset he continued to refine and develop throughout his doctoral research and collaborative activities at NC State University.

Seth's Department of Defense fellowship-funded doctoral research focused on geospatial modeling and field-based approaches to inform estuarine habitat restoration and conservation in North Carolina, and he pursued collaborations and relationships with local government agencies and NGOs to make the resultant information relevant to management and policy. For example, Chapter 1 of his dissertation research involved an extensive field survey of intertidal oyster reefs that quantitatively identified an upper wave energy limit where these reefs, which can protect shorelines from erosion when appropriately placed, would not persist. Working with colleagues at the NC Coastal Reserve and the NOAA Beaufort Lab, they partnered with TNC to make the information accessible to NC decision-makers through TNC's Coastal Resilience Restoration Explorer web-based mapping tool. That experience reinforced to him the importance of effective communication and collaboration amongst partners from diverse groups and the value of leveraging their specialized expertise and resources.

In 2015, Seth was offered a seat on a multi-state, multi-agency steering committee to organize a targeted summit intended to foster inter-state communication on, and encourage

revision of policy related to, living shorelines (i.e., use of living elements instead of hardened structures to stabilize shorelines). The summit contributed significant political momentum that, in part, led the USACE to revise and simplify the federal permitting process for living shorelines. He found it incredibly rewarding to have helped coordinate an event with such a positive, tangible outcome. That experience, along with collaborative activities to apply his research results, showed him how stakeholder engagement and applied science can contribute to lasting progress in marine conservation.

As a passionate marine conservation biologist armed with a suite of ecological and geospatial knowledge and research tools from his PhD and other experiences, Seth intends to dedicate his career to advancing science to inform effective restoration and responsible management of America's coastal and estuarine ecosystems and the livelihoods and traditions that they support. Seth is beginning his career in marine conservation through a joint position with The Nature Conservancy and the National Oceanic and Atmospheric Administration in the Washington, DC area, where he is applying his marine and spatial science skills to support the sustainable growth of marine aquaculture in the United States and globally.

## ACKNOWLEDGMENTS

This dissertation would not have been possible without the unwavering support of many, many people to whom I am forever grateful. To my wife (Katelyn Theuerkauf), our dogs (Raleigh and Beau), my parents (Dan and Tina Theuerkauf), my brothers (Ethan and Elliott Theuerkauf), and all of my friends and family (Kristen Theuerkauf, David Jenkins, Jr. and Sr., Lynn Mendibur, Laura Jenkins, August Jenkins, Kayla Jenkins, Marsha and David Brown, and Jean Jenkins), thank you all for your boundless support and patience over the years—I could not have done it otherwise.

To the small army of mentors I have been privileged to learn under over the past four years—thank you! To my advisor, Dr. David Eggleston, thank you for pushing me to think big and for broadening my perspective as a marine scientist. To Dr. Brandon Puckett, thank you for your patience and guidance, and for helping me solve what I thought were impossible challenges, like finding an intertidal oyster reef in Pamlico Sound or working with Matlab matrices containing ~500,000 cells. I am also deeply appreciative of the guidance provided by my committee members: Dr. Patrick Halpin and Dr. Craig Layman. Thank you both for challenging me to think broadly and to help me to see the forest for the trees with this work. I am also indebted to the broader marine science and conservation community in North Carolina that made valuable contributions to this work, including folks at the NC Division of Marine Fisheries, NOAA Beaufort Lab, UNC Institute of Marine Sciences, NC Coastal Reserve, NC Sea Grant, NC Space Grant, NC Coastal Federation, and The Nature Conservancy.

I thank the past and present members of the Marine Conservation Ecology lab for their assistance in the field. I also thank the many NCSU administrative staff, both in Raleigh and Morehead City, for the critical behind-the-scenes role they played in making this work possible.

Finally, this work would not have been possible without the funding contributions of many groups, both small and large. I am thankful to North Carolina Sea Grant, North Carolina Space Grant, and North Carolina Coastal Reserve for fellowship funding support. I am grateful to have received a National Defense Science and Engineering Graduate Fellowship (contract FA9550-11- C-0028 awarded by the Department of Defense, Air Force Office of Scientific Research, 32 CFR 168a), a North Carolina Coastal Conservation Association Scholarship, and a Beneath the Sea Foundation Scholarship. I am also appreciative of support received through Dr. David Eggleston's funding sources: North Carolina Sea Grant (R12-HCE-2) and the National Science Foundation (OCE-1155609).

## TABLE OF CONTENTS

## LIST OF TABLES

**Page**

**CHAPTER 1**



**CHAPTER 2**



**CHAPTER 3**



**CHAPTER 4**

## LIST OF FIGURES

**Page**

**CHAPTER 1**



**CHAPTER 2**

**CHAPTER 3**



**CHAPTER 4**

## INTRODUCTION AND DISSERTATION OVERVIEW

Oyster reefs, mangroves, saltmarshes and other ecosystem engineers within estuaries provide vital ecosystem services to sustain coastal communities, such as support of viable fisheries, water filtration, and shoreline stabilization (Grabowski and Peterson 2007, Barbier et al. 2011, Hurst et al. 2015). However, as a result of habitat destruction, overharvest, nutrient pollution and other anthropogenic stressors, many of these ecosystem engineers and associated ecosystem services have been severely degraded (Valiela et al. 2001, Barbier et al. 2011, Beck et al. 2011). Oyster reefs represent one of the most imperiled ecosystem engineers in the world, with an estimated > 85% global loss from estuaries (Beck et al. 2011). Ongoing efforts to restore oyster populations have been met with varied success, in part due to insufficient scientific information to support effective restoration decision-making (Powers et al. 2009). This dissertation provides information needed to maximize restored habitat quality, ecosystem services delivery, and metapopulation persistence and connectivity, contributing support needed for a science-based approach to oyster restoration and management.

Intertidal oyster reefs have generated considerable recent interest for their capacity to protect estuarine shorelines from wave erosion and sea-level rise (Scyphers et al. 2011, Ridge et al. 2015, Walles et al. 2016). While intertidal oyster reefs can attenuate wave energy, prior research suggests a causal relationship between high levels of wave exposure and a reduced probability of reef success (Wall et al. 2005). In Chapter 1, I characterized the role of wave exposure in determining the distribution of natural intertidal oyster reefs and of oysters on hardened shorelines (bulkhead and riprap revetments). I identified a narrow wave exposure threshold above which natural intertidal reefs did not occur, and below which reef presence was dependent on other structuring variables, such as salinity and sediment grain size. Wave

exposure was not correlated with the presence of oysters on hardened shorelines. The identification of the structuring role of wave exposure on intertidal oyster reef distribution has implications for the selection of locations for restoration of intertidal oyster reefs and the materials used in their restoration.

Effective restoration of intertidal oyster reefs requires an understanding of the distribution, density, and demographic rates (growth and survival) of oysters inhabiting existing natural reefs and how these may vary as a function of landscape-scale factors, such as tidal range and fetch distances (Ridge et al. 2015, Walles et al. 2016, Theuerkauf et al. 2016). Furthermore, natural intertidal habitats are increasingly being replaced with hardened shoreline structures that may be colonized by oysters (Drexler et al. 2014), yet little is known about habitat quality (as indexed by oyster density and demographic rates) of these hardened structures relative to natural habitats. In Chapter 2, I compared oyster density, demographic rates, and population estimates (1) across estuarine landscape settings to inform natural intertidal oyster reef restoration (i.e., comparing natural intertidal reefs within adjacent water bodies that vary in tidal regimes and fetch distances) and (2) across natural habitats and human-made structures to assess variation in habitat quality between natural reefs and hardened shorelines. Oyster density, growth rates, and population estimates on natural intertidal reefs were greatest within the smaller, more tidally influenced Core Sound versus the larger, wind-driven Pamlico Sound, with no significant difference in survivorship identified between the two water bodies. Natural intertidal reefs and hardened shoreline structures were compared within Pamlico Sound only, with natural intertidal reefs hosting three to eight times higher oyster densities than hardened shoreline structures. An understanding of oyster density and demographic rates on natural intertidal reefs and hardened shorelines can inform future restoration and shoreline management scenarios.

Geospatial habitat suitability index (HSI) models have emerged as powerful tools that integrate pertinent spatial information to guide habitat restoration efforts (Roloff and Kernohan 1999, Theuerkauf and Lipcius 2016, Puckett et al., in review), but have rarely accounted for spatial variation in ecosystem service provision. In Chapter 3, I utilized satellite-derived chlorophyll *a* concentrations for Pamlico Sound, North Carolina, USA in conjunction with data on water flow velocities and dissolved oxygen concentrations to identify potential restoration locations that would maximize the oyster reef-associated ecosystem service of water filtration. I integrated these novel oyster water filtration ecosystem services variables within a broader, existing GIS-based HSI model to identify suitable locations for oyster restoration that maximize: (i) biophysical, (ii) socioeconomic, and (iii) ecosystem services variables essential to long-term persistence of restored populations and maximization of water filtration ecosystem service provision. Furthermore, I compared the 'Water Filtration' optimized HSI with an HSI optimized for 'Reef Persistence,' as well as a hybrid model that optimized for both water filtration and reef persistence. I identified optimal restoration locations (i.e., locations corresponding to the top 1% of suitability scores) that were consistent among the three HSI scenarios (i.e., "win-win" locations), as well as optimal locations unique to a given HSI scenario (i.e., "tradeoff" locations). The modeling framework utilized in Chapter 3 can provide guidance to restoration practitioners to maximize the cost-efficiency and ecosystem services value of habitat restoration efforts.

Metapopulation and source-sink dynamics concepts are increasingly considered within spatially-explicit management of wildlife populations (Hanski 1998, Burgess et al. 2014), but has generally been limited to comparisons of the performance (e.g., demographic rates or dispersal) inside vs. outside protected areas (e.g., Halpern 2003). In Chapter 4, I adapted a size-structured, discrete-time matrix model for eastern oysters (*Crassostrea virginica*) to simulate the dynamics

of an entire oyster metapopulation, including a network of inter-connected no-harvest subtidal sanctuary oyster reefs, restored oyster reefs and harvested oyster reefs, among other reef types, in the Albemarle-Pamlico Estuarine System in North Carolina, USA. I identified: 1) an overall stable, yet slightly declining metapopulation, 2) variable reef type-specific population trajectories depending on spatiotemporal variation in larval recruitment, 3) spatiotemporal variation in the source-sink status of reef subpopulations wherein subtidal sanctuaries and reefs located in the northeastern portion of the system frequently served as sources, and 4) a greater relative importance of inter-reef larval export on metapopulation dynamics relative to local larval retention processes. Based on the results of this research, I recommend future management efforts within this system consider oysters as an interconnected metapopulation. Furthermore, I recommend continued protection of existing oyster sanctuaries and conservation of other identified subpopulations that serve as frequent ‘source’ subpopulations while managing harvest from ‘sink’ subpopulations.

## LITERATURE CITED


Barbier, E. B., Hacker, S. D., Kennedy, C., Koch, E. W., Stier, A. C., & B. R. Silliman. 2011. The value of estuarine and coastal ecosystem services. *Ecological Monographs* 812:169–193.

Beck, M. W., Brumbaugh, R. D., Airoldi, L., Carranza, A., Coen, L. D., Crawford, C., Defeo, O., Edgar, G. J., Hancock, B., Kay, M. C. & H. S. Lenihan. 2011. Oyster reefs at risk and recommendations for conservation, restoration, and management. *Bioscience* 61:107–116.

Burgess, S. C., Nickols, K. J., Griesemer, C. D., Barnett, L. A. K., Dedrick, A. G., Satterthwaite, E. V., Yamane, L., Morgan, S. G., White, J. W., & L. W. Botsford. 2014. Beyond connectivity: how empirical methods can quantify population persistence to improve marine protected-area design. *Ecological Applications* 24:257–270.

Drexler, M., Parker, M. L., Geiger, S. P., Arnold, W. S., & P. Hallock. 2014. Biological assessment of Eastern oysters (*Crassostrea virginica*) inhabiting reef, mangrove, seawall, and restoration substrates. *Estuaries and Coasts* 37:962–972.

Halpern, B. S. 2003. The impact of marine reserves: do reserves work and does reserve size matter? *Ecological Applications* 13:117–137.

Hanski, I. 1998. Metapopulation dynamics. *Nature* 396:41.

Hurst, T.A., Pope, A.J. and G.P. Quinn. 2015. Exposure mediates transitions between bare and vegetated states in temperate mangrove ecosystems. *Marine Ecology Progress Series* 533: 121–134.

Grabowski, J. H. and C. H. Peterson. 2007. Restoring oyster reefs to recover ecosystem services. Pp. 281–298 in Cuddington, K., Byers, J.E., Wilson, W.G., Hastings A., eds. Ecosystem Engineers: Plants to Protists. Elsevier.

Powers, S.P., Peterson, C.H., Grabowski, J.H. and H.S. Lenihan. 2009. Success of constructed oyster reefs in no-harvest sanctuaries: implications for restoration. *Marine Ecology Progress Serie*s 389: 159–170.

Puckett, B. J., Theuerkauf, S. J., Eggleston, D. B., Guajardo, R., Kerr, P., Luettich, R., et al. A GIS-based, habitat suitability index to guide oyster restoration. *PLoS ONE* in review.

Ridge, J.T., Rodriguez, A.B., Fodrie, F.J., Lindquist, N.L., Brodeur, M.C., Coleman, S.E., Grabowski, J.H. and E.J. Theuerkauf. 2015. Maximizing oyster-reef growth supports green infrastructure with accelerating sea-level rise. *Scientific Reports* 5: e14785.

Roloff, G. J. & Kernohan, B. J. 1999. Evaluating reliability of habitat suitability index models. *Wildlife Society Bulletin* 27:973–985.

Scyphers, S.B., Powers, S.P., Heck Jr, K.L. and D. Byron. 2011. Oyster reefs as natural breakwaters mitigate shoreline loss and facilitate fisheries. *PloS one* 6: e22396.

Theuerkauf, S. J. & Lipcius, R. N. 2016. Quantitative validation of a habitat suitability index for oyster restoration. *Frontiers in Marine Science* 3:64.

Theuerkauf, S. J., Eggleston, D. B., Puckett, B. J., and K. W. Theuerkauf. 2016. Wave exposure structures oyster distribution on natural intertidal reefs, but not on hardened shorelines. *Estuaries and Coasts* doi:10.1007/s12237-016-0153-6.

Valiela, I., Bowen, J. L., & J. K. York. 2001. Mangrove forests: one of the world's threatened major tropical environments. *BioScience* 51:807–815.

Wall, L.M., Walters, L.J., Grizzle, R.E. and P.E. Sacks. 2005. Recreational boating activity and its impact on the recruitment and survival of the oyster *Crassostrea virginica* on intertidal reefs in Mosquito Lagoon, Florida. *Journal of Shellfish Research* 24:965–973.

Walles, B., Troost, K., van den Ende, D., Nieuwhof, S., Smaal, A.C. and T. Ysebaert. 2016. From artificial structures to self-sustaining oyster reefs. *Journal of Sea Research* 108: 1–9.

# CHAPTER 1

## WAVE EXPOSURE STRUCTURES OYSTER DISTRIBUTION ON NATURAL INTERTIDAL REEFS, BUT NOT ON HARDENED SHORELINES


## ABSTRACT

Intertidal oyster reefs can protect estuarine shorelines from wave erosion and sea level rise, and recognition of these ecosystem services has fueled global efforts to conserve and restore these reefs. Although intertidal oyster reefs are valued for attenuating wave erosion, little attention has been paid to the effects of wave exposure on their distribution. The present study characterized the role of wave exposure in determining the distribution of natural intertidal oyster reefs and of oysters on hardened shorelines (bulkhead and riprap revetments). Wave exposure was determined using the National Oceanic and Atmospheric Administration (NOAA)-developed Wave Exposure Model (WEMo), which integrates adjacent water depth, fetch, and processed wind information, among other variables. Field mapping of oyster reefs, defined as ≥ 10 oysters $m^{-2}$, in Pamlico and Core Sounds, North Carolina, USA was conducted in summer 2014. Hardened shorelines and associated oyster densities were mapped for Pamlico Sound only. A narrow wave exposure threshold (~ 500 J $m^{-1}$) was identified above which natural intertidal reefs did not occur, and below which reef presence was apparently dependent on other structuring variables, such as salinity at the time of sampling and the grain size of surrounding sediments. Wave exposure was not correlated with the presence of oysters on hardened shorelines. The application of WEMo in the present study should be useful for selecting locations and materials for intertidal oyster reef restoration.

## INTRODUCTION

Geomorphological processes, such as wave erosion and sediment deposition in estuarine systems, can affect the distribution of habitat-forming ecosystem engineers, which, in turn, can modify the impacts of geomorphological processes (Stallins 2006; Stoffel et al. 2013). For example, intertidal oyster reefs, saltmarsh, and mangrove communities can modify sediment dynamics, thereby influencing local geomorphological properties, but basin-scale geomorphological processes, such as wave energy, may control their overall distribution throughout the landscape (Corenblit et al. 2011). Keddy (1983) identified a negative correlation between biodiversity and biomass of shoreline salt marsh plants and wave exposure. Moreover, a recent experimental mangrove restoration project found that wave exposure mediates the transition from bare mudflat (unrestored) to mangrove forest (restored) state, with increasing success of plant restoration with decreasing hydrodynamic energy (Hurst et al. 2015). An improved understanding of the interaction between geomorphological and ecological processes is essential in guiding successful efforts to manage and restore shoreline habitat-forming oyster and plant communities in estuarine systems (Viles and Spencer 1995).

Intertidal oyster reef habitats have been identified as a key component of living shoreline protection strategies in estuarine systems to combat the effects of shoreline erosion and sea-level rise (Scyphers et al. 2011). Their complex, three-dimensional structure provides numerous ecosystem services, including water filtration, sediment stabilization, and nursery habitat for juvenile fish and invertebrate species (Coen et al. 2007; Grabowski et al. 2012). Despite their recognized value, > 85% of oyster reefs have been lost globally from estuarine systems (Beck et al. 2011). In response to this global decline, large-scale oyster restoration programs have been enacted to restore oyster populations to recover these lost ecosystem services. Recent research

has focused on identifying key considerations in siting and monitoring restored intertidal oyster reefs, such as their vertical relief and degree of tidal emersion (Rodriguez et al. 2014; Baggett et al. 2015; Walles et al. 2016). Research has also focused on the potential wave attenuation benefits of intertidal oyster reefs (Manis et al. 2013; La Peyre et al. 2014, 2015), however, less attention has been paid to the effects of wave exposure on their distribution and in the siting of, and materials used for, intertidal reef restoration.

Shoreline erosion and the associated loss of adjacent coastal lands is a major determinant in decisions to deploy hardened shoreline structures (e.g., bulkheads, riprap revetments; Gittman et al. 2015) to reduce erosion. Although these structures may mitigate retreat of the shoreline immediately behind them, structures such as bulkheads reflect erosive wave energies that enhance sediment scour, which extends to the ends of the structure leading to passive erosion of adjacent shorelines (Douglass and Pickel 1999; Scyphers et al. 2011). Living shoreline protection strategies, such as intertidal oyster reefs that can provide a biogenic berm to reduce wave erosion (but see Servold 2015), allow adjacent, shallow habitats such as saltmarshes to thrive, and simultaneously provide shoreline protection benefits and a suite of associated ecosystem services (Borsje et al. 2011; Manis et al. 2014). The structurally complex, three-dimensional structure of intertidal oyster reefs binds sediments thereby promoting vertical reef accretion and maintenance of their own habitat through oyster recruitment and growth (Rodriguez et al. 2014; Walles et al. 2016). As a result of these biophysical feedbacks that promote reef growth and maintenance, intertidal reefs can outpace sea level rise (Rodriguez et al. 2014).

Although the architecture of intertidal oyster reefs attenuates wave energy, prior research suggests a causal relationship between high levels of wave exposure and a reduced probability of reef success (Wall et al. 2005). Lending further support to this notion, Bahr and Lanier (1981)

proposed that: "…a wave energy regime above a certain threshold level will prevent the development of an intertidal oyster reef." Prior field experiments (Wall et al. 2005) and wave tank studies (Campbell 2015) found that wave energy could move individual and clusters of intertidal oysters, resulting in suboptimal reorientation of oysters, which can reduce their probability of survival. This study builds upon this previous work by explicitly quantifying the relationship between wave exposure and distribution patterns of intertidal oyster reefs.

Despite the negative role that hardened shorelines often play in estuarine ecosystems, such as intensification of erosion for adjacent unhardened shorelines and reduction of the land-to-estuary gradient, these structures can also host considerable oyster densities, thereby providing some associated ecosystem services, such as water filtration (Layman et al. 2014; Drexler et al. 2014). Furthermore, given that wave energy can structure the natural distribution of shoreline oyster and plant communities, research into the provision of oyster habitat by existing hardened shorelines can inform the design of bio-engineered shoreline protection strategies to maximize shoreline protection and ecosystem services.

Living shoreline protection strategies involving oyster reefs can take many forms. One form integrates "gray" infrastructure (e.g., concrete and gabions) with traditional restoration materials (i.e., oyster shell; Borsje et al. 2011; Walles et al. 2015). Another form involves construction of mound-shaped reefs composed of recycled or fossilized oyster shells along the shoreline edge of the intertidal (Wall et al. 2005). By evaluating the distribution of oysters on natural intertidal reefs and hardened shorelines, and quantifying the relationship between wave exposure and the distribution of oysters on natural intertidal reefs and hardened shorelines, the present study can inform both forms of oyster reef restoration.

## MATERIALS AND METHODS

### *Study System*

The Albemarle-Pamlico Estuarine System in North Carolina is separated from the Atlantic Ocean by the Outer Banks barrier island system, which limits exchange to relatively small inlets (approximately 1 km wide; Fig. 1; Pietrafesa et al. 1986). Pamlico Sound exchanges water with adjacent lagoonal estuaries, including Albemarle Sound to the north and Core Sound to the south. The estuarine system is relatively shallow, with a mean depth of ~4.5 m and a maximum depth of 7.5 m. Water circulation within the system is dominated by wind-driven currents and riverine freshwater input (Xie and Eggleston 1999). Shoreline fetch distances vary considerably throughout the system (< 1–30 km), with the longest in Pamlico Sound and the shortest in Core Sound. Wind direction varies seasonally, with northeasterly winds dominating in winter and southeasterlies in the summer (Pietrafesa et al. 1986; Eggleston et al. 2010). The variations in shoreline fetch distance and dominant wind direction yield considerable variability in shoreline wave exposure throughout the system. Variation in the dominant wind direction can also initiate a wind-driven seiche lasting from hours to days, which can pile water on the downwind shore and expose the upwind shore (Luettich et al. 2002; Haase et al. 2012).

Tides in and near the inlets of this estuarine system are generally semi-diurnal, with a mean vertical range of 5 cm when averaged across Pamlico Sound (Roelofs and Bumpus 1953) to 30 cm in Core Sound (Dudley and Judy 1973). Tidal range is negligible in Albemarle Sound, and is greatly reduced along the western shore of Pamlico Sound, reducing the majority of intertidal oyster reef distribution to the Pamlico and Core Sound-side shores of the Outer Banks and areas nearest the inlets.

As a result of rapid human population growth and increased tourism, the Outer Banks in North Carolina have experienced significant urban development (Riggs et al. 2008). One consequence is the hardening of shorelines via bulkhead, riprap revetments, and other shoreline structures. Presently, 5.1% of the estuarine system has been hardened (67% as bulkhead, and 33% as riprap revetments, Fig. 1, North Carolina Department of Environmental Quality, Division of Coastal Management, 2012), with much of this hardened shoreline along the Pamlico Sound-side of the Outer Banks barrier island system. Prior studies found high densities of oysters on hardened shoreline structures (Burke 2010, Layman et al. 2014; Drexler et al. 2014), so oyster densities on hardened shorelines in Pamlico Sound were quantified as a part of this study.

***Ground-Truthing Maps of Intertidal Oyster Reefs and Hardened Shorelines***

Initial map layers of the intertidal distribution of shell bottom habitat and hardened shorelines (Fig. 1) in Pamlico and Core Sounds were acquired from the North Carolina Division of Marine Fisheries (NCDMF) Shellfish Mapping program (North Carolina Department of Environmental Quality, Divison of Marine Fisheries 2013) and the North Carolina Division of Coastal Management (NCDCM) Estuarine Shoreline Mapping program (North Carolina Department of Environmental Quality, Division of Coastal Management 2012). The shell bottom habitat layer includes all areas of oyster reef and loose shell, and the hardened shorelines layer includes all areas of bulkhead and riprap revetments. Although hardened shorelines extend beyond the intertidal portions of Pamlico and Core Sounds, only the hardened shorelines within the intertidal were included in this study. The extent of the intertidal zone within Pamlico and Core Sounds was determined using the boundary of the NCDMF intertidal shell bottom habitat map.

Based on our initial ground-truthing of the intertidal shell bottom habitat map within Pamlico and Core Sounds, the distribution of natural intertidal oyster reefs appeared to be a function, in part, of the degree of wave exposure (i.e., high wave exposure precludes intertidal reef formation despite the presence of shell material). I also observed a greater tidal range and shorter overall fetch distances in Core Sound relative to Pamlico Sound. Thus, this study examined natural intertidal shell bottom habitat and associated oyster reefs separately for Pamlico and Core Sounds. Most hardened shorelines were along the Outer Banks-side of Pamlico Sound, and had oyster densities as high as 200 ind $m^{-2}$.

***Quantifying Wave Exposure***

To assess the significance of wave exposure on the distribution of oysters on both natural reefs and hardened shorelines in Pamlico and Core Sounds, I used the National Oceanographic and Atmospheric Administration (NOAA)-developed Wave Exposure Model Version 4.0 (hereafter referred to as WEMo; Fonseca and Malhotra 2010) to quantify representative wave energy, which represents the total wave energy in one wavelength per unit wave crest length (hereafter RWE; in J $m^{-1}$; Currin et al. 2015). WEMo uses a bathymetric grid, shoreline coverage, processed wind information, and a user-defined point grid to calculate RWE based on the combined effects of wind generation, shoaling, dissipation due to wave breaking, and a fetch-weighting process to account for shoreline irregularity. WEMo processes wind data as the mean wind speed and percent wind frequency in cardinal and ordinal directions. To calculate RWE using WEMo, I used a bathymetric grid from NOAA's National Geophysical Data Center (NGCD), shoreline coverage from NOAA's NGDC coastline database, and processed wind data from the NOAA National Data Buoy Center for the period of 2005–2012 from the Cape Hatteras Station (HCGN7) for the Pamlico Sound region, and from the Cape Lookout Station (CLKN7)

for the Core Sound region (sensu Puckett et al. 2014). Only exceedance wind events (average of top 5% of wind speeds measured during 2005-2012) were used to run the model, as these episodic storm events are most likely to influence the distribution of shoreline ecosystem engineers (Keddy 1982, Kelly et al. 2001, Currin et al. 2015).

***Quantifying Oyster Presence-Absence***

To quantify the relationship between RWE and oyster reef distribution on both natural reefs and hardened shorelines, I conducted a presence-absence field survey at randomly selected intertidal shell bottom sites and hardened shoreline sites in Pamlico and Core Sounds. A presence-absence field survey approach was employed because: (1) wave exposure has previously been identified as a variable structuring the distribution of other shoreline habitat forming ecosystem engineers (Keddy 1983; Hurst et al. 2015), and (2) the relationship between RWE and oyster density is confounded by a multitude of abiotic and biotic variables (e.g., larval supply, salinity). A total of 50 intertidal shell bottom sites and 24 hardened shoreline sites (8 riprap revetments, 16 bulkhead) in Pamlico and Core Sounds, respectively were randomly selected from the NCDMF and NCDCM map databases, and were sampled in summer 2014. Sampling effort was scaled to the amount of intertidal shoreline in Pamlico versus Core Sounds, with a total of 36 intertidal shell bottom sites in Pamlico Sound, and 14 in Core Sound. There were fewer hardened shorelines in Core Sound, so they were only surveyed in Pamlico Sound.

During the presence-absence field survey, I used a minimum density criterion of 10 oysters $m^{-2}$ to define an oyster reef (sensu Powers et al. 2009). I quantified oyster density by random quadrat (0.25 $m^2$) sampling, with the number of quadrat samples based on reef area or hardened shoreline length (determined from the map layer of intertidal shell habitat and hardened shorelines), with a maximum number of quadrat samples set at 10. For intertidal shell habitat

sites, the location of each quadrat sample was determined prior to the survey by generating random points within each selected site polygon from the map layer of intertidal shell habitat in ArcGIS (ESRI 2013). The coordinates associated with these points, and the coordinates of randomly selected hardened shoreline sites were entered into a handheld GPS. For hardened shoreline sites, the location of each quadrat sample along the hardened shoreline was determined using a random number generator. Using the handheld GPS to navigate, I traveled to each site by boat, and to each quadrat location on foot. All quadrat samples of intertidal shell bottom habitat sites were hand-excavated to a depth of 10 cm. For sampling hardened shorelines, random quadrat samples (0.25 $m^2$) were taken by removing all oysters from the quadrat. The left valve length (LVL: distance from the umbo to the anterior margin of the shell) of all live oysters was measured to the nearest 1 mm with calipers. At each site, I also recorded salinity, dissolved oxygen concentration, water temperature, maximum tidal elevation for hardened shorelines (for subsequent area calculation), and a qualitative description of sediment type for intertidal shell habitat sites (mud, sandy mud, muddy sand, or sand) (Table 1). I later compared recorded salinity, dissolved oxygen concentrations, and water temperature measurements to similar measurements collected for a concurrent study at the same locations, and the values were determined to sufficiently reflect the local environmental regimes for use in subsequent analyses (S. Theuerkauf, pers. obs.).

***Quantifying the Relationship Between Oyster Reef Presence-Absence and Explanatory Variables***

I used a binary multiple logistic regression statistical approach to identify the relationship between oyster reef presence-absence and explanatory variables, including RWE, salinity, water temperature, dissolved oxygen concentration, and sediment type (categorical data collected for

intertidal shell bottom habitat, converted to mean grain size in millimeters for sediment class). For intertidal shell bottom sites, since sediment type and RWE were identified as correlated ($R^2$ = 0.30, $p < 0.0001$), separate multiple logistic regression models were created for RWE and sediment type (e.g., reef presence-absence as a function of RWE, salinity, water temperature, and dissolved oxygen). For hardened shoreline sites, separate multiple logistic regression models were applied for each substrate type (i.e., bulkhead, riprap) to identify the relationship between oyster presence-absence and explanatory variables (RWE, salinity, water temperature, and dissolved oxygen). In all cases, backwards elimination model selection was used to identify the most parsimonious and statistically significant model. Statistically significant explanatory variables (defined as all $p \leq 0.05$) identified in the multiple logistic regression analysis were subsequently examined individually via simple logistic regression to determine the specific relationship between oyster reef presence-absence and a given explanatory variable; associated p-values and Nagelkerke's $R^2$ values are reported. All statistical analyses were performed using the logistf package within R statistical software package (R Core Team 2016).

***Scaling the Relationship Between Oyster Reef Presence-Absence and Wave Exposure to an Estuary-Wide Scale***

To scale the observed relationship between oyster reef presence-absence and wave exposure (see Results: Relationship Between Intertidal Oyster Reefs and Explanatory Variables) to an estuary-wide scale, I used WEMo to calculate RWE for the entire shoreline of Pamlico and Core Sounds. Using the same bathymetric grid, shoreline coverage, and wind data described above, RWE was calculated for ~3,200 equally spaced shoreline locations throughout Pamlico Sound, and for 900 in Core Sound. I applied the identified wave exposure threshold to the data to determine the amounts of shoreline area above and below the RWE-oyster presence threshold,

and to partition areas most suitable for various forms of intertidal reef restoration (e.g., higher wave exposure areas are most suitable for restoration using heavy, alternative substrates).

## RESULTS

### *Field Survey of Oyster Reef Presence-Absence and Estimates of Reef Area*

Our field reconnaissance of putative intertidal oyster reefs based on the best available data from state agencies yielded varying results. From the initial estimates of intertidal shell bottom distribution from the NCDMF Shellfish Mapping Program, a total of 559,290 $m^2$ and 332,999 $m^2$ of intertidal shell bottom exist in Pamlico and Core Sounds, respectively. Within Pamlico Sound, I observed intertidal oyster reefs (i.e., an oyster density $\geq 10$ $m^{-2}$) on only 5 of 36 (14%) randomly selected intertidal shell bottom sites, whereas 11 of 14 (79%) randomly selected intertidal shell bottom sites in Core Sound hosted intertidal oyster reefs. As a consequence, I reduced the area estimates to 78,301 $m^2$ and 263,069 $m^2$ respectively.

Based on the hardened shoreline distribution dataset from the NCDCM, a total of 65,086 m of hardened shorelines exist within the Pamlico Sound study area. I found that 19 of 24 (79%) of randomly selected hardened shoreline sites hosted oyster reefs. More specifically, a total of 6 of 8 (75%) riprap sites hosted oyster reefs, and 13 of 16 (81%) bulkhead sites hosted oyster reefs. I estimated a mean maximum tidal elevation of 0.412 m, allowing us to convert the linear estimate of hardened shoreline length into an areal estimate of 26,851 $m^2$. Based on the presence of oyster reefs on 79% of hardened shorelines observed in Pamlico Sound, I reduced the area estimate to a total of 21,184 $m^2$.

***Relationship Between Intertidal Oyster Reefs and Explanatory Variables***

*Natural Intertidal Oyster Reefs in Pamlico Sound*

Representative wave energy (RWE) was a statistically significant predictor of oyster reef presence-absence (logistic regression; $\hat{\beta}$ = -0.003, p = 0.007, Nagelkerke's $R^2$ = 0.34), with a relatively narrow threshold RWE value (~500 J $m^{-1}$) above which oyster reefs were absent (Fig. 2A). Salinity was also a statistically significant predictor of oyster reef presence-absence ($\hat{\beta}$ = 0.529, p = 0.0002, Nagelkerke's $R^2$ = 0.59), with a narrow threshold salinity of ~27 below which reefs were not present (Fig. 3A). Sediment type was also a statistically significant predictor of oyster reef presence-absence ($\hat{\beta}$ = -21.223, p = 0.006, Nagelkerke's $R^2$ = 0.16), with a declining prevalence of extant oyster reefs in areas of sand (mean grain size of 0.15 mm, Fig. 4A). Dissolved oxygen concentration and water temperature were not statistically significant predictors of oyster reef presence (both p > 0.4).

*Natural Intertidal Oyster Reefs in Core Sound*

Similar to Pamlico Sound, RWE in Core Sound was a statistically significant predictor of oyster reef presence-absence ($\hat{\beta}$ = -0.008, p = 0.0009, Nagelkerke's $R^2$ = .79), with a narrow threshold RWE value (~500 J $m^{-1}$) above which oyster reefs were absent (Fig. 2B). Salinity was a statistically significant predictor of oyster reef presence-absence ($\hat{\beta}$ = 0.377, p = 0.02, Nagelkerke's $R^2$ = 0.54), with a narrow threshold of ~27, below which reefs did not exist (Fig. 3B). Sediment type was a statistically significant predictor of oyster reef presence-absence ($\hat{\beta}$ = -35.135, p = 0.003, Nagelkerke's $R^2$ = 0.56), with no extant oyster reefs identified in sandy areas (0.15 mm mean grain size, Fig. 4B). Dissolved oxygen concentration and water temperature were not statistically significant predictors of oyster reef presence (both p > 0.4).

*Hardened Shoreline Oyster Reefs in Pamlico Sound*

No explanatory variables sufficiently explained oyster reef presence-absence on riprap or bulkhead hardened shorelines (all $p > 0.1$). For comparison with natural intertidal oyster reefs, I present the relationship between hardened shoreline oyster reef presence-absence and RWE (Fig. 2C) and salinity (Fig. 3C).

***Scaling the Relationship Between Oyster Reef Presence-Absence and Wave Exposure to an Estuary-Wide Scale***

Approximately 19% and 6% of Pamlico and Core Sound's shoreline, respectively, has an associated RWE above the observed 500 J $m^{-1}$ threshold at which natural intertidal reefs were absent (Fig. 5). The most extensive shorelines above the 500 J $m^{-1}$ threshold occur in the southern portion of Pamlico Sound, including portions of the Neuse, Pamlico and Pungo Rivers. Other shorelines above the 500 J $m^{-1}$ threshold occur sporadically throughout the system, indicative of the high degree of variability in local bathymetry topography, and shoreline directional orientation that determine RWE.

## DISCUSSION

While numerous studies have demonstrated the value of intertidal oyster reefs as a key component of living shoreline protection strategies in estuarine systems (Scyphers et al. 2011; Grabowski et al. 2012; Rodriguez et al. 2014; Ridge et al. 2015; Walles et al. 2016), this is the first to quantify the relationship between wave exposure and the distribution of oysters on natural intertidal reefs and hardened shoreline structures. For natural intertidal reefs, a narrow wave exposure threshold was identified above which natural reefs did not exist, and reef presence was conditionally dependent on other structuring variables. For oysters on hardened shorelines, wave

exposure did not appear to structure their distribution. Given the increasing interest in use of intertidal oyster reefs as essential elements of coastal defense schemes (Rodriguez et al. 2014; Walles et al. 2016), these findings have direct implications for the siting of, and materials used for, intertidal reef restoration. For example, intertidal oyster reef restoration in areas of high wave exposure (> 500 J $m^{-1}$) should use relatively heavy, rigid alternative substrate materials (e.g., concrete, Dunn et al. 2014; Oyster Castles ®, Theuerkauf et al. 2015), whereas intertidal oyster reef restoration in areas of low wave exposure (< 500 J $m^{-1}$) could use oyster shells. Moreover, as extant intertidal oyster reefs were only identified at a fraction of visited intertidal shell bottom habitat and hardened shoreline sites, this study confirms the need to ground-truth spatial datasets of habitat types prior to their integration into modeling efforts or use in estimating habitat quality or extent.

The intertidal shell bottom habitat and hardened shoreline map layer developed by North Carolina's state agencies for the estuarine systems are more extensive than for most coastal states in the USA. Prior to ground-truthing these map layers, it was assumed that the intertidal shell bottom habitat layer represented the extent of intertidal oyster reefs in Pamlico and Core Sounds. However, our estimates of actual intertidal reef area (i.e., intertidal shell bottom habitat with an oyster density ≥ 10 $m^{-2}$) were ~14% and 79% of the original estimates for Pamlico and Core Sounds, respectively. All visited intertidal shell bottom habitat sites did contain some form of shell material, ranging from areas of loose shell fragments to high-density reefs, thereby validating the accuracy of the shell bottom habitat layer, but not the assumption that shell bottom habitat equates to oyster reefs (i.e., oyster density ≥ 10 $m^{-2}$). Furthermore, of the sites that hosted oyster reefs, densities varied widely from 10–1,673 oysters $m^{-2}$ (Table 1). This heterogeneity of habitat quality across intertidal shell bottom habitat in North Carolina, from areas of loose shell

fragments containing no live oysters, to scattered, low density assemblages of oysters, to high density, thriving reefs, is important when using this dataset, or similar maps for other regions, to estimate extent and quality of oyster reef habitat. The presence of oyster reefs on 79% of hardened shoreline structures suggests that: (1) hardened shorelines can provide substrate for oyster settlement with the associated ecosystem services, and (2) additional research is needed to quantify associated ecosystem services given the ever-increasing prevalence of hardened shorelines in estuarine environments.

Increasing wave exposure limited the distribution of oysters on natural intertidal shell bottom sites (Fig. 2A, 2B). A consistent and narrow threshold of ~500 J $m^{-1}$ was identified for both Pamlico and Core Sounds, above which natural intertidal oyster reefs were absent. Intertidal shell bottom habitat sites above this exposure level generally consisted of loose shell over sand, occasionally containing a few juvenile oysters (often dead). This loose material was buried by shifting sand or moved and redistributed by waves, which could lead to surface abrasion and subsequent removal of spat (B. Webb, pers. obs.; S. Theuerkauf, pers. obs.). Waves generated by boating activity near intertidal oyster reefs have been shown to reduce juvenile oyster survival relative to unexposed reefs (Wall et al. 2005). Substrate retention in areas of high wave exposure (i.e., preventing suboptimal reorientation of oysters) was identified as a key factor for maximizing juvenile survival and promoting reef growth and persistence.

On hardened shoreline sites in Pamlico Sound, increasing wave exposure did not limit the distribution of oysters (Fig. 2C). Multiple bulkhead and riprap sites hosted oyster densities ≥ 10 $m^{-2}$ above the identified natural intertidal reef wave exposure threshold of ~500 J $m^{-1}$. Substrate stability, as originally posited by Wall et al. (2005) and later La Peyre et al. (2014), is essential in areas of significant boat wake or wind wave exposure. Given that hardened shoreline structures

are composed of heavy, rigid materials, oyster larval settlement on exposed substrate surfaces that are fixed in place is a probable mechanism behind the ability of these substrates to host oyster reefs in high wave exposure areas (Theuerkauf et al. 2015).

The observed negative relationship between RWE and the distribution of natural intertidal reefs aligns with previous studies comparing WEMo-derived RWE with the biomass and distribution of estuarine habitat-forming ecosystem engineers. For example, a significant inverse correlation was identified between RWE and seagrass biomass in the Orbetello Lagoon, Italy (Rubegni et al. 2013). Additionally, in an examination of the relationship between RWE and shoreline habitat types in the New River Estuary, North Carolina, the abundance of saltmarshes was also inversely related to RWE values (Currin et al. 2015). Thus, the present study lends further support to the significance of wave exposure on the distribution of habitat-forming ecosystem engineers, and supports the use of WEMo as a tool to predict this relationship.

Sediment type is a major driver of natural intertidal oyster reef distribution in Pamlico and Core Sounds, with natural intertidal reefs generally absent in sand bottom areas and most reefs occurring in areas of soft sediment, such as sandy mud and muddy sand (Fig. 4A, 4B). This finding supports the observations described by Bahr and Lanier (1981) of natural intertidal reefs along the southeast coast of the USA being primarily in areas of soft sediment types. While sediment type and wave exposure are correlated, the presence of some intertidal reefs in sandy areas in our study suggests that quantitative metrics of wave exposure rather than descriptions of sediment type would be more reliable in predicting success for reef restoration.

Salinity is a major driver of natural intertidal oyster reef distribution in Pamlico and Core Sounds, but not for hardened shoreline reefs in Pamlico Sound. Intertidal shell bottom sites in

Pamlico Sound spanned a wide range of salinities (10–33, Table 1), while intertidal shell bottom sites in Core Sound spanned a narrow, high salinity range (25–36). In both systems, a threshold salinity of ~27 was identified below which natural intertidal oyster reefs do not exist. For hardened shorelines, salinity did not limit the distribution of oysters, with multiple sites hosting oyster densities $\geq 10$ $m^{-2}$ below the salinity threshold of ~27 (range of 13–25). I suggest that, in Pamlico and Core Sounds, this threshold may reflect two processes: 1) the role of lunar tidal emersion (i.e., variation in reef aerial exposure due to the combined effects of reef elevation relative to mean water level and tidal excursion distance), and 2) the effect of an episodic, wind-driven seiche that can expose shorelines (a less predictable, barotropic process that can last from hours to days; Leuttich et al. 2002; Haase et al. 2012). In Pamlico and Core Sounds, as in many other estuarine systems, tidal influence is rapidly attenuated with distance from the tidal influence of ocean inlets (i.e., decreasing salinity). Thus, for areas that are further from the tidal influence of ocean inlets, this episodic, barotropic seiche may have a greater influence on shoreline exposure than lunar tidal emersion. In these areas, irregular extended exposure of oysters to desiccation may preclude natural intertidal reef formation and maintenance (i.e., exposure inducing mortality of juvenile oysters). Hardened shorelines stand in contrast to this by providing extensive vertical relief and settlement substrate across the tidal emersion window and range of aerial exposures. This observation was supported by the qualitative observation of oysters within a uniform horizontal band on hardened shoreline structures. Further understanding of the mechanism behind the identified threshold salinity for reef presence-absence of ~27 is beyond the scope of this study and warrants further research.

Water temperature and dissolved oxygen concentrations at the time of sampling were not significant determinants of natural intertidal or hardened shoreline oyster reef distribution.

Although water temperature and dissolved oxygen concentration vary among sites, the variation is likely not biologically meaningful. As surficial water temperature is strongly correlated with air temperature, and the whole study area is within the same climate zone (Fovell and Fovell 1993), it is not surprising that water temperature was not a significant determinant of natural intertidal or hardened shoreline oyster reef distribution. Furthermore, given that air-sea gas exchange occurs at the water surface (Raymond and Cole 2001), it is not surprising that dissolved oxygen concentration was not a significant driver of natural intertidal or hardened shoreline oyster reef distribution.

Finding a narrow wave exposure threshold that limits the distribution of natural intertidal reefs, but not hardened shoreline reefs, has implications for the siting of, and materials used for, intertidal oyster reef restoration. For areas above the wave exposure threshold, alternative reef substrates less prone to redistribution by wave action, such as riprap, concrete or Oyster Castles® are likely most suitable for intertidal restoration (Dunn et al. 2014; Theuerkauf et al. 2015). For areas below the wave exposure threshold, intertidal restoration using traditional materials, such as loose oyster shell, may be suitable. In all cases, structuring factors such as tidal emersion, sediment type, salinity, and oyster larval supply should also be considered in the restoration planning process (Baggett et al. 2015; Ridge et al. 2015; Walles et al. 2016). Additionally, as waves generated by boating activity can impact oyster survival on intertidal reefs (Wall et al. 2005; Campbell 2015) and could exceed the identified wave exposure thresholds identified in this study, the extent of boat wake exposure should also be considered in planning oyster restorations. Boat wake exposure can be quantified using the NOAA-developed Boat Wake Model (Fonseca and Malhotra 2012).

Application of the observed wave exposure threshold to RWE calculated for the shorelines of Pamlico and Core Sounds (Fig. 5) allows for the information from the present study to be scaled to the entire estuary. The most extensive shorelines above the 500 J $m^{-1}$ threshold in southern Pamlico Sound are the ones most likely to be impacted by the seasonally dominant wind directions (Pietrafesa et al. 1986; Eggleston et al. 2010). Additionally, the sporadic occurrence of shoreline sites above the 500 J $m^{-1}$ threshold, with some sites above the threshold immediately adjacent to shoreline sites below the threshold, suggests that WEMo should be applied at a sufficiently high spatial resolution to encapsulate the small-scale variability in local bathymetry, topography, and shoreline orientation, which can yield dramatically different RWE values for adjacent shoreline locations. Furthermore, application of the observed wave exposure threshold to estuary-scale RWE data provides restoration practitioners with information that can be used to determine where certain materials would be most viable for use in intertidal reef restorations (e.g., areas above the wave exposure threshold should use alternative reef substrates less prone to redistribution by wave action).

The Wave Exposure Model (WEMo) represents a user-friendly extension of ArcGIS (ESRI 2016) that can be used for any region of the world to determine wave exposure in the intertidal zone (Fonseca and Malhotra 2010). With a shoreline layer, bathymetric data, and wind data, WEMo can calculate representative wave energy (in J $m^{-1}$) which can be compared to the values observed in this study. Restoration practitioners should make use of this tool to quantify wave exposure at prospective intertidal reef restoration sites, and should use the results of this study as guidance for selection of sites and materials used in restoration.

Future research should spatially confirm the observed natural intertidal reef wave exposure threshold of ~500 J $m^{-1}$, as well as the lack of an observed wave exposure threshold for

hardened shoreline reefs, at different locations across the biogeographic range of the eastern oyster. Furthermore, future research should quantify the potential simultaneous influence of wave exposure and tidal emersion (i.e., due to variation in reef elevation and tidal excursion distance) on intertidal reef formation and maintenance. Specifically, experimental reefs could be constructed across the wave exposure spectrum and of varying reef elevations across the tidal emersion spectrum to quantify the relative importance of both variables in structuring oyster reef distribution and density. More broadly, research should continue to focus on understanding the interplay between geomorphology and ecology as these interactions can have significant implications for efforts to restore and conserve imperiled habitats.

**ACKNOWLEDGEMENTS**

I thank S. Brown, J. Byrum, O. Caretti, A. Edwards, B. Griffin, R. Lyon, D. McVeigh, O. Phillips, K. Simmons, and R. Ward for their assistance with field collections. Funding for the project and completion of the manuscript was provided by North Carolina Sea Grant (R12-HCE-2) and the National Science Foundation (OCE-1155609) to D. Eggleston, as well as a United States Department of Defense (Office of Naval Research) National Defense Science and Engineering Graduate Fellowship, North Carolina Coastal Conservation Association Scholarship, and Beneath the Sea Foundation Scholarship to S. Theuerkauf.

## LITERATURE CITED


Baggett, L.P., Powers, S.P., Brumbaugh, R.D., Coen, L.D., DeAngelis, B.M., Greene, J.K., Hancock, B.T., Morlock, S.M., Allen, B.L., Breitburg, D.L. and D. Bushek. 2015. Guidelines for evaluating performance of oyster habitat restoration. *Restoration Ecology* 23: 737–745.

Bahr, L.M. and W.P. Lanier. 1981. *The ecology of intertidal oyster reefs of the South Atlantic coast: a community profile* (No. 81/15). US Fish and Wildlife Service.

Beck, M.W., Brumbaugh, R.D., Airoldi, L., Carranza, A., Coen, L.D., Crawford, C., Defeo, O., Edgar, G.J., Hancock, B., Kay, M.C. and H.S. Lenihan. 2011. Oyster reefs at risk and recommendations for conservation, restoration, and management. *Bioscience* 61: 107–116.

Borsje, B.W., van Wesenbeeck, B.K., Dekker, F., Paalvast, P., Bouma, T.J., van Katwijk, M.M. and M.B. de Vries. 2011. How ecological engineering can serve in coastal protection. *Ecological Engineering* 37: 113–122.

Burke, R.P. 2010. Alternative substrates as a native oyster (*Crassostrea virginica*) restoration strategy in Chesapekae Bay. Gloucester Point, Virginia: Dissertation, College of William and Mary.

Campbell, D.E. 2015. *Quantifying the effects of boat wakes on intertidal oyster reefs in a shallow estuary.* (Masters thesis, University of Central Florida, Orlando, Florida).

Coen, L.D., Brumbaugh, R.D., Bushek, D., Grizzle, R., Luckenbach, M.W., Posey, M.H., Powers, S.P. and S. Tolley. 2007. Ecosystem services related to oyster restoration. *Marine Ecology Progress Series* 341: 303–307.

Corenblit, D., Baas, A.C., Bornette, G., Darrozes, J., Delmotte, S., Francis, R.A., Gurnell, A.M., Julien, F., Naiman, R.J. and J. Steiger. 2011. Feedbacks between geomorphology and biota controlling Earth surface processes and landforms: a review of foundation concepts and current understandings. *Earth-Science Reviews* 106: 307–331.

Currin, C., Davis, J., Baron, L.C., Malhotra, A., and M. Fonseca. 2015. Shoreline change in the New River Estuary, North Carolina: rates and consequences. *Journal of Coastal Research* 31: 1069–1077.

Douglass, S.L., and B.H. Pickel. 1999. The tide doesn't go out anymore—the effect of bulkheads on urban shorelines. *Shore Beach* 67: 19–25.

Drexler, M., Parker, M.L., Geiger, S.P., Arnold, W.S., and P. Hallock. 2014. Biological assessment of eastern oysters (*Crassostrea virginica*) inhabitating reef, mangrove, seawall, and restoration substrates. *Estuaries and Coasts* 37: 962–972.

Dudley, D.L., and M.H. Judy. 1973. Seasonal abundance and distribution of juvenile blue crabs in Core Sound, NC 1965–68. *Chesapeake Science* 14: 51–55.

Dunn, R.P., Eggleston, D.B. and N. Lindquist. 2014. Substrate effects on demographic rates of Eastern oyster (*Crassostrea virginica*). *Journal of Shellfish Research* 33: 177–185.

Eggleston, D.B., Reyns, N.B., Etherington, L.L., Plaia, G.R. and L. Xie. 2010. Tropical storm and environmental forcing on regional blue crab (*Callinectes sapidus*) settlement. *Fisheries Oceanography* 19: 89–106.

ESRI. 2016. ArcGIS Desktop: Release 10.3. Redlands, CA: Environmental Systems Research Institute.

Fonseca, M.S., and A. Malhotra. 2010. *WEMo (Wave Exposure Model) for use in Ecological Forecasting* (Vol. 4). National Oceanic and Atmospheric Administration.

Fonseca, M.S. and A. Malhotra. 2012. *Boat wakes and their influence on erosion in the Atlantic Intracoastal Waterway, North Carolina*. National Oceanic and Atmospheric Administration.

Fovell, R.G. and M.Y.C. Fovell. 1993. Climate zones of the conterminous United States defined using cluster analysis. *Journal of Climate* 6: 2103–2135.

Gittman, R.K., Fodrie, F.J., Popowich, A.M., Keller, D.A., Bruno, J.F., Currin, C.A., Peterson, C.H. and M.F. Piehler. 2015. Engineering away our natural defenses: an analysis of shoreline hardening in the US. *Frontiers in Ecology and the Environment* 13: 301–307.

Grabowski, J.H., Brumbaugh, R.D., Conrad, R.F., Keeler, A.G., Opaluch, J.J., Peterson, C.H., Piehler, M.F., Powers, S.P. and A.R. Smyth. 2012. Economic valuation of ecosystem services provided by oyster reefs. *BioScience* 62: 900–909.

Haase, A.T., Eggleston, D.B., Luettich, R.A., Weaver, R.J. and B.J. Puckett. 2012. Estuarine circulation and predicted oyster larval dispersal among a network of r eserves. *Estuarine, Coastal and Shelf Science* 101: 33–43.

Hurst, T.A., Pope, A.J. and G.P. Quinn. 2015. Exposure mediates transitions between bare and vegetated states in temperate mangrove ecosystems. *Marine Ecology Progress Series* 533: 121–134.

Keddy, P.A., 1983. Shoreline vegetation in Axe Lake, Ontario: effects of exposure on zonation patterns. *Ecology* 64: 331–344.

La Peyre, M.K., Furlong, J., Brown, L.A., Piazza, B.P. and K. Brown. 2014. Oyster reef restoration in the northern Gulf of Mexico: Extent, methods and outcomes. *Ocean & Coastal Management* 89: 20–28.

La Peyre, M.K., Serra, K., Joyner, T.A. and A. Humphries. 2015. Assessing shoreline exposure and oyster habitat suitability maximizes potential success for sustainable shoreline protection using restored oyster reefs. *PeerJ* 3: e1317.

Layman, C.A., Jud, Z.R., Archer, S.K. and D. Riera. 2014. Provision of ecosystem services by human-made structures in a highly impacted estuary. *Environmental Research Letters* 9: e044009.

Luettich, R.A., Carr, S.D., Reynolds-Fleming, J.V., Fulcher, C.W. and J.E. McNinch. 2002. Semi-diurnal seiching in a shallow, micro-tidal lagoonal estuary. *Continental Shelf Research* 22:1669–1681.

Manis, J.E., Garvis, S.K., Jachec, S.M. and L.J. Walters. 2015. Wave attenuation experiments over living shorelines over time: a wave tank study to assess recreational boating pressures. *Journal of Coastal Conservation* 19: 1–11.

North Carolina Department of Environmental Quality, Division of Coastal Management. 2016. *Estuarine Shorelines of NC Spatial Dataset.* Shapefile dataset. https://deq.nc.gov/about/divisions/coastal-management/coastal-management-data/spatial-data-maps##Estuarine Shorelines. Accessed 15 March 2016.

North Carolina Department of Environmental Quality, Division of Marine Fisheries. 2012. *Estuarine Benthic Habitat Mapping Program.* Shapefile dataset. http://portal.ncdenr.org/web/mf/shellfish-habitat-mapping. Accessed 15 March 2016.

Pietrafesa, L.J., Janowitz, G.S., Chao, T.Y., Weisberg, R.H., Askari, F. and E. Noble. 1986. *The physical oceanography of Pamlico Sound*. UNC Sea Grant Publication. UNC-WP-86-5, Raleigh.

Powers, S.P., Peterson, C.H., Grabowski, J.H. and H.S. Lenihan. 2009. Success of constructed oyster reefs in no-harvest sanctuaries: implications for restoration. *Marine Ecology Progress Serie*s 389: 159–170.

Puckett, B.J., Eggleston, D.B., Kerr, P.C. and R.A. Luettich. 2014. Larval dispersal and population connectivity among a network of marine reserves. *Fisheries Oceanography* 23: 342–361.

R Core Team. 2015. *R: A Language and Environment for Statistical Computing*. R Foundation for Statistical Computing, Vienna, Austria. https://www.R-project.org.

Raymond, P.A. and J.J. Cole. 2001. Gas exchange in rivers and estuaries: Choosing a gas transfer velocity. *Estuaries and Coasts* 24: 312–317.

Ridge, J.T., Rodriguez, A.B., Fodrie, F.J., Lindquist, N.L., Brodeur, M.C., Coleman, S.E., Grabowski, J.H. and E.J. Theuerkauf. 2015. Maximizing oyster-reef growth supports green infrastructure with accelerating sea-level rise. *Scientific Reports* 5: e14785.

Riggs, S.R., Culver, S.J., Ames, D.V., Mallinson, D.J., Corbett, D.R., and J.P. Walsh. *North Carolina's Coasts in Crisis: A Vision for the Future*. East Carolina University White Paper. https://www.ecu.edu/icsp/ICSP/Reports_files/CoastsinCrisisOct2008.pdf. Accessed 15 March 2016.

Rodriguez, A.B., Fodrie, F.J., Ridge, J.T., Lindquist, N.L., Theuerkauf, E.J., Coleman, S.E., Grabowski, J.H., Brodeur, M.C., Gittman, R.K., Keller, D.A. and M.D. Kenworthy. 2014. Oyster reefs can outpace sea-level rise. *Nature Climate Change* 4: 493–497.

Roelofs, E.W. and D.F. Bumpus. 1953. The hydrography of Pamlico Sound. *Bulletin of Marine Science* 3: 181–205.

Rubegni, F., Franchi, E. and M. Lenzi. 2013. Relationship between wind and seagrass meadows in a non-tidal eutrophic lagoon studied by a Wave Exposure Model (WEMo). *Marine Pollution Bulletin* 70: 54–63.

Scyphers, S.B., Powers, S.P., Heck Jr, K.L. and D. Byron. 2011. Oyster reefs as natural breakwaters mitigate shoreline loss and facilitate fisheries. *PloS one* 6: e22396.

Servold, K.P. 2015. *Observations of wave setup and transmission behind low-crested artificial reef breakwaters.* (Masters thesis, University of South Alabama, Mobile, Alabama).

Stallins, J.A., 2006. Geomorphology and ecology: unifying themes for complex systems in biogeomorphology. *Geomorphology* 77: 207–216.

Stoffel, M., Rice, S. and J.M. Turowski. 2013. Process geomorphology and ecosystems: disturbance regimes and interactions. *Geomorphology* 202: 1–3.

Theuerkauf, S.J., Burke, R.P. and R.N. Lipcius. 2015. Settlement, growth, and survival of eastern oysters on alternative reef substrates. *Journal of Shellfish Research* 34: 241–250.

Viles, H. and T. Spencer. 1995. Coastal problems: geomorphology, ecology and society at the coast. New York: Routledge.

Wall, L.M., Walters, L.J., Grizzle, R.E. and P.E. Sacks. 2005. Recreational boating activity and its impact on the recruitment and survival of the oyster *Crassostrea virginica* on intertidal reefs in Mosquito Lagoon, Florida. *Journal of Shellfish Research* 24: 965–973.

Walles, B., Troost, K., van den Ende, D., Nieuwhof, S., Smaal, A.C. and T. Ysebaert. 2016. From artificial structures to self-sustaining oyster reefs. *Journal of Sea Research* 108: 1–9.

Xie, L. and D.B. Eggleston. 1999. Computer simulations of wind-induced estuarine circulation patterns and estuary-shelf exchange processes: The potential role of wind forcing on larval transport. *Estuarine, Coastal and Shelf Science* 49: 221–234.

Table 1. Range of observed values for environmental variables and mean oyster densities measured at natural intertidal and hardened shoreline reefs in Pamlico and Core Sounds. Note that sediment grain size was recorded as a categorical descriptor, and was converted to a mean grain size for the category (i.e., mud = 0.0078 mm, sandy mud = 0.0156 mm, muddy sand = 0.04 mm, sand = 0.15).

| | RWE (J $m^{-1}$) | Sediment (mm) | Salinity | Water Temperature (°C) | Dissolved Oxygen Concentration (mg $l^{-1}$) | Mean Oyster Density (ind. $m^{-2}$) |
|---|---|---|---|---|---|---|
| **Pamlico Sound Natural Intertidal Reefs** | 3.94–6184.85 | 0.0078–0.15 | 10–33 | 20.9–29.1 | 3.61–7.99 | 0–449 |
| **Core Sound Natural Intertidal Reefs** | 1.34–945.63 | 0.0156–0.15 | 25–36 | 20.7–29.8 | 3.19–9.30 | 0–1673 |
| **Pamlico Sound Hardened Shoreline Reefs (Bulkhead)** | 4.19–519.17 | – | 13–25 | 27.5–30.5 | 5.48–10.09 | 0–96 |
| **Pamlico Sound Hardened Shoreline Reefs (Riprap)** | 2.69–2248.72 | – | 13–28 | 23.0–30.2 | 3.67–9.82 | 0–140 |

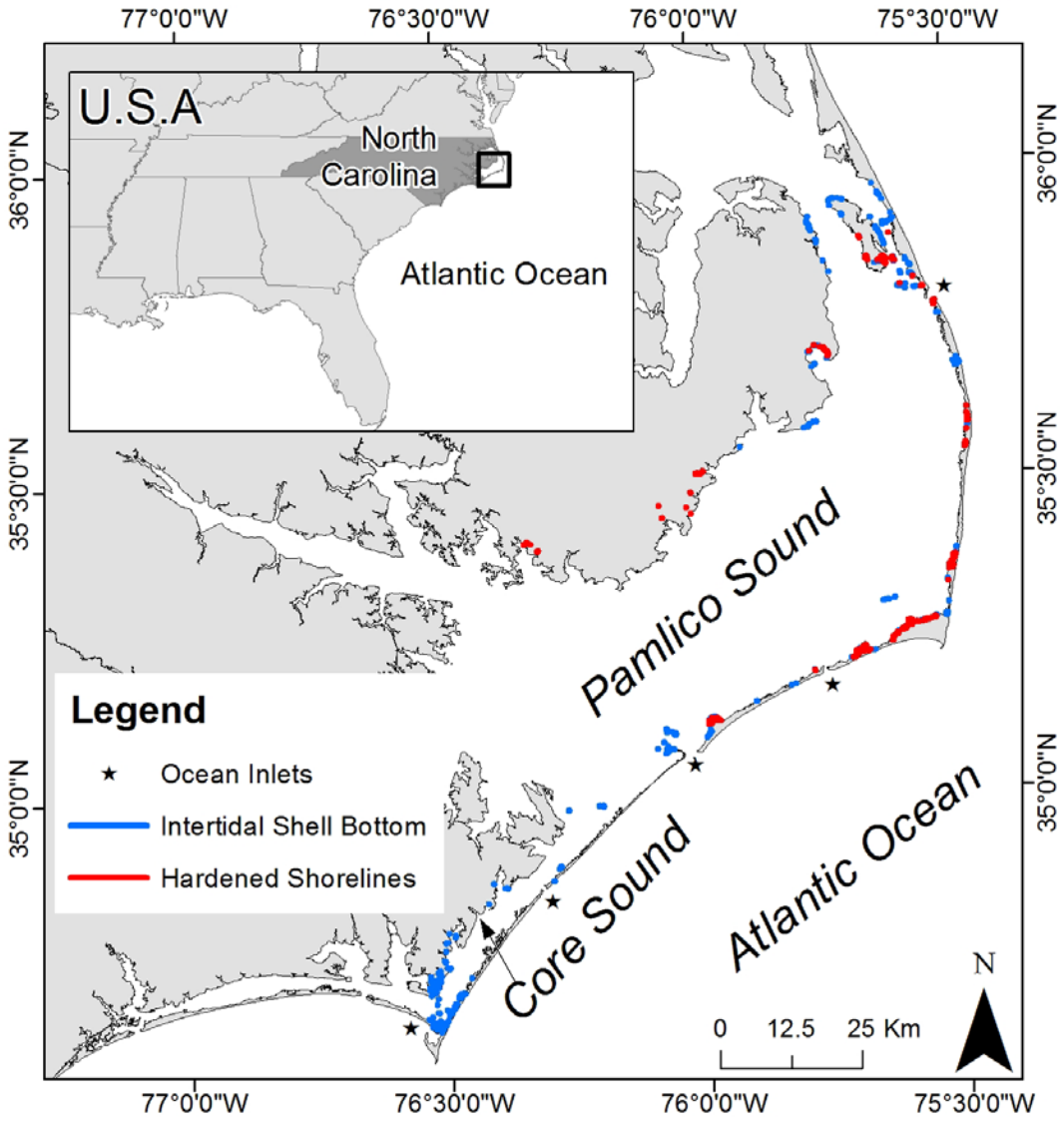


Figure 1. Map of the Albemarle-Pamlico Estuarine System showing distribution of hardened shorelines and intertidal shell bottom habitat. Estuary has limited oceanic exchange through five inlets indicated by stars.

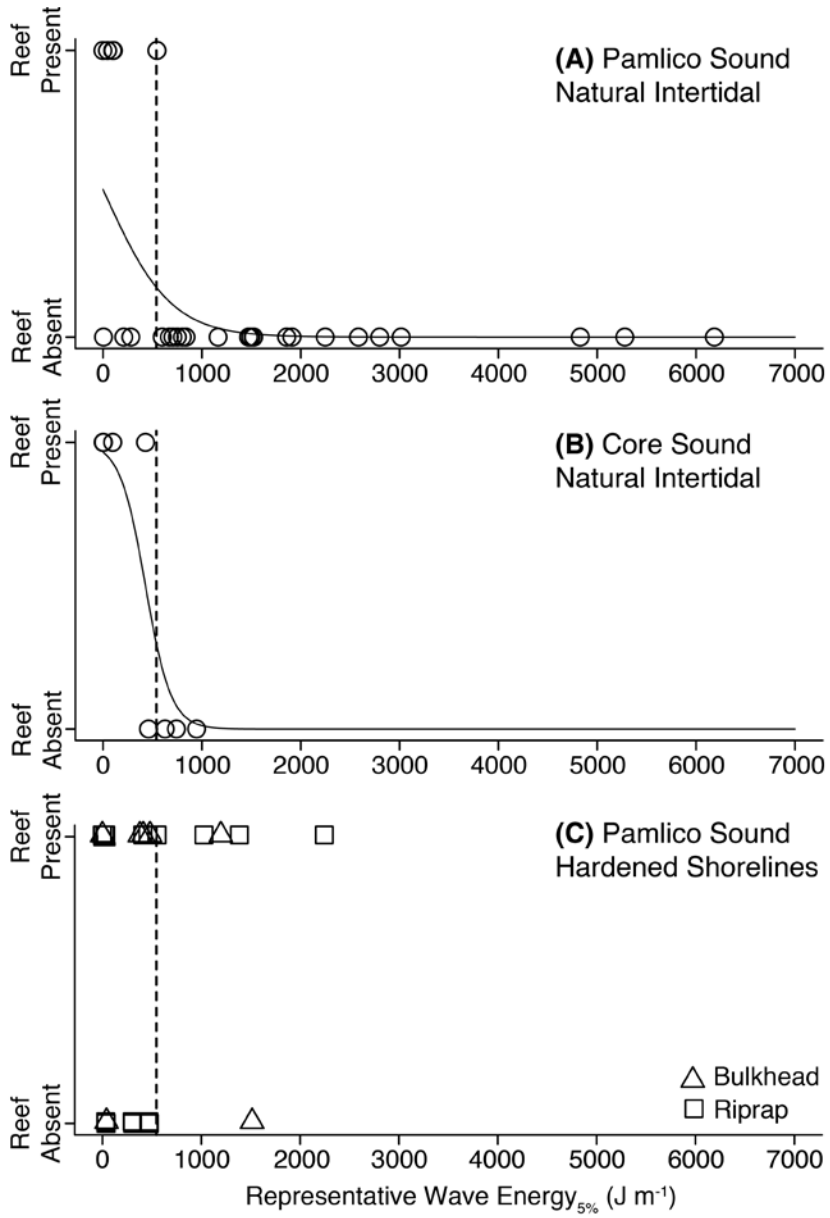


Figure 2. Relationship between oyster reef presence-absence (density ≥ 10 oysters $m^{-2}$) and representative wave energy (Joules per meter) for: A) Pamlico Sound natural intertidal reefs ($\hat{\beta}$ = -0.003, p = 0.007, Nagelkerke's $R^2$ = 0.34), B) Core Sound natural intertidal reefs ($\hat{\beta}$ = -0.008, p = 0.0009, Nagelkerke's $R^2$ = 0.79), and C) Pamlico Sound hardened shorelines (Bulkhead: $\hat{\beta}$ = -0.001, p = 0.43, Nagelkerke's $R^2$ = 0.12; Riprap: $\hat{\beta}$ = 0.0002, p = 0.86, Nagelkerke's $R^2$ = 0.06). Dashed line indicates the lowest threshold RWE value (~500 J $m^{-1}$) above which oyster reef was absent on natural intertidal reefs. RWE calculated using top 5 ($RWE_{5\%}$) percent of the hourly wind data from 2005-2012.

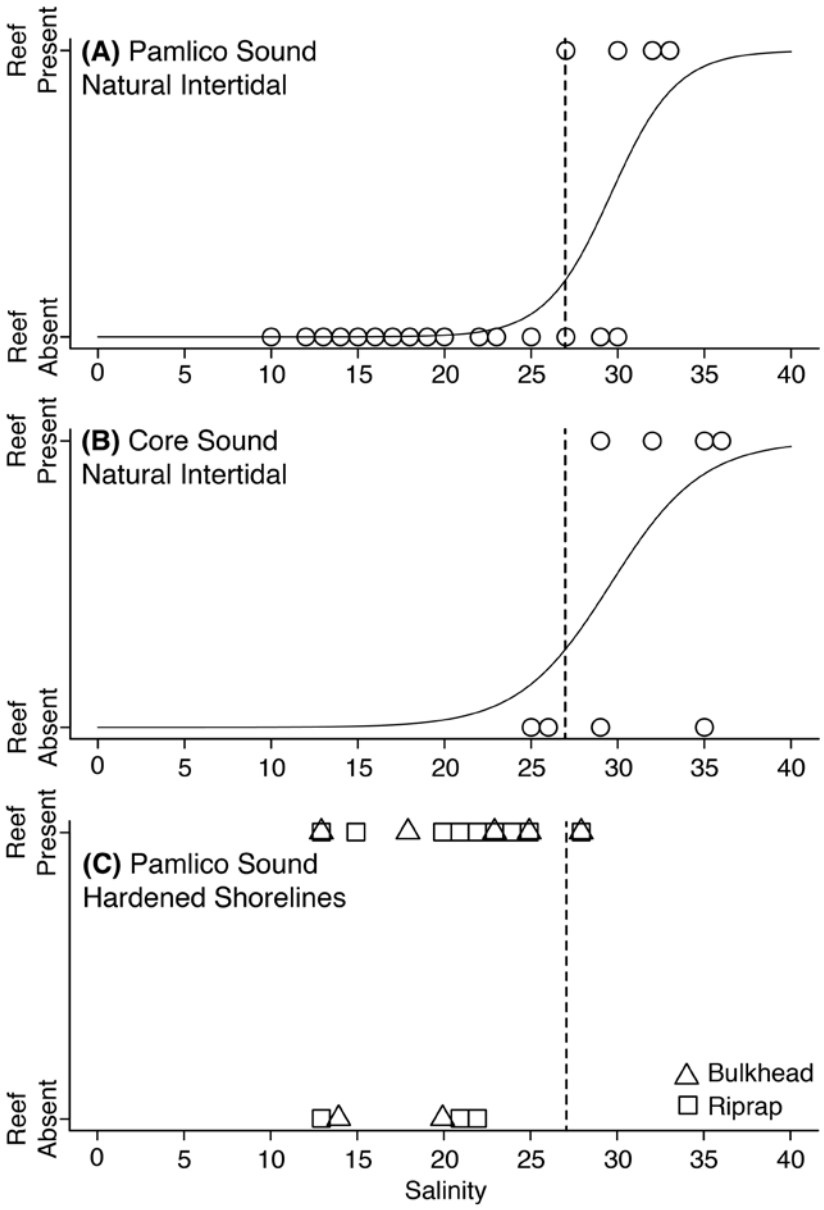


Figure 3. Relationship between oyster reef presence-absence (density ≥ 10 oysters $m^{-2}$) and salinity for: A) Pamlico Sound natural intertidal reefs ($\hat{\beta}$ = 0.529, p = 0.0002, Nagelkerke's $R^2$ = 0.59), B) Core Sound natural intertidal reefs ($\hat{\beta}$ = 0.377, p = 0.02, Nagelkerke's $R^2$ = 0.54) and C) Pamlico Sound hardened shorelines (Bulkhead: $\hat{\beta}$ = 0.116, p = 0.43, Nagelkerke's $R^2$ = 0.21; Riprap: $\hat{\beta}$ = 0.064, p = 0.56, Nagelkerke's $R^2$ = 0.05). Dashed line indicates the lowest threshold salinity value (~27) below which oyster reef was absent on natural intertidal reefs.

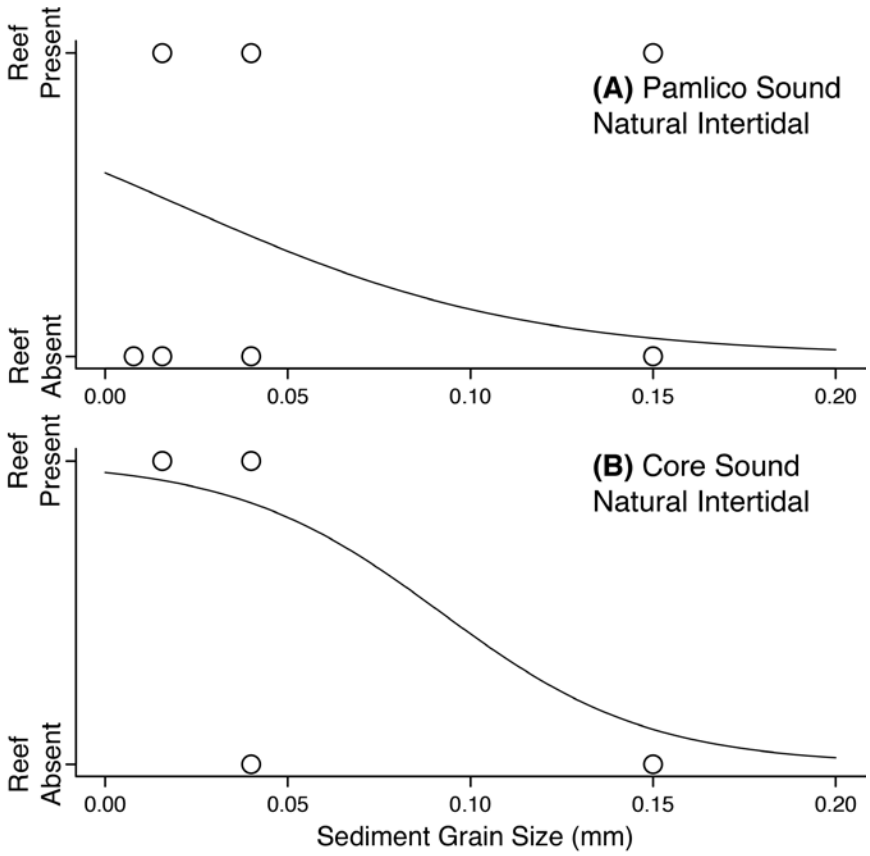


Figure 4. Relationship between oyster reef presence-absence (density ≥ 10 oysters $m^{-2}$) and sediment grain size (mm) for: A) Pamlico Sound natural intertidal reefs ($\hat{\beta}$ = -21.223, p = 0.006, Nagelkerke's $R^2$ = 0.16) and B) Core Sound natural intertidal reefs ($\hat{\beta}$ = -35.135, p = 0.003, Nagelkerke's $R^2$ = 0.56). Note that sediment grain size was recorded as a categorical descriptor and converted to a mean grain size (i.e., mud = 0.0078 mm, sandy mud = 0.0156 mm, muddy sand = 0.04 mm, sand = 0.15).

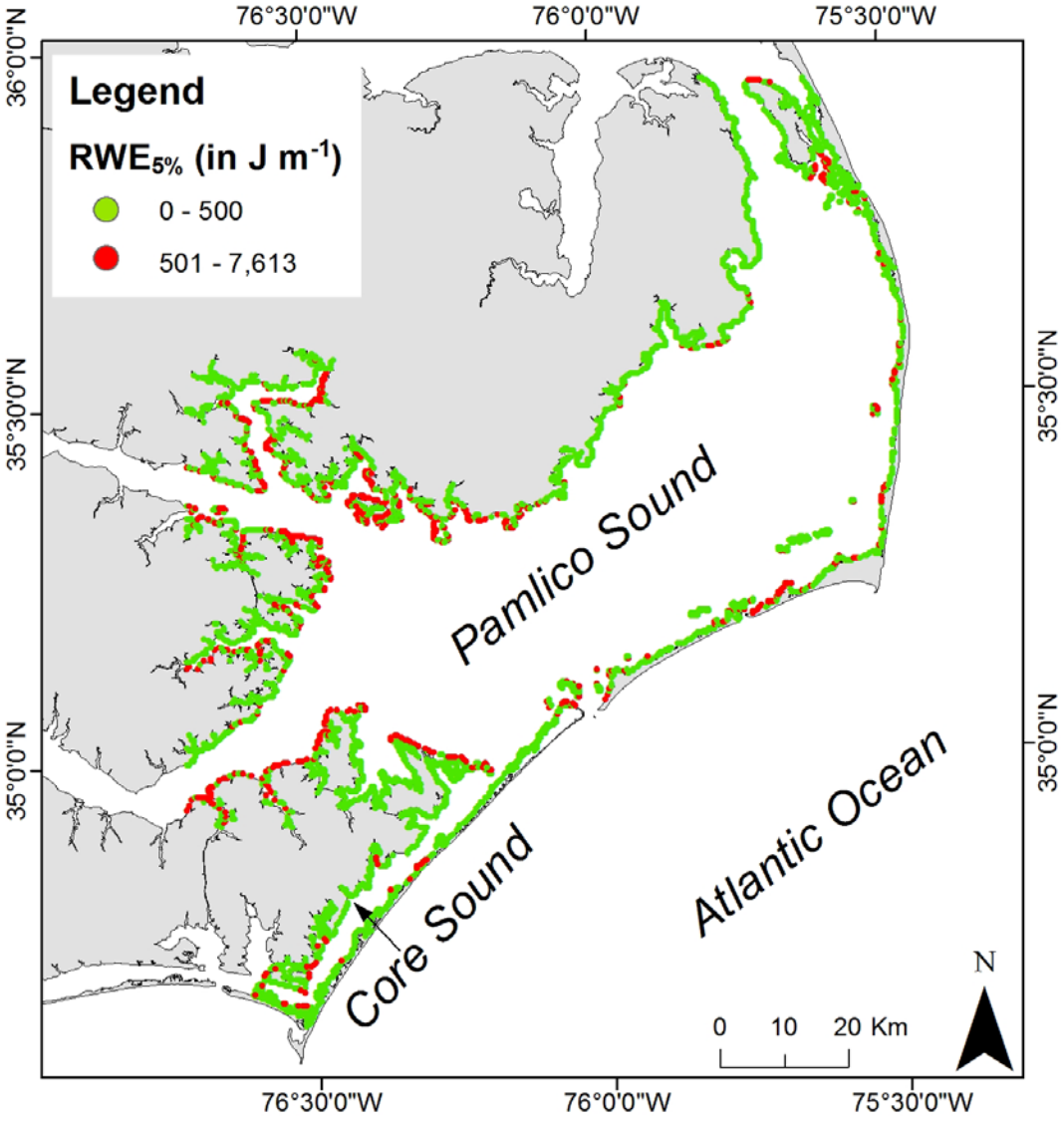


Figure 5. Map of Pamlico and Core Sounds showing distribution of shoreline above and below the identified representative wave energy (RWE) threshold of 500 J $m^{-1}$. RWE calculated using top 5 ($RWE_{5\%}$) percent of the hourly wind data from 2005-2012.

# CHAPTER 2

## OYSTER DENSITY AND DEMOGRAPHIC RATES ON NATURAL INTERTIDAL REEFS AND HARDENED SHORELINE STRUCTURES


## ABSTRACT

The ubiquitous loss of natural intertidal oyster reefs and associated ecosystem services has fueled restoration efforts throughout the world. Effective restoration requires an understanding of the distribution, density, and demographic rates (growth and survival) of oysters inhabiting existing natural reefs and how these may vary as a function of landscape-scale factors, such as tidal range and fetch distances. Furthermore, natural intertidal habitats are increasingly being replaced with hardened shoreline structures that may be colonized by oysters, yet little is known about habitat quality (as indexed by oyster density and demographic rates) of these hardened structures relative to natural habitats. The present study sought to compare oyster density, demographic rates, and population estimates (1) across estuarine landscape settings to inform natural intertidal oyster reef restoration (i.e., comparing natural intertidal reefs within adjacent water bodies that vary in tidal regimes and fetch distances) and (2) across natural habitats and human-made structures to assess variation in habitat quality between natural reefs and hardened shorelines. Oyster density, growth rates, and population estimates on natural intertidal reefs were greatest within the smaller, more tidally influenced Core Sound versus the larger, wind-driven Pamlico Sound, with no significant difference in survivorship identified between the two water bodies. Natural intertidal reefs and hardened shoreline structures were compared within Pamlico Sound only, with natural intertidal reefs hosting three to eight times higher oyster densities than hardened shoreline structures. When mean oyster density/$m^2$ was multiplied by reef area to estimate population size, natural intertidal reefs within Pamlico Sound hosted considerably greater populations of oysters relative to hardened shorelines. The present study fills an existing

need to understand oyster density and demographic rates on natural intertidal reefs and hardened shorelines to better inform future restoration and shoreline management scenarios.

## INTRODUCTION

Intertidal oyster reefs provide essential ecosystem services to coastal communities, yet their distribution and population sizes worldwide have been severely diminished as a result of human activities (Barbier et al. 2011, Beck et al. 2011). Loss of natural intertidal reefs has prompted interest in the restoration of three-dimensional oyster reef structures to promote important ecosystem services such as shoreline stabilization and essential fish habitat (Coen et al. 2007, Grabowski & Peterson 2007, Beck et al. 2011, Grabowski et al. 2012, Pierson & Eggleston 2014, Ridge et al. 2015). The efficacy of oyster restoration efforts is dependent on the ability of restored reefs to recruit larval oysters and to provide favorable conditions to promote their growth and survival (Beck et al. 2011, Theuerkauf et al. 2015). Furthermore, prior landscape-scale research has identified that (1) intertidal oyster density increases with increasing tidal energy and range (Byers et al. 2015) and (2) high levels of wave exposure (i.e., with increasing fetch distances) can restrict the distribution of natural intertidal reefs (Theuerkauf et al. 2016). Thus, effective restoration practices for these shoreline ecosystem engineers requires an understanding of both the distribution, density, demographic rates (growth and survival), and status (population size estimates) of oysters inhabiting natural intertidal reefs, as well as how these may vary as a function of landscape-scale factors (e.g., tidal regimes and fetch distances).

Increasingly, natural shoreline habitats (e.g., intertidal oyster reefs and sandflats) are being replaced with human-made hardened shoreline structures such as bulkheads and riprap revetments in response to shoreline erosion within the coastal zone (Gittman et al. 2015).

Estimates suggest ~14% of the continental U.S. shoreline has been hardened (Gittman et al. 2015), with subsequent reductions or losses of ecosystem services from these intertidal and shallow subtidal habitats (Lotze et al. 2006, Barbier et al. 2011, Layman et al. 2014, Gittman et al. 2016). Consequently, hardened shoreline structures provide a large amount of hard substrate that may be colonized by organisms such as oysters in estuaries when these structures are present (Layman et al. 2014). Studies that have assessed the quality of these human-made structures as habitat for benthic organisms relative to their natural counterparts, however, have yielded variable results. For example, the abundance of oysters on hardened shoreline structures can contribute larvae, habitat, and filtration benefits at levels comparable to, or greater than, natural oyster reefs within their respective estuarine systems (Burke 2010, Drexler et al. 2014, Layman et al. 2014). In contrast, seawalls were found to not sustain viable populations of limpets as they only harbored juveniles relative to natural rocky shores that hosted an expanded size structure (Moreira et al. 2006). Thus, an assessment of variation in habitat quality (as indexed by oyster density and demographic rates) between existing natural intertidal and hardened shoreline structures is needed to better understand the ecological consequences of shoreline armoring on ecosystem service provision and relative demographic contributions of oysters on natural and artificial structures.

The present study sought to compare oyster density, demographic rates, and population estimates (1) across landscape settings to inform natural intertidal oyster reef restoration (i.e., comparing natural intertidal reefs within adjacent water bodies—Core and Pamlico Sounds—that vary in tidal regimes and fetch distances) and (2) across natural habitats and human-made structures to assess variation in habitat quality between natural reefs and hardened shorelines within Pamlico Sound, where ~5.1% of the estuarine shoreline contains hardened shoreline

structures such as bulkhead and riprap revetments (North Carolina Department of Environmental Quality, Division of Coastal Management 2012). This study tested the hypothesis that oyster density, growth, and survivorship rates would be greater (1) on natural intertidal reefs in Core Sound where tidal regime is greater and wave energy is lower relative to Pamlico Sound (Byers et al. 2015, Theuerkauf et al. 2016) and (2) on natural intertidal reefs than hardened structures as hardened shorelines may be suboptimally distributed throughout the landscape with respect to ecological processes, such as larval supply.

## MATERIALS AND METHODS

### *Study Species*

Eastern oysters (*Crassostrea virginica*, hereafter oysters) are distributed throughout estuaries along eastern North America, ranging from the Gulf of St. Lawrence to the Gulf of Mexico, and provide a multitude of ecosystem services, such as water filtration, sediment stabilization, and essential fish habitat (Kennedy et al. 1996, Coen et al. 2007, Grabowski et al. 2012, Pierson & Eggleston 2014). Oysters form dense, three-dimensional reef structures that are connected via larval dispersal, whereby sessile individuals spawn gametes into the water column and fertilized eggs develop into planktonic larvae that are distributed via currents (Kennedy et al. 1996). After a 2- to 3-wk period, larvae seek hard structure on the benthos for permanent settlement.

### *Study System*

The Albemarle-Pamlico Estuarine System (APES) in North Carolina contains (from north to south) Albemarle, Croatan, Roanoke, Pamlico, and Core Sounds. The APES is the largest lagoonal estuary in the United States, and is bounded by a barrier island chain that limits

exchange with the coastal ocean to five relatively small inlets (~1 km wide; Fig. 1; Pietrafesa et al. 1986). Tides in and near the inlets of the APES are generally semidiurnal, with a mean vertical range of 5 cm when averaged across Pamlico Sound (Roelofs & Bumpus 1953) to 30 cm in Core Sound (Dudley & Judy 1973). Tidal range is negligible in Albemarle Sound, and is greatly reduced along the western shore of Pamlico Sound, reducing the majority of intertidal oyster reef distribution in Pamlico Sound to areas near inlets. Intertidal oyster reefs are distributed more homogenously throughout the more tidally influenced Core Sound.

The APES is relatively shallow with a mean depth of ~4.5 m and a maximum depth of 7.5 m (Epperly & Ross 1986). Shoreline fetch distances vary considerably throughout the system (<1–30 km), with the longest in Pamlico Sound and the shortest in Core Sound (Fig. 1). Correspondingly, representative wave energy (RWE; J/m), which incorporates adjacent water depth, fetch distances, and mean wind speed and percent wind frequency in cardinal and ordinal directions for the top 5% of wind speeds, varies from 1.34–945.63 J/m in Core Sound to 3.94–6184.85 J/m in Pamlico Sound (Theuerkauf et al. 2016). Water circulation patterns within the APES are due predominately to wind-driven currents and riverine freshwater input, with an increasing tidal influence from north to south (Xie & Eggleston 1999). Circulation during the summer, when primary and secondary peaks in oyster spawning occur (Ballance et al. 2009, Mroch et al. 2012), is driven predominately by southwesterly winds. These winds derive from synoptic-scale frontal systems that transverse the region. Wind patterns in the region have a strong influence on spatiotemporal variation in larval dispersal patterns of oysters (Haase et al. 2012, Puckett et al. 2014). The contrast in fetch and tide between Core and Pamlico Sounds, two adjacent water bodies, provides an ideal model system for comparing intertidal oyster demographics across these two important landscape-scale factors.

Multiple oyster reef types, both natural and restored, occur within the subtidal and intertidal zones of the APES. Within the subtidal zone, natural oyster reefs, restored cultch reefs (i.e., reefs restored for commercial harvest with shell, concrete, or limestone marl), and restored, no-take oyster sanctuaries exist (Puckett & Eggleston 2012, Peters 2014). Within the intertidal zone, oysters exist on natural reefs and hardened shoreline structures, such as bulkhead and riprap revetments (Theuerkauf et al. 2016). All reefs exist within a salinity range of approximately 10–36 psu, and are separated from each other by ~1–125 km.

***Site Selection***

To quantify intertidal oyster density and demographic rates, an initial oyster reef presence–absence field survey was conducted during summer 2014 at randomly selected intertidal shell bottom and hardened shoreline sites within the intertidal zone of Pamlico and Core Sounds. These sites were selected from map layers of the distribution of shell bottom habitat and hardened shoreline structures obtained from the North Carolina Division of Marine Fisheries Shellfish Mapping Program (North Carolina Department of Environmental Quality, Division of Marine Fisheries 2013) and the North Carolina Division of Coastal Management Estuarine Shoreline Mapping Program (North Carolina Department of Environmental Quality, Division of Coastal Management 2012). The shell bottom habitat layer, as described in more explicit detail in Theuerkauf et al. (2016), includes a range of shell habitat quality from areas of loose shell fragments containing no live oysters at the time of North Carolina Division of Marine Fisheries surveys (≥2 y before the present study), to scattered, low-density assemblages of oysters, to high-density oyster reefs. The hardened shoreline structures layer includes all areas of bulkhead and riprap revetments installed before 2012. Based on ground-truthing of these maps (Theuerkauf et al. 2016), wave exposure appeared to restrict the distribution of natural intertidal

oyster reefs such that high wave exposure precluded intertidal reef formation despite the presence of shell material. Because of the greater tidal range and shorter fetch distances in Core Sound relative to Pamlico Sound, oyster density and demographic rates of natural intertidal shell bottom habitat and associated oyster reefs were examined for each sound separately. In addition, given the paucity of hardened shoreline structures along the less developed shoreline of Core Sound, only hardened shoreline sites in Pamlico Sound were included in subsequent comparisons of oyster density and demographic rates between natural intertidal reefs and hardened shoreline structures.

A minimum density criterion of 10 live oysters per $m^2$ was used to define the presence of oyster reefs (sensu Powers et al. 2009) for subsequent samplings in 2014 and 2015 to quantify oyster density and demographic rates. From the initial ground-truthing and mapping of intertidal oyster reefs and hardened structures in Pamlico and Core Sounds (Theuerkauf et al. 2016), 5 (of 36) natural intertidal reef sites were identified in Pamlico Sound that met the minimum density criterion, and 11 (of 14) natural intertidal reef sites in Core Sound. Furthermore, 6 (of 8) riprap revetment and 13 (of 16) bulkhead-hardened shoreline sites were identified in Pamlico Sound that met the minimum density criterion.

***Oyster Density and Demographic Rates***

To quantify oyster density and demographic rates on natural intertidal oyster reefs and hardened shorelines, the reef sites from the ground-truthing survey that met the minimum density criterion (10 live oysters per $m^2$; sensu Powers et al. 2009, Theuerkauf et al. 2016) were revisited and continuously sampled. Because of accessibility issues, two of the bulkheads and one of the riprap revetments were unable to be revisited and continuously sampled, and thus these sites were not included in subsequent analyses. The present study's sampling protocol was adapted

from Drexler et al. (2014) and ensured that the reported measurements represented all living oysters existing on all available substrate material within a fixed 1-$m^2$ footprint. For natural intertidal reefs, oysters were sampled using a 1-$m^2$ quadrat randomly placed on a reef with the number of quadrat samples determined as a function of reef area, and a maximum number of quadrat samples set at 10. When densities appeared likely to exceed 500/$m^2$, a 0.25-$m^2$ quadrat was substituted and subsequent oyster density estimates were standardized to 1 $m^2$. All samples were hand-excavated to a depth of 10 cm. To sample hardened shoreline structures, a tape measure was first run along the horizontal length of the structure. The number of quadrat samples was determined as a function of structure length, and a maximum number of quadrat samples set at 10. A 1-$m^2$ quadrat was placed at randomly selected intervals along the tape measure and immediately below the high tide line (i.e., encompassing the entirety of the narrow tidal range that exists in Pamlico Sound). Quadrat samples were taken by destructively harvesting all oysters from the substrate within a quadrat. Natural intertidal oyster reefs were sampled during June, August, and October of 2014 and 2015, and hardened structures during August and October 2014, and June and August 2015. These sampling intervals followed several annual peak oyster recruitment pulses in North Carolina estuarine waters in May and a secondary peak in August (Ortega & Sutherland 1992, Ballance et al. 2009, Mroch et al. 2012), with the intention of tracking various oyster cohorts to quantify post-settlement growth and survivorship. The left valve length (LVL; distance from the umbo to the anterior margin of the shell) of all live oysters was measured to the nearest 1 mm with calipers.

**Oyster Density**

As the experimental unit was each Reef sampled, oyster density data were averaged from all quadrats for a given reef site for each sampling event and was subsequently partitioned into

three size classes: (1) recruit (LVL < 30 mm), (2) sublegal (30 mm ≤ LVL < 75 mm), and (3) legal oysters (LVL ≥ 75 mm; legally harvestable size) for statistical analyses. Four separate, linear mixed-effects models tested if a given response variable (total oyster density, recruit density, sublegal, and legal density) on natural intertidal oyster reefs varied according to Water Body (Pamlico versus Core Sound) or Time (June 2014, August 2014, October 2014, June 2015, August 2015, or October 2015), where the fixed factors were Water Body and Time (repeated measure), and the Reef sampled was considered as a random effect. Four separate linear mixed-effects models were also used to test if a given response variable (oyster total density, recruit density, sublegal, and legal density) on natural intertidal and hardened shoreline oyster reefs within Pamlico Sound varied by Habitat Type (bulkhead versus riprap versus natural intertidal) or Time (August 2014 to August 2015), where the fixed factors were Habitat Type and Time (repeated measure), and the Reef sampled was considered as a random effect. All data analyses were conducted using the PROC MIXED procedure within SAS version 9.4. All data were tested for normality; natural log transformation of total, recruit, sublegal, and legal oyster density were required to satisfy the model assumption of normality. In cases where transformed data failed to meet the assumption of homoscedasticity, denominator degrees of freedom were computed using Satterthwaite's method, which adjusts the degrees of freedom for unequal variances (Keselman et al. 1999). Comparisons among treatments within a factor were conducted with a Tukey–Kramer multiple comparisons test.

**Oyster Demographic Rates**

To estimate oyster growth and survivorship, a modal analysis of oyster LVL length frequency distributions was conducted to follow cohort modal progression at size–class intervals of 5 mm (sensu Puckett & Eggleston 2012). Modes within each site's monthly oyster length

frequency distribution were identified using FiSAT NORMSEP ©, which treats length frequency distributions as a combination of normal distributions and applies a maximum likelihood procedure to separate length frequency distributions into its normal distribution subcomponents (Gayanilo & Sparre 2005). Adjacent modes were considered significantly different in the procedure when their separation indices were >2 (Sparre & Venema 1996), and therefore assumed to be distinct oyster cohorts. Thus, in this study, the number of modes was specified a priori such that the modes were initially over-fit to the length frequency data. The number of modes was then stepped backward to reach the maximum number of modes with a minimum separation index >2 for all modes. At each time step, the procedure provides an estimate of mean LVL and density for each cohort. For a more detailed explanation of methods and visualization of cohort modal progression analyses, see Puckett and Eggleston (2012).

To estimate cohort-specific growth rates (*G*) on natural intertidal and hardened shoreline oyster reef sites, mean cohort LVL from modal analysis was plotted for each sampling event to observe changes in mean LVL of a cohort over time. Cohort-specific growth rates (mm/day) for each site were calculated between successive sampling dates (e.g., June 2014 to August 2014) as:

$$G = \frac{(\mathrm{LVL}_{t2} - \mathrm{LVL}_{t1})}{d}$$

where LVL is mean left valve length for the cohort, *t*1 is the initial sampling date, *t*2 is the subsequent sampling date, and *d* is the number of days between *t*1 and *t*2.

Changes in cohort density over time were used to estimate oyster mortality, and to subsequently estimate oyster survivorship (*S*) at each site. Mortality rates (*M*, %/day) were determined between successive sampling dates noted earlier as:

$$M = \frac{\left[(\mathrm{CD}_{t1} - \mathrm{CD}_{t2}) / \mathrm{CD}_{t1}\right] \times 100}{d}$$

where CD is cohort density and $t1$, $t2$, and $d$ are defined earlier. Daily percent survivorship ($S$) was calculated as $1 - M$. A caveat of the cohort analysis method used in the present study to estimate growth and survivorship is the underlying assumption that changes in total number of individuals in a cohort between $t1$ and $t2$ are due to mortality alone and not due to growth stasis of individuals or merging of cohorts between successive time steps. This potential artifact of the analysis would most significantly impact oysters within larger size classes as they have the slowest growth rates and would tend to increase estimates of survivorship of the largest cohort and decrease estimates of growth of the largest cohort.

Two separate linear mixed-effects models tested if cohort-specific oyster growth rates and survivorship on natural intertidal reefs varied by Water Body (Pamlico versus Core Sound), Size Class (recruit versus sublegal versus legal), or Time (Summer 2014, Fall 2014, Winter 2014–2015, Summer 2015, Fall 2015), where the fixed factors were Water Body, Size Class, and Time (repeated measure), and the Reef sampled was considered as a random effect. Two separate linear mixed-effects models were also used to test if cohort-specific growth rates and survivorship on natural intertidal and hardened shoreline oyster reefs within Pamlico Sound varied by Habitat Type (bulkhead versus riprap versus natural intertidal) or Time, where the fixed factors were Habitat Type, Size Class, and Time (repeated measure), and the Reef sampled was considered as a random effect.

***Oyster Population Size Estimates***

To estimate the population size of oysters from different intertidal reef habitat types of various size classes, the mean density of oysters (no. of oysters per $m^2$) within a size class (i.e., total, recruit, sublegal, and legal oysters) was multiplied by the areal footprint ($m^2$) of a given habitat type (i.e., natural intertidal, bulkhead, riprap). The areal footprint of a given habitat type was

determined by adjusting initial estimates of intertidal shell bottom habitat and hardened shoreline area by the percentage of reefs and structures meeting the minimum oyster density criterion (10 live oysters per $m^2$; North Carolina Department of Environmental Quality, Division of Coastal Management 2012, North Carolina Department of Environmental Quality, Division of Marine Fisheries 2013). For example, maps suggested there were 559,290 $m^2$ of intertidal shell bottom habitat in Pamlico Sound, yet reefs were observed at only 5 of 36 sites (14%). So, 559,290 $m^2$ was multiplied by 14% to get an adjusted natural intertidal reef area of 78,301 $m^2$ for Pamlico Sound. For a more detailed description of reef area estimation methods, see Theuerkauf et al. 2016.

## RESULTS

An overview of measured oyster density, reef area, relevant environmental covariates and sampling metrics for the natural intertidal oyster reefs, and hardened shorelines sampled in this study is provided in Table 1.

### *Oyster Density and Demographics on Natural Intertidal Reefs by Water Body*

#### Oyster Density

Mean oyster densities of all size classes examined in this study were 2–10 times higher in Core Sound versus Pamlico Sound (Fig. 2). Mean total, sublegal, and legal oyster density on natural intertidal reefs within Core Sound were significantly greater than in Pamlico Sound, but did not vary by Time (June 2014 to October 2015, Table 2). Mean recruit oyster density was ~2 times higher in Core Sound than Pamlico Sound; however, mean recruit density did not vary significantly by Water Body or Time (Table 2).

**Oyster Growth Rates**

Mean cohort-specific oyster growth rates on natural intertidal oyster reefs varied by Water Body, Size Class, and Time (Table 2). Mean oyster growth rates on natural intertidal oyster reefs in Core Sound were ~0.05 mm/day faster than those in Pamlico Sound (Fig. 3A). Within Core Sound, oysters in the recruit size class grew at a mean growth rate that was ~0.07 mm/day faster than those in the sublegal size class ($P < 0.0001$), and oysters in the sublegal size class also grew at a mean growth rate that was ~0.06 mm/day faster than those in the legal size class, though the difference was not significant ($P = 0.11$, Fig. 3B). Seasonally, mean oyster growth rates in Core Sound did not vary significantly between summer and fall of 2014 or 2015 ($P > 0.06$, means range between ~0.25 and ~0.31 mm/day), but were significantly slower during winter than other months (all $P < 0.0001$, mean growth rate ~0.07 mm/day, Fig. 3C). Within Pamlico Sound, oysters in both the recruit and sublegal size classes grew at approximately the same mean growth rate, which was ~0.06 mm/day faster than those in the legal size class, though there were no significant differences in growth rates between size classes (all $P > 0.21$, Fig. 3B). Seasonally, mean oyster growth rates in Pamlico Sound did not vary significantly between summer and fall of 2014 or 2015 ($P > 0.06$, means range between ~0.15 and ~0.25 mm/day), but were significantly higher during fall and summer as compared with winter (all $P < 0.0001$, Fig. 3C).

**Oyster Survivorship**

Mean cohort-specific oyster survivorship on natural intertidal oyster reefs varied by Size Class and Time, but not by Water Body (Table 2, Fig. 4A). Mean daily survivorship was ~0.2% higher for oysters in the recruit size class relative to those in the sublegal size class ($P = 0.07$); and oysters in the sublegal size class similarly had a mean daily survivorship that was ~0.2%

higher than those in the legal size class ($P < 0.0001$, Fig. 4B). Mean daily survivorship did not vary significantly between summer and fall of 2014 or 2015 ($P > 0.89$, means range between ~99.1% and ~99.2%), but was significantly higher during Winter 2014–2015 (all $P < 0.001$, mean daily percent survivorship ~99.8%, Fig. 4C).

### *Oyster Density and Demographics by Habitat Type within Pamlico Sound*

#### Oyster Density

Within Pamlico Sound, mean oyster densities of all size classes (with the exception of the legal size class) were three to eight times higher on natural intertidal reefs than hardened shorelines (Fig. 5). Mean total oyster density was ~4 times higher on natural intertidal reefs than bulkhead or riprap; however, mean total density did not vary significantly by Habitat Type or Time (Table 3, Fig. 5A). Mean recruit oyster density varied significantly by Habitat Type, but not by Time (Table 3). Specifically, mean recruit density was significantly higher (~8 times) on natural intertidal reefs than bulkhead ($P < 0.0001$) or riprap ($P < 0.0001$), but did not vary significantly between bulkhead or riprap ($P = 0.38$). Mean sublegal oyster density was ~3 times higher at natural intertidal reefs than bulkhead or riprap, though mean sublegal density did not vary significantly by Habitat Type or Time (Table 3, Fig. 5C). Mean legal oyster density varied significantly by Habitat Type, but not by Time (Table 3). Mean legal oyster density was significantly greater (~4 times higher) on bulkhead than riprap or natural intertidal oyster reefs (both $P = 0.01$), but did not vary significantly between riprap or natural intertidal oyster reefs ($P = 0.99$, Fig. 5D).

#### Oyster Growth Rates

Mean cohort-specific oyster growth rates on natural intertidal reefs and hardened shorelines varied by Size Class and Time, but not by Habitat Type (Table 3, means range

between 0.17 and 0.19 mm/day, Fig. 6A). Oysters in the recruit size class grew at a mean growth rate that was ~0.05 mm/day faster than those in the sublegal size class ($P = 0.003$), and oysters in the sublegal size class similarly grew at a mean growth rate that was ~0.08 mm/day faster than those in the legal size class ($P < 0.0001$, Fig. 6B). Mean oyster growth rates were significantly higher during summer and fall as compared with winter (all $P < 0.0001$, Fig. 6C).

**Oyster Survivorship**

Mean cohort-specific oyster survivorship on shoreline oyster reefs varied by Size Class and Time, but not by Habitat Type (Table 3). Mean daily survivorship was ~0.15% higher for oysters on bulkhead than riprap ($P = 0.02$), but did not vary significantly between other habitat types (all $P > 0.05$, Fig. 7A). Mean daily survivorship was ~0.2% higher for oysters in the recruit size class relative to those in the sublegal size class ($P = 0.001$); oysters in the sublegal size class had a mean daily survivorship that was comparable with those in the legal size class ($P = 0.69$, Fig. 7B). Mean daily survivorship did not vary significantly between Fall 2014 or Summer 2015 ($P > 0.10$, means range between ~99.1% and ~99.2%), but was significantly higher during Winter 2014–2015 (all $P < 0.0001$, mean daily percent survivorship ~99.8%, Fig. 7C).

***Multiplying Density by Area to Estimate Population Size***

Natural intertidal oyster reef area in Core Sound (263,069 $m^2$) was ~3 times greater than that in Pamlico Sound (78,301 $m^2$), yet Core Sound natural intertidal reefs hosted ~10 times more oysters (total population estimate ~15E+7 individuals; Fig. 8A). In Pamlico Sound, natural intertidal reef area was ~4 times greater than the combined hardened shoreline area (bulkhead = 14,122 $m^2$; riprap = 7,061 $m^2$), yet hosted ~20 times more oysters than bulkheads (total population estimate of ~8E+5 individuals), and ~40 times more than riprap (total population

estimate of ~4E+5 individuals). Patterns in recruit, sublegal, and legal oyster population estimates (Fig. 8B–D) largely reflected the patterns observed within total population estimates.

## DISCUSSION

The present study is among the first to quantify oyster density and demographic rates as a function of both landscape setting (i.e., comparing natural intertidal reefs within adjacent water bodies that vary in tidal regimes and fetch distances) and habitat type (i.e., hardened shorelines versus natural reefs). Oyster density, growth rates, and population estimates on natural intertidal reefs were greatest within the smaller, more tidally influenced Core Sound versus the larger, wind-driven Pamlico Sound, with no significant difference in survivorship identified between the two water bodies. These results suggest that within more tidally influenced, shorter fetch water bodies (e.g., Core Sound), restoration planning efforts should focus primarily on reef-scale considerations, such as identifying locations within the optimal tidal emersion range to maximize oyster survival (Ridge et al. 2015, Walles et al. 2016). Within larger, wind-driven water bodies (e.g., Pamlico Sound), restoration planning efforts should focus primarily on landscape-scale considerations, such as identifying locations with limited wave exposure (Theuerkauf et al. 2016). In all cases, restoration efforts should consider the range of relevant biophysical variables and parameters (e.g., larval supply, tidal emersion, wave exposure) necessary to maximize probability of restoration success (Walles et al. 2016). Furthermore, within Pamlico Sound, natural intertidal reefs harbored three to eight times more oysters than hardened shoreline structures and when mean density/$m^2$ was multiplied by reef area to estimate population sizes, natural intertidal reefs hosted considerably greater populations of oysters relative to hardened shorelines. These results suggest that natural intertidal reefs provide enhanced habitat quality for

oysters on a per unit area basis relative to hardened shorelines and thus conserving and/or rehabilitating degraded natural intertidal reefs should be a management priority within Pamlico Sound.

Oyster density was significantly greater within the smaller, more tidally influenced Core Sound as compared with the larger, wind-driven Pamlico Sound for all sizes classes, with the exception of the recruit size class (Fig. 2). Statistically significant differences in the mean density of both sublegal and legal oyster size classes between Core and Pamlico Sound, despite a lack of a significant difference in recruit density over 2 y of sampling, implies greater survivorship of recruit-size oysters within Core Sound relative to Pamlico Sound. Survivorship of oysters into sublegal and legal size classes is highly dependent on individuals reaching a size-dependent predation refuge (Eggleston 1990), or settlement on substrate that is not prone to burial by shifting sand or redistribution by wave action that can lead to surface abrasion and subsequent removal of spat (Wall et al. 2005, Taylor & Bushek 2008, Campbell 2015, Theuerkauf et al. 2016). Both mechanisms may explain the observed greater sublegal and legal oyster densities in Core Sound relative to Pamlico Sound. The greater fetch distances and higher levels of wave exposure within Pamlico Sound as compared with those in Core Sound (Table 1), coupled with the observation of burial of shell material between sampling events (S. Theuerkauf, personal observation), suggests a greater role of substrate redistribution leading to reduced recruit survival rather than predation; however, further testing of this hypothesis is needed. A more detailed description of the impact of substrate redistribution on oyster survival can be found in Wall et al. (2005) and Campbell (2015).

Mean total oyster densities on natural intertidal reefs observed in this study (~200–550 individuals/$m^2$; Fig. 2A) compared favorably with densities observed on intertidal reefs in

southern North Carolina (~300–1,200; Byers et al. 2015). Intertidal oyster density along the estuaries of the South Atlantic Bight was previously found to peak in Georgia and South Carolina estuaries, with declining densities identified in more northern and southern latitudes, presumably as a result of decreasing tidal energy and range (i.e., potentially reduced flow velocities and net water volume delivery per unit time; Byers et al. 2015). This observation may also partially explain the observed lower total oyster densities in Pamlico Sound versus Core Sound due to the relatively low tidal range in Pamlico Sound compared with Core Sound.

Oyster growth rates were significantly greater within the relatively high salinity waters of Core Sound as compared with the lower salinity waters of Pamlico Sound—a finding that is consistent with prior observations of enhanced growth rates in higher salinity waters (Table 3, Fig. 3A; Shumway 1996 and references therein, Puckett & Eggleston 2012). In both the Water Body– and Habitat Type–specific analyses, growth rates generally declined with increasing age of size class, consistent with previous studies of size-specific oyster growth rates (Figs. 3B, 6B; Puckett & Eggleston 2012). Furthermore, mean growth rates were most rapid during the summer, generally slowed during the fall, and were slowest overwinter (Figs. 3C, 6C). This is consistent with the previously identified winter growth stasis of oysters due to reduced primary production and reduced metabolic rates associated with colder water temperatures (Kennedy et al. 1996, Puckett & Eggleston 2012). When compared with annualized reef growth rates from prior studies in southern North Carolina, the growth rates observed in the present study compared favorably. Extrapolating the season-specific growth rates observed in this study (Fig. 3C) to yearly growth rates resulted in mean individual growth rates of ~50 mm/y. This rate falls within the ~40–80 mm/y reef growth rate range previously observed for natural intertidal oyster reefs in Back Sound, North Carolina (Ridge et al. 2015).

Oyster survivorship rates did not vary significantly between Core versus Pamlico Sound (Fig. 4A). Observed survivorship was greatest over winter months, and was reduced during summer and fall months. This observation is consistent with a general reduction in activity of oyster predators, such as the oyster drill (*Urosalpinx cinerea*), during winter months (Stauber 1950), as well as prior research that identified little overwinter mortality of oysters in Delaware Bay (Powell & Ashton-Alcox 2013). In both the Water Body– and Habitat Type–specific analyses in this study, recruit survivorship was greatest, followed by sublegal and legal survivorship (Figs. 4B, 7B). This observation was unexpected as predation impacts are generally greatest on recruit-size oysters (Eggleston 1990), and survivorship of juvenile marine invertebrates is generally lowest relative to adults (Gosselin & Qian 1997). This unexpected finding may be an artifact of the present study's sampling design where recruitment included individuals up to 30-mm LVL, which is presumably a month or more after settlement. Because mortality immediately following settlement can be high (Powell et al. 1984), this may have resulted in an overestimate of recruit survivorship. Powell et al. (1984) quantified larval settlement and post-settlement recruitment processes of various mollusc species using both death assemblages and living communities and determined that recruit survivorship estimates based on sampling the living community alone with a ≥6-wk sampling regimen resulted in an ~90% underestimate of true mortality rates. The authors attributed this discrepancy to post-settlement mortality occurring during the time between sampling intervals that would not otherwise be evident when examining size frequency distributions of the living community. Thus, the finding in the present study of the greatest survivorship rates occurring within the recruit size class should be interpreted cautiously and future studies that intend to assess recruit survivorship

should carefully consider the length of their sampling interval (i.e., weekly rather than monthly intervals for post-settlement processes).

Within Pamlico Sound, oyster density was generally higher on natural intertidal reefs than on hardened shoreline structures (Fig. 5). The greatest observed difference in total oyster density between natural intertidal reefs and hardened shoreline structures was driven by a higher density of recruit and sublegal oysters on natural intertidal reefs relative to those on hardened shorelines. Recruit density was significantly greater on natural intertidal reefs as compared with bulkhead and riprap revetments. This recruitment differentiation may indicate that natural intertidal reefs are distributed throughout the seascape in a manner that yields more consistent larval recruitment and post-settlement survivorship, whereas hardened structures, which are haphazardly placed with respect to ecological processes, such as larval supply, may be placed in locations that receive episodic recruitment with more variable post-settlement survivorship. The lack of a statistically significant differentiation of sublegal density between natural intertidal reefs and hardened shoreline structures implies potentially greater survivorship of recruit-size oysters on hardened shoreline structures relative to natural intertidal reefs despite the observed nonsignificant difference in survivorship between habitat types (Fig. 7A). This may be due to the previously described mechanism of enhanced survival due to the substrate stability afforded by hardened shorelines relative to natural intertidal reefs. The higher density of legal oysters on bulkheads, as compared with natural intertidal and riprap, implies considerable mortality of sublegal oysters on natural intertidal reefs and riprap relative to those on bulkhead, despite a nonsignificant difference in survivorship between habitat types. Oyster growth rates also did not vary significantly between habitat types (Fig. 6A), implying similarity in growing conditions

(e.g., food availability, flow rates) between natural intertidal reefs and hardened shoreline structures within Pamlico Sound.

On hardened shoreline structures in the present study, mean total oyster densities (~50 individual/$m^2$ on both bulkhead and riprap) were considerably lower than those observed on intertidal riprap in the Lynnhaven River System of Chesapeake Bay (~1,000 individual/$m^2$; Burke 2010) and seawalls in Tampa Bay, Florida (~2,400 individual/$m^2$; Drexler et al. 2014). In both previous studies, high levels of recruitment on hardened shoreline structures were observed and posited as drivers of the high total densities observed, whereas relatively low recruitment was observed on the hardened shoreline structures in the present study (Fig. 5B). The considerably lower tidal range within Pamlico Sound (5 cm) relative to the Lynnhaven River System of Chesapeake Bay (50 cm) and Tampa Bay (125 cm) yields a narrower intertidal window for oyster settlement and growth on hardened shorelines within Pamlico Sound, potentially contributing to the lower observed densities on hardened shorelines in the present study (Roelofs & Bumpus 1953, United States Army Corps of Engineers, Norfolk District 2013, Drexler et al. 2014).

The lack of variability of oyster density by Time in both the Water Body– and Habitat Type–specific analyses in this study is likely due to the age of natural intertidal and hardened shoreline structures, and a general lack of fishery harvest from these reefs. Natural intertidal reefs examined in this study appeared to be unrestored, naturally occurring and well established (S. Theuerkauf, personal observation), whereas hardened shoreline structures examined had been in place for a minimum of 3 y before the study (North Carolina Department of Environmental Quality, Division of Coastal Management 2012). Prior studies of oyster reefs in North Carolina that examined subtidal oyster sanctuaries and fished subtidal reefs identified a significant effect

of Time on oyster density. For the newly established subtidal oyster sanctuaries in Pamlico Sound, density varied significantly with Time as these reefs experienced rapid initial recruitment postconstruction (Puckett & Eggleston 2012). For fished subtidal reefs in Pamlico Sound, oyster density varied significantly with Time due to fishery harvest, resulting in decreased total and legal oyster density after the fishery season ensued (Peters 2014). Given that natural intertidal reefs and hardened shoreline structures in the regions examined in this study appeared to be unharvested and well established, the lack of a significant Time effect on oyster density is likely indicative of relatively stable densities on these habitat types. Furthermore, as described earlier, the lack of variability of recruit density by Time may be a result of post-settlement mortality occurring between the sampling intervals (i.e., ≥60 days; Powell et al. 1984).

Comparison of population estimates between natural intertidal reefs in Core Sound versus Pamlico Sound revealed ~10 times more oysters (15E+8 individuals) within Core Sound despite the footprint of natural intertidal reefs in Core Sound being only ~3 times that of Pamlico Sound (Fig. 8). The ~3 times greater density of oysters/$m^2$ on Core Sound natural intertidal reefs combined with their ~3 times greater areal footprint yielded an ~10 times greater population size within Core Sound relative to Pamlico Sound. The greater population size of natural intertidal oyster reefs in Core Sound as compared with Pamlico Sound may be due to the previously described mechanisms of enhanced recruit survival, faster growth rates, and enhanced tidal energy and range (sensu Byers et al. 2015). Furthermore, within Pamlico Sound, natural intertidal reefs hosted an estimated total population size that was ~20 times that of bulkhead reefs, and ~40 times that of riprap reefs. Given that natural intertidal reefs in Pamlico Sound occupy a footprint that is only ~4 times the combined footprint of bulkhead and riprap reefs, yet host a substantially larger total oyster population than hardened shoreline structures, this finding

highlights the importance of conserving and/or rehabilitating degraded natural intertidal reefs as a management priority within Pamlico Sound. Natural intertidal reefs, however, harbored reduced legal oyster densities relative to bulkhead reefs due to the likely physical redistribution of substrate harboring oysters on natural intertidal reefs (Wall et al. 2005, Taylor & Bushek 2008, Theuerkauf et al. 2016). Thus, substrate stability (i.e., use of alternative reef substrates in areas prone to redistribution by wave action; Burke 2010, Theuerkauf et al. 2015) is an important consideration for future intertidal restoration efforts.

The present study identified that oyster density, growth rates, and population estimates can be higher on natural intertidal reefs in smaller, more tidally influenced water bodies (e.g., Core Sound) relative to larger, wind-driven water bodies (e.g., Pamlico Sound) with no significant difference in survivorship identified between the two water bodies. These results indicate that within more tidally influenced, shorter fetch water bodies (e.g., Core Sound), restoration planning efforts should focus primarily on reef-scale considerations (e.g., optimal tidal emersion range to maximize oyster survival; Ridge et al. 2015, Walles et al. 2016), whereas within larger, wind-driven water bodies (e.g., Pamlico Sound), restoration planning efforts should focus primarily on landscape-scale considerations (e.g., locations with limited wave exposure; Theuerkauf et al. 2016). Furthermore, the present study also provides evidence that despite the reduced habitat quality (as indexed by oyster density and demographic rates) of hardened shorelines relative to natural intertidal reefs, each habitat type has a unique set of advantages and disadvantages. For example, natural intertidal reefs exhibited the highest total, recruit, and sublegal densities, yet bulkhead reefs exhibited the highest legal densities relative to other habitat types in Pamlico Sound. These results further highlight the need for additional research to test hypotheses that ultimately determine the success of restored intertidal reefs, such

as the potential role of substrate redistribution on recruit survivorship in natural intertidal reefs, and the potential role of larval supply versus post-settlement processes in leading to relatively low recruitment on hardened shoreline structures.

**ACKNOWLEDGEMENTS**

I thank S. Brown, J. Byrum, O. Caretti, A. Edwards, B. Griffin, R. Lyon, D. McVeigh, O. Phillips, K. Simmons, and R. Ward for their assistance with field collections. Funding for the project and completion of the manuscript was provided by North Carolina Sea Grant (R12-HCE-2) and the National Science Foundation (OCE-1155609) to D. Eggleston, well as a National Defense Science and Engineering Graduate Fellowship (contract FA9550-11- C-0028 awarded by the Department of Defense, Air Force Office of Scientific Research, 32 CFR 168a), North Carolina Coastal Conservation Association Scholarship, and Beneath the Sea Foundation Scholarship to S. Theuerkauf.

## LITERATURE CITED


Ballance, G., Eggleston, D. B., Plaia, G., & B. J. Puckett. 2009. Oyster settlement and reef mapping in Pamlico Sound. Final Report for the Fisheries Research Grant, 07-EP-04. NC Division of Marine Fisheries, Morehead City, NC, 20 pp.

Barbier, E. B., Hacker, S. D., Kennedy, C., Koch, E. W., Stier, A. C., & B. R. Silliman. 2011. The value of estuarine and coastal ecosystem services. *Ecological Monographs* 812:169–193.

Beck, M. W., Brumbaugh, R. D., Airoldi, L., Carranza, A., Coen, L. D., Crawford, C., Defeo, O., Edgar, G. J., Hancock, B., Kay, M. C. & H. S. Lenihan. 2011. Oyster reefs at risk and recommendations for conservation, restoration, and management. *Bioscience* 61:107–116.

Burke, R. P. 2010. *Alternative substrates as a native oyster (*Crassostrea virginica*) reef restoration strategy in Chesapeake Bay* (Doctoral dissertation, College of William and Mary, Gloucester Point, Virginia).

Byers, J. E., Grabowski, J. H., Piehler, M. F., Hughes, A. R., Weiskel, H. W., Malek, J. C., & D. L. Kimbro. 2015. Geographic variation in intertidal oyster reef properties and the influence of tidal prism. *Limnology and Oceanography* 60:1051–1063.

Campbell, D. E. 2015. *Quantifying the effects of boat wakes on intertidal oyster reefs in a shallow estuary* (Masters thesis, University of Central Florida, Orlando, Florida).

Coen, L. D., Brumbaugh, R. D., Bushek, D., Grizzle, R., Luckenbach, M. W., Posey, M. H., Powers, S. P. & S. Tolley. 2007. Ecosystem services related to oyster restoration. *Marine Ecology Progress Series* 341:303–307.

Drexler, M., Parker, M. L., Geiger, S. P., Arnold, W. S., & P. Hallock. 2014. Biological assessment of Eastern oysters (*Crassostrea virginica*) inhabiting reef, mangrove, seawall, and restoration substrates. *Estuaries and Coasts* 37:962–972.

Dudley, D. L., & M. H. Judy. 1973. Seasonal abundance and distribution of juvenile blue crabs in Core Sound, NC 1965–68. *Chesapeake Science* 14:51–55.

Eggleston, D. B. 1990. Foraging behavior of the blue crab, Callinectes sapidus, on juvenile oysters, *Crassostrea virginica*: effects of prey density and size. Bulletin of Marine Science 46:62–82.

Epperly, S. P., & S. W. Ross. 1986. *Characterization of the North Carolina Pamlico-Albemarle complex*. National Oceanic and Atmospheric Administration Technical Memorandum. NMFS-SEFC-175. Washington, D.C.

Gayanilo, F. C. J. and P. Sparre. 2005. *FAO-ICLARM Stock Assessment Tools II (FiSAT II). Revised version. User's guide.* Food and Agriculture Organization of the United Nations Computerized Information Series (Fisheries) 8. Rome, Italy.

Gittman, R. K., Fodrie, F. J., Popowich, A. M., Keller, D. A., Bruno, J. F., Currin, C. A., Peterson, C. H. and M. F. Piehler. 2015. Engineering away our natural defenses: an analysis of shoreline hardening in the US. *Frontiers in Ecology and the Environment* 13:301–307.

Gittman, R. K., Peterson, C. H., Currin, C. A., Fodrie, F. J., Piehler, M. F., and J. F. Bruno. 2016. Living shorelines can enhance the nursery role of threatened estuarine habitats. *Ecological Applications* 26:249–263.

Gosselin, L. A. and P. Qian. 1997. Juvenile mortality in benthic marine invertebrates. *Marine Ecology Progress Series* 146:265–282.

Grabowski, J. H. and C. H. Peterson. 2007. Restoring oyster reefs to recover ecosystem services. Pp. 281–298 in Cuddington, K., Byers, J.E., Wilson, W.G., Hastings A., eds. Ecosystem Engineers: Plants to Protists. Elsevier.

Grabowski, J. H., Brumbaugh, R. D., Conrad, R. F., Keeler, A. G., Opaluch, J. J., Peterson, C. H., Piehler, M. F., Powers, S. P. and A. R. Smyth. 2012. Economic valuation of ecosystem services provided by oyster reefs. *BioScience* 62:900–909.

Haase, A. T., Eggleston, D. B., Luettich, R. A., Weaver, R. J. and B. J. Puckett. 2012. Estuarine circulation and predicted oyster larval dispersal among a network of reserves. *Estuarine, Coastal and Shelf Science* 101:33–43.

Kennedy, V. S., R. I. E. Newell & A. F. Eble. 1996. The eastern oyster (*Crassostrea virginica*). College Park, MD: Maryland Sea Grant Press. 734 pp.

Keselman, H. J., Algina, J., Kowalchuk, R. K., and R. D. Wolfinger. 1999. The analysis of repeated measurements: A comparison of mixed-model Satterthwaite F tests and a non-pooled adjusted degrees of freedom multivariate test. *Communications in Statistics-Theory and Methods* 28:2967–2999.

Layman, C. A., Jud, Z. R., Archer, S. K. and D. Riera. 2014. Provision of ecosystem services by human-made structures in a highly impacted estuary. *Environmental Research Letters* 9:e044009.

Lotze, H. K., Lenihan, H. S., Borque, B. J., Bradbury, R. H., Cooke, R. G., Kay, M. C., Kidwell, S. M., Kirby, M. X., Peterson, C. H., and J. B. Jackson. 2006. Depletion, degradation, and recovery potential of estuaries and coastal seas. *Science* 312:1806–1809.

Moreira, J., Chapman, M. G., and A. J. Underwood. 2006. Seawalls do not sustain viable populations of limpets. *Marine Ecology Progress Series* 322:179–188.

Mroch III, R. M., Eggleston, D. B., and B. J. Puckett. 2012. Spatiotemporal variation in oyster fecundity and reproductive output in a network of no-take reserves. *Journal of Shellfish Research* 31:1091–1101.

North Carolina Department of Environmental Quality, Division of Coastal Management. 2012. *Estuarine Shorelines of NC Spatial Dataset.* Shapefile dataset. https://deq.nc.gov/about/divisions/coastal-management/coastal-management-data/spatial-data-maps##Estuarine Shorelines. Accessed 15 March 2016.

North Carolina Department of Environmental Quality, Division of Marine Fisheries. 2013. Estuarine benthic habitat mapping program. Shapefile dataset. http://portal.ncdenr.org/web/mf/shellfish-habitat- mapping. Accessed 15 Mar 2016.

Ortega, S., and J. P. Sutherland. 1992. Recruitment and growth of the Eastern oyster, *Crassostrea virginica,* in North Carolina. *Estuaries* 15:158–170.

Peters, J. W. 2014. *Oyster demographic rates in sub-tidal fished areas: recruitment, growth, mortality, and potential larval output* (Masters thesis, North Carolina State University, Raleigh, North Carolina).

Pierson, K. and D. B. Eggleston. 2014. Response of estuarine fish to large-scale oyster reef restoration. *Transactions of the American Fisheries Society* 143:273−288.

Pietrafesa, L. J., Janowitz, G. S., Chao, T. Y., Weisberg, R. H., Askari, F. and E. Noble. 1986. *The physical oceanography of Pamlico Sound*. UNC Sea Grant Publication. UNC-WP-86-5, Raleigh, NC, USA.

Powell, E. N., Cummins, H., Stanton, R. J., Staff, G. 1984. Estimation of the size of molluscan larval settlement using the death assemblage. *Estuarine, Coastal and Shelf Science* 18:367–384.

Powell, E. N. and K. A. Ashton-Alcox. 2013. Is overwinter mortality commonplace in Delaware Bay oyster populations? The ambiguity of dredge efficiency. *Journal of Shellfish Research* 32:639–645.

Powers, S. P., Peterson, C. H., Grabowski, J. H. and H. S. Lenihan. 2009. Success of constructed oyster reefs in no-harvest sanctuaries: implications for restoration. *Marine Ecology Progress Serie*s 389:159–170.

Puckett, B. J. and D. B. Eggleston. 2012. Oyster demographics in a network of no-take reserves: recruitment, growth, survival, and density dependence. *Marine and Coastal Fisheries* 4:605–627.

Puckett, B. J., Eggleston, D. B., Kerr, P. C., and R. A. Luettich. 2014. Larval dispersal and population connectivity among a network of marine reserves. *Fisheries Oceanography* 23:342-361.

Ridge, J. T., Rodriguez, A. B., Fodrie, F. J., Lindquist, N. L., Brodeur, M. C., Coleman, S. E., Grabowski, J. H. and E. J. Theuerkauf. 2015. Maximizing oyster-reef growth supports green infrastructure with accelerating sea-level rise. *Scientific Reports* 5:e14785.

Roelofs, E. W. and D. F. Bumpus. 1953. The hydrography of Pamlico Sound. *Bulletin of Marine Science* 3:181–205.

Shumway, S. E. 1996. Natural environmental factors. Pp. 467–503 in Kennedy, V. S., R. I. E. Newell & A. F. Eble., eds. The eastern oyster (*Crassostrea virginica*). College Park, MD: Maryland Sea Grant Press. 734 pp.

Sparre, P and S. C. Venema. 1996. Introduction à l'évaluation des stocks de poissons tropicaux. FAO document technique sur les pêcheries, Première partie manuel N°306/1, FAO, Rome: 400p.

Stauber, L. A. 1950. The problem of physiological species with special reference to oysters and oyster drills. *Ecology* 31:109–118.

Taylor, J. and D. Bushek. 2008. Intertidal oyster reefs can persist and function in a temperate North American Atlantic estuary. *Marine Ecology Progress Series* 361:301–306.

Theuerkauf, S. J., Burke, R. P., and R. N. Lipcius. 2015. Settlement, growth, and survival of eastern oysters on alternative reef substrates. *Journal of Shellfish Research* 34:241–250.

Theuerkauf, S. J., Eggleston, D. B., Puckett, B. J., and K. W. Theuerkauf. 2016. Wave exposure structures oyster distribution on natural intertidal reefs, but not on hardened shorelines. *Estuaries and Coasts* doi:10.1007/s12237-016-0153-6.

United States Army Corps of Engineers, Norfolk District. 2013. *Final Feasibility Report and Integrated Environmental Assessment: Appendix A. Lynnhaven River Basin Ecosystem Restoration.* Norfolk, Virginia.

Wall, L. M., Walters, L. J., Grizzle, R. E. and P. E. Sacks. 2005. Recreational boating activity and its impact on the recruitment and survival of the oyster *Crassostrea virginica* on intertidal reefs in Mosquito Lagoon, Florida. *Journal of Shellfish Research* 24:965–973.

Walles, B., Troost, K., van den Ende, D., Nieuwhof, S., Smaal, A. C. and T. Ysebaert. 2016. From artificial structures to self-sustaining oyster reefs. *Journal of Sea Research* 108:1–9.

Table 1. Overview of natural intertidal oyster reefs and hardened shoreline sampled in this study.

| | Reef | Reef area ($m^2$) | Number of quadrats | Average total density (ind $m^{-2}$) | Average recruit density | Average sublegal density | Average legal density | RWE (J $m^{-1}$) | Average salinity (standard deviation) |
|---|---|---|---|---|---|---|---|---|---|
| Natural Intertidal – Core Sound | 1 | 3,364 | 10 | 2,378 | 1,059 | 1,216 | 104 | 428.64 | 32.67 (3.56) |
| | 2 | 418 | 4 | 93 | 18 | 55 | 20 | 3.12 | 32.33 (4.97) |
| | 3 | 1,070 | 6 | 102 | 28 | 70 | 4 | 0.00 | 33.33 (1.97) |
| | 4 | 192 | 3 | 482 | 131 | 317 | 35 | 2.52 | 33.33 (1.75) |
| | 5 | 130 | 3 | 204 | 37 | 164 | 2 | 3.68 | 29.80 (4.32) |
| | 6 | 343 | 4 | 795 | 252 | 535 | 8 | 4.40 | 31.17 (4.36) |
| | 7 | 170 | 3 | 865 | 150 | 676 | 39 | 97.02 | 31.83 (2.93) |
| | 8 | 590 | 5 | 428 | 99 | 313 | 17 | 1.34 | 30.83 (3.76) |
| | 9 | 263 | 4 | 40 | 5 | 28 | 7 | 4.26 | 29.00 (3.03) |
| | 10 | 334 | 4 | 340 | 82 | 230 | 28 | 1.98 | 29.17 (6.55) |
| | 11 | 651 | 5 | 167 | 21 | 128 | 18 | 3.56 | 28.25 (4.27) |
| Natural Intertidal – Pamlico Sound | 12 | 787 | 5 | 103 | 63 | 40 | 0 | 0.56 | 26.70 (5.15) |
| | 13 | 272 | 4 | 749 | 234 | 496 | 18 | 0.00 | 27.58 (5.02) |
| | 14 | 192 | 3 | 91 | 66 | 25 | 0 | 45.73 | 26.00 (5.25) |
| | 15 | 165 | 3 | 10 | 0 | 6 | 3 | 98.33 | 24.07 (2.60) |
| | 16 | 763 | 5 | 84 | 47 | 34 | 3 | 103.64 | 16.98 (5.94) |
| Hardened Shorelines – Bulkhead | 17 | 13 | 5 | 38 | 3 | 31 | 4 | 4.46 | 13.75 (4.35) |
| | 18 | 9 | 4 | 59 | 0 | 26 | 33 | 413.03 | 24.75 (2.50) |
| | 19 | 9 | 4 | 77 | 1 | 20 | 56 | 36.71 | 24.25 (2.87) |
| | 20 | 7 | 3 | 74 | 10 | 48 | 16 | 36.95 | 24.25 (2.22) |
| | 21 | 16 | 6 | 20 | 1 | 17 | 2 | 3.58 | 9.75 (2.75) |
| | 22 | 7 | 3 | 64 | 9 | 50 | 5 | 29.00 | 25.75 (3.20) |
| | 23 | 10 | 4 | 77 | 13 | 55 | 9 | 1,389.1 | 24.25 (3.30) |
| | 24 | 10 | 4 | 8 | 0 | 7 | 0 | 305.29 | 13.75 (4.35) |
| | 25 | 11 | 4 | 32 | 2 | 19 | 10 | 2,248.72 | 21.50 (2.08) |
| | 26 | 6 | 3 | 21 | 1 | 13 | 7 | 556.37 | 19.50 (4.20) |
| | 27 | 8 | 4 | 116 | 1 | 47 | 68 | 464.90 | 22.00 (2.16) |
| Hardened Shorelines – Riprap | 28 | 11 | 4 | 71 | 1 | 50 | 20 | 4.19 | 16.75 (1.50) |
| | 29 | 7 | 3 | 35 | 5 | 29 | 1 | 1,031.50 | 24.50 (1.29) |
| | 30 | 25 | 8 | 69 | 19 | 49 | 2 | 485.43 | 23.75 (1.71) |
| | 31 | 7 | 3 | 48 | 3 | 45 | 0 | 3.86 | 10.00 (3.92) |
| | 32 | 9 | 4 | 40 | 2 | 35 | 3 | 417.03 | 21.50 (2.89) |

Table 2. Mixed model results (type III test of fixed effects) for each parameter examined in Water Body–specific (Core versus Pamlico Sound) analyses of oyster density, growth rates, and survivorship rates on natural intertidal reefs. Degrees of freedom are expressed as (numerator degrees of freedom, denominator degrees of freedom).

| | **Parameter** | ***F* value (df)** | ***P* value** |
|---|---|---|---|
| **Oyster density** | | | |
| Total | Water Body | 16.96 (1, 88) | 0.0001 |
| | Time | 0.12 (5, 83) | 0.99 |
| Recruit | Water Body | 3.78 (1, 88) | 0.06 |
| | Time | 0.53 (5, 88) | 0.76 |
| Sub-Legal | Water Body | 24.53 (1, 88) | <0.0001 |
| | Time | 0.09 (5, 88) | 0.99 |
| Legal | Water Body | 36.89 (1, 88) | <0.0001 |
| | Time | 0.30 (5, 83) | 0.87 |
| **Growth rates** | | | |
| | Water Body | 10.29 (1, 140) | 0.002 |
| | Size Class | 25.06 (2, 140) | <0.0001 |
| | Time | 48.51 (4, 140) | <0.0001 |
| **Survivorship rates** | | | |
| | Water Body | 0.13 (1, 12.4) | 0.73 |
| | Size Class | 7.90 (2, 184) | 0.0005 |
| | Time | 18.79 (4, 181) | <0.0001 |

Table 3. Mixed model results (type III test of fixed effects) for each parameter examined in Habitat Type–specific (riprap versus bulkhead versus natural intertidal reef in Pamlico Sound) analyses of oyster density, growth rates, and survivorship rates. Degrees of freedom are expressed as (numerator degrees of freedom, denominator degrees of freedom).

| | Parameter | *F* value (df) | *P* value |
|---|---|---|---|
| **Oyster density** | | | |
| Total | Habitat Type | 1.99 (2, 78) | 0.14 |
| | Time | 1.03 (3, 78) | 0.38 |
| Recruit | Habitat Type | 28.24 (2, 78) | <0.0001 |
| | Time | 0.97 (3, 78) | 0.41 |
| Sub-Legal | Habitat Type | 0.93 (2, 78) | 0.40 |
| | Time | 1.57 (3, 78) | 0.20 |
| Legal | Habitat Type | 6.99 (2, 78) | 0.00 |
| | Time | 0.17 (3, 78) | 0.92 |
| **Growth rates** | | | |
| | Habitat Type | 0.42 (2,105) | 0.66 |
| | Size Class | 28.58 (2,105) | <0.0001 |
| | Time | 85.82 (2,105) | <0.0001 |
| **Survivorship rates** | | | |
| | Habitat Type | 3.00 (2, 16.8) | 0.07 |
| | Size Class | 5.11 (2, 167) | 0.01 |
| | Time | 119.43 (2, 179) | <0.0001 |

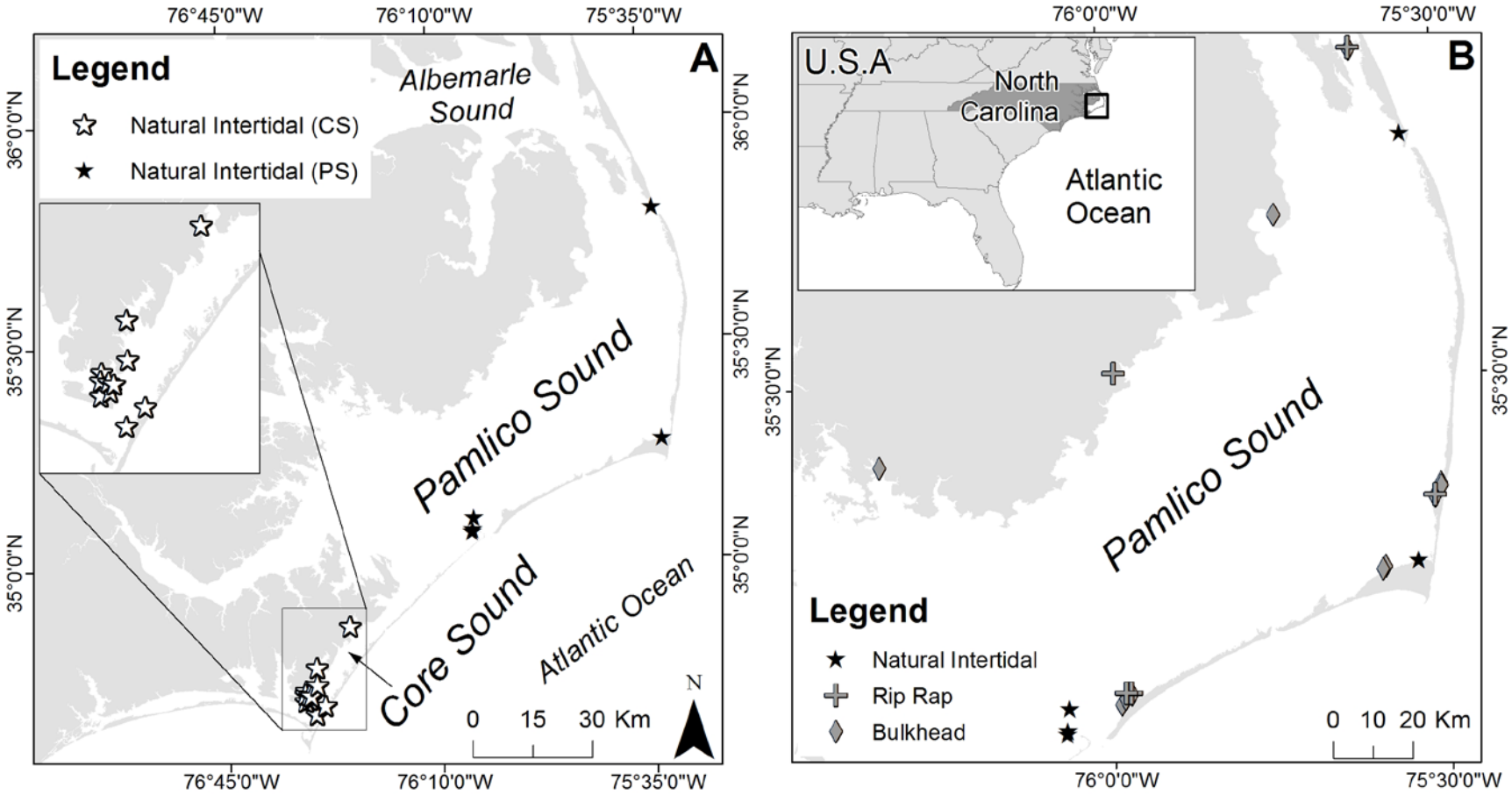


Figure 1. A) Map of the Albemarle-Pamlico Estuarine System showing the distribution of natural intertidal oyster reef study sites within Core Sound (white stars) and Pamlico Sound (black stars). B) Map of the natural intertidal oyster reefs (black stars), rip rap revetments (gray crosses), and bulkhead hardened shoreline (gray diamonds) study sites within Pamlico Sound.

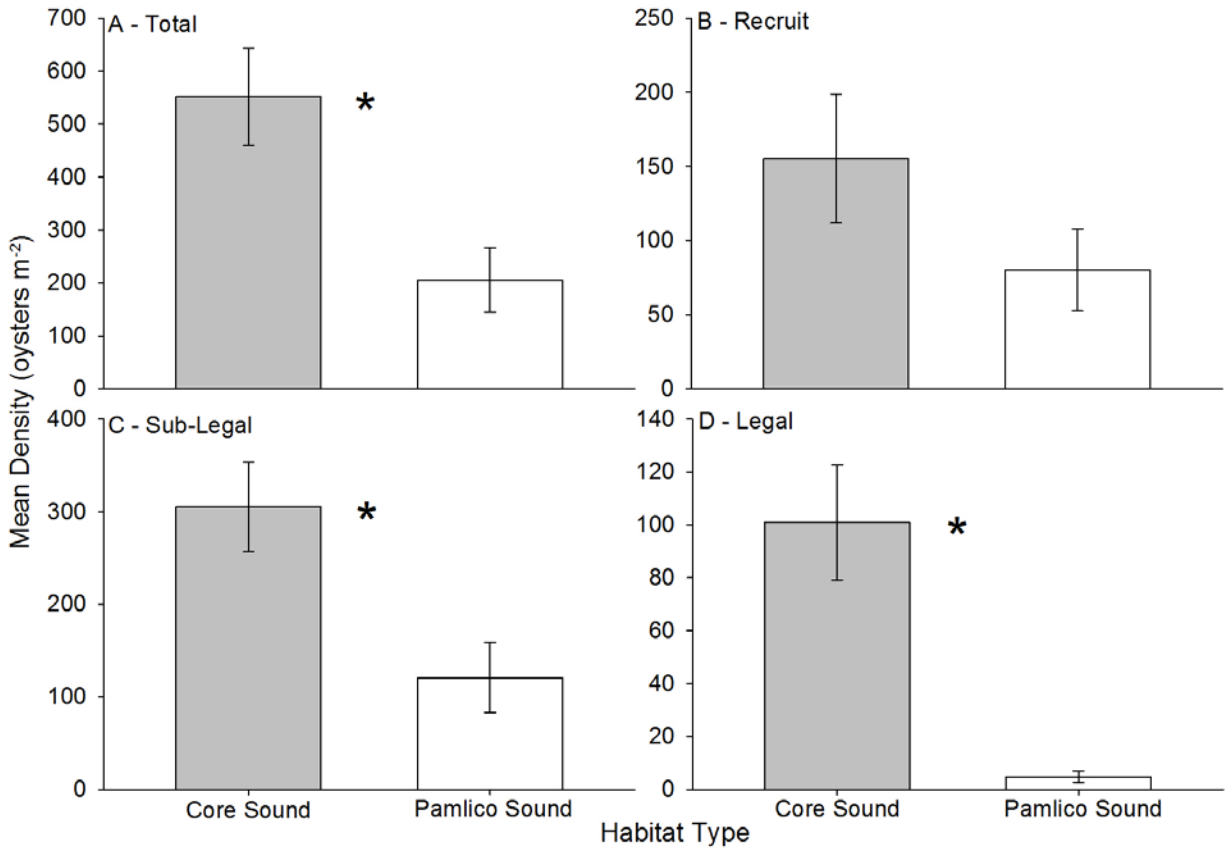


Figure 2. Mean oyster density (oysters $m^{-2}$) on natural intertidal reefs in Core Sound versus Pamlico Sound for a) total (all size classes), b) recruit (LVL < 30 mm), c) sub-legal (30mm ≤ LVL<75mm), and d) legal (LVL ≥75mm) size classes. Error bars designate standard error. Significant differences as determined by the linear mixed-effects model are denoted by an asterisk (*).

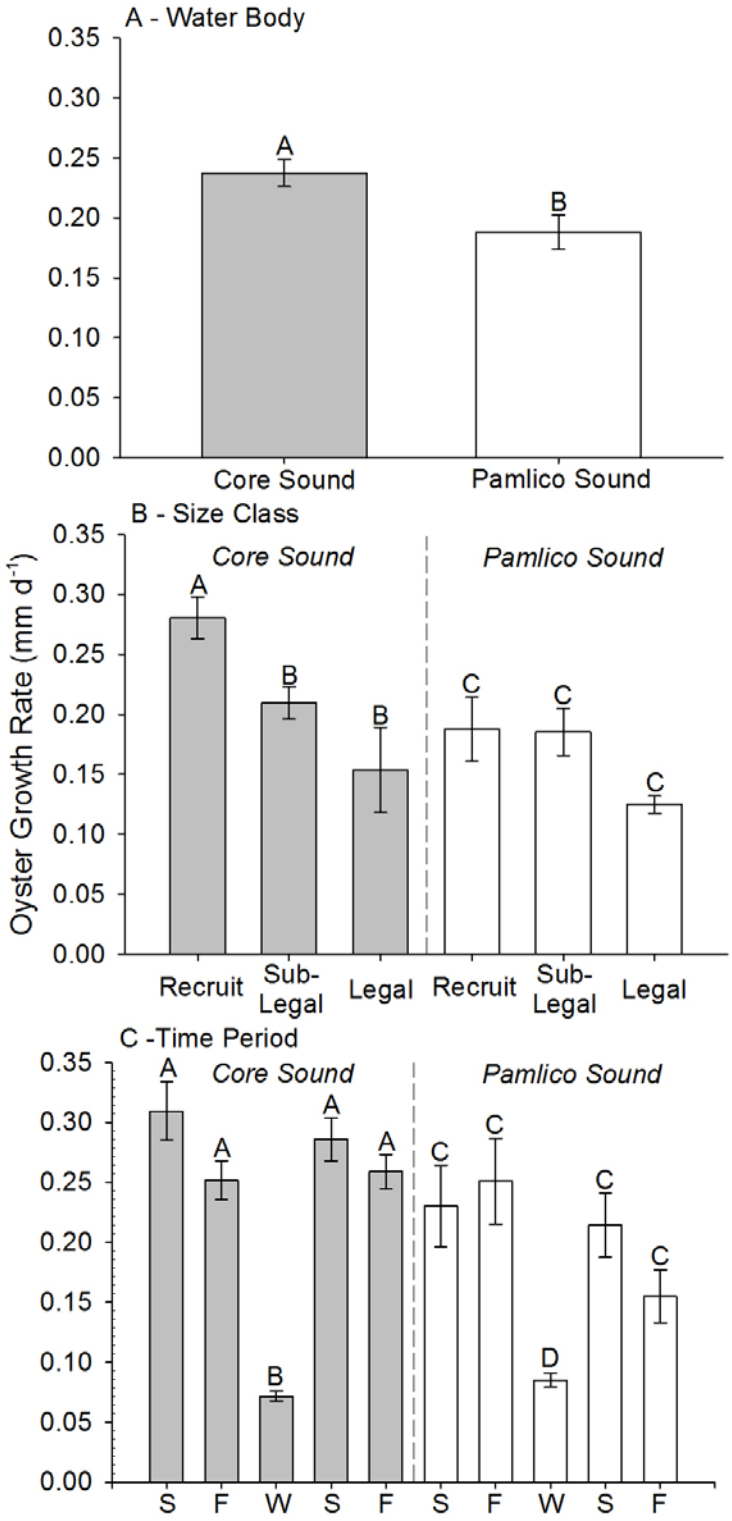


Figure 3. Mean oyster growth rate (mm $d^{-1}$) for natural intertidal reefs compared among: a) water body, b) size class within a water body, and c) time period within a water body (S = spring, F = fall, W = winter; temporal range from 2014–2015). Error bars designate standard error. Letters indicate significant differences between levels of a factor as determined with a Tukey-Kramer multiple comparison test.

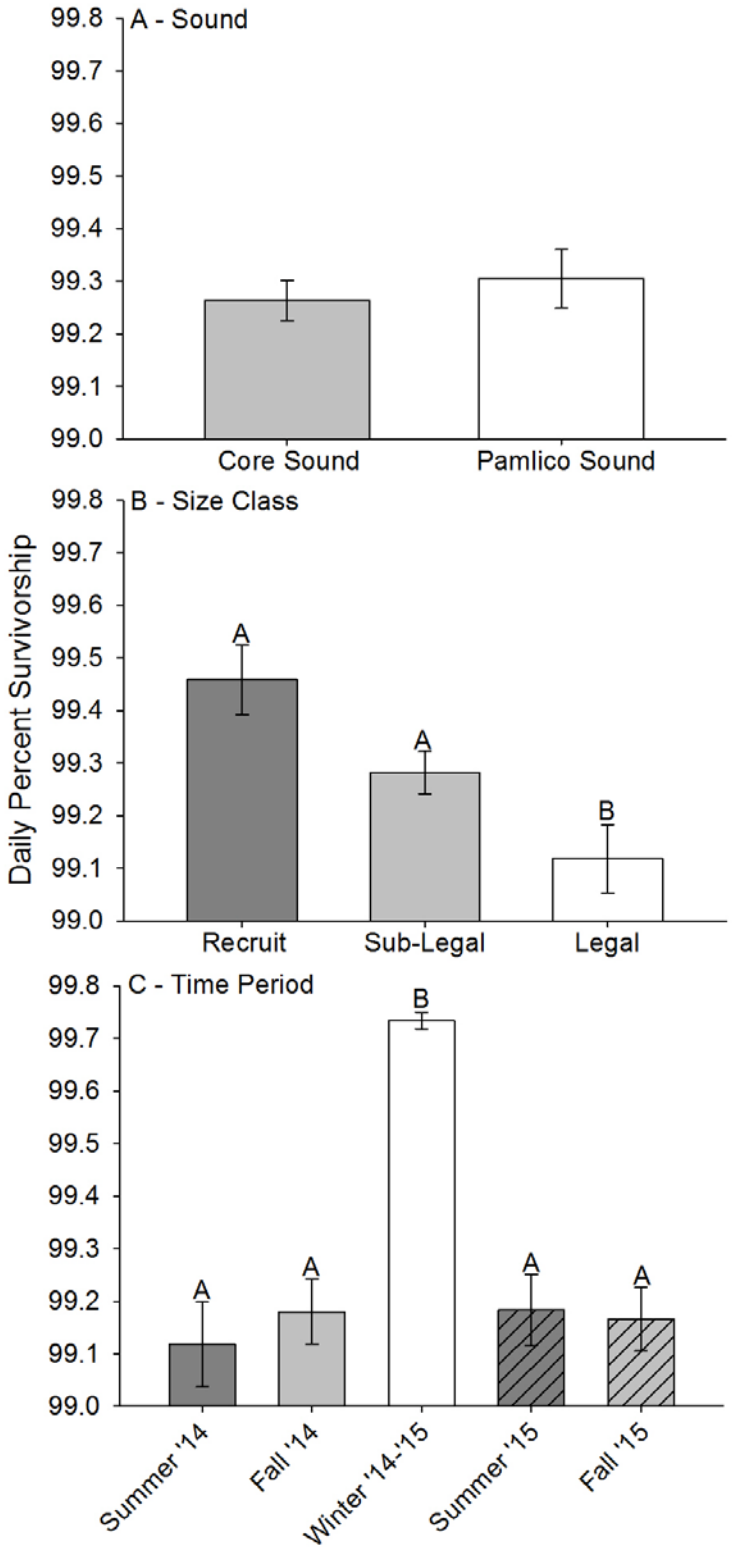


Figure 4. Mean daily percent survivorship for oysters on natural intertidal reefs compared among: a) water body, b) size class, and c) time period. Error bars designate standard error. Letters indicate significant differences between levels of a factor as determined with a Tukey-Kramer multiple comparison test.

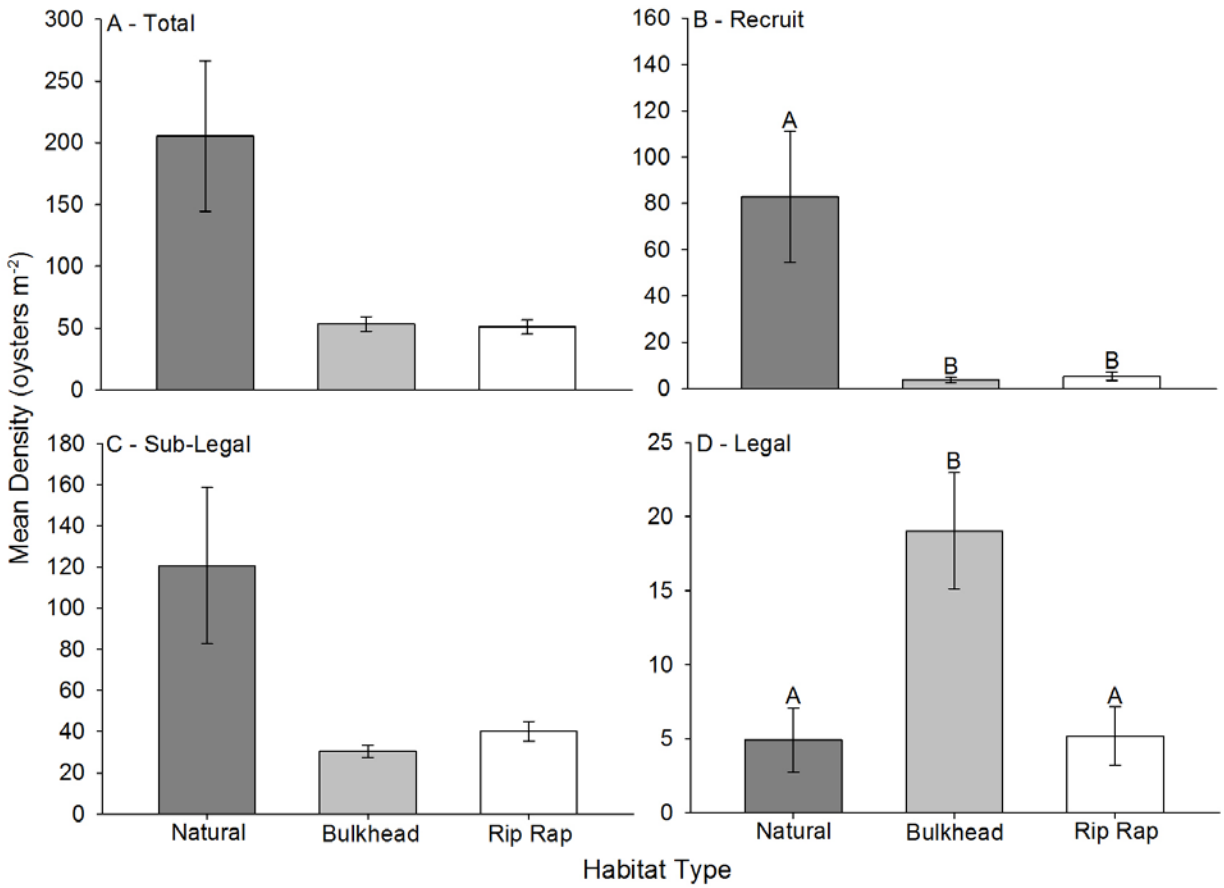


Figure 5. Mean oyster density (oysters $m^{-2}$) on natural intertidal, bulkhead, and riprap habitat types in Pamlico Sound. for a) total (all size classes), b) recruit (LVL < 30 mm), c) sub-legal (30mm ≤ LVL<75mm), and d) legal (LVL ≥75mm) size classes. Error bars designate standard error. Letters indicate significant differences between levels of a factor as determined with a Tukey-Kramer multiple comparison test.

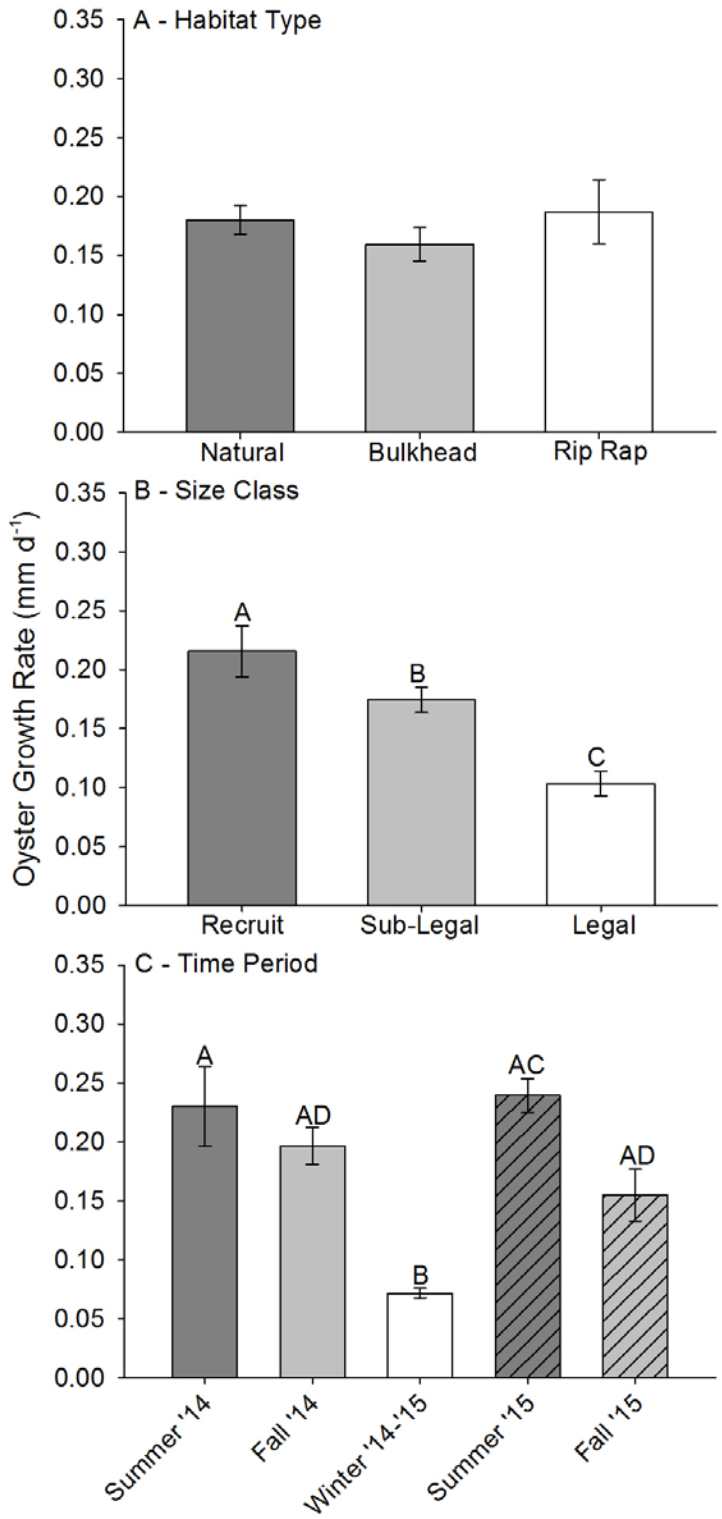


Figure 6. Mean oyster growth rate (mm $d^{-1}$) compared among: a) habitat type, b) size class, and c) time period. Error bars designate standard error. Letters indicate significant differences between levels of a factor as determined with a Tukey-Kramer multiple comparison test.

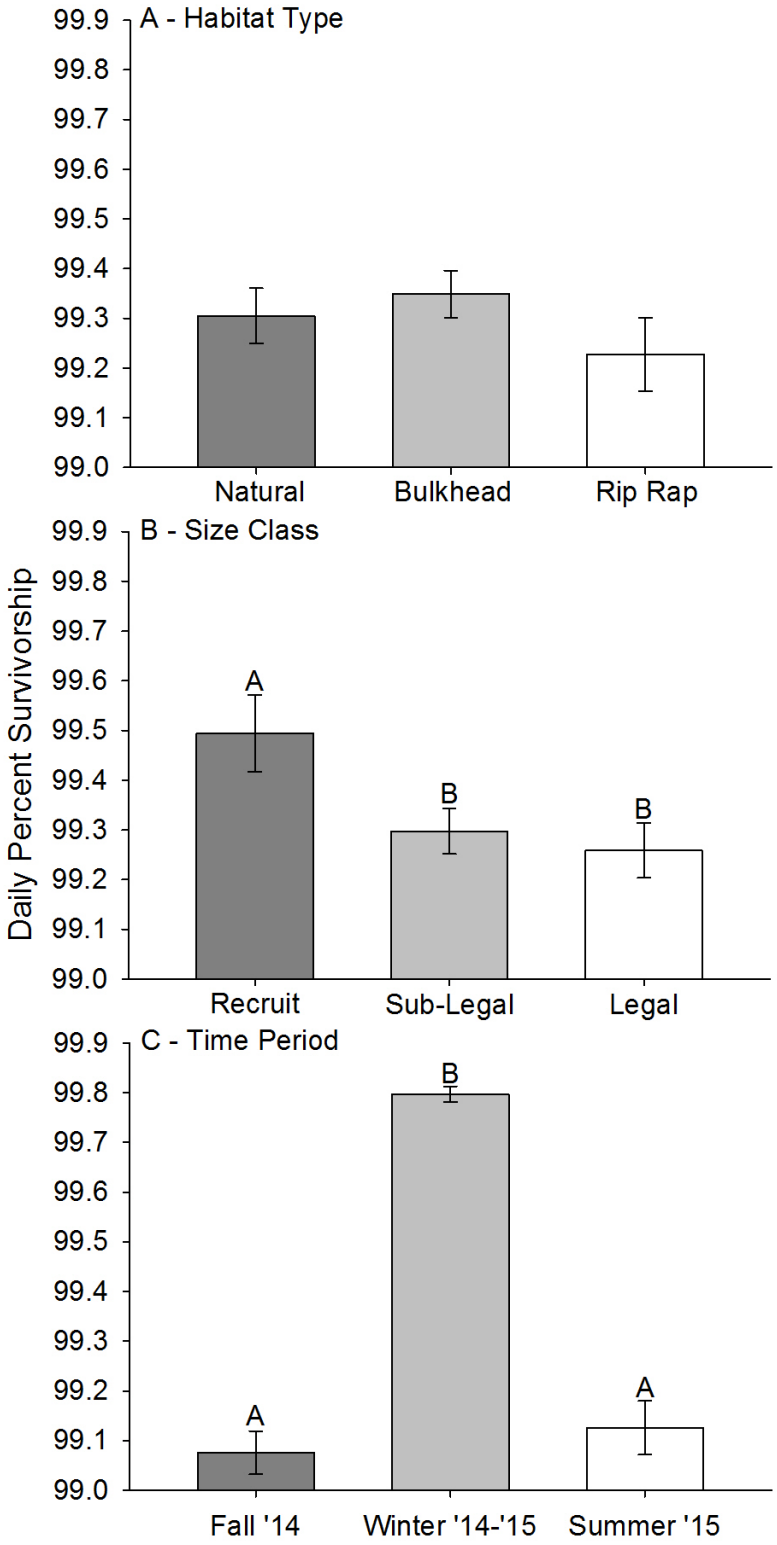


Figure 7. Mean daily percent survivorship for oysters compared among: a) habitat type, b) size class, and c) time period. Error bars designate standard error. Letters indicate significant differences between levels of a factor as determined with a Tukey-Kramer multiple comparison test.

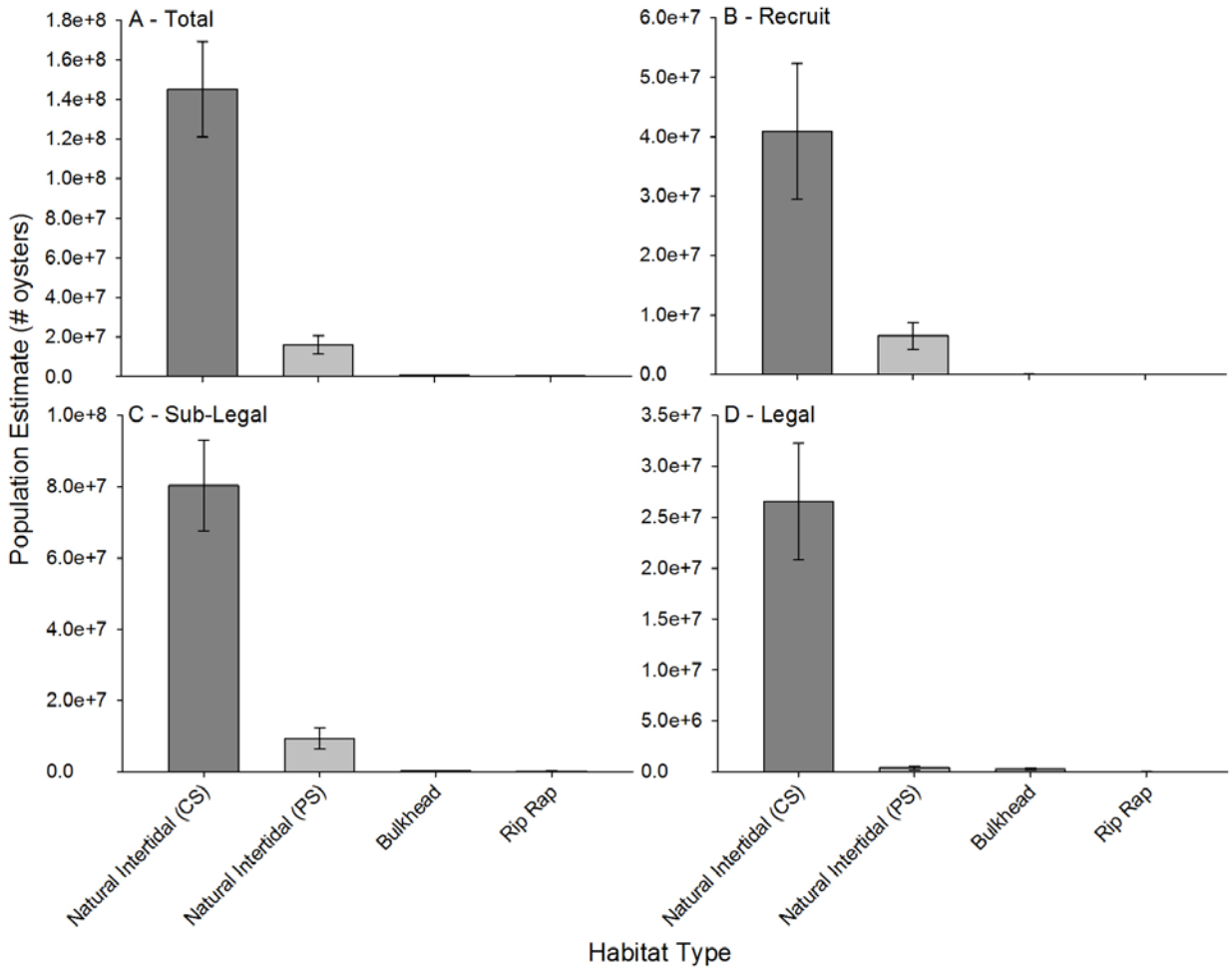


Figure 8. Population estimates (number of oysters) on different habitat types within Core and Pamlico Sounds for a) total (all size classes), b) recruit (LVL < 30 mm), c) sub-legal (30mm ≤ LVL<75mm), and d) legal (LVL ≥75mm) size classes. Estimates calculated by scaling habitat type-specific density estimates to overall reef area footprints. Error bars designate standard error.

# CHAPTER 3

# INTEGRATING ECOSYSTEM SERVICES WITHIN A GIS-BASED HABITAT SUITABILITY INDEX FOR OYSTER RESTORATION


## ABSTRACT

Geospatial habitat suitability index (HSI) models have emerged as powerful tools that integrate pertinent spatial information to guide habitat restoration efforts, but have rarely accounted for spatial variation in ecosystem service provision. In this study, I utilized satellite-derived chlorophyll *a* concentrations for Pamlico Sound, North Carolina, USA in conjunction with data on water flow velocities and dissolved oxygen concentrations to identify potential restoration locations that would maximize the oyster reef-associated ecosystem service of water filtration. I integrated these novel oyster water filtration ecosystem services variables within a broader, existing GIS-based HSI model to identify suitable locations for oyster restoration that maximize: (i) biophysical (e.g., salinity, oyster larval connectivity), (ii) socioeconomic (e.g., distance to nearest restoration material stockpile site), and (iii) ecosystem services (i.e., water filtration) variables essential to long-term persistence of restored populations and maximization of water filtration ecosystem service provision. Furthermore, I compared the 'Water Filtration' optimized HSI with an HSI optimized for 'Reef Persistence,' as well as a hybrid model that optimized for both water filtration and reef persistence. I identified optimal restoration locations (i.e., locations corresponding to the top 1% of suitability scores) that were consistent among the three HSI scenarios (i.e., "win-win" locations), as well as optimal locations unique to a given HSI scenario (i.e., "tradeoff" locations). The modeling framework utilized in this study can provide guidance to restoration practitioners to maximize the cost-efficiency and ecosystem services value of habitat restoration efforts. Furthermore, the functional relationships between oyster water

filtration and chlorophyll *a* concentrations, water flow velocities, and dissolved oxygen developed in this study can guide field- and lab-testing of hypotheses related to optimal conditions for oyster reef restoration to maximize water quality enhancement benefits.

## INTRODUCTION

Recovery of ecosystem services is often cited as a principal motivation for habitat restoration activities (Benayas et al. 2009). Yet, the quantity and quality of ecosystem services provided by restored habitats can vary in space and time and are often mediated by restored habitat quality (Koch et al. 2009, Palmer and Filoso 2009, Bullock et al. 2011). Geospatial habitat suitability indices (hereafter 'HSI') have emerged as powerful, spatially explicit decision support tools to guide habitat restoration to areas of highest probable habitat quality (Roloff and Kernohan 1999). HSIs are commonly generated through application of wildlife-habitat relationships to relevant geospatial environmental data within a Geographic Information System (GIS) to develop a composite HSI score with a range of 0 to 1, representing unsuitable (0) to optimal (1) habitat (Brooks 1997). Previous efforts have sought to map and quantify spatial variation in ecosystem services provided by existing habitats (e.g., Crossman et al. 2013), however, relatively few efforts have attempted to assess where habitat restoration might provide enhanced levels of ecosystem service provision relative to other locations. Given the need and desire to maximize provision of ecosystem services associated with habitat restoration efforts, as well as the significant associated costs (e.g., US$10,000 per ha per cm of substrate material for oyster habitat restoration in Chesapeake Bay; Theuerkauf et al. 2015), there is a need for a geospatial modeling framework to inform where habitat restoration efforts might be most successful and yield the greatest ecosystem services benefit.

Oyster reefs provide important ecosystem services within estuaries, including water filtration, sediment stabilization, and provision of essential fish habitat (Kennedy et al. 1996). Despite their recognized value, native oyster populations worldwide are at ~10-15% of their historic levels due to a combination of overfishing, habitat destruction, and disease (Beck et al. 2011). The global loss of native oyster reefs has prompted the establishment of large-scale oyster restoration programs to restore oyster populations to recover these lost ecosystem services. Recent research into the water quality enhancement benefits associated with oyster reef restoration (e.g., removal of phytoplankton biomass from the water column and enhancement of denitrification rates; Grizzle et al. 2008, Kellogg et al. 2013), coupled with the rising cost of infrastructural means of reducing nutrient pollution (e.g., improvements to wastewater treatment facilities) has generated considerable interest in the role of strategic oyster restoration as a cost-effective means to improve water quality and meet nutrient reduction mandates (Kellogg et al. 2014). Restoration of oyster reefs to maximize potential water quality benefits requires, in part, a spatial understanding of where the ecosystem service of oyster filtration would be greatest.

Geospatial HSI models that integrate relevant environmental, biological, and socioeconomic factors are useful tools to identify optimal sites for habitat restoration within the broader landscape or seascape of interest (Roloff and Kernohan 1999). Multiple HSI models have been developed to guide aquaculture, fishery production, and restoration of oyster species (Cake 1983, Brown and Hartwick 1988, Cho et al. 2012, Theuerkauf and Lipcius 2016, Puckett et al., in review). These models have incorporated a range of abiotic and biotic factors of relevance to oyster restoration, such as salinity, bottom type, and water depth. The combinations of factors incorporated into these waterbody-specific HSIs have varied depending upon both data availability and relevance in determining habitat suitability for a given system. To date, none of

the published oyster restoration HSIs has directly incorporated variables pertinent to, and for purposes of, identification of suitable restoration locations that would maximize ecosystem service provision.

The present study extends an HSI originally developed by Puckett et al. (in review) to guide oyster habitat restoration activities in Pamlico Sound, North Carolina, USA by incorporating ecosystem services-related factors to identify oyster reef restoration locations that maximize provision of water filtration ecosystem services (Puckett et al., in review). The original HSI developed by Puckett et al. (in review) incorporates biophysical (e.g., salinity, oyster larval connectivity) and socioeconomic (e.g., distance to nearest restoration material stockpile site) factors essential to long-term restoration of persistent oyster populations (hereafter 'Reef Persistence HSI'). In the present study, I utilize satellite-derived chlorophyll *a* concentrations for Pamlico Sound in conjunction with data on water flow velocities, dissolved oxygen concentrations, and varying combinations of factors considered within the original 'Reef Persistence HSI' to generate two additional HSI scenarios: one focused primarily on identifying restoration locations that would maximize oyster water filtration ecosystem services (hereafter, 'Water Filtration HSI'), and another that balanced long-term oyster population persistence criteria with oyster water filtration ecosystem services considerations (hereafter, 'Water Filtration & Reef Persistence HSI'). I subsequently compared both suitability patterns and optimal locations (i.e., locations corresponding to the top 1% of HSI values) identified within and between all three HSI model scenarios to determine optimal restoration locations that were consistent among scenarios (i.e., "win-win" locations), as well as optimal locations unique to each scenario (i.e., "tradeoff" locations). I also evaluated the sensitivity of each HSI scenario to its respective parameterization to determine which variables are major drivers of suitability within a given HSI. The conceptual framework utilized in this study wherein restoration goal-specific HSIs (e.g., maximizing long-term population persistence, maximizing ecosystem service

provision) were developed and “win-win” versus “tradeoff” locations were identified can broadly inform development of similar restoration goal-specific HSI models in other systems. Moreover, the functional relationships between oyster water filtration and chlorophyll *a* concentrations, water flow velocities, and dissolved oxygen developed in this study can guide field- and lab-testing of hypotheses related to optimal conditions for oyster reef restoration to maximize water quality enhancement benefits.

## MATERIALS AND METHODS

### *Study System*

The Albemarle-Pamlico Estuarine System (APES) in North Carolina, USA is the largest lagoonal estuary in the United States (~6,600 $km^2$), and is bounded by a barrier island chain that limits exchange with the coastal ocean to five relatively small inlets (~1 km wide; Figure 1; Epperly and Ross 1986, Pietrafesa et al. 1986). Pamlico Sound, the largest component of the APES (~120 x 40 km), is relatively shallow with a mean depth of ~4.5 m and a maximum depth of 7.5 m (Epperly and Ross 1986). The shallow nature of this wind-driven estuary coupled with limited oceanic exchange yields a relatively long water residence time and negligible vertical stratification of the water column (i.e., high degree of vertical mixing of the water column; Roelofs and Bumpus 1953). Previous research has indicated that phytoplankton community structure and biomass is consistent vertically throughout the water column in the well-mixed portion of North Carolina estuaries (Burkholder et al. 2003), congruent with patterns identified in previous studies of well-mixed estuaries, such as San Francisco Bay, California, USA and Bay of Brest, France (Conomos 1979, Cloern and Oremland 1982).

Subtidal oyster reefs, a once prevalent benthic habitat in Pamlico Sound, are believed to occupy ~1-10% of their historical footprint (Beck et al. 2011, Puckett et al., in review). Multiple

subtidal oyster habitat restoration methods are ongoing, including: (1) cultch planting, the deployment of a thin veneer of oyster shell or other settlement substrate to replace shell removed through commercial harvest, and (2) no-harvest sanctuaries, the designation of areas protected from harvest within which large, high-relief artificial reefs are constructed to provide settlement substrate (Pucket and Eggleston 2012, Peters et al. 2017). The present study provides spatial guidance to inform both forms of subtidal oyster reef restoration.

***Original HSI Model Characteristics***

This study extends a previous GIS-based habitat suitability index (HSI) developed for restoration of eastern oysters (*Crassostrea virginica*) in Pamlico Sound, North Carolina, USA (Puckett et al., in review). The original model was developed by: 1) convening stakeholder meetings to identify model input parameters and their relative importance to oyster restoration, 2) using a GIS-based modeling approach to integrate 17 physical, biological, and socioeconomic parameters to identify optimal locations for habitat restoration that maximize persistence of oyster populations on restored reefs (i.e., 'Reef Persistence HSI'; Appendix 1), and 3) conducting sensitivity analysis and model validation analyses to assess model performance.

Using ArcMap 10.3 (ESRI 2016), a grid was developed consisting of 5,987 1 km x 1 km (1 $km^2$) grid cells covering the waters of Pamlico Sound (Puckett et al., in review). Using expert stakeholder input (i.e., academics, non-governmental organizations, and state resource managers engaged in oyster restoration), 17 GIS layers were projected onto the grid of Pamlico Sound such that each cell contained a "value" for each layer. Layers were partitioned into two categories: (1) "threshold" layers—those assigned values based on thresholds and weights relevant to suitability (Appendix 2), and (2) "exclusion" layers—binary, 0 or 1 layers used to exclude unsuitable sites (Appendix 3). Threshold values and weights, as well as exclusion layer values were determined

through literature reviews, stakeholder input, and regulatory statutes (Table 2, Appendix 1). A complete list of all threshold and exclusion layers, and their associated details can be found in Appendix 1.

Using the GIS-raster calculator, the suitability of each cell ($S_j$) for siting restored oyster reefs within the 'Reef Persistence' HSI was calculated in a two-step process as:

$$C_j = \sum_{x=1}^{10} (L_{xj} \cdot W_x)$$

$$S_j = C_j \cdot E_j,$$

where $C_j$ is the cumulative value of cell $j$ calculated as the product of the threshold value $L$ of cell $j$ in threshold layer $x$ and the weight $W$ of layer $x$ summed across all 10 threshold layers, and $E_j$ is the binary (0 or 1) score for cell $j$ based on the product of all 7 binary exclusion layers. On a scale of 0 to 1, cell suitability scores for restored oyster reefs were ranked from lowest (least suitable) to highest (most suitable). Output from the original 'Reef Persistence HSI' is provided in Figures 2C, 2G. The present study extends this original modeling effort by integrating novel spatial layers related to water quality enhancement ecosystem services within a 'Water Filtration HSI', and a hybrid HSI optimized for 'Water Filtration & Reef Persistence.'

***Water Filtration Ecosystem Services Layer Development***

To develop a 'Water Filtration HSI', I focused on relevant input parameters for which: 1) spatially-explicit datasets were available for our study system, and 2) functional relationships between these abiotic and biotic parameters and suitability for oyster filtration could be inferred from the literature. Based on these criteria, I included: chlorophyll *a* concentrations, water flow velocities, and dissolved oxygen (DO) concentrations. I subsequently applied suitability functions based on literature-inferred relationships to available spatial datasets and integrated

these layers along with other layers relevant to each HSI scenario (i.e., 'Water Filtration,' 'Water Filtration & Reef Persistence,' and 'Reef Persistence'; see '*Methods, HSI Integration'* below).

Chlorophyll *a* concentrations serve as a surrogate variable for phytoplankton biomass (i.e., food availability). Recent oyster reef growth modeling efforts have described the importance of selecting restoration locations with greatest food availability in determining long-term reef survival (Housego and Rosman 2016). Water flow velocity is an important factor regulating food delivery and oyster filtration. Increasing water flow velocities across reefs to 15 cm $s^{-1}$ increases the rate of food delivery (Dame et al. 1989, Wilson-Ormond et al. 1997), however exceedance of 15 cm $s^{-1}$ can result in sediment resuspension or cessation of oyster filtration, yielding no net reduction in seston concentrations (Lenihan et al. 1996, Grizzle et al. 2008). Areas of high chlorophyll *a* concentrations have been associated with areas of low benthic DO concentrations (i.e., hypoxic or anoxic "dead zones") that can be lethal to oysters; therefore, DO concentrations are a critical additional consideration (Cerco 1995). A more detailed review of the literature surrounding the functional relationships applied to the spatial datasets in this study is provided in the "Discussion."

Chlorophyll *a* concentration (μg chl *a* $l^{-1}$) information was derived from monthly-averaged satellite images (i.e., average of all satellite passes within a given month for the period of January 2003 through December 2011) captured by the European Space Agency's Environmental Satellite 1 (EnviSat-1) Medium Resolution Imaging Spectrometer (MERIS). All chlorophyll *a* data products were provided in a pre-processed form by the United States Environmental Protection Agency (Blake Schaeffer, personal communication). Keith (2014) performed validation of MERIS-derived chlorophyll *a* concentrations for Pamlico Sound and tributaries using *in situ*-measured chlorophyll *a* concentrations, and identified a statistically-

significant ~1:1 relationship between the two data sources. MERIS imagery is highly suitable for estimation of chlorophyll *a* concentrations given its high spatial resolution (300 m) and narrow spectral bands with a high signal to noise ratio (Sokoletsky et al. 2011). To determine which month across the nine-year data series represented the average chlorophyll *a* maximum when phytoplankton biomass within Pamlico Sound overall is maximized, I averaged chlorophyll *a* concentrations across all pixels within a map for a given sampling period to obtain a single value for a monthly mean chlorophyll *a* concentration and subsequently averaged across years within a given month (e.g., averaged across January 2003 through 2011). From this analysis, September, which corresponds with the fall phytoplankton bloom in Pamlico Sound, was determined to be the month of maximum average chlorophyll *a* concentration for the period of 2003 through 2011 (Table 1).

I calculated the: 1) mean and 2) coefficient of variation for chlorophyll *a* for each cell within the model grid using data from September of 2003 through 2011. The coefficient of variation ($c_v = \sigma \mu^{-1}$) was utilized as it provides a standardized statistic to compare the degree of variation amongst data points irrespective of mean values. I evaluated the form of the relationship between mean chlorophyll *a* concentration and the coefficient of variation using the local polynomial regression fitting (loess) function in R (R Core Team 2017). Based on the relationships from the loess fits, mean chlorophyll *a* concentration and the variance to mean ratio appeared to be uncorrelated, which was further confirmed by simple linear regression (Figure 3A, $R^2 = 0.008$). Thus, I developed separate spatial layers to represent: 1) mean chlorophyll a concentration and 2) coefficient of variation of chlorophyll a. I considered areas of high mean chlorophyll *a* concentration to be most suitable for reef restoration (i.e., greatest food availability) and areas of low mean chlorophyll *a* concentration to be least suitable (Figure 4A).

Furthermore, I considered areas of low coefficient of variation to be most suitable (i.e., most stable food availability) and high coefficient of variation to be least suitable (Figure 4B).

Water flow velocity (cm $s^{-1}$) data was derived from the Advanced Three-Dimensional Circulation Model (ADCIRC), a nonlinear, finite-element hydrodynamic model developed by Luettich et al. (1992) and validated in Pamlico Sound and adjacent estuarine and coastal waters of North Carolina by (Luettich et al. 2002, Reyns et al. 2006, Haase et al. 2012). ADCIRC solves the shallow water form of the momentum equations over the entire APES domain represented by an unstructured grid developed by Reyns et al. (2006) consisting of 22,425 nodes and 41,330 elements (resolution = 0.3–1 km). ADCIRC is forced with hourly wind velocities. To determine times of 'average,' 'strongest,' and 'weakest' winds corresponding with the range of wind conditions possible within the APES, I conducted residual sums of squares (RSS) analysis (sensu Puckett et al. 2014) on wind speed and direction recorded at the Cape Hatteras Meteorological Station for September of 2012-2016 (i.e., 5 most recent years of available data provided by the Climate Office of North Carolina). During this period, 'average,' 'strongest,' and 'weakest' winds corresponded with September of 2014, 2015, and 2012, respectively. The model was subsequently forced with hourly wind velocities for these three monthly time periods. Bottom current velocities were output at hourly intervals for each of the 22,425 nodes. For each node, I subsequently calculated a: 1) mean water velocity, and 2) percent frequency of water velocities exceeding 15 cm $s^{-1}$ (hereafter 'exceedance frequency'). I evaluated the form of the relationship between mean water velocity and exceedance frequency using the loess function in R (R Core Team 2017). The relationship from the loess fit was nonlinear and sigmoid, which was confirmed after fitting a statistically significant four-parameter logistic function to the data within a global curve-fitting program (Figure 3B; Sigmaplot 2007). As mean water velocity and

exceedance frequency were significantly correlated, I developed a single spatial layer to represent water flow velocity suitability. Based on the identified inflection point of the sigmoid relationship between mean water velocity and exceedance frequency (i.e., 10.17 cm $s^{-1}$), I generated and applied a left-skewed Weibull function to describe the relationship between mean water velocity and suitability for oyster water filtration. The form of this function yields increasing suitability to mean water velocities up to 10.17 cm $s^{-1}$, and decreasing suitability beyond. At the inflection point of 10.17 cm $s^{-1}$ at which suitability was decreased, exceedance frequency was 20–50% of the time (Figure 4C).

DO concentration (mg $l^{-1}$) was derived from benthic DO concentration point measurements taken within the study area during the fall portion (i.e., corresponding with timing of peak hypoxia) of the North Carolina Division of Marine Fisheries Program 195 fishery-independent trawl survey program (North Carolina Division of Marine Fisheries, personal communication). Data were collected at 522 unique stations between September of 1996 through 2014 (~52 randomly chosen stations sampled per year during September). As not all stations were revisited at the same interval, I considered the minimum observed DO concentration for each station in subsequent analyses. I utilized ordinary kriging within ArcMap (ESRI 2016) to generate an interpolated minimum DO concentration layer for the study area (i.e., a conservative estimate of DO). I considered areas of highest observed DO concentrations to be most suitable, and areas of lowest observed DO concentration to be least suitable (Figure 4D).

### *HSI Integration*

Similar to the development of the 'Reef Persistence HSI' (Puckett et al., in review), I utilized expert stakeholder input (e.g., local academics [University of North Carolina at Chapel

Hill Institute of Marine Sciences, North Carolina State University], non-governmental organizations [The Nature Conservancy], and state resource managers [North Carolina Division of Marine Fisheries]) to assign percentage weights to each of the individual layers considered within an updated HSI that simultaneously maximizes for both water filtration ecosystem services and reef persistence (i.e., 'Water Filtration & Reef Persistence HSI;' Table 2). Layer weights reflected expert stakeholders perceived relative importance of each layer for water filtration and reef persistence (higher weight = more important). I generated weights for the 'Water Filtration HSI' by proportionally rescaling the assigned weights for the four oyster water filtration ecosystem service-associated layers (i.e., chlorophyll *a* mean, chlorophyll *a* variation, flow mean and variation, and dissolved oxygen) such that they summed to ~70% of the overall model for direct comparison with the 'Reef Persistence' optimized HSI (Table 2), wherein four layers (salinity, larval export, larval import and dissolved oxygen; Table 2) accounted for 70% of that overall model. Other secondary considerations within the 'Water Filtration HSI' focused primarily on increasing oyster densities within a given reef location (i.e., larval export), minimizing potential predation and disease stressors (i.e., salinity), and certain socioeconomic considerations (e.g., proximity to reef-building material stockpile sites).

***Model Sensitivity***

To determine and compare the sensitivity of the three HSI models to individual layers, I: 1) sequentially removed the four threshold layers with the highest weight, 2) re-weighted the remaining layers proportionally based on the weight of the removed layer, 3) re-ran the models, and 4) calculated the percent change in suitability of each cell ($S_j$) with removal of each layer.

To determine the sensitivity of the three HSI models to our weightings, I ran the model with equal weightings for each of the threshold layers considered within each respective model

(i.e., null model). As above, I similarly removed the four threshold layers with the highest weight from each null model and compared the impact of layer removal between final HSIs and the respective null models.

## RESULTS

### *Water Filtration Ecosystem Service Layers*

Chlorophyll *a* concentration – Chlorophyll *a* concentrations varied widely spatially across Pamlico Sound and temporally across September 2003-2011 (i.e., Appendix 4 depicts the wide range in September chlorophyll *a* concentrations across years). Mean September chlorophyll *a* concentrations across the nine-year time series and across the 5,987 grid cells contained within the model domain ranged from 9.12–98.98 μg chl *a* $l^{-1}$, whereas coefficient of variation of September chlorophyll *a* concentrations ranged from 0.01–1.67. Mean chlorophyll *a* concentrations were generally highest and most variable near-shore within the bays, tributaries, and rivers flowing into Pamlico Sound (Figure 5A, 5B). Chlorophyll *a* concentrations were generally lowest and least variable within the central portion of Pamlico Sound (Figure 5A, 5B).

Water flow velocity – Mean bottom current flow velocities were generally greatest in the shallow near-shore environment of Pamlico Sound, however near-shore locations generally exceeded 15 cm $s^{-1}$ frequently. Deeper portions of the major bays, tributaries, and rivers flowing into Pamlico Sound, along with the central portion of the sound, generally had lower mean bottom current flow velocities. Suitability of mean water flow velocity was generally greater in shallow near-shore locations and lower in deeper waters (Figure 5C). Mean September bottom current flow velocities across the three-year time series and across the 22,425 nodes contained

within the model domain ranged from 0.58–18.26 cm $s^{-1}$. Mean September exceedance frequency (i.e., percent frequency flow velocity exceeds 15 cm $s^{-1}$) ranged from 0–52%.

DO concentration – Minimum observed benthic DO concentrations ranged from 2–8 mg $l^{-1}$ and were generally lowest within the major rivers flowing into Pamlico Sound and near their confluence in southwestern Pamlico Sound (Figure 5D). DO concentrations were generally highest and most suitable within the central portion of Pamlico Sound.

***Model Simulations***

Water Filtration HSI – Suitability patterns of the 'Water Filtration HSI' (Figure 2) were driven largely by mean chlorophyll *a* concentration, DO concentration, water flow velocity, and coefficient of variation of chlorophyll *a* concentration—these four layers had a combined weighting of 73% (Table 2). Highly suitable restoration locations were primarily nearshore and located in the northwestern and western portions of Pamlico Sound, with some additional highly suitable areas in the southern and southwestern portions of the sound.

Water Filtration & Reef Persistence HSI – Suitability patterns of the 'Reef Persistence and Water Filtration HSI' (Figure 2) were driven largely by mean chlorophyll *a* concentration, salinity, dissolved oxygen concentration, and larval export from oyster sanctuaries (i.e., settlement location of oyster larvae spawned from existing oyster sanctuaries). These four layers had a combined weighting of 55% (Table 2). Highly suitable restoration locations based on this HSI scenario balancing both reef persistence- and water filtration-related criteria were located similarly to the 'Reef Persistence HSI' in the southwestern and northwestern portions of Pamlico Sound (Figure 2). These suitable locations were generally more near-shore and included a greater portion of western Pamlico Sound than in the 'Reef Persistence HSI'.

Reef Persistence HSI – Suitability patterns of the original 'Reef Persistence HSI' (Figure 2; Puckett et al., in review) were driven largely by salinity, sanctuary larval export, sanctuary larval import (i.e., natal location of oyster larvae settling within existing oyster sanctuaries), and dissolved oxygen—these four layers had a combined weighting of 69% (Table 2). Highly suitable restoration locations based on the reef persistence-related criteria considered within this model were located in the southwestern (mouth of Neuse and Pamlico Rivers and bays) and northwestern portions of Pamlico Sound (Figure 2). A detailed description of model output, suitability drivers, sensitivity analysis, and model validation results for this model is provided in Puckett et al. (in review).

*Optimal Restoration Locations*

Suitability scores associated with optimal restoration locations (defined as the top 1% of suitability scores) identified within the three HSI scenarios ranged from: 0.63–0.55 in the 'Water Filtration HSI,' 0.61–0.52 in the 'Water Filtration & Reef Persistence HSI,' and 0.69–0.52 in the 'Reef Persistence HSI.' Optimal locations within the 'Water Filtration HSI' were primarily located nearshore in the northwestern and western portions of Pamlico Sound, with two additional optimal locations near Ocracoke Inlet (Figure 6). Within the 'Reef Persistence HSI,' optimal locations were primarily located within southwestern Pamlico Sound near the mouths of the Neuse and Pamlico Rivers. Optimal locations within the 'Water Filtration & Reef Persistence HSI' overlapped entirely with optimal locations identified within the two other HSI scenarios (i.e., contained within the 'Top 1% for 2 & 3 Models' categories in Figure 6). Optimal locations identified within two or three HSI scenarios (i.e., 'win-win' restoration locations) were located primarily within northwestern and western Pamlico Sound (Figure 6).

*Model Sensitivity*

The 'Water Filtration HSI' was generally most sensitive to layers in order of their weightings, except for the coefficient of variation of chlorophyll *a* layer (9.66%), which the model was more sensitive to removal of than the water flow velocity layer (9.32%; Figure 7A). The percent change in HSI averaged among all grid cells was 21.10% +/- 0.11% SE with the removal of the mean chlorophyll *a* layer (weighted at 28%) and 14.73% +/- 0.12% SE with removal of the dissolved oxygen layer (weighted at 19%). The null model, with equal layer weightings, was most sensitive to removal of the chlorophyll *a* variation layer, followed by dissolved oxygen, water flow velocity, and chlorophyll *a* mean.

In general, the 'Water Filtration & Reef Persistence HSI' was equally sensitive to each of the top four highest weighted layers (Figure 7B), with a marginally greater sensitivity to the removal of the salinity layer. The percent change in HSI with the removal of the mean chlorophyll *a* layer (weighted at 17%) and averaged among all grid cells was 11.73 +/- 0.07 SE%, and 13.45 +/- 0.10 SE% with removal of the salinity layer (weighted at 15%). The null model with equal layer weightings was most sensitive to removal of the salinity layer, followed by dissolved oxygen, sanctuary larval export, and chlorophyll *a* mean.

The 'Reef Persistence HSI' was most sensitive to layers in order of their weightings, except for the dissolved oxygen layer, which the model was more sensitive to removal than the sanctuary larval import layer (Figure 7C). The percent change in the HSI after the removal of the salinity layer (weighted at 23%) and averaged among all grid cells was 32.9 +/- 0.2 SE%, and 22.4 +/- 0.2 SE% with removal of the oyster larval export layer (weighted at 20%). The null model with equal layer weightings was most sensitive to removal of the dissolved oxygen layer

(i.e., layer with the greatest degree of spatial variability), followed by salinity, sanctuary larval import, and sanctuary larval export.

## DISCUSSION

Habitat suitability indices (HSI) are valuable quantitative tools to guide spatial planning of habitat restoration efforts in locations with the greatest potential for success (Brooks 1997, Roloff and Kernohan 1999, Theuerkauf et al. 2016). However, these models have generally not incorporated factors of direct relevance to siting restoration in locations that would maximize ecosystem service provision. Furthermore, given the financial costs and varying goals attributed to specific habitat restoration projects (e.g., restoring oyster reefs to support oyster fishery harvest, provide shoreline stabilization benefits, or to provide essential fish habitat / recreational fishing opportunities), multiple HSI models optimized for multiple restoration goals within a given waterbody are warranted to identify locations that are 'win-win' and locations where 'tradeoffs' must be considered. In this study, novel oyster water filtration ecosystem services layers were integrated with an existing GIS-based HSI model to identify suitable locations for oyster restoration that maximize: (i) ecosystem services (i.e., water filtration) factors, (ii) biophysical (e.g., salinity, oyster larval connectivity), and (iii) socioeconomic (e.g., distance to nearest restoration material stockpile site) variables. I compared both suitability patterns and optimal locations (i.e., locations corresponding to the top 1% of suitability score) identified within and between three HSI scenarios optimized for varying restoration goals, including a 'Water Filtration HSI', a 'Reef Persistence HSI', and a hybrid model that optimized for 'Water Filtration & Reef Persistence.' The conceptual framework utilized in this study, wherein restoration goal-specific HSIs were developed and "win-win" (i.e., optimal restoration locations

identified in multiple goal-specific HSIs) versus "tradeoff" (i.e., optimal restoration locations identified in a single goal specific HSI) restoration locations were identified, can inform development of similar restoration goal-specific HSI models in other systems.

Chlorophyll *a* concentrations, water flow velocities, and dissolved oxygen concentrations were selected to generate oyster water filtration ecosystem services layers as: 1) spatially-explicit datasets were available for our study system, and 2) functional relationships between suitability for oyster filtration and these abiotic and biotic parameters could be inferred from the literature. Chlorophyll *a* serves as a reliable surrogate for phytoplankton biomass (Falkowski and Kiefer 1985), and previous field and modeling research identified a significant, positive relationship between chlorophyll *a* concentrations and oyster growth rates (Battista 1999, Housego and Rosman 2016). Laboratory experiments that examined bivalve feeding under varying food particle concentrations identified both minimum and maximum particle concentrations that function as an "on-off switch" for filtration (Bernard 1983). Below a minimum particle concentration threshold (e.g., 25 mg $l^{-1}$ for *Crassostrea gigas*), active filtration is energetically unfavorable as caloric expenditure exceeds caloric uptake (Bernard 1983). Above a critical particle concentration threshold (e.g., 500 mg $l^{-1}$ for *Crassostrea gigas*), filtration is also energetically unfavorable as excess energy is expended to clear clogged mucus from the gills. It is probable that, under field environmental conditions wherein particle concentrations fluctuate continuously as a function of flow velocity and direction, bivalves mediate between periods of active filtration and inactivity dependent upon ambient particle concentrations. Field-based studies are needed to examine if this "on-off switch" occurs within individual oysters on reefs under hypothesized field conditions and, if so, its impact on oyster filtration rates and capacity in areas along a gradient of mean phytoplankton biomass (i.e., areas of low to high mean

chlorophyll *a* concentrations). Resultant information from these field-based studies could be used to update the functional relationships between oyster water filtration and chlorophyll *a* concentrations (Figure 4A, 4B) used in this study or other future HSI models.

Water flow velocities, combined with seston composition and concentration, have been previously identified as a significant driver of overall oyster filtration capacity (Wildish and Kristmanson 1997, Harsh and Luckenbach 1999). Increasing water flow velocities yields enhanced food delivery to individual oysters on reefs (Grizzle et al. 2008), yet water flow velocities above 15 cm $s^{-1}$ can inhibit individual feeding and growth (Wildlish and Kristmanson 1997, Grizzle et al. 2001). The exact causal mechanisms underlying this threshold remain unknown and should be the subject of future research, however, it is probable that high flow velocities (i.e., > 15 cm $s^{-1}$) can result in turbulent resuspension of reef sediments that may trigger cessation of filtration (i.e., exceedance of the maximum particle concentrations above which filtration is energetically favorable; Bernard 1983, Grizzle et al. 2008).

Hypoxic or anoxic conditions are increasingly common within urbanized estuaries because of eutrophication (Diaz and Rosenburg 2008). Low dissolved oxygen conditions within bottom waters can yield lethal impacts to benthic organisms, such as oysters (Lenihan and Peterson 1998). Thus, incorporation of spatial information on dissolved oxygen concentrations is an essential consideration when developing spatial guidance tools for restoration of benthic organisms that incorporate indicator variables of phytoplankton biomass (e.g., chlorophyll *a* concentrations). Water temperature, turbidity, freshet frequency, and salinity variation are additional environmental parameters that have been included in previous HSI models (Soniat and Brody 1988, Battista 1999, Barnes et al. 2007, Swannack et al. 2014). These factors are relevant for consideration in future 'Water Filtration' optimized HSI models, but data of sufficient spatial

and temporal resolution were unavailable for the present study. For example, oyster filtration rates are constant between 16–28 °C, but increase rapidly above 28 °C (Korringa 1952).

Overall suitability patterns varied spatially between the three HSI scenarios. Within the 'Water Filtration HSI' (Figure 2A, 2E), highly suitable restoration locations were concentrated primarily nearshore within the northwestern and western portions of Pamlico Sound, driven largely by the highly suitable chlorophyll *a*, water flow velocities, and dissolved oxygen conditions that co-occur in those areas. Within the 'Reef Persistence HSI' (Figure 2C, 2G), highly suitable restoration locations were located in the southwestern (mouth of Neuse and Pamlico Rivers and bays) and northwestern portions of Pamlico Sound, driven largely by the highly suitable salinity and larval connectivity with oyster sanctuaries in those areas. The 'Water Filtration & Reef Persistence' HSI (Figure 2B, 2F), given its incorporation of factors from both the 'Water Filtration' and the 'Reef Persistence' HSI models, largely reflected an average of the suitability patterns observed in those two HSI scenarios (i.e., high suitability nearshore within the northwestern, western, and southwestern portions of Pamlico Sound).

Optimal restoration locations identified in each HSI generally reflected the suitability patterns of the respective HSI (Figure 6). "Tradeoff" locations, or locations identified as optimal within a single HSI scenario, included areas in northwestern and western Pamlico Sound for the 'Water Filtration' HSI and areas in southwestern Pamlico Sound for the 'Reef Persistence' HSI. "Win-win" restoration locations, or locations identified as optimal within multiple HSI scenarios, were primarily located within the northwestern and western portions of Pamlico Sound. The development of restoration goal-specific HSI models (e.g., maximizing long-term population persistence, maximizing ecosystem service provision) provides restoration practitioners with valuable spatial information to guide where habitat restoration efforts might be most successful

or yield the greatest ecosystem services benefit. By understanding where “win-win” or “tradeoff” optimal restoration locations occur based on these goal-specific HSI models, practitioners can prioritize or select locations that are most likely to meet the goals of a specific restoration project.

Model sensitivity analyses and quantitative model validation are important steps in the HSI model development process (Theuerkauf and Lipcius 2016, Puckett et al., in review). I quantitatively evaluated the sensitivity of each HSI model to individual layers and their assigned weightings (Table 2, Figure 7). The order of sensitivity of each full HSI model to layer removal generally followed the corresponding order of the assigned layer weights (i.e., a greater percent change in model output with removal of higher weighted layers), with a few notable exceptions. For example, in the ‘Water Filtration’ HSI (Figure 7A), a greater percent change in model output was observed with removal of the chlorophyll *a* variation layer relative to the higher weighted flow velocity layer. This enhanced sensitivity to layer removal is likely due to the more spatially dynamic nature of certain layers within these models (i.e., high degree of spatial heterogeneity with considerable small- and large-scale variability) relative to the other more highly weighted layers. The impact of the greater degree of spatial heterogeneity associated with certain layers was further emphasized in the sensitivity analysis of the null models (i.e., where all layers are weighted equally). For example, within the ‘Water Filtration’ HSI null model, removal of the highly spatially heterogeneous chlorophyll *a* variation layer (Figure 5B) resulted in the greatest percent change in model output with layer removal relative to other layers considered within the model. These results highlight the importance of acquiring spatial data layers for parameters that are spatially dynamic (e.g., dissolved oxygen, chlorophyll *a*) when developing similar HSI models for other systems.

Rigorous validation of the ecosystem services-optimized HSI models presented here would require construction of reefs along a gradient of suitability (e.g., constructing reefs in areas of high to low suitability within each HSI scenario) and assessment of response variables of interest (e.g., oyster density, growth and survival rates, chlorophyll *a* reduction). Thus, quantitative validation of the ecosystem services-optimized HSI models presented here is beyond the scope of this study (but see Puckett et al., in review for model validation results for the 'Reef Persistence' HSI). However, the functional relationships between oyster water filtration and chlorophyll *a* concentrations, water flow velocities, and dissolved oxygen developed in this study can guide field- and lab-testing of hypotheses related to optimal conditions for oyster reef restoration to maximize water quality enhancement benefits. For example, as described above, field-based studies are needed to examine if a threshold particle concentration "on-off switch" occurs within individual oysters on reefs and, if so, its impact on oyster filtration rates and capacity in areas along a gradient of mean phytoplankton biomass. Information from these proposed studies could be used to update the functional relationships between oyster water filtration and chlorophyll *a* concentrations, water flow velocities, and dissolved oxygen (Figure 4) developed and utilized in this study or other similar models in the future. Thorough literature reviews were an essential component in the development of the suitability functions used within this ecosystem services HSI. Future studies that incorporate ecosystem services considerations within HSI models should utilize relevant results from field- and lab-based studies to develop meaningful suitability functions that relate biophysical parameters with the capacity of a species or habitat to provide ecosystem services.

The conceptual framework utilized in this study, wherein HSIs developed to meet specific restoration goals (e.g., maximizing long-term population persistence, maximizing

ecosystem service provision) were developed and “win-win” versus “tradeoff” optimal restoration locations were identified, can broadly inform development of similar restoration goal-specific HSI models in other systems. Furthermore, the approach utilized in this study, and originally developed by Puckett et al. (in review), provides a useful case study wherein stakeholder input was directly used to shape model development and parameterization that, in-turn, enhanced stakeholder ‘buy-in” to the modeling approach and adoption of the model output for restoration planning.

**ACKNOWLEDGEMENTS**

I thank the North Carolina Division of Marine Fisheries, North Carolina State Climate Office, and United States Environmental Protection Agency for providing datasets used in the study. I also thank M. Piehler, B. Boutin, A. McCall, J. Peters, G. Wright, K. Theuerkauf for helpful comments. Funding for the project and completion of the manuscript was provided by a North Carolina Sea Grant and North Carolina Space Grant Fellowship, a National Defense Science and Engineering Graduate Fellowship (contract FA9550-11- C-0028 awarded by the Department of Defense, Air Force Office of Scientific Research, 32 CFR 168a), a North Carolina Coastal Conservation Association Scholarship, and a Beneath the Sea Foundation Scholarship to S. Theuerkauf, as well as North Carolina Sea Grant (R12-HCE-2) and the National Science Foundation (OCE-1155609) to D. Eggleston.

## LITERATURE CITED


Barnes, T. K., Volety, A. K., Chartier, K., Mazzoti, F. J., & Pearlstine, L. 2007. A habitat suitability index model for the eastern oyster (*Crassostrea virginica*), a tool for restoration of the Caloosahatchee Estuary, Florida. Journal of Shellfish Research 26:949–959.

Battista, T. A. 1999. Habitat suitability index model for the eastern oyster, *Crassostrea virginica*, in the Chesapeake Bay: A geographic information system approach. M.Sc. Thesis, University of Maryland.

Beck, M. W., Brumbaugh, R. B., Airoldi, L., Carranza, A., Coen, L. D., Crawford, C., et al. 2011. Oyster reefs at risk and recommendations for conservation, restoration, and management. *BioScience* 61:107–116.

Benayas, J. M. R., Newton, A. C., Diaz, A., & Bullock, J. M. 2009. Enhancement of biodiversity and ecosystem services by ecological restoration: a meta-analysis. *Science* 325:1121–1124.

Bernard, F. R. 1983. Physiology and the mariculture of some northeastern Pacific bivalve molluscs. Ottawa: Department of Fisheries and Oceans No. 63.

Brooks, R. P. 1997. Improving habitat suitability index models. *Wildlife Society Bulletin* 25:163–167.

Brown, J. R. & Hartwick, E. B. 1988. A habitat suitability index model for suspended tray culture of the Pacific oyster, *Crassostrea gigas* Thunberg. *Aquaculture Research* 19:109–126.

Bullock, J. M., Aronson, J., Newton, A. C., Pywell, R. F., & Benayas, J. M. R. 2011. Restoration of ecosystem services and biodiversity: conflicts and opportunities. *Trends in Ecology & Evolution* 26:541–549.

Burkholder, J., Eggleston, D., Glasgow, H., Brownie, C., Reed, R., Janowitz, G., et al. 2003. Comparative impacts of two major hurricane seasons on the Neuse River and western Pamlico Sound ecosystems. *Proceedings of the National Academy of Science* 101:9291–9296.

Cake, E. W. 1983. Habitat suitability index models: Gulf of Mexico American Oyster. U.S. Fish and Wildlife Service: No. 82/10.57.

Cerco, C. F. 1995. Response of Chesapeake Bay to nutrient load reductions. *Journal of Environmental Engineering* 121:549–557.

Cho, Y., Lee, W., Hong, S., Kim, H., Kim, J. B. 2012. GIS-based suitable site selection using habitat suitability index for oyster farms in Geoje-Hansan Bay, Korea. *Ocean & Coastal Management* 56:10–16.

Cloern, J. E. & Oremland, R. S. 1982. Does the benthos control phytoplankton biomass in South San Francisco Bay? *Marine Ecology Progress Series* 9:192–202.

Coen, L. D. & Luckenbach, M. W. 2000. Developing success criteria and goals for evaluating oyster reef restoration: ecological function or resource exploitation? *Ecological Engineering* 15:323–343.

Conomos, T. J. 1979. Properties and circulation of San Francisco Bay waters. In: San Francisco Bay – The Urbanized Estuary. San Francisco: American Association for the Advancement of Science – Pacific Division; pp. 47–84.

Crossman, N. D., Burkhard, B., Nedkov, S., Willeman, L., Petz, K., Palomo, I., et al. 2013. A blueprint for mapping and modeling ecosystem services. *Ecosystem Services* 4:4–14.

Dame, R. F., Spurrier, J. D., & Wolaver, T. G. 1989. Carbon, nitrogen and phosphorus processing by an oyster reef. *Marine Ecology Progress Series* 54:249–256.

Diaz, R. J. & Rosenburg, R. 2008. Spreading dead zones and consequences for marine ecosystems. *Science* 321:926–929.

Epperly, S. P. & Ross, S. W. 1986. Characterization of the North Carolina Pamlico-Albemarle complex. Washington: National Oceanic and Atmospheric Administration Technical Memorandum: NMFS-SEFC-175.

ESRI. ArcGIS Desktop: Release 10.3.2016. Redlands: Environmental Systems Research Institute.

Falkowski, P. & Kiefer DA. 1985. Chlorophyll *a* fluorescence in phytoplankton: relationship to photosynthesis and biomass. *Journal of Plankton Research* 7:715–731.

Grizzle, R. E., Bricelj, M. V. & Shumway, S. E. 2001. Physiological ecology of *Mercenaria mercenaria*. In: Kraetuer, J. N., Castagna, M., editors. Biology of the hard clam. Elsevier; pp. 305–382.

Grizzle, R. E., Greene, K. J., & Coen, L. D. 2008. Seston removal by natural and constructed intertidal eastern oyster (*Crassostrea virginica*) reefs: A comparison with previous laboratory studies, and the Value of in situ Methods. *Estuaries and Coasts* 31:1208–1220.

Haase, A. T., Eggleston, D. B., Luettich, R. A., Weaver, R. J., & Puckett, B. P. 2012. Estuarine circulation and predicted oyster larval dispersal among a network of reserves. *Estuarine, Coastal and Shelf Science* 101:33–43.

Harsh, D. A. & Luckenbach, M. W. 1999. Materials processing by oysters in patches: Interactive roles of current speed and seston composition. In: Luckenbach MW, Mann R, Wesson JA, editors. Oyster reef habitat restoration: a synopsis and synthesis of approaches. Gloucester Point: Virginia Institute of Marine Science Press; pp. 251–265.

Housego, R. M. & Rosman, J. H. 2016. A model for understanding the effects of sediment dynamics on oyster reef development. *Estuaries and Coasts* 39:495–509.

Keith, D. J. 2014. Satellite remote sensing of chlorophyll *a* in support of nutrient management in the Neuse and Tar-Pamlico River (North Carolina) estuaries. *Remote Sensing of Environment* 153:61–78.

Kellogg, M. L., Cornwell, J. C., Owens, M. S., & Paynter, K. T. 2013. Denitrification and nutrient assimilation on a restored oyster reef. *Marine Ecology Progress Series* 480:1–19.

Kellogg, M. L., Smyth, A. R., Luckenbach, M. W., Carmichael, R. H., Brown, B. L., Cornwell, J. C., et al. 2014. Use of oysters to mitigate eutrophication in coastal waters. *Estuarine, Coastal and Shelf Science* 151:156–168.

Kennedy, V. S., Newell, R. I. E., & Eble, A. F. 1996. The eastern oyster, *Crassostrea virginica*. 2nd ed. College Park: University of Maryland Sea Grant College Press.

Koch, E. W., Barbier, E. B., Silliman, B. R., Reed, D. J., Perill, G. M. E., Hacker, S. D., et al. 2009. Non-linearity in ecosystem services: temporal and spatial variability in coastal protection. *Frontiers in Ecology and the Environment* 7:29–37.

Korringa, P. 1952. Recent advances in oyster biology. *The Quarterly Review of Biology* 27: 266–308.

Lenihan, H. S., Peterson, C. H., & Allen, J. M. 1996. Does flow speed also have a direct effect on growth of active suspension feeders: An experimental test on oysters. *Limnology and Oceanography* 41:1359–1366.

Lenihan, H. S. & Peterson, C. H. 1998. How habitat degradation through fishery disturbance enhances impacts of hypoxia on oyster reefs. *Ecological Applications* 8:128–140.

Luettich, R. A., Westerink, J. J., & Scheffner, N. W. 1992. ADCIRC: An advanced three-dimensional circulation model for shelves, coasts, and estuaries. Vicksburg: Report 1: Theory and Methodology of ADCIRC-2DDI and ADCIRC-3DL. NO. CERC-TR-DRP-92-6.

Luettich, R. A., Carr, S. D., Reyonlds-Fleming, J. V., Fulcher, C. W., & McNinch, J. E. 2002. Semi-diurnal seiching in a shallow micro-tidal lagoonal estuary. *Continental Shelf Research* 22:1669–1681.

Palmer, M. A. & Filoso, S. 2009. Restoration of ecosystem services for environmental markets. *Science* 325:575–576.

Peters, J., Eggleston, D. B., Puckett, B. J., & Theuerkauf, S. J. 2017. Oyster demographics in harvested reefs versus no-take reserves: Implications for larval spillover and restoration. *Frontiers in Marine Science*: in press.

Pietrafesa, L. J., Janowitz, G. S., Chao, T. Y., Weisberg, R. H., Askari, F., & Noble, E. 1986. The physical oceanography of Pamlico Sound. Raleigh: UNC Sea Grant Publication: UNC-WP-86-5.

Puckett, B. J. & Eggleston, D. B. 2012. Oyster demographics in a network of no-take reserves: recruitment, growth, survival, and density dependence. *Marine and Coastal Fisheries* 4:605–627.

Puckett, B. J., Eggleston, D. B., Kerr, P. C., & Luettich, R. A. 2014. Larval dispersal and population connectivity among a network of marine reserves. *Fisheries Oceanography* 23:342–361.

Puckett, B. J., Theuerkauf, S. J., Eggleston, D. B., Guajardo, R., Kerr, P., Luettich, R., et al. A GIS-based, habitat suitability index to guide oyster restoration. *PLoS ONE* in review.

R Core Team. 2017. R foundation for statistical computing. Vienna.

Reyns, N. B., Eggleston, D. B., & Luettich, R. A. 2006. Secondary dispersal of early juvenile blue crabs within a wind-driven estuary. *Limnology and Oceanography* 51:1982–1995.

Roelofs, E. W. & Bumpus, D. F. 1953. The hydrography of Pamlico Sound. *Bulletin of Marine Science* 3:181–205.

Roloff, G. J. & Kernohan, B. J. 1999. Evaluating reliability of habitat suitability index models. *Wildlife Society Bulletin* 27:973–985.

Sigmaplot: Release 10. 2007. San Jose: Systat Software Inc.

Sokoletsky, L. G., Lunetta, R. S., Wetz, M. S., & Paerl, H. W. 2011. MERIS retrieval of water quality components in the turbid Albemarle-Pamlico Sound Estuary, USA. *Remote Sensing* 3:684–707.

Soniat, T. M. & Brody, M. S. 1988. Field validation of a habitat suitability index for the American oyster. *Estuaries and Coasts* 11:87–95.

Swannack, T. M., Reif, M., & Soniat, T. M. 2014. A robust, spatially explicit model for identifying oyster restoration sites: Case studies on the Atlantic and Gulf coasts. *Journal of Shellfish Research* 33:395–408.

Theuerkauf, S. J., Burke, R. P., & Lipcius, R. N. 2015. Settlement, growth, and survival of eastern oysters on alternative reef substrates. *Journal of Shellfish Research* 34:241–250.

Theuerkauf, S. J. & Lipcius, R. N. 2016. Quantitative validation of a habitat suitability index for oyster restoration. *Frontiers in Marine Science* 3:64.

Wildish, D. J. & Kristmanson, D. D. 1997. Benthic suspension feeders and flow. Cambridge: Cambridge University Press.

Wilson-Ormond, E. A., Powell, E. N., & Ray, S. M. 1997. Short-term and small-scale variation in food availability to natural oyster populations: Food, flow and flux. *Marine Ecology* 18:1–34.

## TABLES

Table 1. Mean (± standard error of the mean) monthly-averaged chlorophyll *a* concentration for Pamlico Sound across the nine-year MERIS satellite imagery data series (2003-2011) used to determine the timing of average peak phytoplankton biomass within the system. Chlorophyll *a* concentrations were averaged across all pixels for a given sampling period to obtain a single value for a monthly mean chlorophyll *a* concentration and subsequently averaged across years within a given month (e.g., averaged across January 2003 through 2011). September, which corresponds with the fall phytoplankton bloom in Pamlico Sound, was determined to be the month of maximum average chlorophyll *a* concentration for the period of 2003 through 2011.

| **Month** | **Mean Chlorophyll *a* Concentration ± SE (2003-2011; µg $l^{-1}$)** |
|---|---|
| January | 21.63 ± 4.91 |
| February | 18.06 ± 5.49 |
| March | 17.76 ± 4.44 |
| April | 17.73 ± 2.71 |
| May | 20.21 ± 2.87 |
| June | 22.24 ± 3.03 |
| July | 22.88 ± 4.27 |
| August | 22.08 ± 3.02 |
| September | 22.92 ± 4.98 |
| October | 19.47 ± 1.96 |
| November | 16.92 ± 2.09 |
| December | 17.86 ± 3.71 |

Table 2: Threshold layers and associated weights utilized to compute suitability in the three HSI scenarios. Weights were applied to each layer, and the assigned weight corresponds to the relative importance of each threshold layer to siting oyster restoration efforts in a given HSI scenario. The assigned weights of all threshold layers sum to 100%.

| Threshold Layers | Water Filtration HSI | Water Filtration & Reef Persistence HSI | Reef Persistence HSI |
|---|---|---|---|
| Salinity | 10% | 15% | 23% |
| Sanctuary Reef Larval Export | 8% | 11% | 20% |
| Sanctuary Reef Larval Import | - | 6% | 15% |
| Dissolved Oxygen | 19% | 12% | 11% |
| Cultch Reef Larval Import | - | 2% | 7% |
| Natural Reef Larval Import | - | 2% | 7% |
| Cultch Reef Larval Export | 3% | 5% | 5% |
| Natural Reef Larval Export | 3% | 5% | 5% |
| Material Stockpile Site Proximity | 1.5% | 4% | 4% |
| Boat Ramp Proximity | 1.5% | 4% | 3% |
| Chlorophyll a (Mean) | 28% | 17% | - |
| Chlorophyll a (Variation) | 10% | 7% | - |
| Flow (Mean + Variation) | 16% | 10% | - |

**FIGURES**

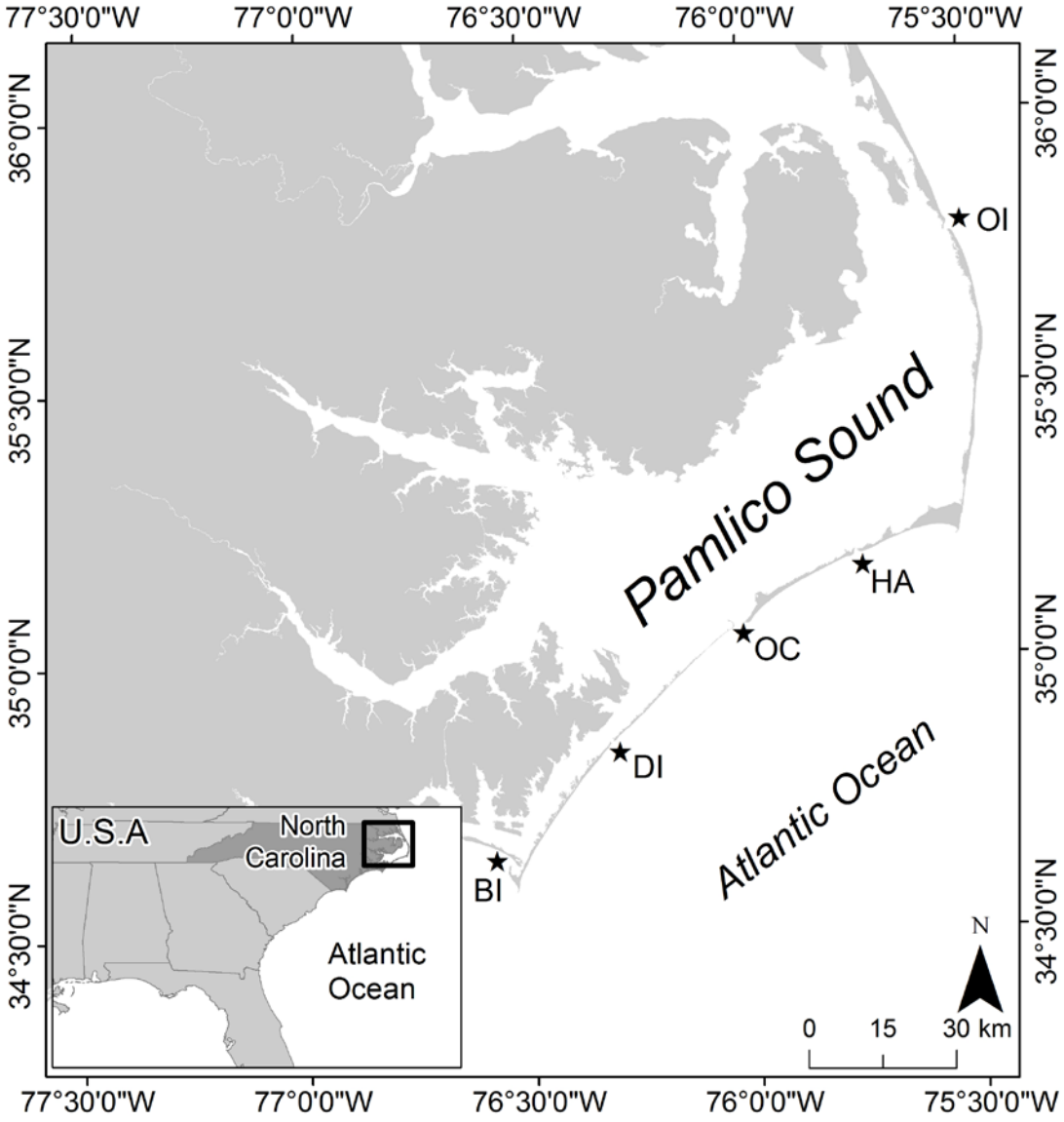


Figure 1. Map showing the location of the study area, Pamlico Sound, within the Albemarle-Pamlico Estuarine System (APES); stars denote oceanic inlets (OI = Oregon Inlet, HA = Hatteras Inlet, OC = Ocracoke Inlet, DI = Drum Inlet, BI = Bardens Inlet).

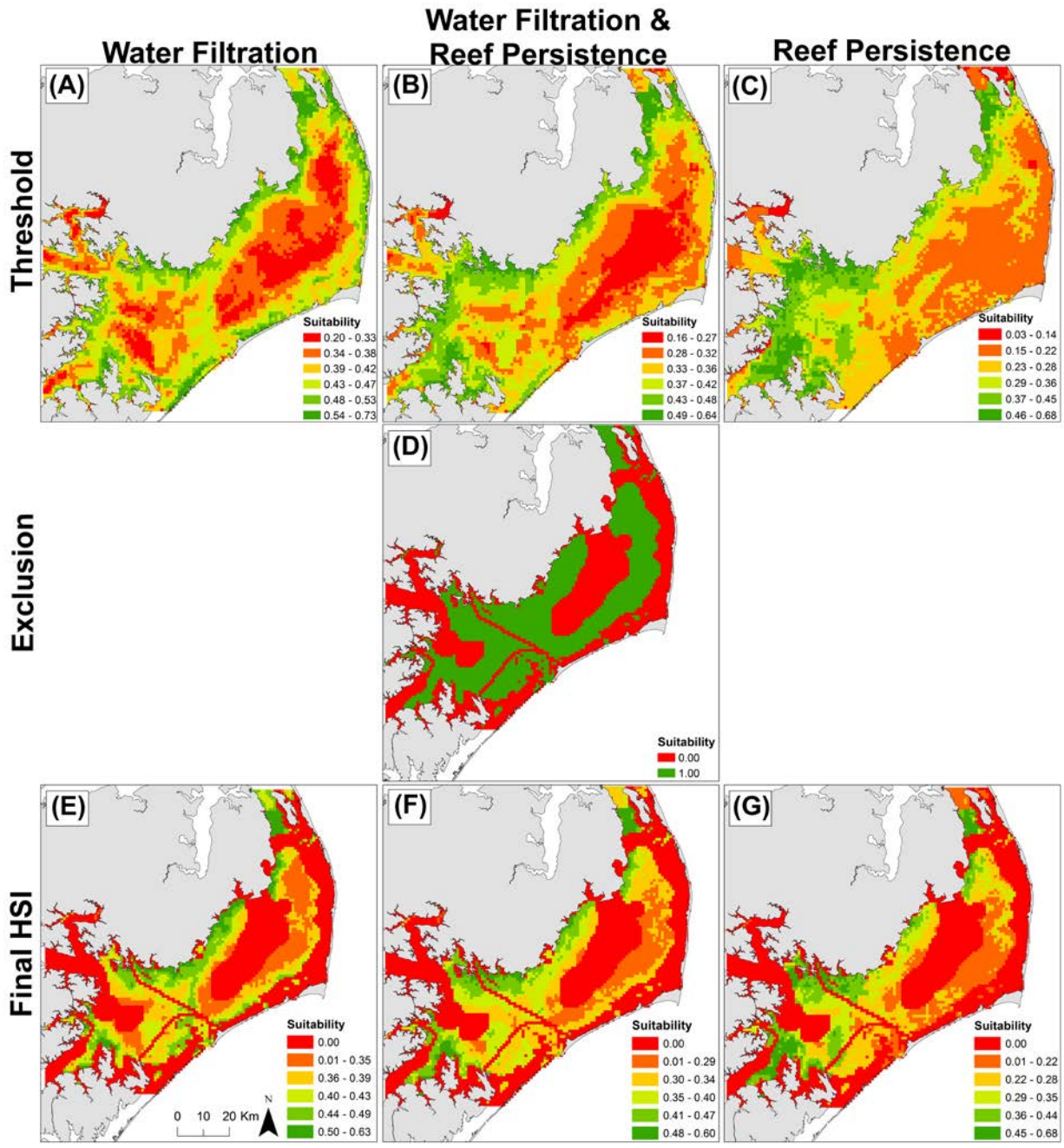


Figure 2. Habitat suitability based on: (A-C) aggregated threshold layers, (D) aggregated exclusion layers, (E-G) aggregated exclusion and threshold layers combined for the three model scenarios: 'Water Filtration,' 'Water Filtration & Reef Persistence,' and 'Reef Persistence.' Suitability in panels A-C and E-G is continuous, while suitability in panel D is binary. Suitability increases from low (red) to high (green) HSI. Panels C, D, and G adapted from Puckett et al. (in review).

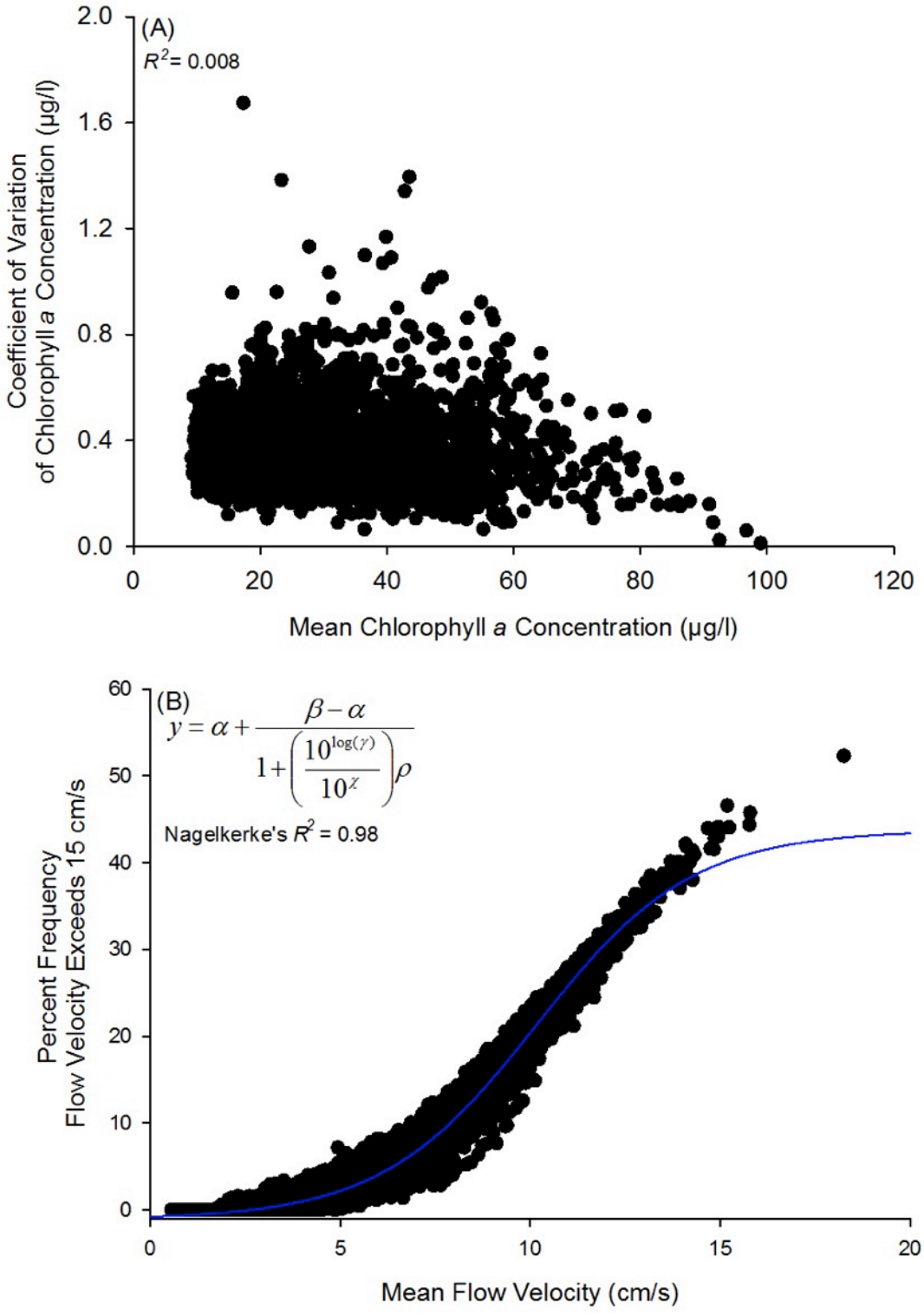


Figure 3. Relationships between: (A) mean chlorophyll *a* concentration and coefficient of variation, and (B) mean flow velocity (cm/s) and percent frequency flow velocity exceeds 15 cm/s. A description of the analysis methods used to identify these relationships can be found in '*Methods, Water Filtration Ecosystem Services Layer Development.'*

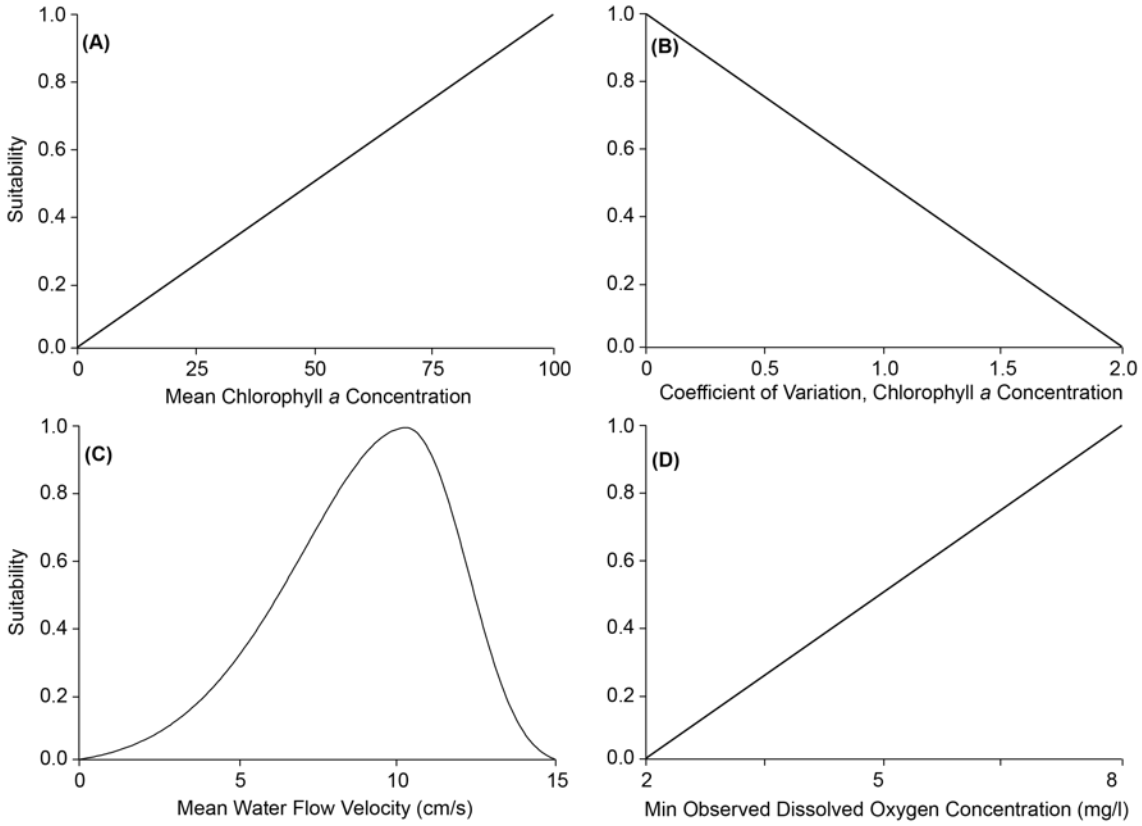


Figure 4. Relationship between actual values of: (A) mean chlorophyll *a* concentration, (B) coefficient of variation of chlorophyll *a* concentration, (C) mean water flow velocity (cm/s), and (D) minimum observed dissolved oxygen concentrations, and their associated suitability values. A description of the analysis methods used to develop these functions can be found in '*Methods, Water Filtration Ecosystem Services Layer Development.*

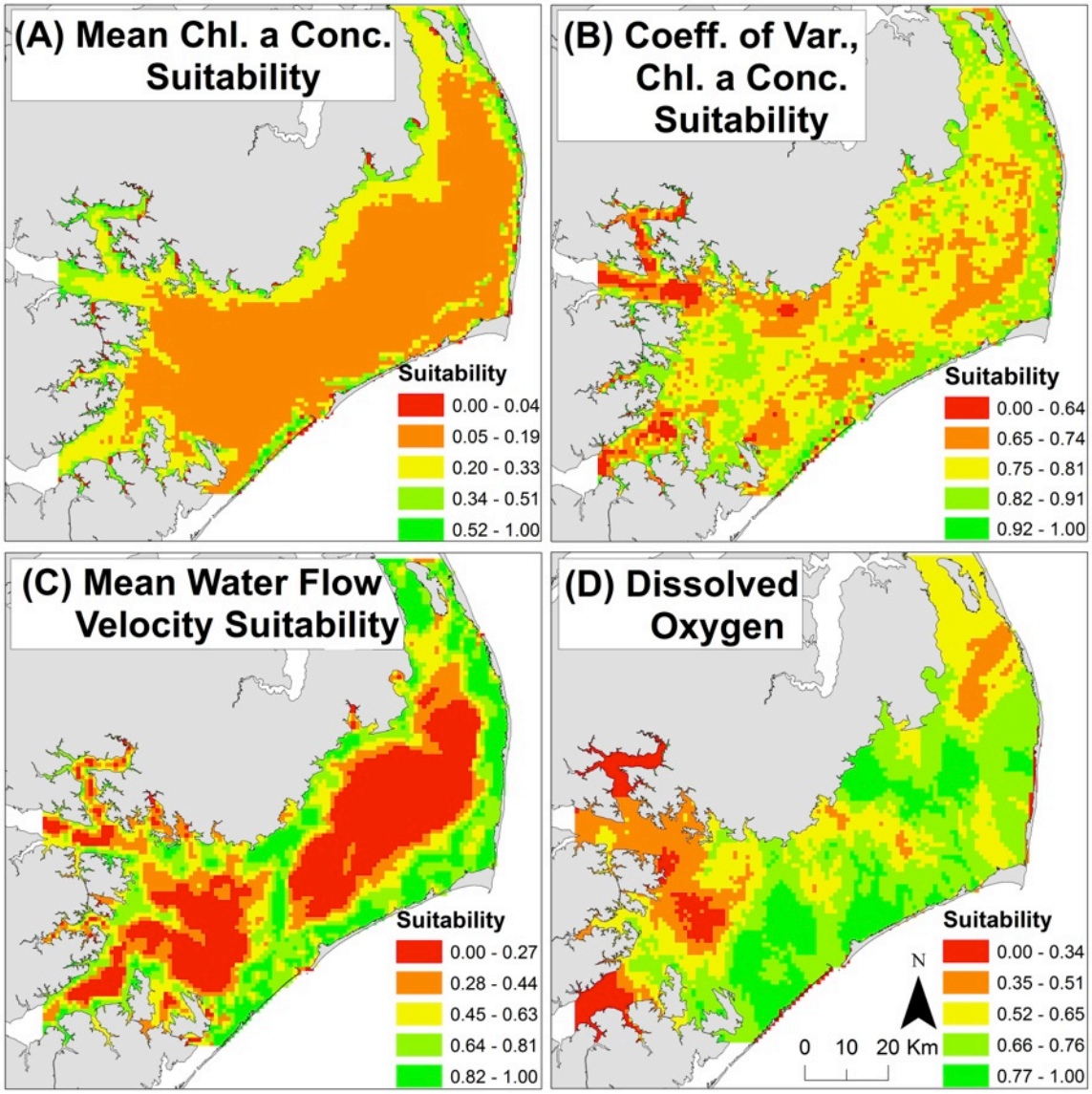


Figure 5. Suitability layer for: (A) mean chlorophyll *a* concentration, (B) coefficient of variation of chlorophyll *a* concentration, (C) mean water flow velocity, and (D) minimum observed dissolved oxygen concentration. Suitability for oyster restoration increases from low (red) to high (green) HSI.

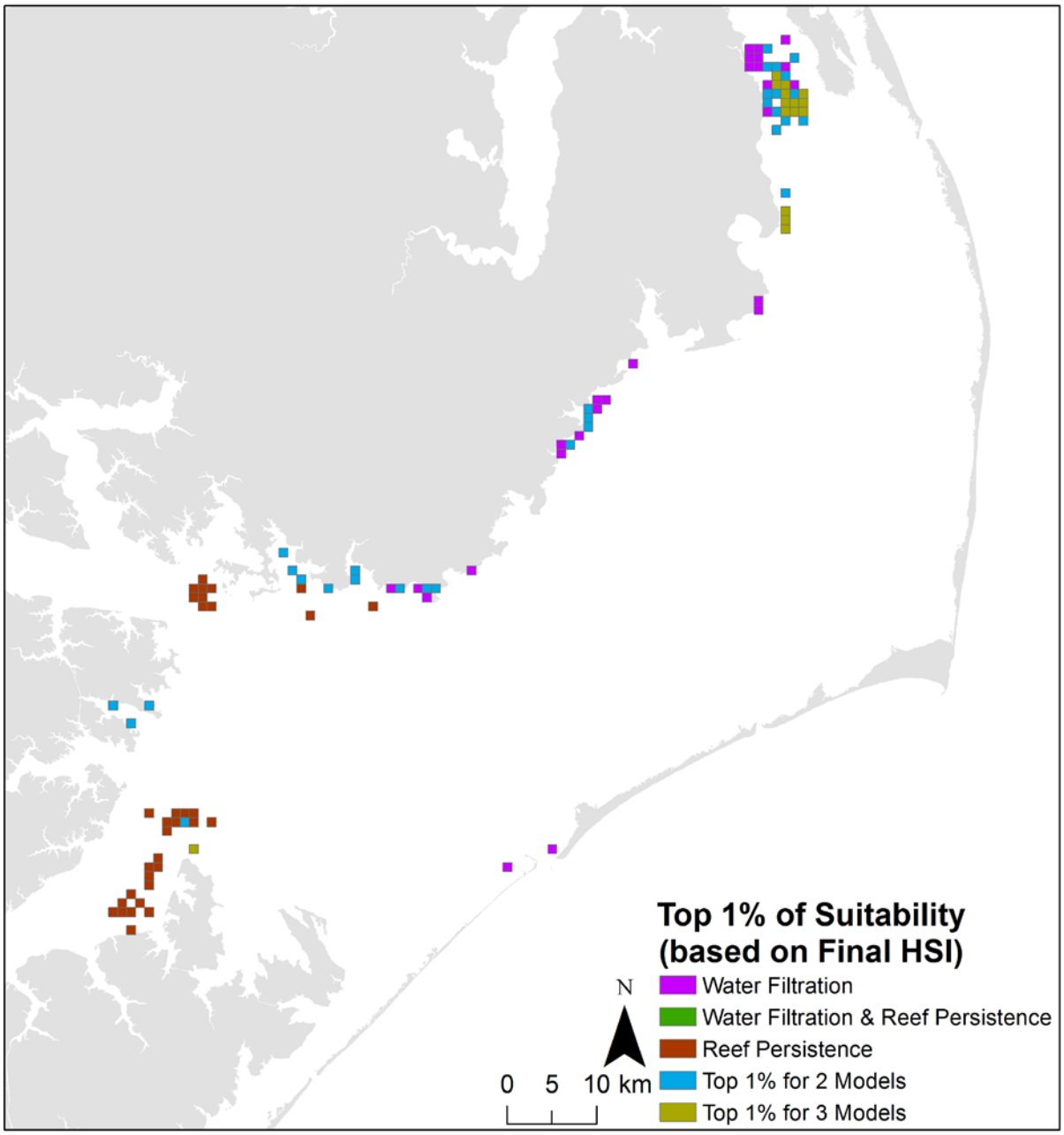


Figure 6. Optimal locations for restoration (i.e., top 1% highest HSI scores) identified in each HSI scenario as derived from the final HSI (i.e., aggregated threshold combined with aggregated exclusion layers). Locations that were identified within the top 1% for multiple HSI scenarios are indicated in red (2 models) and orange (3 models). For example, 'Top 1% for 2 Models' may include areas identified within the top 1% for the 'Water Filtration' and the 'Water Filtration & Reef Persistence' HSI scenarios, whereas 'Top 1% for 3 Models' includes areas identified within the top 1% for all three HSI scenarios.

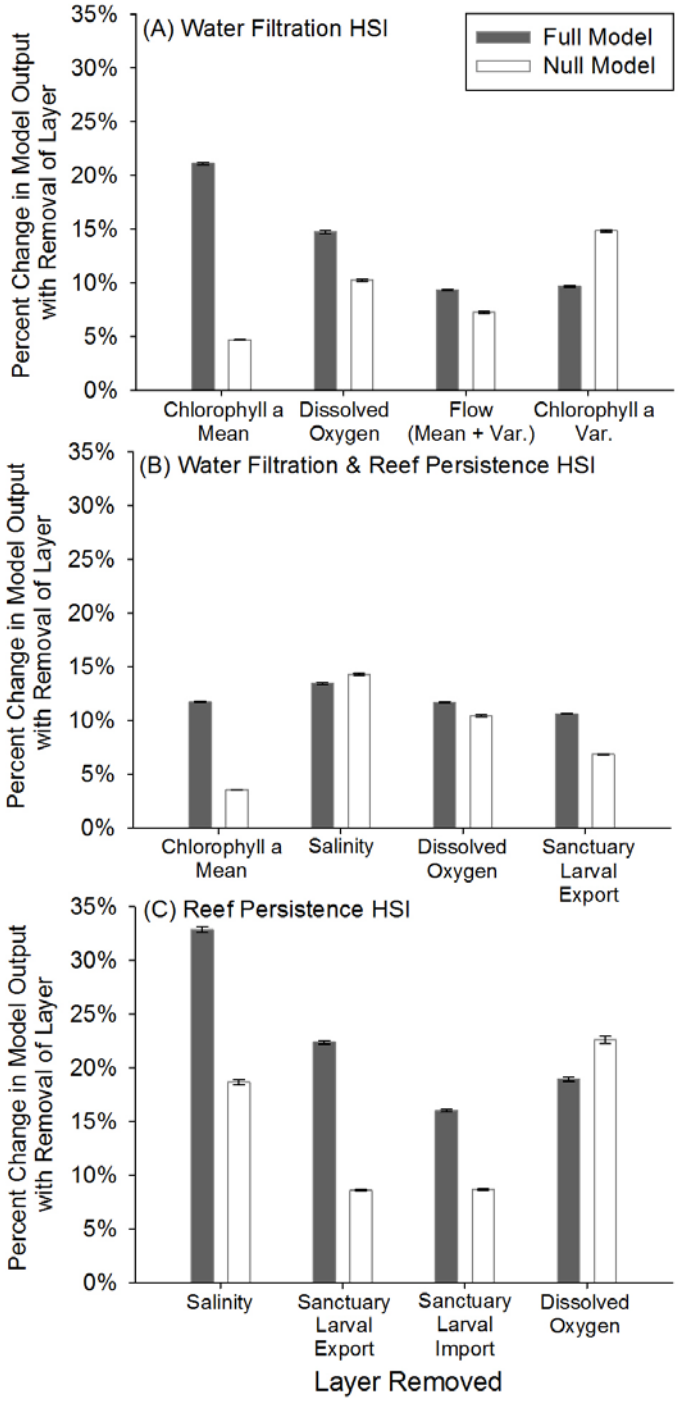


Figure 7. Results of model sensitivity analysis conducted for each of the three HSI scenarios where I: 1) removed the four threshold layers with the highest weight individually, 2) re-weighted the remaining layers proportionally based on the weight of the removed layer, 3) re-ran the model, and 4) calculated on a cell-by-cell basis the percent change in model output with removal of each layer. Error bars represent standard error of the mean (n = 5,987) of the percent change in model output with removal of a layer. Weights associated with the threshold layers in each HSI scenario can be found in Table 2.

# CHAPTER 4

# OYSTER METAPOPULATION DYNAMICS: INTEGRATING DEMOGRAPHICS AND LARVAL DISPERSAL FROM PROTECTED, RESTORED, NATURAL AND HARVESTED REEFS


## ABSTRACT

Metapopulation and source-sink dynamics concepts are increasingly considered within spatially-explicit management of wildlife populations, but has generally been limited to comparisons of the performance (e.g., demographic rates or dispersal) inside vs. outside protected areas. In the present study, I adapted a size-structured, discrete-time matrix model for eastern oysters (*Crassostrea virginica*) to simulate the dynamics of an oyster metapopulation, including a network of inter-connected no-harvest subtidal sanctuary oyster reefs, restored oyster reefs and harvested oyster reefs, among other reef types, in the Albemarle-Pamlico Estuarine System in North Carolina, USA. I identified: 1) an overall stable, yet slightly declining metapopulation, 2) variable reef type-specific population trajectories depending on spatiotemporal variation in larval recruitment, 3) spatiotemporal variation in the source-sink status of reef subpopulations wherein subtidal sanctuaries and reefs located in the northeastern portion of the system frequently served as sources, and 4) a greater relative importance of inter-reef larval export on metapopulation dynamics relative to local larval retention processes. I further examined the management and broader implications of this work and recommend future management efforts within this system consider oysters as an interconnected metapopulation. Furthermore, I recommend continued protection of existing oyster sanctuaries and conservation of other identified subpopulations that serve as frequent ‘source’ subpopulations while managing harvest from ‘sink’ subpopulations.

## INTRODUCTION

Metapopulation concepts—wherein subpopulations are viewed as interconnected networks with asynchronous demographic (i.e., birth, death) and dispersal rates (i.e., immigration, emigration)—are a critical underpinning of spatially-explicit management of wildlife populations (Hanski 1998, Beissinger et al. 1998, Burgess et al. 2014). Where management of wildlife populations is multifaceted and parts of the population are harvested, others protected in reserves, or are undergoing restoration, the application of metapopulation concepts is particularly important (Puckett and Eggleston 2016). However, attempts to characterize and simulate metapopulation dynamics as they relate to spatial management have often taken the form of comparisons (e.g., demographic rates or dispersal) inside vs. outside protected areas (e.g., Halpern 2003). Rarely is the performance of protected areas or other managed subpopulations considered within the broader context of the entire metapopulation, wherein dynamics are simulated within and amongst all subpopulations. Comprehensive evaluation of metapopulation dynamics is needed to inform appropriate application of metapopulation concepts to inform spatial management of populations such that disparate management strategies (e.g., reserves, harvest, and restoration) can be integrated and evaluated within a single framework.

Demographics and dispersal drive metapopulation dynamics (Pulliam 1988, Hanksi 1998). In marine systems, the relative importance of demographic rates on metapopulation dynamics is poorly understood because most populations are ‘open’ and inter-connected via pelagic larval dispersal (hereafter referred to as ‘larval connectivity’; Planes et al. 2009). Thus, understanding the drivers of metapopulation dynamics in marine systems requires knowledge of both demographic rates and the direction and magnitude of larval connectivity among

subpopulations, including the degree of local larval retention (i.e., larvae that originate from a given reef that settle on the same reef) versus larval export (i.e., larvae that originate from a given reef that settle on a different reef). When rates of local larval retention are low and larval export are high, the importance of local demographics on metapopulation dynamics diminishes as subpopulation recruitment is decoupled from local reproduction (Warner and Cowen 2002, Figueira 2009). Conversely, as local larval retention increases (e.g., subpopulations are more isolated), local demographics often become increasingly important.

Source-sink dynamics, wherein 'sink' subpopulations have insufficient reproduction to balance local mortality and thus are dependent upon an external supply of recruits from more productive 'source' subpopulations, is a key component of the metapopulation concept (Pulliam 1988). 'Source' subpopulations are generally in areas of high habitat quality where birth rates exceed death rates. Conversely, 'sink' subpopulations are generally in areas of reduced habitat quality where death rates exceed birth rates—often leading 'sink' subpopulations towards extinction unless sufficient individuals emigrate from a 'source' subpopulation. Source-sink status of a given subpopulation is generally non-binary and can fluctuate spatiotemporally dependent upon local conditions. For example, variation in local water current direction and magnitude has been found to isolate or connect subpopulations of coral reef-associated fish (Figueira 2009). An understanding of spatiotemporal variation in source-sink dynamics of subpopulations of interest is essential to effective management of wildlife metapopulations, wherein management efforts generally attempt to protect or restore 'source' subpopulations and manage harvest from 'sink' subpopulations.

Metapopulation and source-sink dynamics are increasingly considered within the context of management for sessile marine species such as corals and oysters, wherein subpopulations are

only connected via larval dispersal (Botsford et al. 2003, Figueira and Crowder 2006, Burgess et al. 2014, Holstein et al. 2015, Puckett and Eggleston 2016). These systems are particularly amenable to testing metapopulation and source-sink concepts because of: (1) the presence of spatially separated reefs, (2) spatial variation in the timing of spawning (Ballance et al. 2009, Mroch et al. 2012), (3) spatiotemporal variation in demographic rates such as fecundity, growth and survival (Mroch et al. 2012, Puckett and Eggleston 2012, Theuerkauf et al. 2017, Peters et al. 2017), and (4) variation in potential larval connectivity due to hydrodynamics that vary with synoptic-scale forcings such as wind (Puckett et al. 2014).

In the present study, I adapted a size-structured, discrete-time matrix metapopulation model originally developed by Puckett and Eggleston (2016) for eastern oysters (*Crassostrea virginica*) in the Albemarle-Pamlico Estuarine System in North Carolina, USA to simulate the dynamics of an entire oyster metapopulation, including a network of inter-connected no-harvest sanctuary oyster reefs, restored oyster reefs, harvested oyster reefs, and oysters on hardened shoreline structures. Using this modeling framework, I estimated: 1) overall metapopulation trends, 2) reef type- and size class-specific population trajectories, 3) the degree and relative importance of local larval retention and inter-reef connectivity on metapopulation dynamics, and 4) spatiotemporal variation in source-sink structure within this metapopulation. I further examined the management and broader implications of this work.

## MATERIALS AND METHODS

### *Study System*

The Albemarle-Pamlico Estuarine System (APES) in North Carolina contains (from north to south) Albemarle, Pamlico, and Core Sounds. The APES is the largest lagoonal estuary in the

United States, and is bounded by a barrier island chain that limits exchange with the coastal ocean to five relatively small inlets (~1 km wide; Figure 1; Pietrafesa et al. 1986). Tides in and near the inlets of the APES are generally semi-diurnal, with a mean vertical range of 5 cm when averaged across Pamlico Sound (Roelofs and Bumpus 1953) to 30 cm in Core Sound (Dudley and Judy 1973). The APES is relatively shallow with a mean depth of ~4.5 m and a maximum depth of 7.5 m (Epperly and Ross 1986). Water circulation patterns within the APES are due predominately to wind-driven currents and riverine freshwater input, with an increasing tidal influence from north to south (Xie and Eggleston 1999). Circulation during the summer, when primary and secondary peaks in oyster spawning occur (Ballance et al. 2009, Mroch et al. 2012), is driven predominately by southwesterly winds (Puckett and Eggleston 2012). These winds derive from synoptic-scale frontal systems that transverse the region (Pietrafesa et al. 1986). Wind patterns in the region have a strong influence on spatiotemporal variation in larval dispersal patterns of oysters (Haase et al. 2012, Puckett et al. 2014).

***Study Species***

Eastern oysters (*Crassostrea virginica*, hereafter oysters) are distributed throughout estuaries along eastern North America, ranging from the Gulf of St. Lawrence to the Gulf of Mexico, and provide a multitude of ecosystem services within estuaries, such as water filtration, sediment stabilization, and essential fish habitat (Kennedy et al. 1996, Coen et al. 2007, Grabowski et al. 2007, Pierson and Eggleston 2014). Oysters form dense, three-dimensional reef structures that are connected via larval dispersal, whereby sessile individuals spawn gametes into the water column and fertilized eggs develop into planktonic larvae that are distributed via currents (Kennedy et al. 1996). After a two-to-three week period, larvae seek hard structure on the benthos for permanent settlement.

Multiple natural and restored oyster reef types exist within the subtidal and intertidal zones of the APES (Figure 1). Within the subtidal zone there are: commercially harvested natural oyster reefs, commercially harvested reefs restored with shell, concrete, or limestone marl reef substrates (i.e., cultch reefs), and reefs restored with high vertical relief and protected from commercial harvest (i.e., sanctuaries; Puckett and Eggleston 2012, Peters et al. 2017). Within the intertidal zone, oysters exist on natural reefs and hardened shoreline structures, such as bulkhead and riprap revetments (Theuerkauf et al. 2016, 2017). All reefs exist within a salinity range of approximately 10 to 36 psu, and are separated from each other by < 1–125 km.

***General Modeling Approach***

Our general modeling approach incorporated: (1) the spatial distribution, areal footprint, and initial population size of all oyster reef types within the APES, (2) reef type- and intra-annual-specific oyster size-class transition probabilities (i.e., probability of surviving and remaining in a given size class or surviving and growing into the next size class; sensu Caswell 2001), (3) size-specific oyster fecundity estimates, and (4) local larval retention and inter-reef connectivity via larval dispersal simulations. With this modeling approach, I simulated metapopulation dynamics throughout the APES using a demographic matrix model over a 5 year time period (2012-2016) and evaluated consistency in metapopulation source-sink structure over space and time.

***Estimating Reef Footprints***

I aggregated multiple geospatial data sources to generate estimates of oyster reef areal footprints for all reef types within the APES. All natural and restored (i.e., cultch planting and sanctuary) oyster reef footprints were provided as map layers by the North Carolina Division of Marine Fisheries Shellfish Mapping Program (North Carolina Department of Environmental

Quality, North Carolina Division of Marine Fisheries 2013), and were adjusted where appropriate based on ground-truth surveys conducted by Peters et al. (2017) and Theuerkauf et al. (2016). For a more detailed description of methods used to adjust subtidal reef areal footprints refer to Peters et al. (2017), and for adjustment of intertidal reef areal footprint refer to Theuerkauf et al. (2016). Subtidal natural oyster reef footprints were further adjusted based on density data collected by the North Carolina Division of Marine Fisheries Shellfish Mapping Program from 2007–2009. It is important to note that the original map layers provided by the North Carolina Division of Marine Fisheries Shellfish Mapping Program include a range of shell habitat quality from areas of loose shell fragments containing no live oysters, to scattered, low-density assemblages of oysters, to high-density oyster reefs (Theuerkauf et al. 2017). Adjustment of these map layers was required to ensure the distribution of reef footprints considered in subsequent modeling reflected the distribution of oyster reefs with densities > 10 $m^{-2}$ (i.e., minimum density criterion to define a reef; sensu Powers et al. 2009, Theuerkauf et al. 2016). The distribution of hardened shorelines from map layers included all areas of bulkhead and riprap revetments installed prior to 2012, and were provided by the North Carolina Division of Coastal Management Estuarine Shoreline Mapping Program (North Carolina Department of Environmental Quality, North Carolina Division of Coastal Management 2012). Map layers of hardened shoreline structures were adjusted to reflect the distribution of structures with oyster densities > 10 $m^{-2}$ based on a ground-truthing (Theuerkauf et al. 2016). A total of 646 reefs were identified and utilized in the present study. Table 1 provides summary statistics by reef type including number of unique reefs, total reef area, average reef area, average initial density, average initial population size, and average initial size structure and Figure 1 displays the spatial distribution of these reefs within the APES by reef type.

***Estimating Demographic Rates via Field Sampling***

Oyster density and length frequency were quantified on a subset of subpopulations of all reef types via repeated field sampling of existing reefs (2–3 samplings per year, coinciding with the timing of major recruitment events, over a 2–3 year time period) using comparable methods between 2006 and 2015. Puckett and Eggleston (2012) sampled no-harvest oyster sanctuaries ($n$ = 6, 3 samplings per year, 2006–2008), Peters et al. (2017) sampled subtidal natural reefs ($n$ = 8, 3 samplings per year, 2011–2013) and cultch reefs ($n$ = 16, 3 samplings per year, 2011–2013), and Theuerkauf et al. (2017) sampled intertidal natural reefs ($n$ = 16, 3 samplings per year, 2014–2015) and hardened shoreline structures ($n$ = 19, 2 samplings per year (2014–2015). The subset of subpopulations examined for all reef types spanned the length-width axis of the APES. Oyster density and length frequency were quantified on reefs randomly selected from maps of existing reefs via random quadrat sampling (0.25–1 $m^2$). The number of quadrat samples collected per reef was proportional to reef area. Quadrat samples for subtidal oyster reefs were obtained via SCUBA divers. It is important to note that in addition to random quadrat sampling of oyster sanctuaries, Puckett and Eggleston (2012) conducted a mark-recapture study of oysters to validate growth and survival rates as estimated via random quadrat sampling and cohort analyses (see below). This mark-recapture data was used to develop the method described below for utilizing size structure data collected via quadrats from the oyster subpopulations examined in the APES to estimate growth and survival transition probabilities, which was required for subsequent demographic matrix modeling. Size class-specific densities observed at the first sampling of a given reef type were also used to seed the demographic matrix model with initial population estimates for all reefs. Specifically, observed density estimates (individuals $m^{-2}$) were interpolated via ordinary kriging (ESRI 2016) to predict reef type-specific oyster densities across

the APES. Predicted oyster density estimates for non-sampled reef locations were then extracted from this continuous, interpolated data and multiplied by reef area to generate initial population estimates for each reef considered within the model domain.

***Estimating Growth and Survival Transition Probabilities***

Field-derived, oyster size structure data was used to estimate reef type- and season-specific growth and survival transition probabilities (i.e., probability of surviving and remaining in a given size class or surviving and growing into the next size class; sensu Caswell 2001). Specifically, for each reef type, I averaged oyster density data from all quadrats for a given reef site for each sampling event and subsequently partitioned density estimates into three size classes: (1) recruit (LVL < 30mm), (2) sub-adult (30mm ≤ LVL < 75mm), and (3) adult oysters (LVL ≥ 75mm; legally harvestable size). I used a linear optimization approach to determine the least squares estimate for five growth and survival transition probabilities based on size-class specific density data from time *t* and *t+1*. These five transition probabilities included the probability of surviving and remaining in a size class (i.e., recruit at *t* to recruit at *t+1*, sub-adult at *t* to sub-adult at *t+1*, adult at *t* to adult at *t+1*), and the probability of surviving and growing into larger size classes (i.e., recruit at *t* to sub-adult at *t+1*, sub-adult at *t* to adult at *t+1*). Specifically, linear optimization was used to adjust the five transition probabilities that were multiplied by the observed size class-specific densities at *t* and summed where appropriate (e.g. to predict least squares size class-specific density estimates at *t+1* and minimize the total sums of squares difference between predicted and observed densities for the three size classes at *t + 1*). As transition probabilities cannot exceed 1 (equivalent to 100% growth and/or survival), and cannot be less than 0 (e.g., 0% survival), I established initial constraints within the linear optimization for each of the five transition probabilities as 0.01 and 0.99. I also constrained the

sum of the recruit at *t* to recruit at *t+1* and the recruit at *t* to sub-adult at *t+1*, as well as the sub-adult at *t* to sub-adult at *t+1* and the sub-adult at *t* to adult at *t+1* to be no greater than 1.

I evaluated the efficacy of this method by comparing season-specific transition probabilities determined empirically from a mark-recapture study used previously to characterize transition probabilities for subtidal oyster sanctuary reefs (see Puckett and Eggleston 2012 for description of methods) with those estimated using the linear optimization method described above. The same field-derived size structure data for subtidal sanctuaries in the APES from Puckett and Eggleston (2012) was used in both methods, providing a standardized basis for comparison. Initial comparison of these transition probabilities identified that linear optimization with wide constraints for each possible transition probability (i.e., 0.01 to 0.99) resulted in underestimates of various transition probabilities relative to those determined from the mark-recapture study. I subsequently modified the constraints within the linear optimization for all recruit and sub-legal transitions to reflect the minimum and maximum observed values for transition probabilities from the mark-recapture study (i.e., empirically derived spatially- and season-specific transition probabilities for six oyster sanctuaries in the APES; Puckett and Eggleston 2016). This resulted in narrower constraints for the various transition probabilities within the linear optimization and yielded an improved fit of estimated transition probabilities derived from the mark-recapture study (Figure 2). Since I intended to develop a universal method for using linear optimization to estimate transition probabilities for all reef types within our study system, I did not constrain the adult transition (i.e., adult at *t* to the adult at *t + 1*) using minimum and maximum observed values as harvest is not prohibited from other subpopulations and thus the observed minimum and maximum ranges for the transition from the no-take oyster sanctuaries likely do not apply (i.e., fishing mortality occurs on other reef types). I also

developed unique transition probability estimates for intertidal natural reefs in Core versus Pamlico Sounds as prior research indicated significant differences in density and demographic rates between water bodies (Theuerkauf et al. 2017). A summary of reef type- and season-specific oyster growth and survival transition probabilities utilized in model simulations are included in Table 2.

***Estimating Fecundity***

Size-specific oyster fecundity was estimated from a previous study that quantified size class-specific mean total egg content (i.e. per capita fecundity) of oysters (Mroch et al. 2012). Fecundity estimates were generated from this dataset for three size classes (i.e., 0–30 mm (recruit), 30–75 mm (sub-adult), and 75+ mm (adult). Specifically, randomly selected oysters (*n* = 2,067) were collected from six reef sites throughout the APES during May and August of 2006–2007. Oysters were processed individually to determine per capita fecundity following the general procedures in Cox and Mann (1992). Mean per capita fecundity was calculated for each oyster size class across six reef sites to generate a mean per capita fecundity for each of the three size classes, and temporally corresponding with the primary and secondary peaks in oyster reproductive output for the APES (i.e., May–June and July–August; Table 3). Males were included in the calculations of mean per capita fecundity, thereby incorporating the sex ratio of a given size class. For a more detailed description of fecundity methods, see Mroch et al. (2012).

***Estimating Larval Connectivity***

I used a validated and coupled hydrodynamic and particle tracking model to quantify local larval retention and inter-reef larval connectivity (Luettich et al. 2002, Haase et al. 2012, Puckett et al. 2014). The hydrodynamic model was forced with hourly wind velocities measured from May through August of 2012–2016 at Cape Hatteras Meteorological Station. Water current

velocities were output from the model at hourly intervals following an 8-day model "spin-up." Nine particles were released from evenly spaced grid nodes within each of 646 reefs at 24-hour intervals over a 14-day period in late May and late July of each year to coincide with the primary and secondary peaks in oyster reproductive output in the APES (i.e., 252 particles/reef/year for a total of 1,260 particles). Particles (hereafter 'larvae') were assumed to be passive surface drifters and subjected to predicted surface currents. Previous research in this shallow, well-mixed system revealed that connectivity was driven primarily by location of natal reef, date of spawning, and their interaction—larval behavior and the number of larvae released were of secondary importance (Puckett et al. 2014, Puckett and Eggleston 2016). Moreover, as described above, the APES is a shallow, wind-driven lagoonal estuary with a well-mixed water column and no distinct halocline (Reyns et al. 2007). Larvae were tracked hourly over a 21-day larval duration. As described in more detail below, I applied three proportional daily larval mortality rates: 7.5% $day^{-1}$, 10% and 20%, under three separate, unique metapopulation model scenarios based on literature-derived relationships between larval duration and mortality (Mann and Evans 1998). Larvae were assumed competent to settle from day 14 through day 21, after which larvae remaining in the water column died (e.g., North et al. 2008, Puckett et al. 2016). Settlement was assumed to occur if larvae that were competent to settle were located within reef polygon boundaries.

Oyster metapopulation connectivity matrices were generated for May–June and July–August of 2012–2016 (i.e., 2 matrices/year x 5 years = 10 connectivity matrices). Matrix elements represent the proportion of larvae released from a row-referenced reef that settled in a column-referenced reef. Local retention—the probability of larvae spawned from a reef returning to settle within their natal reef—was obtained from the diagonal elements of the connectivity

matrix. Inter-reef connectivity—the proportion of larvae spawned from a reef that successfully settled in any non-natal reef—was calculated by summing each row of the connectivity matrix excluding local retention.

***Metapopulation Model Structure***

I modified a size-structured, discrete-time matrix metapopulation model originally developed by Puckett and Eggleston (2016) of the form,

$$n(t+1) = \mathbf{A}n(t)$$

where $n$ is a vector containing the number of individuals in each size class at time $t$ and $\mathbf{A}$ is a metapopulation projection matrix that represents demographic transitions and per capita fecundity (Caswell 2001). I divided $n$ on the basis of size classes where elements in vector $n$ contained the abundance of oysters in one of three size classes: 0–30 mm (recruits), 30–75 mm (sub-adults), 75+ mm (adults, harvestable size).

The model time step was divided into three intra-annual seasonal periods corresponding to demographic sampling (see *Estimating Demographic Rates via Field Sampling* above) and oyster biology (Puckett and Eggleston 2016). The projection matrix, **A**, was parameterized separately for each season: $\mathbf{A}^{\text{spring}}$–1 May to 30 June corresponding to peak oyster fecundity, $\mathbf{A}^{\text{summer}}$–1 July to 31 August corresponding to secondary peaks in oyster fecundity, and $\mathbf{A}^{\text{fall/winter}}$–1 September to 30 April corresponding to no fecundity. Growth and survival also differed in each seasonal projection matrix (see description of transition probabilities below). Projection matrices did not vary inter-annually as reef type-specific demographic data were pooled to ensure sufficient sample sizes for estimating demographic parameters in $\mathbf{A}^{x}$ (McMurray et al. 2010, Puckett and Eggleston 2016).

Seasonal metapopulation projection matrices were parameterized separately for each *k* reef ($\mathbf{A}_k^x$) and decomposed into the sum of two matrices, $\mathbf{T}_k^x$ and $\mathbf{F}_k^x$, where $\mathbf{T}_k^x$ describes transition probabilities in reef *k* during season *x* and $\mathbf{F}_k^x$ describes per capita fecundity in reef *k* during season *x*. The diagonal elements of $\mathbf{T}_k^x$ describe the probability of individuals in reef *k* and size class *i* surviving and remaining in size-class *i* (i.e., stasis; $P_{i,k}$; Figure 3), and the subdiagonal elements describe the probability of surviving and growing into size-class *j* ($G_{i,k}$). Reef type- and season-specific growth and survival transition probabilities were estimated using the methods described in '*Estimating Growth and Survival Transition Probabilities'* above. Elements along the first row of $\mathbf{F}_k^x$, the only non-zero values in **F**, describe per capita fecundity of individuals in reef *k* and size class *i* ($F_{i,k}$). Elements of $\mathbf{F}_k^x$ were adjusted for density-dependent fertilization success based on Levitan (1991) as:

$$\% \text{ fertilization} = 0.49 \text{ x } D^{0.72}$$

where *D* is total oyster density per $m^2$. Fertilization success was capped at 100% in the event oyster densities were sufficiently high to generate fertilization success >100%. The larvae spawned from reef *j* were calculated as the product of a reef's per capita fecundity matrix ($\mathbf{F}_j^x$) and $n_{j(t)}$. Larvae were distributed among reefs based on elements of the connectivity matrix, **M**, at time *t*. Elements of **M** describe the proportion of larvae released from reef *j* that survive to settle in reef *j* ($m_{j,k}$; Figure 3). Connectivity pathways included both local retention and inter-reef connectivity. I assumed settlement occurred at the midpoint of the model time step (i.e., *t* + 0.5) and new settlers in reef *j* survived to time *t* + 1 with probability $P_{1,j}^*$ adjusted for half a time step (Caswell 2001, Puckett and Eggleston 2016).

The complete metapopulation model, adapted from Puckett and Eggleston's (2016) original model, was expressed as:

$$N(t+1) = \sum \begin{pmatrix} n_{1(t+1)} \\ \vdots \\ n_{646(t+1)} \end{pmatrix} = \left( \begin{bmatrix} \mathrm{T}_1{}^x & \cdots & 0 \\ \vdots & \ddots & \vdots \\ 0 & \cdots & \mathrm{T}_{646}{}^x \end{bmatrix} + \begin{bmatrix} P^*_{1,1}(m_{1,1}\mathbf{F}_1^x) & \cdots & P^*_{1,646}(m_{646,1}\mathbf{F}_{646}^x) \\ \vdots & \ddots & \vdots \\ P^*_{1,646}(m_{1,646}\mathbf{F}_1^x) & \cdots & P^*_{1,646}(m_{646,646}\mathbf{F}_{646}^x) \end{bmatrix} \right) \begin{pmatrix} n_{1(t)} \\ \vdots \\ n_{646(t)} \end{pmatrix}$$

where $\boldsymbol{N}$ is metapopulation size at time *t*, $\boldsymbol{n}_{k(t)}$ is a subvector containing the abundance of oysters in each size class in reef *k* at time *t*, $\mathbf{T}_k^x$ is a submatrix representing the transition probabilities of each size class in reef *k* at time *t* during season *x*, $\mathbf{F}_k^x$ is a submatrix representing the per capita fecundity of each size-class in reef *k* at time *t* during season *x* and $m_{j,k}$ and $P^*_{1,j}$ are defined as above (Lewis 1997, Caswell 2001, Puckett and Eggleston 2016). Population vectors at each reef, $n_k$, were initially seeded with reef-specific empirical estimates (or interpolated for reefs not sampled) of oyster density and size structure scaled to reef area (Table 1, see '*Estimating Demographic Rates via Field Sampling'* above). Metapopulation abundance was projected over a 5-year period from May 2012 to April 2017.

***Quantifying Metapopulation and Source-Sink Dynamics***

I calculated the overall metapopulation growth rate as:

$$\lambda_M(t) = \sum_{j=1}^{646} \lambda_{C,j}(t) \left(\frac{n_{j(t)}}{N(t)}\right)$$

where ($\lambda_{C,j}$(t)) is reef *j*'s contribution to the metapopulation at time *t* (Figuiera and Crowder 2006, Puckett and Eggleston 2016) and $N(t)$ and $n_{j(t)}$ are defined above. Values of $\lambda_M(t) \geq 1$ indicate a persistent or expanding metapopulation during time *t*, whereas $\lambda_M(t) < 1$ indicate a contracting metapopulation during time *t.* I generated a time series plot to depict $\lambda_M$ across the five-year model timeframe.

Each reef's contribution to the metapopulation (i.e., subpopulation status as a net source or sink) was calculated based on Figuiera and Crowder (2006) as:

$$\lambda_{C,j}(t) = \left[\mathbf{T}_j^x n_{j(t)}\right] + \left[\sum_{j=1}^{646} P^*_{1,k}\left(m_{jk}\mathbf{F}_j^x n_{j(t)}\right)\right]$$

where variables are defined as above and $\lambda_{C,j}(t) \geq 1$ indicates reef *j* functioned as a source during time *t* and $\lambda_{C,j}(t) < 1$ indicates reef *j* functioned as a sink during time *t*. By calculating reef source-sink status in this manner, reefs are credited with births to any reef within the metapopulation (including itself) and penalized for deaths that occur within the reef. By this definition, a source is a net contributor to the metapopulation regardless of whether local retention is sufficient for self-persistence.

Metapopulation and source-sink dynamics were evaluated under three distinct proportional daily larval mortality rates: 7.5% $day^{-1}$, 10% and 20%, based on literature-derived relationships between larval duration and mortality (Mann and Evans 1998). As further described below in 'Results,' each larval mortality scenario yielded widely varying metapopulation and source-sink dynamics outcomes. I describe each scenario and provide detailed descriptions of the 10% proportional daily larval mortality scenario for brevity and given alignment of the model output with prior field-based observations.

*Evaluating Reef Type- and Size Class-Specific Population Trajectories* – Time series plots were generated to depict reef-type and size class-specific population trajectories. Specifically, I plotted the mean per-reef population size associated with a given reef type and size class across the five-year model timeframe.

*Evaluating Spatiotemporal Variation in Source-Sink* Structure – Box and whisker plots were generated to depict season- (i.e., May-June vs. July-August) and reef type-specific source-sink status (i.e., $\lambda_c$). I generated a map depicting the frequency of $\lambda_c \geq 1$ at all reefs across the five-year model timeframe.

*Estimating the Degree and Relative Importance of Local Larval Retention vs. Inter-Reef Connectivity* – I determined on a reef type-specific basis the average percent of larvae (i.e.,

across all 10 simulated dispersal events) retained locally versus exported between reefs. Local larval retention includes all larvae originating from a given reef that settle on the same reef. Larval export includes all larvae originating from a given reef that settle on a different reef. I also determined, dependent upon the frequency of $\lambda_c \geq 1$, the average percent of larvae retained locally versus exported between reefs for each level of frequency of $\lambda_c \geq 1$ (i.e., 10-50%) to evaluate possible larval connectivity-derived drivers of frequent population sources.

*Assessing Validity of Model Output* – Observed versus model predicted population sizes were compared to quantitatively assess validity of model output (Figure 4). Specifically, I compared estimates of observed population size derived from field sampling of subtidal natural and cultch reefs in August 2012 with estimates of predicted population size derived from metapopulation simulations corresponding to the same time period in the present study. As density estimates derived from field samplings at different time points (i.e., 2006-2008 for subtidal sanctuary reefs and 2014-2015 for intertidal natural and hardened shoreline reefs) were used to parameterize the model, and the model timestep was initialized to May 2012, the above-stated field-derived data represented the only available data for valid comparison.

## RESULTS

### *Areal Footprint, Density, and Population Estimates by Reef Type*

Subtidal natural reefs are the predominant reef type within the APES, with 301 unique reefs encompassing a total reef area of 934.27 ha (Table 1, Figure 1). Subtidal sanctuary reefs are the next largest reef type, with the boundaries of these 14 reefs encompassing a total reef area of 66.02 ha. Individual subtidal sanctuary reefs occupy ~1.5x greater area than natural subtidal reefs. Subtidal cultch reefs are the third largest reef type by total reef area, with 53 reefs

encompassing 15.32 ha. Intertidal natural reefs in Pamlico and Core Sounds occupy similar total reef areas, with 59 intertidal natural reefs occupying 10.43 ha in Pamlico Sound, and 72 intertidal natural reefs occupying 11.82 ha in Core Sound. Hardened shoreline reefs occupy the smallest total reef area, with 149 hardened shorelines encompassing 2.69 ha.

Average initial population densities were highest on intertidal natural reefs in Core Sound, followed closely by subtidal sanctuary reef (842 oysters $m^{-2}$ versus 670, respectively; Table 1). Subtidal cultch reefs and intertidal natural reefs in Pamlico Sound harbored lower initial population densities (152 oysters $m^{-2}$ and 121, respectively). Hardened shoreline reefs and subtidal natural reefs harbored the lowest initial population densities (69 ind. $m^{-2}$ and 61, respectively). When initial density was scaled by reef area to estimate the initial population size of individual reefs used to seed the metapopulation model (see '*Estimating Demographic Rates via Field Sampling'* above), the average initial population size of subtidal sanctuary reefs was approximately one order of magnitude greater than the next highest reef types, which were subtidal natural reefs and intertidal natural reefs in Core Sound (Table 1). Subtidal cultch reefs and intertidal natural reefs in Pamlico Sound contained similar initial population sizes (average of ~400,000 individuals). Hardened shoreline reefs contained the smallest initial population sizes (average of ~70,000 individuals; Table 1).

The average initial size structure of subtidal natural reefs and subtidal cultch reefs was comparable, with ~one-half of the population contained within the sub-adult size class, ~one-third of the population within the recruit size class, and ~one-sixth of the population within the adult size class. Intertidal natural reefs in Pamlico and Core Sounds contained similar average size structures to subtidal natural and cultch reefs, with slightly greater populations of sub-adults and recruits and less than one-tenth of the population within the adult size class. Average initial

size structure of subtidal sanctuary reefs contained ~one-quarter of the population within the recruit size class, ~two-thirds of the population within the sub-adult size class, and less than one-tenth of the population within the adult size class. Hardened shoreline reefs contained an average initial size structure with ~two-thirds of the population within the sub-adult size class, ~one-third within the adult size class, and less than one-twentieth of the population within the recruit size class.

***Larval Connectivity***

Variability in the dominant wind direction during a given dispersive period (e.g., May-June and July-August of 2012–2016) yielded widely varying larval dispersal patterns. I utilized residual sums of squares (RSS) analysis of average frequencies for wind speed and direction (i.e., across 5 m $s^{-1}$ speed bins and 10° directional bins; sensu Puckett et al. 2014) to determine times of 'average' wind conditions when the RSS was lowest and anomalous wind conditions when the RSS was highest. Based on this analysis, winds within the APES were predominately southwesterly (towards northeast) at mean speeds of 4–5 m $s^{-1}$. Average wind conditions from 2012 to 2016 were best represented by July–August 2013, and larval dispersal patterns during this time largely reflected northeast transport of larvae (Figure 5). The period of May–June of 2012 represented anomalously strong and variable northeasterly winds (towards southwest), with dispersal patterns displaying highly variable directionality of larval connections between natal and settled reefs (Figure 6). July–August of 2012 represented the strongest southwesterly winds (towards northeast) and dispersal patterns reflected strong larval transport from southern natal reefs in the APES towards northeastern reefs (Figure 7). Additional figures depicting larval connectivity during the other dispersal periods are included in Appendices 5-11.

Larvae were more frequently exported to different reefs than they were retained locally (Table 4). On average, ~0.5% of larvae were retained locally (i.e., all larvae originating from a given reef that settle on the same reef), whereas ~18% of larvae were exported (i.e., all larvae originating from a given reef that settle on a different reef). Natural subtidal reefs exported the greatest percentage of larvae to other reefs (~26%), followed by subtidal cultch and sanctuary reefs. Hardened shorelines and natural intertidal reefs in Pamlico Sound exported similar amounts of larvae and retained very few locally. Natural intertidal reefs in Core Sound exported the lowest percentage of larvae to other reefs (~5%).

***Metapopulation Status and Source-Sink Dynamics***

Variation in proportional daily larval mortality rates between 7.5% $day^{-1}$, 10% and 20% yielded widely varying outcomes for total metapopulation abundance (Figure 8). The 7.5% $day^{-1}$ larval mortality rate yielded a rapidly growing metapopulation (Figure 8a), the 10% $day^{-1}$ larval mortality rate yielded a generally stable, but slightly declining metapopulation (Figure 8b), whereas the 20% $day^{-1}$ larval mortality rate yielded a rapidly declining metapopulation (Figure 8c). As the 10% $day^{-1}$ larval mortality rate yielded overall metapopulation trends most closely aligned with field-based observations (e.g., episodic recruitment on hardened shorelines, Theuerkauf et al. 2017), I present figures depicting reef type- and size class-specific population trajectories under the 10% $day^{-1}$ larval mortality rate (Figures 9–12). Population trajectories and metapopulation summary statistics under the 7.5% and 20% $day^{-1}$ larval mortality rates are provided in Appendix 12-18.

Overall oyster population trends by reef type showed an overall slight decline across reef types (Figure 9), however, spatiotemporal variation in recruitment yielded substantial differences in population trajectories (Figure 10). For example, the population trajectory for subtidal natural

and cultch reefs (Figure 10a, 10b) was oscillatory in response to consistently high recruitment, but was generally stable across time around a mean population size. In contrast, the population trajectory for hardened shorelines and intertidal natural reefs in Pamlico Sound (Figure 10d, 10e) showed overall decline with punctuated increases in response to episodic recruitment. Spatiotemporal variation in recruitment patterns were generally manifested in sub-adult and adult size classes in subsequent time steps (Figures 11, 12). For example, substantial recruitment on hardened shorelines during the May-June recruitment event of 2014 (Figure 10D) yielded increases in sub-adult (Figure 11D) and adult (Figure 12D) populations on hardened shorelines in the subsequent time steps after the major recruitment event. In contrast, periods of low recruitment yielded decreases in sub-adult and adult populations. For example, low levels of recruitment on hardened shorelines in 2015 (Figure 10D) yielded declining sub-adult (Figure 11D) and adult (Figure 12D) populations. The exception occurred on subtidal sanctuaries where sub-adult (Figure 11C) and adult (Figure 12C) dynamics were not as oscillatory in response to variation in recruitment patterns (Figure 10C).

Overall metapopulation growth rate ($\lambda_M$) exceeded 1 (i.e., indicative of a persistent metapopulation) during all model time steps corresponding to the peak primary spawning event (May-June), but was less than 1 during all other model time steps (i.e., indicative of a non-persistent metapopulation; Figure 13). Source-sink status ($\lambda_c$) of reefs varied widely by reef type and between the May-June and July-August spawning peaks for oysters in Pamlico Sound (Figures 14, 15). During primary spawning and recruitment periods in May-June, subtidal sanctuaries were the only reef type with a mean $\lambda_c$ exceeding one (i.e., on average, subtidal sanctuaries function as sources to the metapopulation; Figure 14). Some subtidal natural and cultch reefs served as sources, whereas fewer intertidal natural reefs in Pamlico and Core Sounds

served as sources. No hardened shorelines functioned as sources during the May-June time steps. During secondary spawning and recruitment periods in July-August, no reef types had a mean $\lambda_c$ exceeding one (Figure 15). Infrequently, individual subtidal sanctuaries, intertidal natural reefs in Core Sound, and hardened shorelines functioned as sources.

Reefs serving as frequent sources to the metapopulation (i.e., high frequency of $\lambda_c > 1$ across recruitment events) were generally located in the northeastern portion of Pamlico Sound (Figure 16). Other frequent sources were distributed widely throughout Pamlico Sound, often in central locations within the sound and not within embayments. Subtidal sanctuaries were the most frequent sources to the metapopulation (Table 5), followed by natural subtidal reefs and subtidal cultch reefs. Natural intertidal reefs and hardened shorelines were occasional sources. Of the reefs that served as frequent sources to the metapopulation, local larval retention was generally greater than average (e.g., ~2% and ~3% versus ~0.5%) and larval export was also generally greater than average (>22% versus ~18%).

## DISCUSSION

While metapopulation concepts are increasingly recognized as a critical underpinning of spatially-explicit wildlife management methods (e.g., marine protected areas; Botsford et al. 2003, Figueira and Crowder 2006, Burgess et al. 2014, Holstein et al. 2015, Puckett and Eggleston 2016), metapopulations have rarely been evaluated holistically wherein demographic rates and dispersal are integrated to simulate dynamics of the entire metapopulation and performance of individual subpopulations. In the present study, I aggregated demographic (e.g, initial population estimates, demographic rates) and spatial information (e.g., reef distribution, areal footprint) for all subpopulations, evaluated larval connectivity via dispersal simulations,

and simulated dynamics of an entire marine metapopulation. Using this modeling framework applied to oyster reefs in the Albemarle-Pamlico Estuarine System, North Carolina, USA, I identified: 1) an overall stable, yet slightly declining metapopulation, 2) variable reef type-specific population trajectories depending on spatiotemporal variation in larval recruitment, 3) spatiotemporal variation in the source-sink status of reef subpopulations wherein subtidal sanctuaries and reefs located in the northeastern portion of the system frequently served as sources, and 4) a greater relative importance of inter-reef larval export on metapopulation dynamics relative to local larval retention processes. I further examined the management and broader implications of this work and recommend future management efforts within this system consider oysters as an interconnected metapopulation.

***Metapopulation and Source-Sink Dynamics***

Overall Metapopulation Trends – The 10% $day^{-1}$ larval mortality rate yielded an overall stable, yet slightly declining metapopulation (Figure 8b). Increases in overall metapopulation abundance corresponded with the period following the primary spawning peak (i.e., May-June) within the system. Increases in recruit abundance after the spawning peak were followed in subsequent periods with increases in sub-adult and adult abundance (i.e., corresponding with survival and growth of individuals into the next size class). The overall pattern of metapopulation decline with slight recovery following the spawning peak (Figure 8B) is indicative of the importance of recruitment within the system—a finding consistent with previous studies (e.g., Caley et al. 1996). The patterns of the overall metapopulation growth rate ($\lambda_M$) provide further support for this notion (Figure 13), wherein $\lambda_M$ exceeds 1 and the metapopulation is considered persistent only in the period following the primary spawning peak. These findings, wherein a network of oyster reef subpopulations was buffered and subsidized

through larval dispersal, lend strong support to the notion of an oyster metapopulation within the APES (sensu Levins 1969).

Population Trajectories – Overall oyster population trends by reef type exhibited an overall slight decline across reef type (Figure 9) and spatiotemporal variation in recruitment generally impacted population trajectories. Subtidal natural and cultch reefs generally received consistent recruitment during the annual primary and secondary spawning peaks (Figure 9A, 9B, 10A, 10B). Other reef types, such as hardened shorelines and intertidal natural reefs in Pamlico Sound (Figure 9D, 9E, 10D, 10E) received episodic recruitment—a finding consistent with a recent field-based study that examined oyster density and demographic rates on hardened shorelines and intertidal natural reefs in Pamlico Sound (Theuerkauf et al. 2017). The spatial distribution of reef types yielded a substantial influence on recruitment patterns. For example, subtidal natural and cultch reefs, which are distributed consistently throughout the APES, generally receive regular recruitment (Figure 10A, 10B). Conversely, hardened shorelines, which are concentrated primarily along the eastern shore of Pamlico Sound, received substantial, episodic recruitment following the May-June 2014 spawning event (Figure 10D), which corresponded with a period of strong southwesterly winds (Appendix 6).

Observed spatiotemporal variation in recruitment patterns generally led to similar subsequent patterns in sub-adult and adult size classes (Figures 11, 12). For example, substantial recruitment on hardened shorelines following the May-June recruitment event of 2014 (Figure 10D) yielded increases in sub-adult (Figure 11D) and adult (Figure 12D) populations on hardened shorelines in the subsequent time steps after the major recruitment event. Variation in demographics (i.e., growth and survival transition probabilities; Table 2) also yielded varied population-level outcomes by reef type. For example, while subtidal natural reefs exhibited

substantial, oscillatory population "booms and busts" (Figure 12A), the improved demographics (i.e., growth and survival transition probabilities) associated with subtidal sanctuaries (Figure 12C) yielded subpopulations less directly impacted by recruitment variation, although still in decline. The more stable (i.e., less oscillatory) sub-adult (Figure 11C) and adult (Figure 12C) subpopulations on subtidal sanctuaries in response to variation in recruitment patterns (Figure 10C) provides evidence of the buffering capacity of protected subpopulations and ability to withstand periods of reduced recruitment. This finding is consistent with field-based observations of these protected reefs within the system (Puckett and Eggleston 2012).

Spatiotemporal Variation in Source-Sink Dynamics – Source-sink status ($\lambda_c$) of reefs varied widely by reef type and between the May-June and July-August spawning peaks for oysters in APES (Figures 14, 15). During the primary spawning event (May-June), subtidal sanctuaries were the only reef type with a mean $\lambda_c$ exceeding one (i.e., on average, subtidal sanctuaries function as sources; Figure 14). The larger initial population size (Table 1) and enhanced demographic rates (Table 2) relative to other reef types likely allowed subtidal sanctuaries to function as sources. Some subtidal natural and cultch reefs, fewer intertidal natural reefs in Pamlico and Core Sounds, and no hardened shorelines served as sources during the May-June time steps (Figure 14). For the July-August dispersive periods, no reef types had a mean $\lambda_c$ exceeding one, although infrequently, subtidal sanctuaries, intertidal natural reefs in Core Sound, and hardened shorelines functioned as sources (Figure 15). Reefs serving as sources likely exhibited high population sizes (i.e., greater fecundity and associated larval output), enhanced demographic rates (e.g., enhanced survival), and ideal geographic placement (e.g., along dispersal pathways that connected multiple reefs) relative to reefs serving as sinks.

Frequent source reefs (i.e., high frequency of $\lambda_c > 1$ across recruitment events) exhibited greater rates of both larval export and local retention relative to other reefs. For example, for reefs where $\lambda_c > 1$ occurred 50% of the time, ~24% of larvae were exported to other reefs relative to ~18% exported for all reefs, and ~2% of larvae were retained locally relative to ~0.5% retained locally for all reefs (Table 4, 5). As frequent source reefs were generally located in the northeastern portion of Pamlico Sound (Figure 16), it is likely that these reefs are located along dispersal pathways that enhance potential connectivity. The process underlying enhanced local retention for frequent sources reefs is unknown, but previously identified semi-diurnal seiching within the APES (Luettich et al. 2002) may reduce dispersal distances in northeastern Pamlico Sound and promote greater local retention. Further evaluation of the processes underlying larval export and local retention is warranted.

Processes Underlying Metapopulation Dynamics and Source-Sink Structure – Inter-reef larval export substantially impacted metapopulation dynamics relative to local larval retention. Across all reefs, ~18% of larvae originating from a given reef successfully settled on a different reef (Table 4). This value ranged from as high as ~26% for natural subtidal reefs to a low of ~5% for natural intertidal reefs in Core Sound. The geographic distribution of reefs of differing reef types likely contributed to the variation in inter-reef larval connectivity. For example, natural subtidal reefs are distributed homogeneously throughout the APES, however natural intertidal reefs and hardened shorelines are limited to shoreline locations. Local retention occurred less frequently than inter-reef larval export (e.g., ~0.5% vs. ~18%), and likely yielded less impact on metapopulation dynamics. Inter-reef larval connectivity and local retention rates were substantially higher in the present study (~18% and ~0.5%, respectively) than in a previous study that examined inter-reef larval connectivity and local retention of 10 subtidal sanctuaries within

the APES (~0.1% and ~0.3%, respectively; Puckett and Eggleston 2016). The elevated inter-reef larval connectivity and local retention rates observed in the present study is due to the inclusion of all known reefs within the system relative to the previous study that included only subtidal sanctuaries (i.e., greater probability of larvae originating from a given reef encountering and settling in a different reef when connections between all reefs are possible).

Given the high rates of inter-reef larval connectivity relative to local retention observed in the present study, it is probable that larval connectivity is a more important driver of metapopulation dynamics than subpopulation demographics within this system. High levels of inter-reef larval connectivity decouple subpopulation reproduction and recruitment (i.e., reefs are less dependent upon recruitment derived from local retention; Warner and Cowen 2002, Figueira 2009). For example, Figueira (2009) documented a declining importance of demographic rates on metapopulation dynamics at low levels of local retention. Contrastingly, when local retention is equivalent or greater than larval import from other reefs, subpopulation demographic rates (e.g., growth and survival) are potentially more important drivers of metapopulation dynamics. However, to quantitatively evaluate the relative importance of within-reef demographics, local retention, and inter-reef larval connectivity on metapopulation dynamics and source-sink dynamics (i.e., $\lambda_c$), elasticity analyses are needed and are the subject of ongoing research (Theuerkauf et al., unpublished data). Elasticity values represent the proportional contribution of each model parameter to $\lambda_c$ by assessing how $\lambda_c$ changes in response to proportional perturbations of model parameters (e.g., increase/decrease by 5%; Puckett and Eggleston 2016).

Although it is appears that inter-reef larval connectivity is a more substantial driver of metapopulation dynamics within this system, the role of demographics on metapopulation dynamics was still evident. For example, 12 of 14 (86%) of subtidal sanctuaries served as

metapopulation sources, but only 7–49% of other reef types served as sources at least once (Table 5). It is probable that the enhanced demographics associated with subtidal sanctuaries relative to other reef types contributed to their capacity to serve as metapopulation sources (Table 2). Heightened vertical relief, protection from fishery harvest, and placement within areas of suitable habitat are likely contributing factors to the capacity of subtidal sanctuaries to serve as sources (Schulte et al. 2009, Puckett and Eggleston 2012, Peters et al. 2017). Fishing mortality, reduced vertical relief, and reduced habitat quality likely contribute to the poorer demographic rates of other reef types (Peters et al. 2017).

***Caveats Regarding Model Assumptions***

Several assumptions were made to simplify the metapopulation model applied in the present study. First, to estimate reef type- and season-specific growth and survival transition probabilities, I averaged oyster density data from all quadrats for a given reef site for each sampling event and subsequently partitioned density estimates into the three size classes. I then pooled this data and applied a linear optimization approach to determine the least squares estimate for five growth and survival transition probabilities based on size-class specific density data from time *t* and *t+1*. This approach allowed for reef type- and season-specific variation in growth and survival transition probabilities, but did not allow for spatial variation in transition probabilities within a reef type or season.

Second, distinct proportional daily larval mortality rates: 7.5% $day^{-1}$, 10% and 20%, yielded widely varying metapopulation and source-sink dynamics outcomes. While I provide population trajectories and metapopulation summary statistics under the 7.5% and 20% $day^{-1}$ larval mortality rates in the Appendix to show the range of possible metapopulation outcomes, the 10% proportional daily larval mortality scenario qualitatively aligned with prior field-based

observations. Given the impact of this parameter on metapopulation outcomes, further field-based evaluation of proportional daily larval mortality rates within the APES is warranted.

Third, larval dispersal was modeled as passive drift driven solely by surface currents despite evidence that oyster larvae migrate vertically and are generally distributed in the water column according to their ontogenetic stage (Carriker 1951, Dekshenieks et al. 1996, Puckett and Eggleston 2016). Given the well-mixed nature of the APES, it is unclear what water column features oyster larvae might respond to (if any) to regulate their depth, other than a general ontogenetic shift towards deeper depths as sinking speeds exceed swimming speeds (Dekshenieks et al. 1996). In our study system, larval dispersal and connectivity were more sensitive to location and the date of spawning than to larval behavior (Puckett et al. 2014). Including larval behavior may have reduced dispersal distances, thereby increasing local retention, decreasing inter-reef connectivity and ultimately influencing our projection of metapopulation abundance (North et al. 2008, Puckett et al. 2014, Puckett and Eggleston 2016).

***Management and Broader Implications***

The present study provides strong evidence for the management of oysters within the APES as an interconnected metapopulation driven largely by inter-reef larval connectivity. Thus, oyster restoration and conservation strategies within the APES that focus on maximizing inter-reef connectivity are likely to be most effective. Subtidal sanctuaries served as the most frequent sources to the metapopulation, likely due to a combination of their high population sizes, enhanced demographic rates, and optimal geographic placement to enhance inter-reef connectivity relative to reefs serving as sinks. This finding is consistent with previous studies documenting the value of no-harvest marine protected areas (e.g., Agardy 1994, Botsford et al. 2003, Schulte et al. 2009). Continued protection of subtidal sanctuaries from fishery harvest and

construction of additional sanctuaries in areas likely to promote inter-reef connectivity should be a management priority within this system. Additionally, as some subtidal natural and cultch reefs served as frequent sources to the metapopulation, this study provides evidence of the potential metapopulation source value of fished reefs that should be accounted for in fishery management plans.

***Conclusions***

The present study applied an empirically-based, metapopulation modeling framework to simulate an entire oyster metapopulation to understand underlying source-sink dynamics. Within the APES, inter-reef larval connectivity appears to be a major driver of oyster metapopulation dynamics, and reef-specific population sizes, demographics, and location likely combined to mediate source-sink status. While inter-reef larval connectivity was likely the major driver of metapopulation dynamics, demographics also played an underlying role in mediating metapopulation dynamics (e.g., 86% of sanctuaries served as metapopulation sources). Oyster management efforts should aim to protect and restore frequent 'source' subpopulations while managing harvest from 'sink' subpopulations.

**ACKNOWLEDGEMENTS**

I thank K. Theuerkauf, K. Shertzer, P. Sullivan for their assistance with analyses and interpretation. I thank the NC State Climate Office for providing wind data. Funding for the project and completion of the manuscript was provided by North Carolina Sea Grant (R12-HCE-2) and the National Science Foundation (OCE-1155609) to D. Eggleston, well as a National Defense Science and Engineering Graduate Fellowship (contract FA9550-11- C-0028 awarded by the Department of Defense, Air Force Office of Scientific Research, 32 CFR 168a), North

Carolina Coastal Conservation Association Scholarship, and Beneath the Sea Foundation Scholarship to S. Theuerkauf.

## LITERATURE CITED


Agardy, M. T. 1994. Advances in marine conservation: the role of marine protected areas. *Trends in Ecology and Evolution* 9:267–270.

Ballance, G., Eggleston, D. B., Plaia, G., & B. J. Puckett. 2009. Oyster settlement and reef mapping in Pamlico Sound. Final Report for the Fisheries Research Grant, 07-EP-04. NC Division of Marine Fisheries, Morehead City, NC, 20 pp.

Beissinger, S. R., & M. I. Westphal. 1998. On the use of demographic models of population viability in endangered species management. *The Journal of Wildlife Management* 62:821–841.

Botsford, L. W., Micheli, F., & A. Hastings. 2003. Principles for the design of marine reserves. *Ecological Applications* 13:S25–S31.

Burgess, S. C., Nickols, K. J., Griesemer, C. D., Barnett, L. A. K., Dedrick, A. G., Satterthwaite, E. V., Yamane, L., Morgan, S. G., White, J. W., & L. W. Botsford. 2014. Beyond connectivity: how empirical methods can quantify population persistence to improve marine protected-area design. *Ecological Applications* 24:257–270.

Caley, M. J., Carr, M. H., Hixon, M. A., Hughes, T. P., Jones, G. P., & B. A. Menge. 1996. Recruitment and the local dynamics of open marine populations. *Annual Review of Ecology and Systematics* 27:477–500.

Carriker, M. R. 1951. Ecological observations on the distribution of oyster larvae in New Jersey estuaries. *Ecological Monographs* 21:19–38.

Caswell, H. 2001. Matrix population models. New York, NY: John Wiley & Sons, Ltd. 722 pp.

Coen, L. D., Brumbaugh, R. D., Bushek, D., Grizzle, R., Luckenbach, M. W., Posey, M. H., Powers, S. P. & S. Tolley. 2007. Ecosystem services related to oyster restoration. *Marine Ecology Progress Series* 341:303–307.

Cox, C. & R. Mann. 1992. Temporal and spatial changes in fecundity of eastern oysters, *Crassostrea virginica* (Gmelin, 1791) in the James River, Virginia. *Journal of Shellfish Research* 11:49–54.

Dekshenieks, M. M., Hofmann, E. E., Klinck, J. M. & E. N. Powell. 1996. Modeling the vertical distribution of oyster larvae in response to environmental conditions. *Marine Ecology Progress Series* 136:97–110.

Dudley, D. L., & M. H. Judy. 1973. Seasonal abundance and distribution of juvenile blue crabs in Core Sound, NC 1965–68. *Chesapeake Science* 14:51–55.

Epperly, S. P., & S. W. Ross. 1986. *Characterization of the North Carolina Pamlico-Albemarle complex*. National Oceanic and Atmospheric Administration Technical Memorandum. NMFS-SEFC-175. Washington, D.C.

ESRI. 2016. ArcGIS Desktop: Release 10.3. Redlands, CA: Environmental Systems Research Institute.

Figueira, W. F., & L. B. Crowder. 2006. Defining patch contribution in source-sink metapopulations: the importance of including dispersal and its relevance to marine systems. *Population Ecology* 48:215–224.

Figueira, W. F. 2009. Connectivity or demography: defining sources and sinks in coral reef fish metapopulations. *Ecological Modelling* 220:1126–1137.

Grabowski, J. H. & C. H. Peterson. 2007. Restoring oyster reefs to recover ecosystem services. Pp. 281–298 in Cuddington, K., Byers, J.E., Wilson, W.G., Hastings A., eds. Ecosystem Engineers: Plants to Protists. Elsevier.

Halpern, B. S. 2003. The impact of marine reserves: do reserves work and does reserve size matter? *Ecological Applications* 13:117–137.

Haase, A. T., Eggleston, D. B., Luettich, R. A., Weaver, R. J. & B. J. Puckett. 2012. Estuarine circulation and predicted oyster larval dispersal among a network of reserves. *Estuarine, Coastal and Shelf Science* 101:33–43.

Hanski, I. 1998. Metapopulation dynamics. *Nature* 396:41.

Holstein, D. M., Smith, T. B., Gyory, J., & C. B. Paris. 2015. Fertile fathoms: deep reproductive refugia for threatened shallow corals. *Scientific Reports* 5:e12407.

Kennedy, V. S., R. I. E. Newell & A. F. Eble. 1996. The eastern oyster (*Crassostrea virginica*). College Park, MD: Maryland Sea Grant Press. 734 pp.

Levins, R. 1969. Some demographic and genetic consequeneces of environmental heterogeneity for biological control. *Bulletin of the Entomological Society of America* 15:237–240.

Levitan, D. R. 1991. Influence of body size and population density on fertilization success and reproductive output in a free-spawning invertebrate. *The Biological Bulletin* 181:262–268.

Lewis, O., Thomas, C., Hill, J., Brookes, M., Crane, T. P., Graneau, Y., Mallet, J. & O. Rose. 1997. Three ways of assessing metapopulation structure in the butterfly *Plebejus argus*. *Ecological Entomology* 22:283–293.

Luettich, R. A., Carr, S. D., Reynolds-Fleming, J. V., Fulcher, C. W. & J. E. McNinch. 2002. Semi-diurnal seiching in a shallow, micro-tidal lagoonal estuary. *Continental Shelf Research* 22:1669–1681.

Mann, R., & D. A. Evans. 1998. Estimation of oyster, *Crassostrea virginica*, larval production and advective loss in relation to observed recruitment in the James River, Virginia. *Journal of Shellfish Research* 17:239–254.

McMurray, S. E., Henkel, T. P., & J. R. Pawlik. 2010. Demographics of increasing populations of the giant barrel sponge *Xestospongia muta* in the Florida Keys. *Ecology* 91:560–570.

Mroch III, R. M., Eggleston, D. B., & B. J. Puckett. 2012. Spatiotemporal variation in oyster fecundity and reproductive output in a network of no-take reserves. *Journal of Shellfish Research* 31:1091–1101.

North, E. W., Schlag, Z., Hood, R. R., Li, M., Zhong, L., Gross, T., & V. S. Kennedy. 2008. Vertical swimming behavior influences the dispersal of simulated oyster larvae in a coupled particle-tracking and hydrodynamic model of Chesapeake Bay. *Marine Ecology Progress Series* 359:99–115.

North Carolina Department of Environmental Quality, Division of Coastal Management. 2012. *Estuarine Shorelines of NC Spatial Dataset.* Shapefile dataset. https://deq.nc.gov/about/divisions/coastal-management/coastal-management-data/spatial-data-maps##Estuarine Shorelines. Accessed 15 March 2016.

North Carolina Department of Environmental Quality, Division of Marine Fisheries. 2013. Estuarine benthic habitat mapping program. Shapefile dataset. http://portal.ncdenr.org/web/mf/shellfish-habitat- mapping. Accessed 15 Mar 2016.

Peters, J., Eggleston, D. B., Puckett, B. J., & S. J. Theuerkauf. 2017. Oyster demographics in harvested reefs versus no-take reserves: implications for larval spillover and restoration. *Frontiers in Marine Science* 4:e326.

Pierson, K. & D. B. Eggleston. 2014. Response of estuarine fish to large-scale oyster reef restoration. *Transactions of the American Fisheries Society* 143:273−288.

Pietrafesa, L. J., Janowitz, G. S., Chao, T. Y., Weisberg, R. H., Askari, F. and E. Noble. 1986. *The physical oceanography of Pamlico Sound*. UNC Sea Grant Publication. UNC-WP-86-5, Raleigh, NC, USA.

Planes, S., Jones, G. P., & S. R. Thorrold. 2009. Larval dispersal connects fish populations in a network of marine protected areas. *Proceedings of the National Academy of Sciences* 106:5693–5697.

Powers, S. P., Peterson, C. H., Grabowski, J. H. & H. S. Lenihan. 2009. Success of constructed oyster reefs in no-harvest sanctuaries: implications for restoration. *Marine Ecology Progress Serie*s 389:159–170.

Puckett, B. J. & Eggleston, D. B. 2012. Oyster demographics in a network of no-take reserves: recruitment, growth, survival, and density dependence. *Marine and Coastal Fisheries* 4:605–627.

Puckett, B. J., Eggleston, D. B., Kerr, P. C., & Luettich, R. A. 2014. Larval dispersal and population connectivity among a network of marine reserves. *Fisheries Oceanography* 23:342–361.

Puckett, B. J., & D. B. Eggleston. 2016. Metapopulation dynamics guide marine reserve design: importance of connectivity, demographics, and stock enhancement. *Ecosphere* 7.6.

Pulliam, H. R. 1988. Sources, sinks, and population regulation. *The American Naturalist* 132:652–661.

Reyns, N. B., D. B. Eggleston, & R. A. Luettich. 2007. Dispersal dynamics of postlarval blue crabs, *Callinectes sapidus*, within a wind-driven estuary. *Fisheries Oceanography* 16:257–272.

Roelofs, E. W. & D. F. Bumpus. 1953. The hydrography of Pamlico Sound. *Bulletin of Marine Science* 3:181–205.

Schulte, D. M., Burke, R. P., & R. N. Lipcius. Unprecedented restoration of a native oyster metapopulation. *Science* 325:1124–1128.

Theuerkauf, S. J., Eggleston, D. B., Puckett, B. J., and K. W. Theuerkauf. 2016. Wave exposure structures oyster distribution on natural intertidal reefs, but not on hardened shorelines. *Estuaries and Coasts* doi:10.1007/s12237-016-0153-6.

Theuerkauf, S. J., Eggleston, D. B., Theuerkauf, K. W., & B. J. Puckett. 2017. Oyster density and demographic rates on natural intertidal reefs and hardened shoreline structures. *Journal of Shellfish Research* 36:87–100.

Warner, R. R., & R. K. Cowen. Local retention of production in marine populations: evidence, mechanisms, and consequences. *Bulletin of Marine Science* 70:245–249.

Xie, L. and D. B. Eggleston. 1999. Computer simulations of wind-induced estuarine circulation patterns and estuary-shelf exchange processes: The potential role of windforcing on larval transport. *Estuarine, Coastal and Shelf Science* 49:221–234.

Table 1. Summary information on number of unique reefs, total reef area, average reef area, average initial density (ind. $m^{-2}$), average initial population size, and average initial size structure by reef type for model simulations. Reef location and area information was derived from the North Carolina Division of Marine Fisheries Shellfish Mapping Program and the North Carolina Division of Coastal Management Estuarine Shoreline Mapping Program. Average initial densities for each reef type were derived from Peters et al. (in review), Theuerkauf et al. 2017, and Puckett et al. 2016. Average initial population size was calculated by multiplying spatially-explicit oyster densities $m^{-2}$ by reef area. Average initial size structure represents the average percentage of individuals within a given size class on a given reef used to initialize the metapopulation model.

| Reef Type | Number of Unique Reefs | Total Reef Area (ha) | Average Reef Area (ha) | Average Initial Density (ind. $m^{-2}$) | Average Initial Population Size (% of metapopulation) | Average Initial Size Structure (% in size class) | | |
|---|---|---|---|---|---|---|---|---|
| | | | | | | Recruits (0-30mm) | Sub-Adults (30-75mm) | Adults (75mm+) |
| Subtidal Natural Reefs | 301 | 934.27 | 3.12 | 61 | 2,307,464 | 29% | 55% | 16% |
| Subtidal Cultch Reefs | 53 | 15.32 | 0.29 | 152 | 438,967 | 28% | 54% | 18% |
| Subtidal Sanctuary Reefs | 14 | 66.02 | 4.72 | 670 | 26,323,847 | 25% | 68% | 7% |
| Hardened Shoreline Reefs | 149 | 2.69 | 0.10 | 69 | 69,653 | 2% | 65% | 33% |
| Intertidal Natural Reefs (Pamlico Sound) | 57 | 10.43 | 0.28 | 121 | 384,183 | 34% | 58% | 8% |
| Intertidal Natural Reefs (Core Sound) | 72 | 11.82 | 0.24 | 842 | 2,483,700 | 39% | 55% | 6% |

Table 2: Reef type- and season-specific transition probabilities utilized in model simulations. Transition probabilities represent the probability of surviving and remaining in a given size class or surviving and growing into the next size class (sensu Caswell 2001).

| Reef Type | stage at *t+1* | Time Period: May-June (spring) — stage at *t* | | | Time Period: July-August (summer) — stage at *t* | | | Time Period: September-April (fall/winter) — stage at *t* | | |
|---|---|---|---|---|---|---|---|---|---|---|
| | | **Recruits** | **Sub-Adults** | **Adults** | **Recruits** | **Sub-Adults** | **Adults** | **Recruits** | **Sub-Adults** | **Adults** |
| **Natural (Subtidal)** | **Recruits** | 0.21 | 0 | 0 | 0.23 | 0 | 0 | 0.16 | 0 | 0 |
| | **Sub-Adults** | 0.29 | 0.70 | 0 | 0.58 | 0.65 | 0 | 0.38 | 0.49 | 0 |
| | **Adults** | 0 | 0.08 | 0.58 | 0 | 0.01 | 0.22 | 0 | 0.23 | 0.07 |
| **Cultch (Subtidal)** | **Recruits** | 0.21 | 0 | 0 | 0.23 | 0 | 0 | 0.21 | 0 | 0 |
| | **Sub-Adults** | 0.29 | 0.61 | 0 | 0.58 | 0.65 | 0 | 0.38 | 0.49 | 0 |
| | **Adults** | 0 | 0.01 | 0.62 | 0 | 0.08 | 0.23 | 0 | 0.08 | 0.06 |
| **Sanctuary (Subtidal)** | **Recruits** | 0.1 | 0 | 0 | 0.11 | 0 | 0 | 0.11 | 0 | 0 |
| | **Sub-Adults** | 0.45 | 0.71 | 0 | 0.73 | 0.72 | 0 | 0.08 | 0.71 | 0 |
| | **Adults** | 0 | 0.1 | 0.87 | 0 | 0.11 | 0.79 | 0 | 0.49 | 0.04 |
| **Hardened Shorelines** | **Recruits** | 0.21 | 0 | 0 | 0.08 | 0 | 0 | 0.21 | 0 | 0 |
| | **Sub-Adults** | 0.29 | 0.61 | 0 | 0.92 | 0.65 | 0 | 0.38 | 0.77 | 0 |
| | **Adults** | 0 | 0.04 | 0.65 | 0 | 0.03 | 0.38 | 0 | 0.21 | 0.99 |
| **Natural (Intertidal, Core Sound)** | **Recruits** | 0.21 | 0 | 0 | 0.23 | 0 | 0 | 0.21 | 0 | 0 |
| | **Sub-Adults** | 0.29 | 0.61 | 0 | 0.58 | 0.77 | 0 | 0.42 | 0.49 | 0 |
| | **Adults** | 0 | 0.05 | 0.68 | 0 | 0.01 | 0.36 | 0 | 0.09 | 0.01 |
| **Natural (Intertidal, Pamlico Sound)** | **Recruits** | 0.21 | 0 | 0 | 0.23 | 0 | 0 | 0.21 | 0 | 0 |
| | **Sub-Adults** | 0.29 | 0.61 | 0 | 0.77 | 0.77 | 0 | 0.71 | 0.77 | 0 |
| | **Adults** | 0 | 0.02 | 0.99 | 0 | 0.02 | 0.99 | 0 | 0.02 | 0.01 |

Table 3. Size class- (i.e., 0-30 mm, 30-75 mm, and 75+ mm) and season-specific (i.e., May-June and July-August) per capita oyster fecundity estimates (# eggs / oyster) for oyster reefs in APES used in metapopulation simulations (derived from Mroch et al. 2012).

| | **Season** | |
|---|---|---|
| **Size Class** | **May-June** | **July-August** |
| **0–30 mm** | 345.98 | 51.92 |
| **30–75 mm** | 7,166.70 | 472.35 |
| **75+ mm** | 37,333.25 | 1,737.92 |

Table 4: Average percent of larvae (i.e., across all 10 simulated dispersal events) retained locally versus exported between reefs. Local larval retention includes all larvae originating from a given reef that settle on the same reef. Larval export includes all larvae originating from a given reef that settle on a different reef.

| | Local Retention | Larval Export |
|---|---|---|
| All Reef Types | 0.38% | 17.66% |
| Natural (Subtidal) | 0.64% | 26.03% |
| Cultch (Subtidal) | 0.10% | 23.77% |
| Sanctuary (Subtidal) | 0.71% | 19.76% |
| Hardened Shorelines | 0.06% | 8.35% |
| Natural (Intertidal, Core Sound) | 0.41% | 5.33% |
| Natural (Intertidal, Pamlico Sound) | 0.01% | 7.17% |

Table 5: Total number of reefs of a specific reef type associated with a $\lambda_c > 1$ (i.e., $\lambda_c \geq 1$ indicates a given reef functioned as a source during time *t*) at varying frequencies. For each level of frequency of $\lambda_c \geq 1$, the corresponding average percent of larvae retained locally versus exported between reefs is provided. Local larval retention includes all larvae originating from a given reef that settle on the same reef. Larval export includes all larvae originating from a given reef that settle on a different reef.

| | Reef Type | | | | | | | |
|---|---|---|---|---|---|---|---|---|
| Frequency of $\lambda_c > 1$ | Natural (Subtidal) | Cultch (Subtidal) | Sanctuary (Subtidal) | Hardened Shorelines | Natural (Intertidal, Core Sound) | Natural (Intertidal, Pamlico Sound) | Local Retention | Larval Export |
| 50% | 1 | 0 | 3 | 0 | 0 | 0 | 1.51% | 24.36% |
| 40% | 7 | 0 | 4 | 0 | 0 | 0 | 2.50% | 24.89% |
| 30% | 25 | 4 | 4 | 2 | 0 | 0 | 0.24% | 27.61% |
| 20% | 29 | 5 | 1 | 5 | 3 | 0 | 1.36% | 26.87% |
| 10% | 53 | 17 | 0 | 16 | 22 | 4 | 0.38% | 22.05% |

**FIGURES**

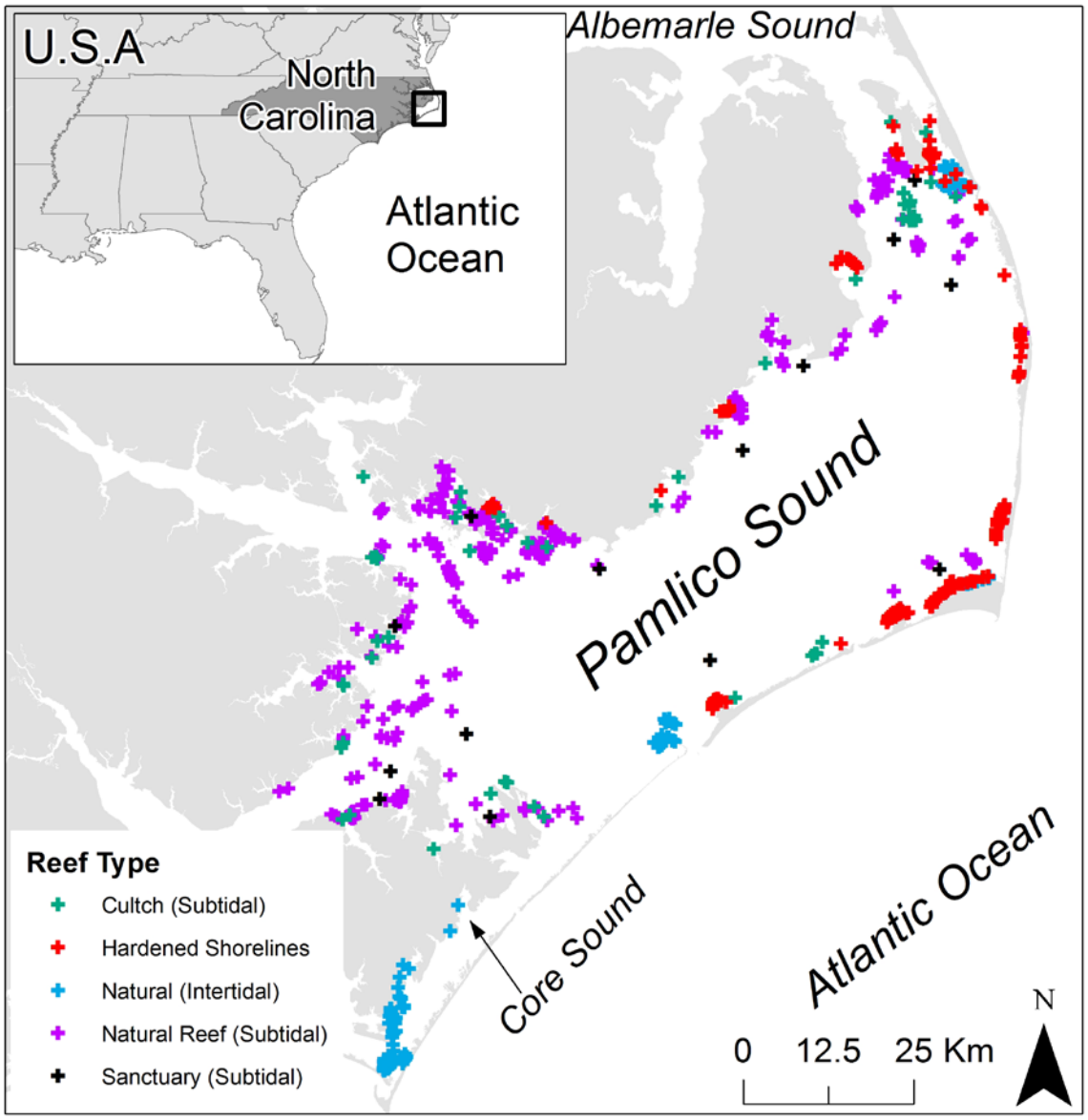


Figure 1: A) Map of the Albemarle-Pamlico Estuarine System showing the distribution of various oyster reefs by reef type, including cultch (teal), hardened shorelines (red), natural intertidal (blue), natural subtidal (purple), and sanctuary (black) reefs. Reefs not to scale.

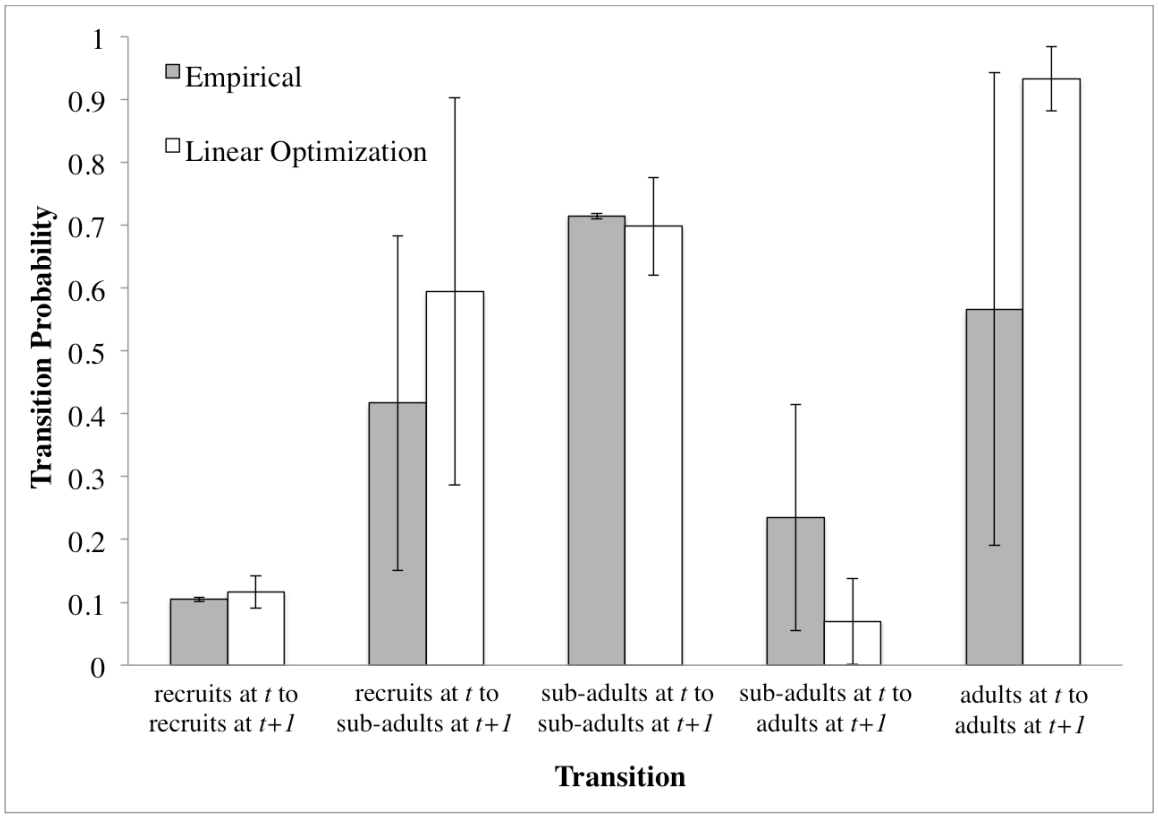


Figure 2: Comparison of transition probability estimates for oyster sanctuaries derived empirically (gray; based on Puckett and Eggleston 2016) and from linear optimization (white). Error bars represent standard deviation.

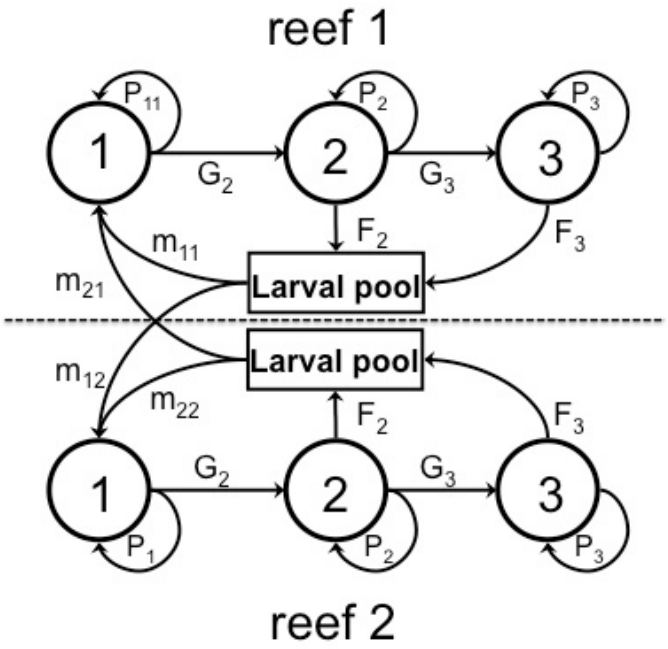


Figure 3: A simplified life cycle graph (adapted from Puckett and Eggleston 2016) depicting the spatially explicit, size-structured matrix metapopulation model used in this study. Two subpopulations (separated by dotted line) and three size classes (circles) are shown. The model used in the present study consisted of 646 reefs and three size classes. Model parameters are as follows: $P_i$ is the probability of surviving and remaining in size class $i$; $G_j$ is the probability of surviving and growing into size class $j$; $F_i$ is the per capita fecundity of size class $i$, and $m_{jk}$ is the proportion of larvae spawned in reef $j$ that settle in reef $k$.

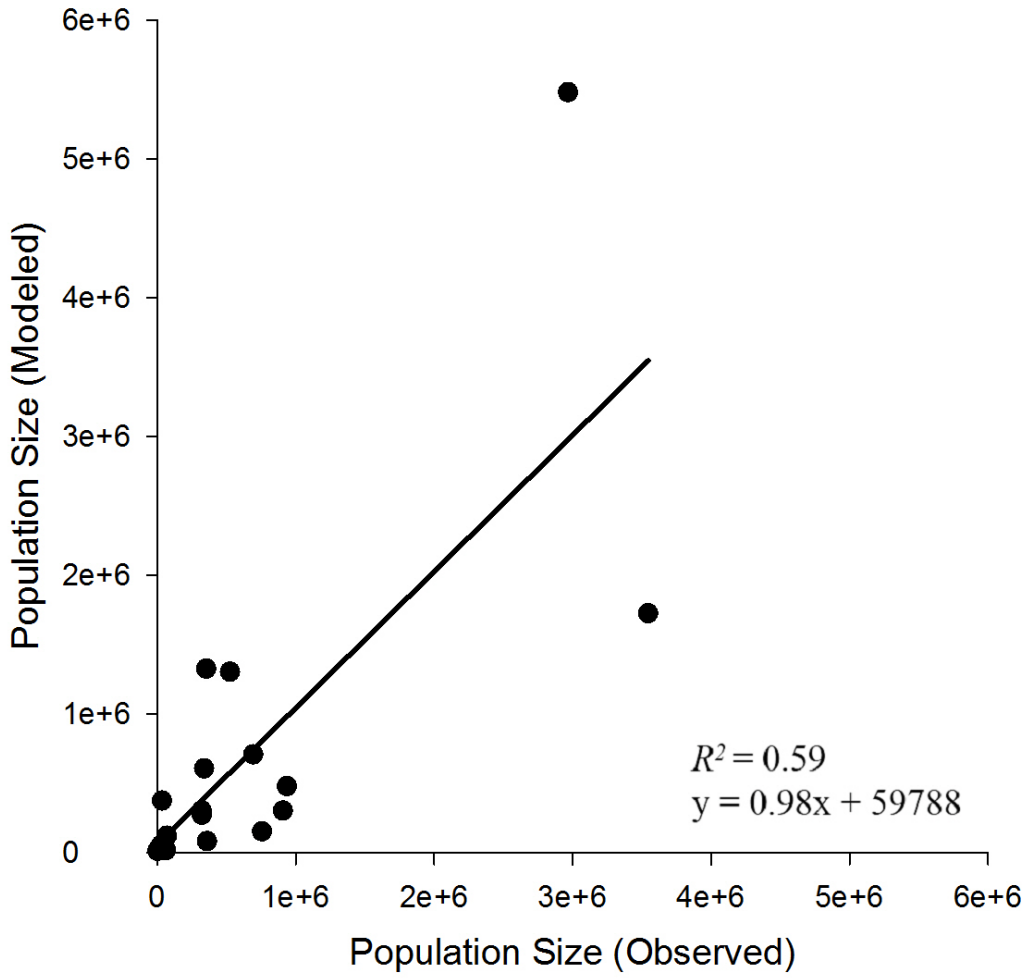


Figure 4. Relationship between observed and predicted population size at natural subtidal and cultch reefs. Estimates of observed population size are derived from field sampling of natural subtidal and cultch reefs in August of 2012 and estimates of predicted population size are derived from metapopulation model simulations corresponding to the same time period in the present study (under the 10% larval mortality day$^{-1}$ scenario).

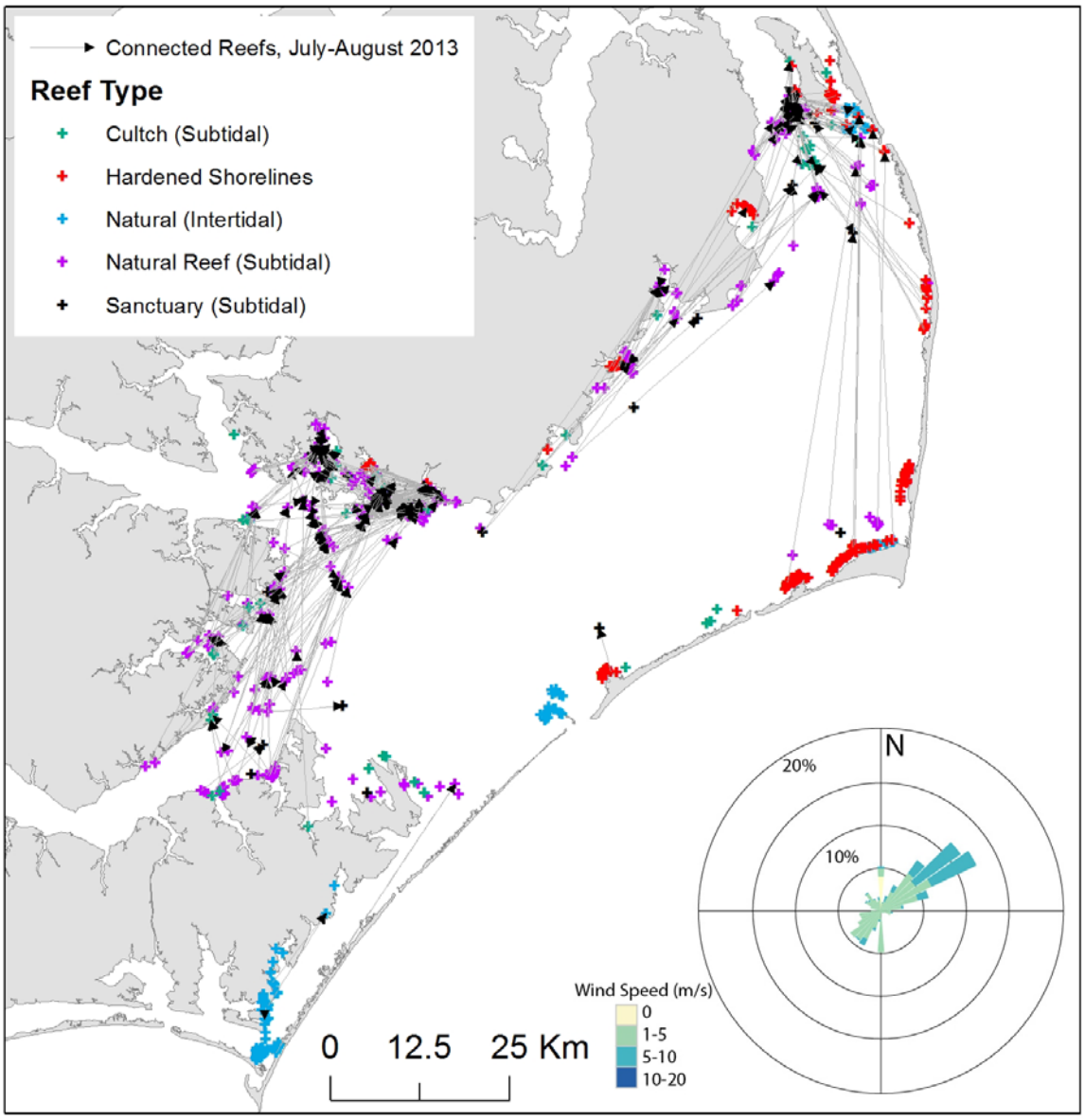


Figure 5. Map depicting larval dispersal patterns during a period of average wind conditions (i.e., predominantly southwesterly winds, towards northeast) during July–August of 2013. Lines depict connections between natal and settled reef locations (arrowheads point towards settled reef locations). Note that lines depict the least-cost path between reefs and not the actual dispersal path, and only a random subset (5%) of all connections are shown for illustrative purposes.

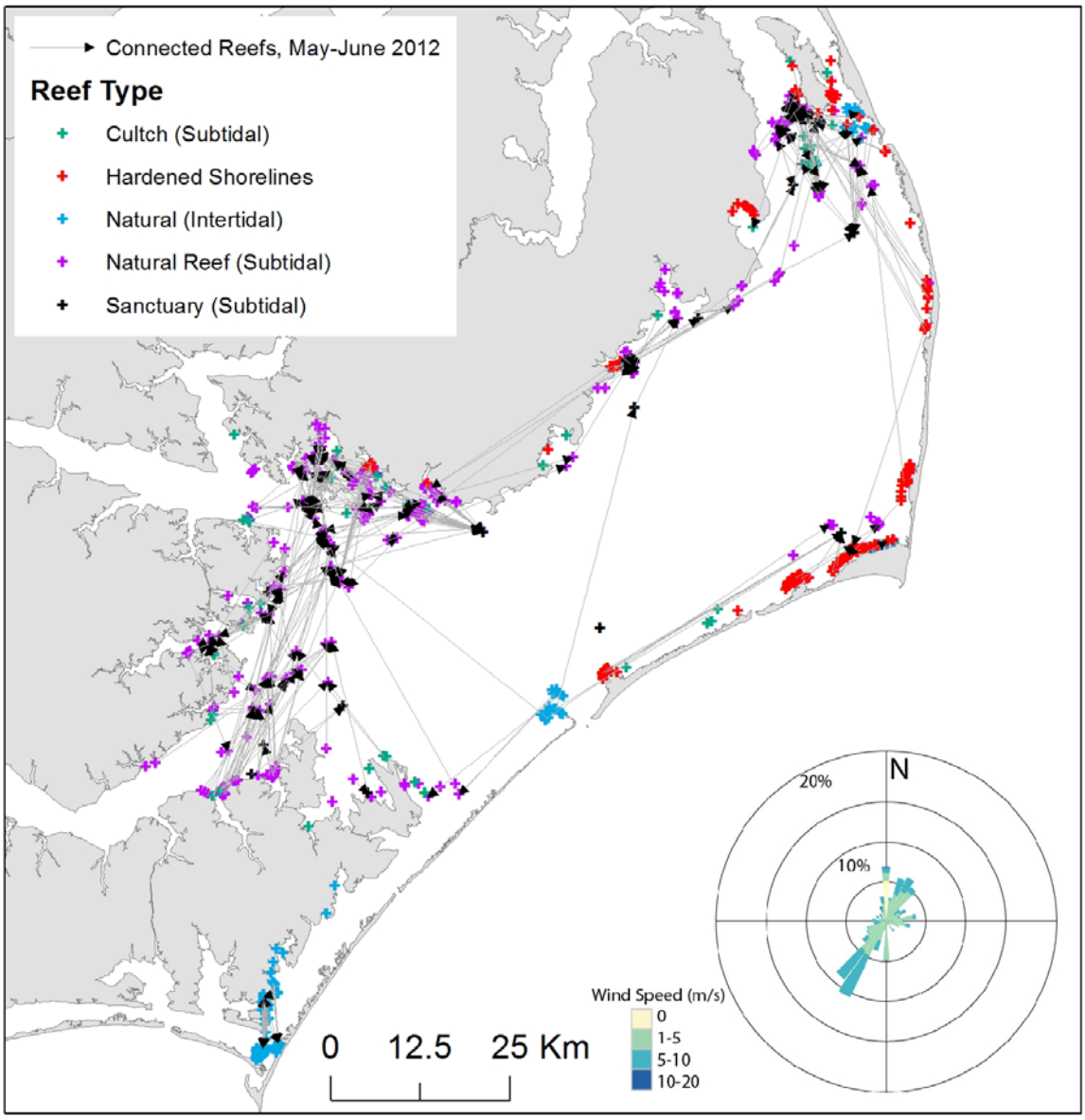


Figure 6. Map depicting larval dispersal patterns during a period of anomalously strong northeasterly winds (towards southwest) during May–June of 2012. Lines depict connections between natal and settled reef locations (arrowheads point towards settled reef locations). Note that lines depict the least-cost path between reefs and not the actual dispersal path, and only a random subset (5%) of all connections are shown for illustrative purposes.

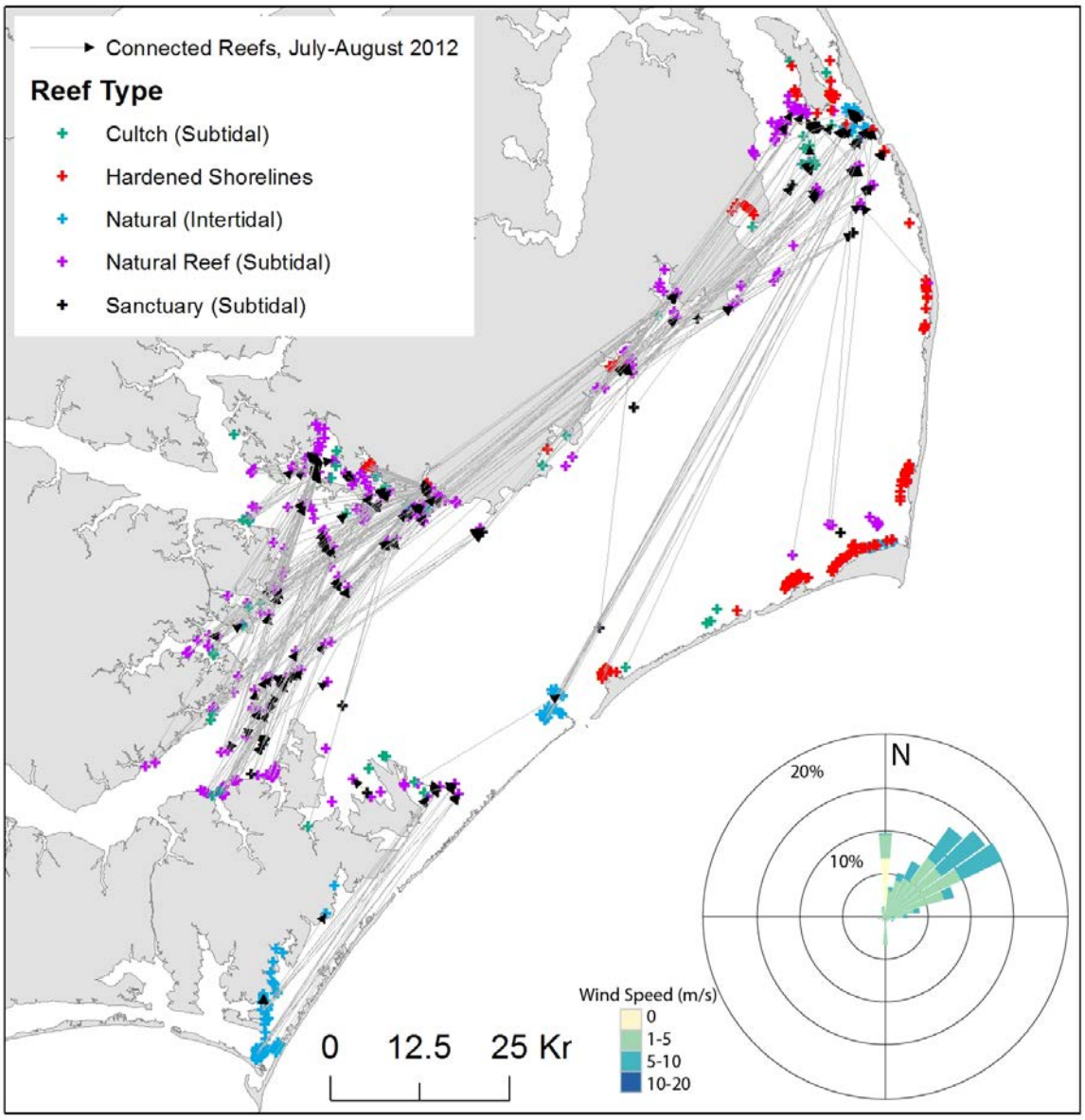


Figure 7. Map depicting larval dispersal patterns during a period of anomalously strong southwesterly winds (towards northeast) during July–August of 2012. Lines depict connections between natal and settled reef locations (arrowheads point towards settled reef locations). Note that lines depict the least-cost path between reefs and not the actual dispersal path, and only a random subset (5%) of all connections are shown for illustrative purposes.

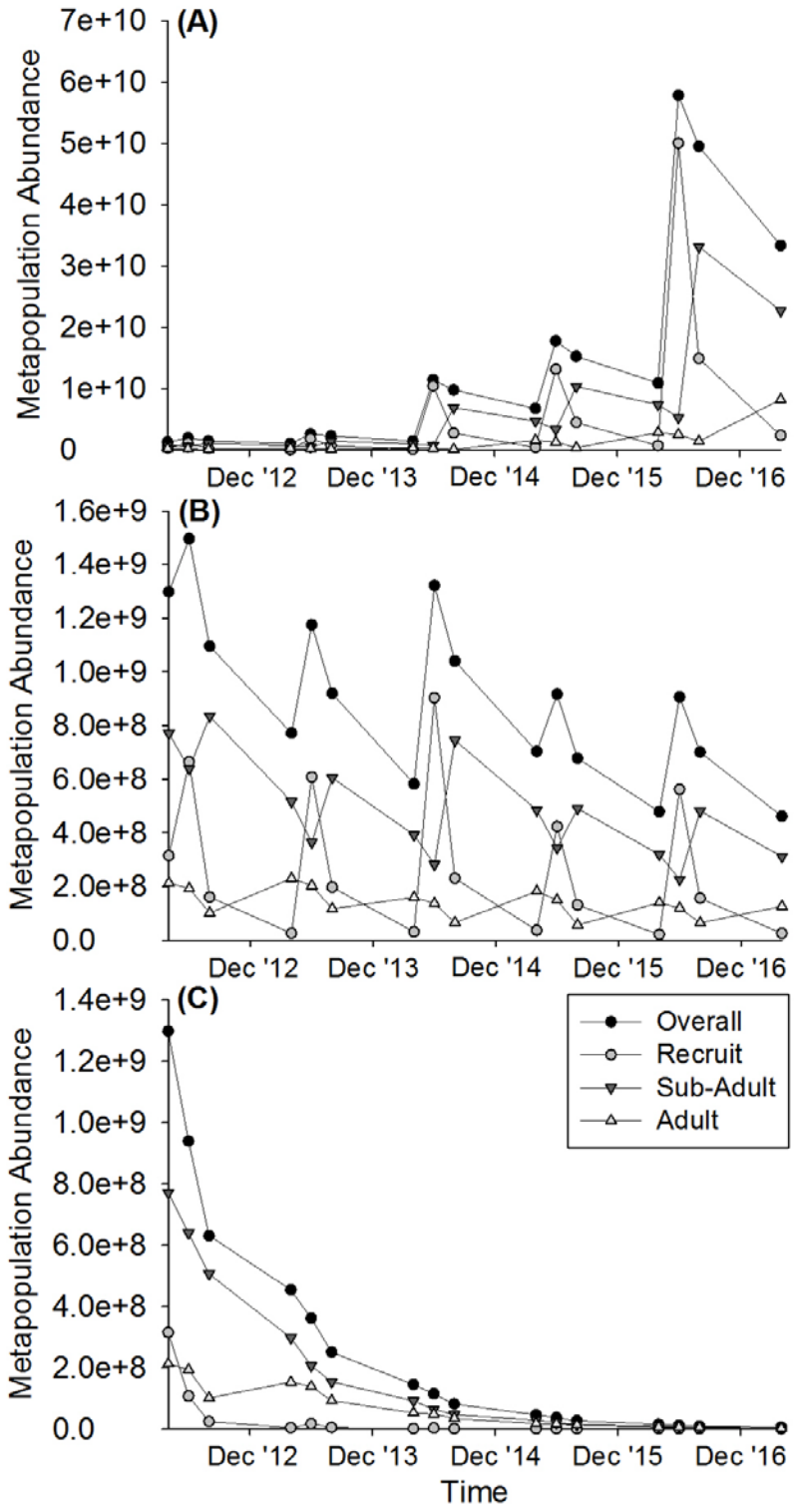


Figure 8. Total metapopulation abundance (overall and size-class specific) across the five year model timeframe under three larval mortality scenarios: (A) – 7.5% mortality day$^{-1}$, (B) – 10% mortality day$^{-1}$, (C) – 20% mortality day$^{-1}$. Further information on selection of these larval mortality rates can be found in the 'Methods.'

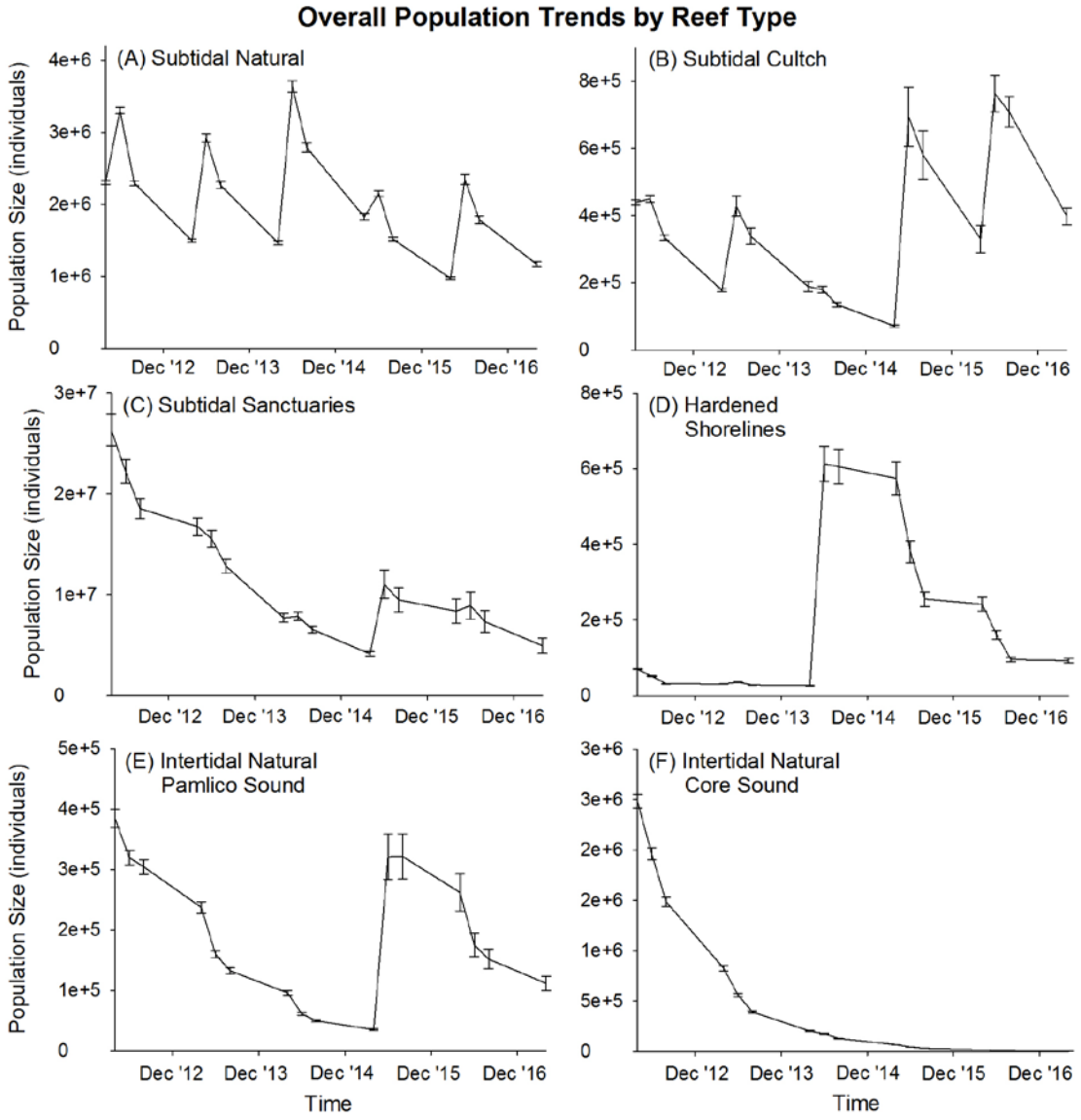


Figure 9: Overall population trends (i.e., inclusive of all size classes) by reef type across the five-year model timeframe under the 10% larval mortality day$^{-1}$ scenario. Points represent the average population size on a given reef type at a given time step; error bars represent standard error of the mean.

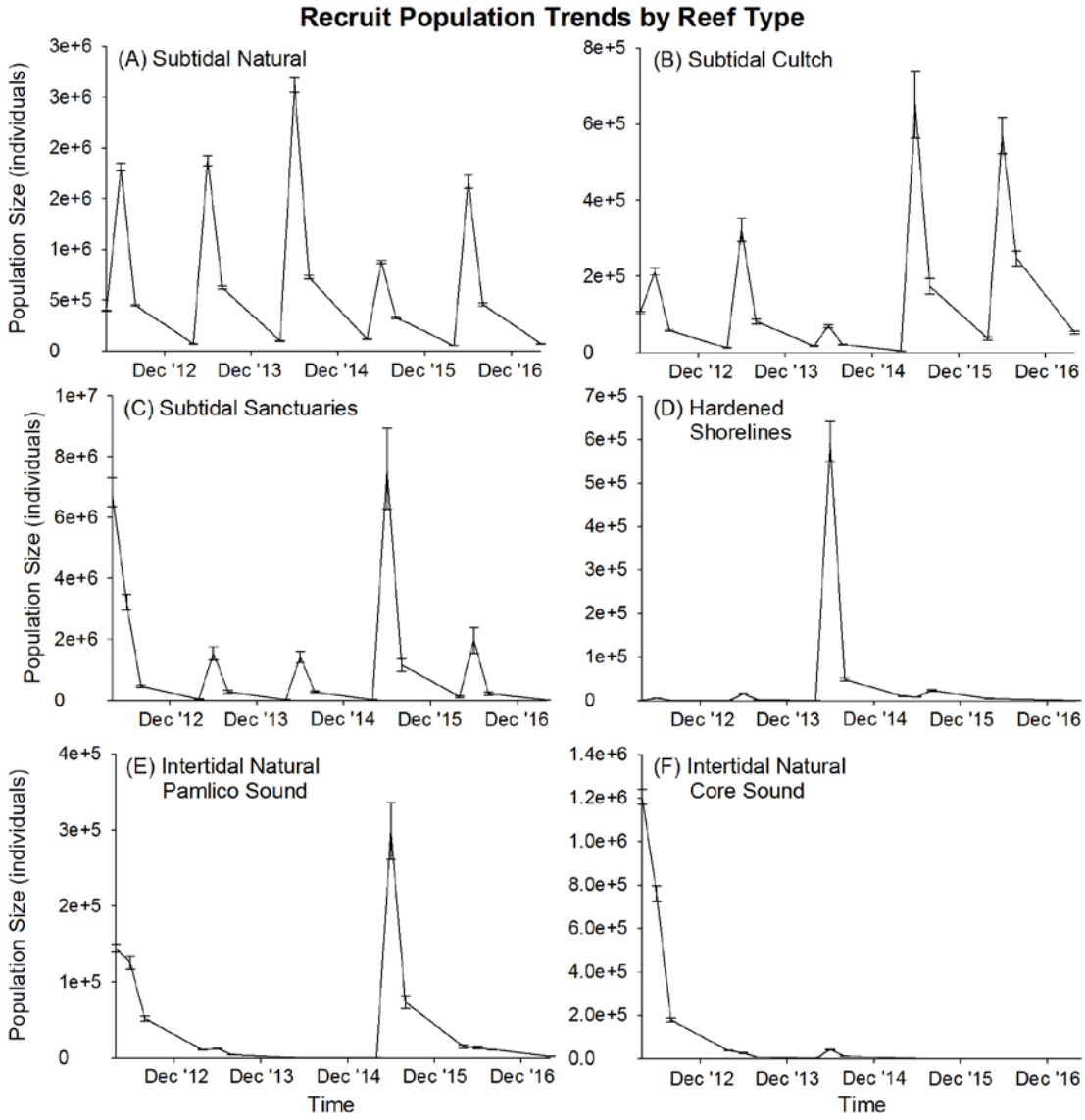


Figure 10: Recruit size class population trends by reef type across the five-year model timeframe under the 10% larval mortality day$^{-1}$ scenario. Points represent the average recruit population size on a given reef type at a given time step; error bars represent standard error of the mean.

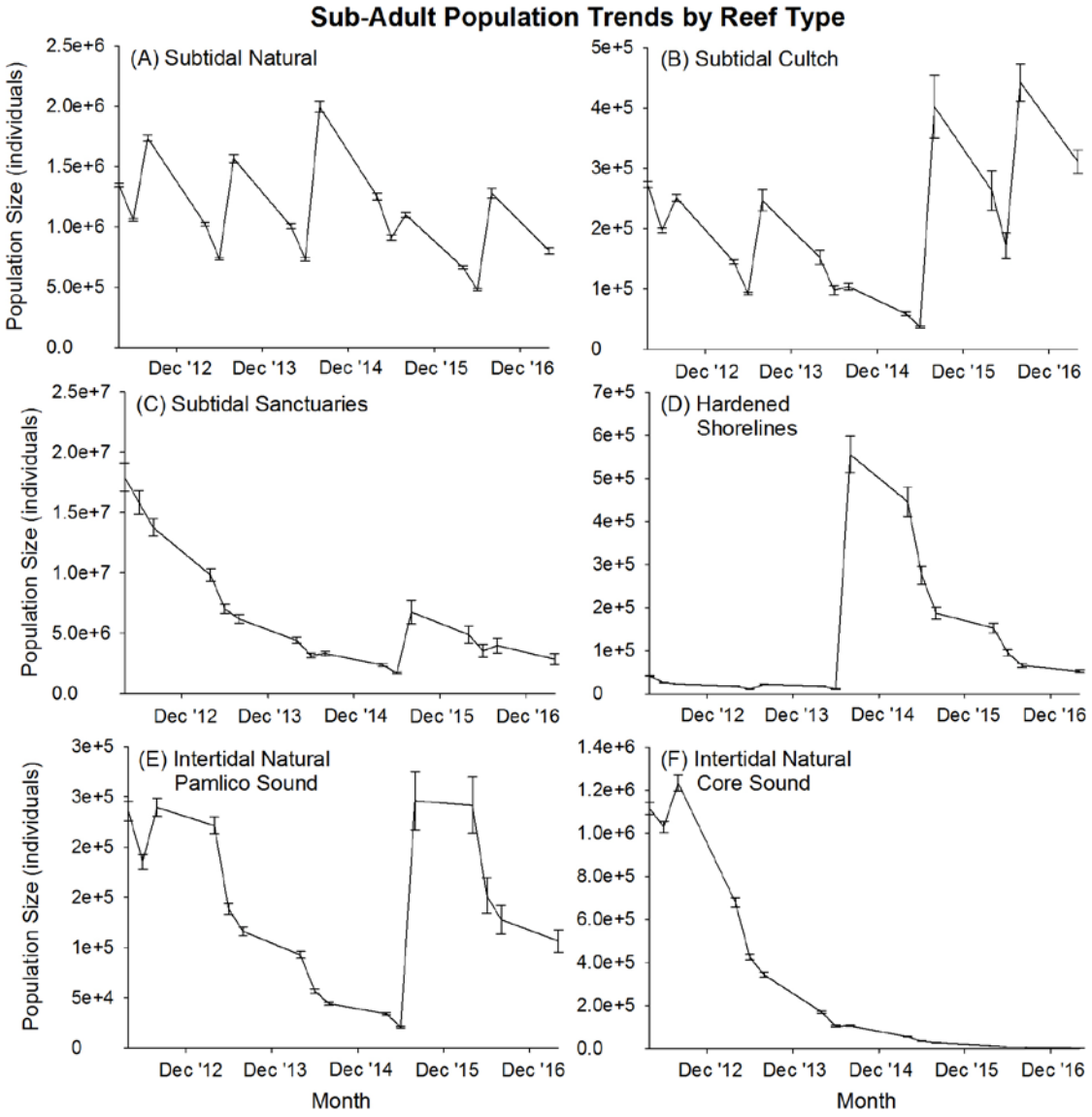


Figure 11: Sub-adult size class population trends by reef type across the five-year model timeframe under the 10% larval mortality day$^{-1}$ scenario. Points represent the average sub-adult population size on a given reef type at a given time step; error bars represent standard error of the mean.

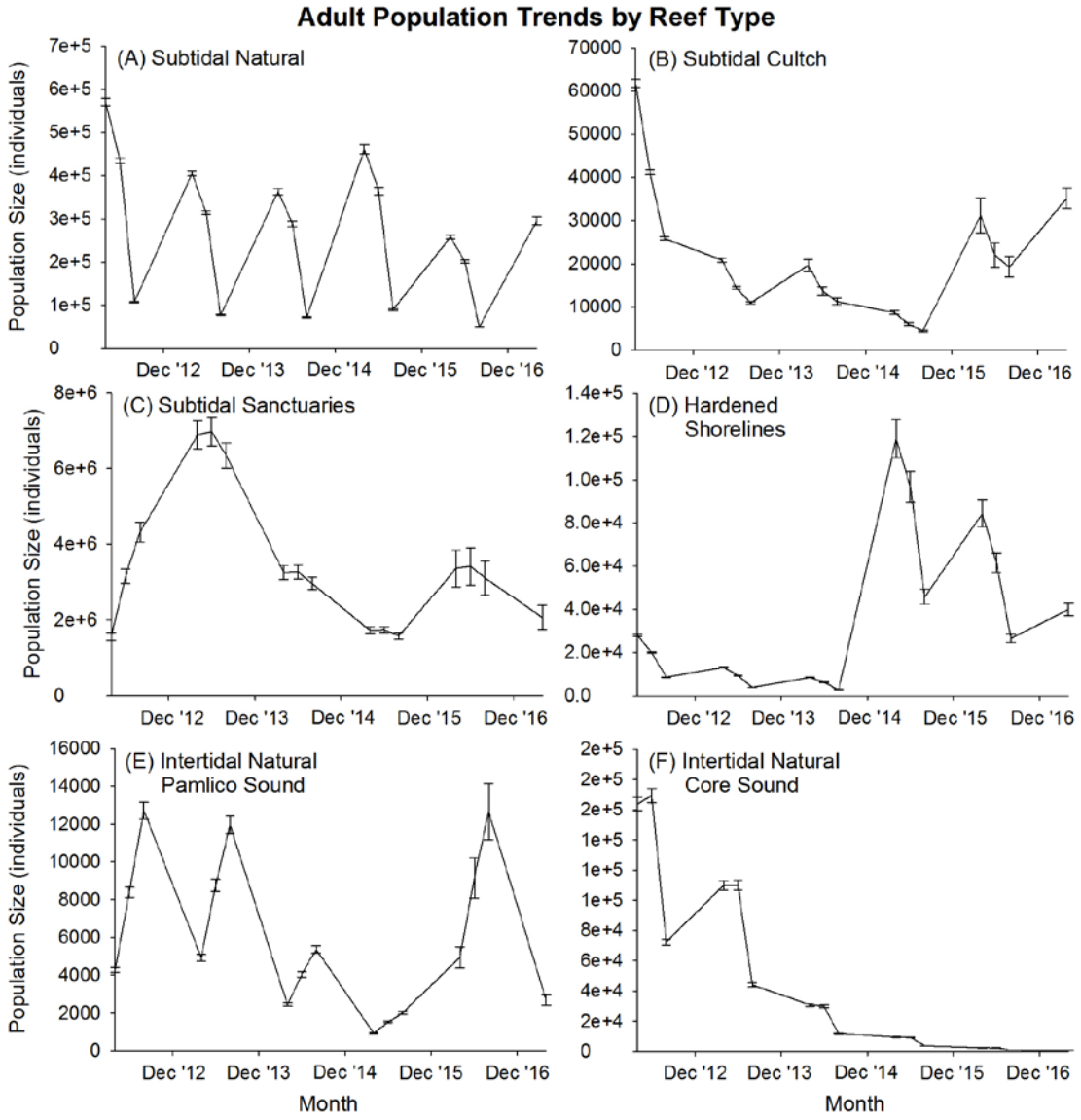


Figure 12: Adult size class population trends by reef type across the five-year model timeframe under the 10% larval mortality day$^{-1}$ scenario. Points represent the average adult population size on a given reef type at a given time step; error bars represent standard error of the mean.

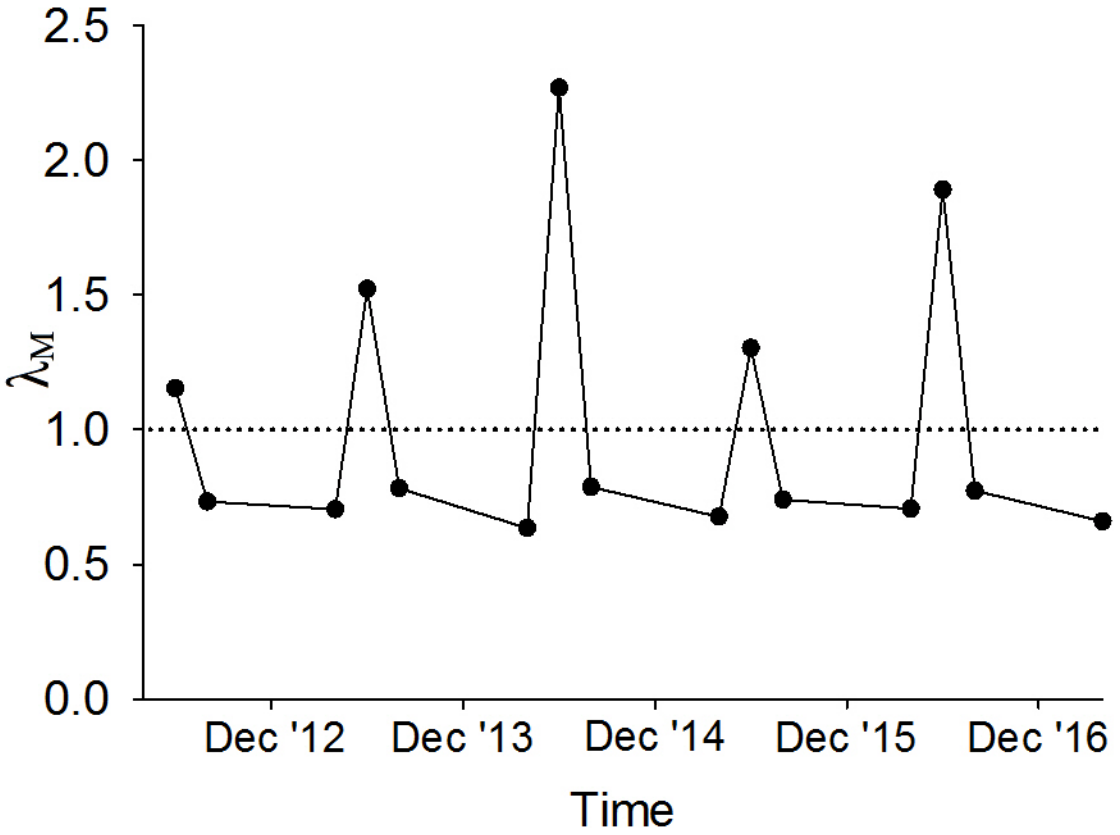


Figure 13: Overall metapopulation growth ($\lambda_M$) across the five-year model timeframe under the 10% larval mortality day$^{-1}$ scenario. The dashed line indicates a $\lambda_M = 1$, above or equal to which a metapopulation is persistent during time *t*, and below which a metapopulation is non-persistent during time *t*.

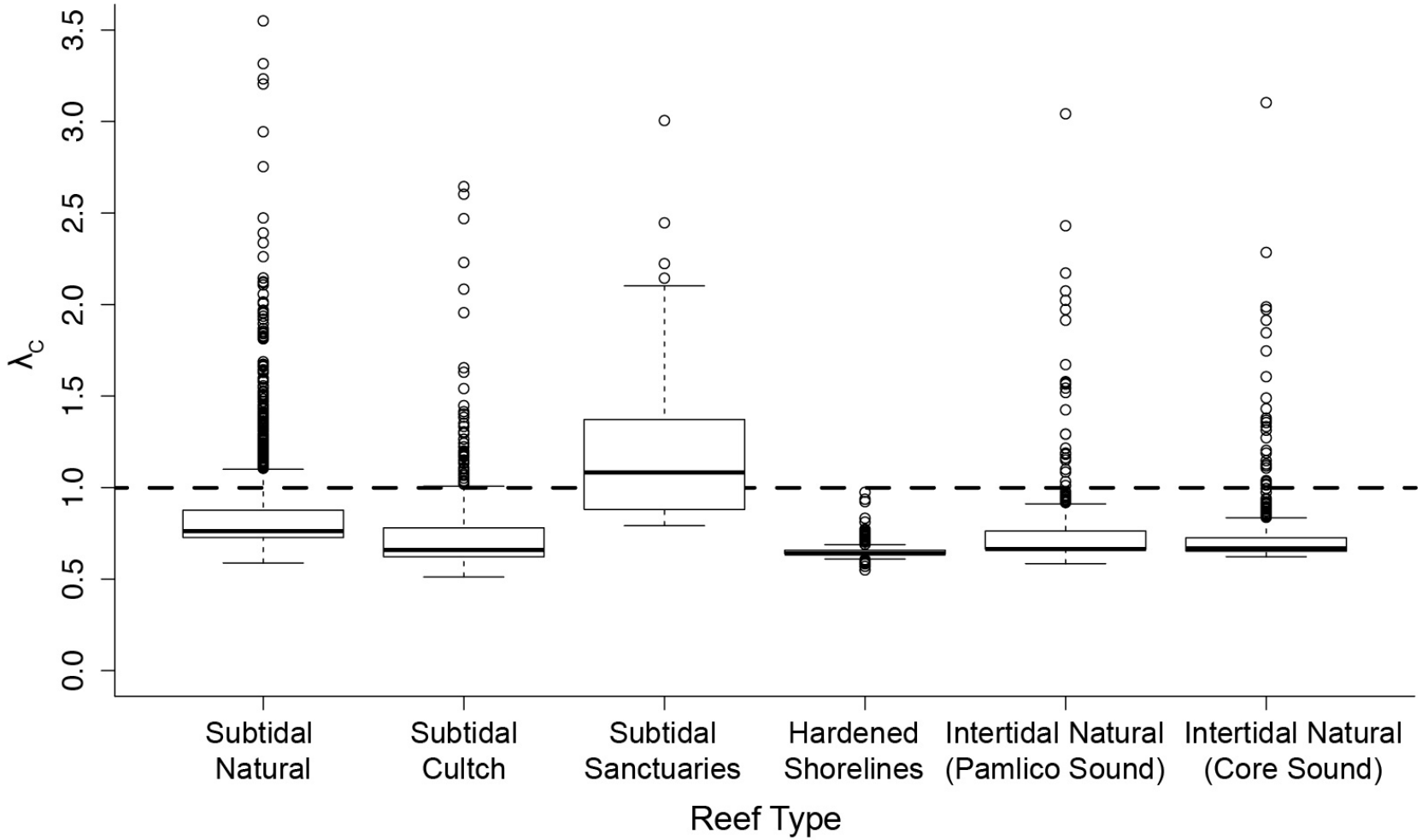


Figure 14: Source-sink status ($\lambda_c$) of each reef (by reef type) during each May-June time step between 2012-2016 under the 10% larval mortality day$^{-1}$ scenario. $\lambda_c \geq 1$ indicates a given reef functioned as a source during time *t*, and $\lambda_c < 1$ indicates a given reef functioned as a sink during time *t*.

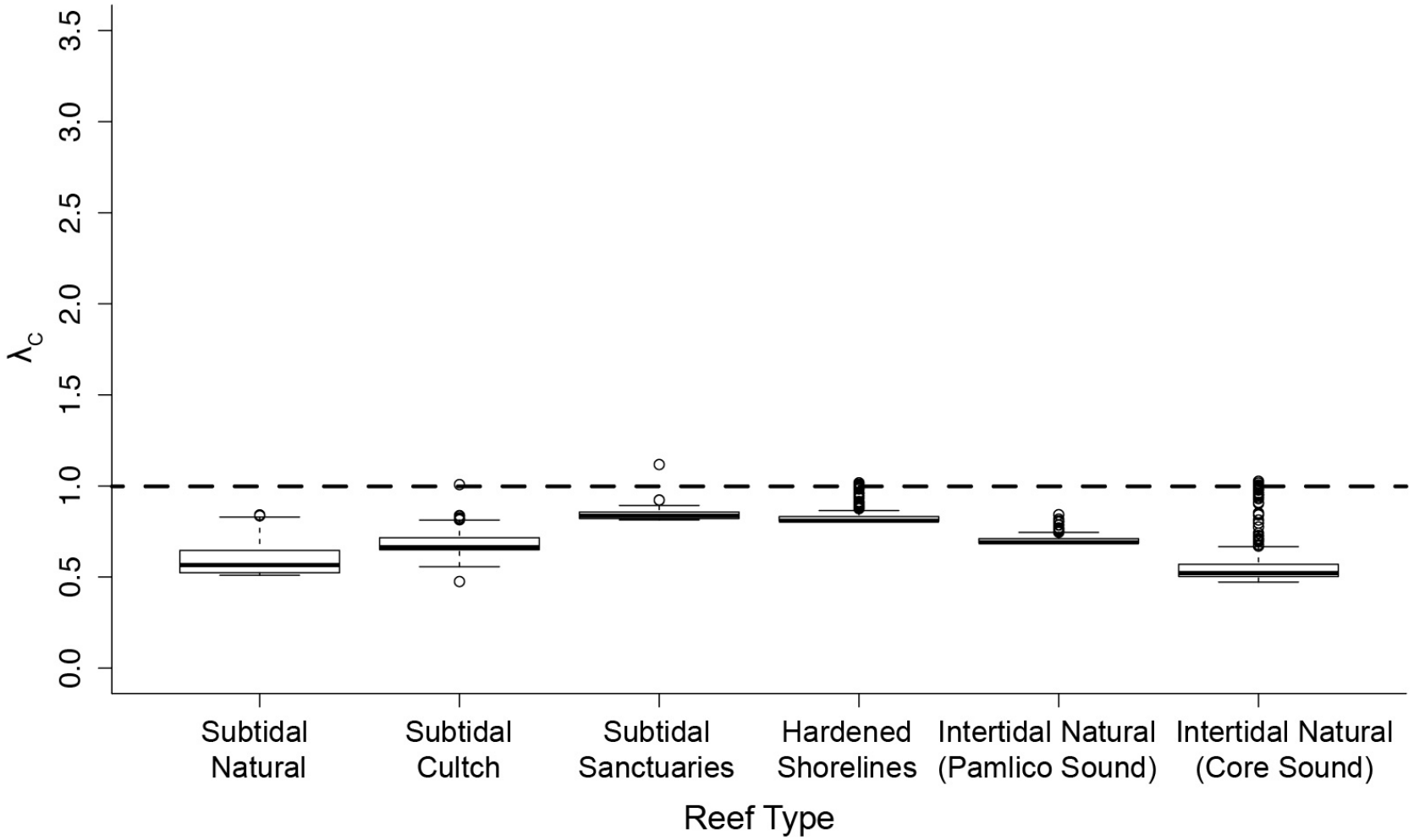


Figure 15: Source-sink status ($\lambda_c$) of each reef (by reef type) during each July-August time step between 2012-2016 under the 10% larval mortality day$^{-1}$ scenario. $\lambda_c \geq 1$ indicates a given reef functioned as a source during time *t*, and $\lambda_c < 1$ indicates a given reef functioned as a sink during time *t*.

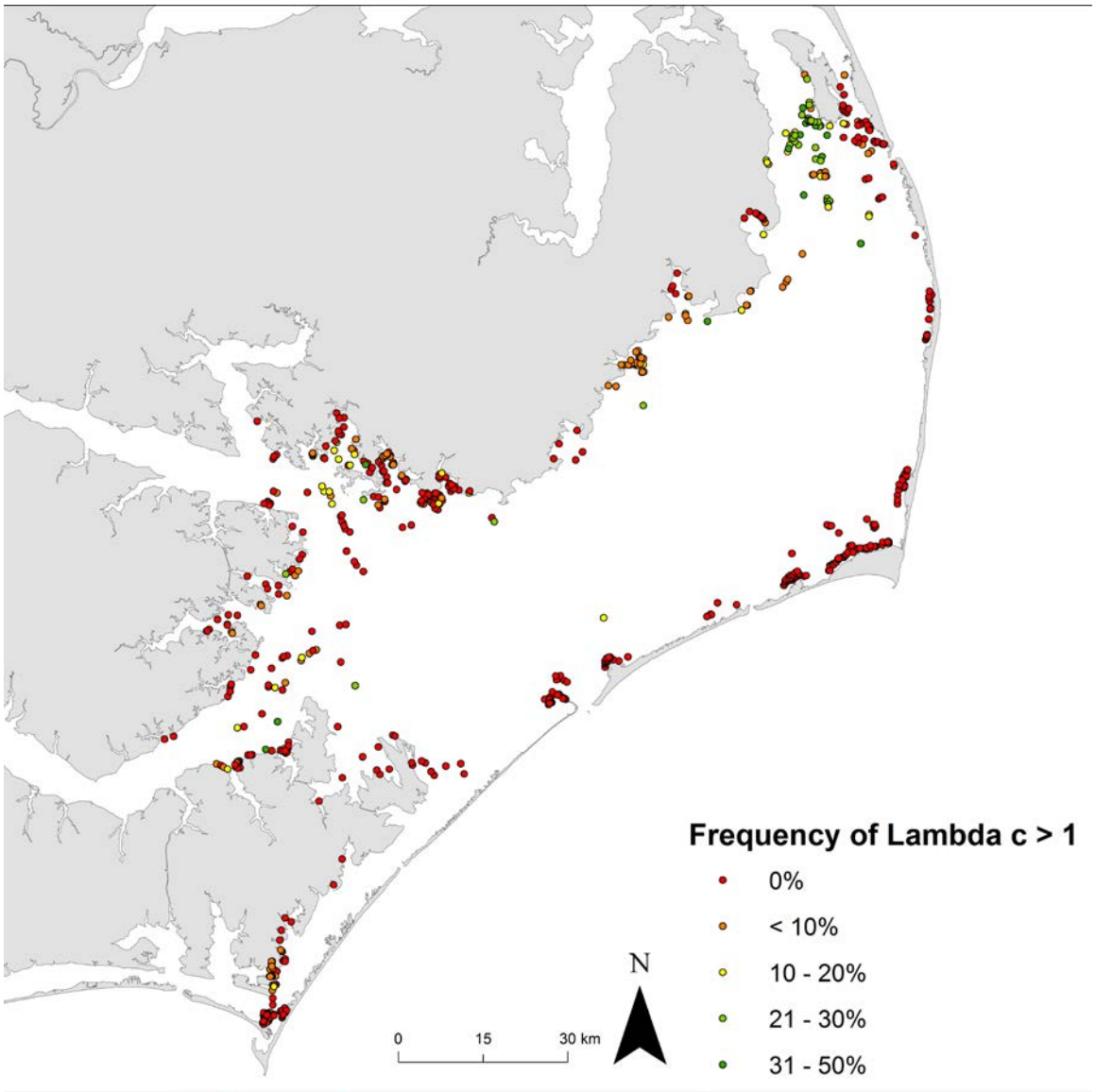


Figure 16: Frequency of $\lambda_c \geq 1$ at all reefs across the five-year model timeframe under the 10% larval mortality day$^{-1}$ scenario. $\lambda_c \geq 1$ indicates a given reef functioned as a source during time *t*, and $\lambda_c < 1$ indicates a given reef functioned as a sink during time *t*. Green dots represent frequent 'source' reefs (i.e., $\lambda_c \geq 1$ 31-50% of the time), red dots represent 'sink' reefs (i.e, $\lambda_c \geq 1$ 0% of the time).

## CONCLUSIONS AND MANAGEMENT APPLICATIONS

Humanity depends upon the services afforded by natural ecosystems (Dobson et al. 1997, Hobbs and Harris 2001). However, human-induced change and damage to Earth's ecosystems necessitates their repair and restoration. Coastal habitats, such as oyster reefs, mangroves, and saltmarshes provide essential ecosystem services to humanity, but anthropogenic impacts render these habitats among the most imperiled ecosystems on earth (Grabowski and Peterson 2007, Barbier et al. 2011, Hurst et al. 2015). Oyster reefs have been subject to extensive restoration efforts over the past century with varied success (Powers et al. 2009), leading coastal managers to increasingly value scientific guidance to aid in their successful restoration (Baggett et al. 2015). Through a combination of field- and computer modeling-based approaches, this dissertation aimed to contribute geomorphological-, ecosystem services-, and population dynamics-related guidance needed for a science-based approach to oyster restoration and management.

In Chapter 1, I characterized the structuring role of wave exposure on natural intertidal oyster reef distribution and identified a narrow wave exposure threshold above which natural intertidal reefs did not occur, and below which reef presence was dependent on other structuring variables, such as salinity and sediment grain size. The identification of the structuring role of wave exposure on intertidal oyster reef distribution has implications for the selection of locations for restoration of intertidal oyster reefs and the materials used in their restoration. Specifically, this research indicates that in areas of high wave exposure, intertidal oyster reef restoration efforts should incorporate alternative reef substrates less prone to redistribution by wave action, such as riprap, concrete or Oyster Castles® (Dunn et al. 2014, Theuerkauf et al. 2015). For areas

below the wave exposure threshold, intertidal restoration using traditional materials, such as loose oyster shell, may be suitable.

In Chapter 2, I evalauted the role of increasingly pervasive hardened shoreline structures as oyster habitat, and evaluated how intertidal oyster reefs vary as a function of landscape-scale factors. Oyster density, growth rates, and population estimates on natural intertidal reefs were greatest within the smaller, more tidally influenced Core Sound versus the larger, wind-driven Pamlico Sound, with no significant difference in survivorship identified between the two water bodies. Natural intertidal reefs and hardened shoreline structures were compared within Pamlico Sound only, with natural intertidal reefs hosting three to eight times higher oyster densities than hardened shoreline structures. These results indicate that within more tidally influenced, shorter fetch water bodies (e.g., Core Sound), restoration planning efforts should focus primarily on reef-scale considerations (e.g., optimal tidal emersion range to maximize oyster survival; Ridge et al. 2015, Walles et al. 2016), whereas within larger, wind-driven water bodies (e.g., Pamlico Sound), restoration planning efforts should focus primarily on landscape-scale considerations (e.g., locations with limited wave exposure; Theuerkauf et al. 2016). Furthermore, the present study also provides evidence that hardened shorelines provide habitat value for oysters, albeit reduced relative to natural intertidal reefs.

In Chapter 3, I utilized satellite-derived chlorophyll *a* concentrations for Pamlico Sound, North Carolina, USA in conjunction with data on water flow velocities and dissolved oxygen concentrations to identify potential restoration locations that would maximize the oyster reef-associated ecosystem service of water filtration. I integrated these novel oyster water filtration ecosystem services variables within a broader, existing GIS-based HSI model to identify suitable locations for oyster restoration that maximize: (i) biophysical, (ii) socioeconomic, and (iii)

ecosystem services variables essential to long-term persistence of restored populations and maximization of water filtration ecosystem service provision. I further compared the 'Water Filtration' optimized HSI with an HSI optimized for 'Reef Persistence,' as well as a hybrid model that optimized for both water filtration and reef persistence. I identified optimal restoration locations that were consistent among the three HSI scenarios (i.e., "win-win" locations), as well as optimal locations unique to a given HSI scenario (i.e., "tradeoff" locations). The modeling framework utilized in Chapter 3 can provide guidance to restoration practitioners to maximize the cost-efficiency and ecosystem services value of habitat restoration efforts in Pamlico Sound, and can be adapted and applied to guide oyster restoration in other systems.

In Chapter 4, I adapted a size-structured, discrete-time matrix model for eastern oysters (*Crassostrea virginica*) to simulate the dynamics of an entire oyster metapopulation, including a network of inter-connected no-harvest subtidal sanctuary oyster reefs, restored oyster reefs and harvested oyster reefs, among other reef types, in the Albemarle-Pamlico Estuarine System in North Carolina, USA. I identified: 1) an overall stable, yet slightly declining metapopulation, 2) variable reef type-specific population trajectories depending on spatiotemporal variation in larval recruitment, 3) spatiotemporal variation in the source-sink status of reef subpopulations wherein subtidal sanctuaries and reefs located in the northeastern portion of the system frequently served as sources, and 4) the importance of inter-reef larval export on metapopulation dynamics relative to local larval retention processes. Based on the results of this research, I recommend future management efforts within this system consider oysters as an interconnected metapopulation. Furthermore, as subtidal sanctuaries served as frequent sources to the metapopulation, I recommend continued efforts to protect and restore frequent 'source' subpopulations (e.g., subtidal sanctuaries) while managing harvest from 'sink' subpopulations.

## LITERATURE CITED


Baggett, L.P., Powers, S.P., Brumbaugh, R.D., Coen, L.D., DeAngelis, B.M., Greene, J.K., Hancock, B.T., Morlock, S.M., Allen, B.L., Breitburg, D.L. and D. Bushek. 2015. Guidelines for evaluating performance of oyster habitat restoration. *Restoration Ecology* 23: 737–745.

Barbier, E. B., Hacker, S. D., Kennedy, C., Koch, E. W., Stier, A. C., & B. R. Silliman. 2011. The value of estuarine and coastal ecosystem services. *Ecological Monographs* 812:169–193.

Dobson, A. P., Bradshaw, A. D., & A. J. M. Baker. 1997. Hopes for the future: restoration ecology and conservation biology. *Science* 277:515–522.

Dunn, R.P., Eggleston, D.B. and N. Lindquist. 2014. Substrate effects on demographic rates of Eastern oyster (*Crassostrea virginica*). *Journal of Shellfish Research* 33: 177–185

Hobbs, R. J., & J. A. Harris. 2001. Restoration ecology: repairing the Earth's ecosystems in the New Millenium. *Restoration Ecology* 9:239–246.

Hurst, T.A., Pope, A.J. and G.P. Quinn. 2015. Exposure mediates transitions between bare and vegetated states in temperate mangrove ecosystems. *Marine Ecology Progress Series* 533: 121–134.

Grabowski, J. H. and C. H. Peterson. 2007. Restoring oyster reefs to recover ecosystem services. Pp. 281–298 in Cuddington, K., Byers, J.E., Wilson, W.G., Hastings A., eds. Ecosystem Engineers: Plants to Protists. Elsevier.

Ridge, J.T., Rodriguez, A.B., Fodrie, F.J., Lindquist, N.L., Brodeur, M.C., Coleman, S.E., Grabowski, J.H. and E.J. Theuerkauf. 2015. Maximizing oyster-reef growth supports green infrastructure with accelerating sea-level rise. *Scientific Reports* 5: e14785.

Theuerkauf, S. J., Eggleston, D. B., Puckett, B. J., and K. W. Theuerkauf. 2016. Wave exposure structures oyster distribution on natural intertidal reefs, but not on hardened shorelines. *Estuaries and Coasts* doi:10.1007/s12237-016-0153-6.

Theuerkauf, S.J., Burke, R.P. and R.N. Lipcius. 2015. Settlement, growth, and survival of eastern oysters on alternative reef substrates. *Journal of Shellfish Research* 34: 241–250.

Walles, B., Troost, K., van den Ende, D., Nieuwhof, S., Smaal, A.C. and T. Ysebaert. 2016. From artificial structures to self-sustaining oyster reefs. *Journal of Sea Research* 108: 1–9.

# APPENDICES

Appendix Table 1: List of 17 GIS layers used originally by Puckett et al. (in review) and in the present study to determine suitability of sites in Pamlico Sound, North Carolina USA for placement of oyster reefs to maximize the probability of reef persistence (i.e., 'Reef Persistence HSI'). Threshold layers were assigned thresholds (e.g., optimal [score = 1], suitable [0.5], and unsuitable [0]) and subsequently weighted based on the layer's relative importance. A stakeholder panel was used to assign thresholds and weights. Exclusion layers were binary (suitable [score = 1] or unsuitable [0]). A detailed description of the methods used to develop these layers is provided in Puckett et al. (in review). Layer abbreviations are as follows: Submerged Aquatic Vegetation (SAV). Source abbreviations are as follows: National Oceanic and Atmospheric Administration (NOAA), NC Division of Marine Fisheries (DMF), NC Department of Environmental Quality (DEQ), US Geological Survey (USGS), NC Wildlife Resource Commission (WRC).

| Layer | Description | Type | Threshold and Exclusion Values | Rationale | Source |
|---|---|---|---|---|---|
| **Salinity (psu)** | Summer sound-wide salinity during average freshwater input from 1987-2008. | Threshold | Optimal (1): 10-15<br>Suitable (0.5): 6-10; 15-25<br>Unsuitable (0): <6; >25<br><br>Thresholds based on values reported in Kennedy (1996). | Important to oyster biological processes (e.g., growth and survival). | NC DMF Trawl Survey Program; Durham 2009 |
| **Sanctuary Larval Export** | Settlement location of oyster larvae spawned from existing sanctuaries. | Threshold | Continuous (0-1)<br><br>Log-transformed abundance of larval settlers in a cell, standardized on a 0 (lowest abundance) to 1 (highest abundance) scale. | Goal for existing sanctuaries to export larvae to future sanctuaries to create sanctuary network. | Puckett et al. 2016; Puckett et al. (in review) |
| **Sanctuary Larval Import** | Natal location of oyster larvae settling within existing sanctuaries. | Threshold | Continuous (0-1)<br><br>Log-transformed abundance of larvae spawned in a cell, standardized on a 0 (lowest abundance) to 1 (highest abundance) scale. | Goal for existing sanctuaries to import larvae from future sanctuaries to create sanctuary network. | NC DMF Oyster Sanctuary Program; This Study |

Appendix Table 1 Continued

| | | | | | |
|---|---|---|---|---|---|
| **Dissolved Oxygen** | Fall sound-wide minimum dissolved oxygen concentrations from 1996-2014. | Threshold | Continuous (0-1)<br><br>Minimum dissolved oxygen values linearly transformed on a 0 (lowest) to 1 (highest) scale. | Important to oyster biological processes (e.g., survival). | NC DMF Trawl Survey Program; This Study |
| **Cultch-planting Site Larval Import** | Natal location of oyster larvae settling within cultch-planting sites—locations where oyster shell is deployed to replace shell removed through commercial oyster harvest. Cultch-planting sites established from 2010-2014 were used. | Threshold | Continuous (0-1)<br><br>Log-transformed abundance of larvae spawned in a cell, standardized on a 0 (lowest abundance) to 1 (highest abundance) scale. | Goal for existing sanctuaries to export larvae to commercially harvested cultch-planting sites. Promotes larval exchange among strategies within the oyster restoration portfolio. | NC DMF Habitat Enhancement Program; This Study |
| **Natural Reef Larval Import** | Natal location of oyster larvae settling within natural subtidal reefs. | Threshold | Continuous (0-1)<br><br>Log-transformed abundance of larvae spawned in a cell, standardized on a 0 (lowest abundance) to 1 (highest abundance) scale. | Goal for existing sanctuaries to export larvae to commercially harvested natural reefs. | NC DMF Estuarine Benthic Habitat Mapping Program; This Study |
| **Cultch-planting Site Larval Export** | Settlement location of oyster larvae spawned from cultch-planting sites. Cultch-planting sites established from 2010-2014 were used. | Threshold | Continuous (0-1)<br><br>Log-transformed abundance of larval settlers standardized on a 0 (lowest abundance) to 1 (highest abundance) scale. | Enables selection of sites that promotes larval exchange among strategies within the oyster restoration portfolio. | NC DMF Habitat Enhancement Program; This Study |

Appendix Table 1 Continued

| | | | | | |
|---|---|---|---|---|---|
| **Natural Reef Larval Export** | Settlement location of oyster larvae spawned from natural subtidal oyster reefs. | Threshold | Continuous (0-1)<br><br>Log-transformed abundance of larval settlers standardized on a 0 (lowest abundance) to 1 (highest abundance) scale. | Enables selection of sites that promotes larval exchange among natural and restored oyster reefs. | NC DMF Estuarine Benthic Habitat Mapping Program; This Study |
| **Material Stockpile Sites (km)** | Location of material stockpile sites accessed by vessels for loading material (e.g., reef balls) used for restoration. | Threshold | Optimal (1): <5 km<br>Suitable (0.5): 5-10 km<br>Unsuitable (0): >10 km<br><br>Thresholds based on vessel range (trips per day), fuel costs, and vessel load capabilities. | Enables selection of sites based on economic and logistical constraints associated with transporting large amounts of hard substrate needed for restoration. | NC DMF Oyster Sanctuary Program |
| **Boat Ramps (nm)** | Location of boat ramps where recreational fishermen can launch boats. | Threshold | Optimal (1): <10 km<br>Unsuitable (0): >10 km<br><br>Thresholds based on average travel distance reported for inshore recreational vessels by Ramos et al. (2006). | Enables selection of sites based on accessibility to recreational (fin)fishing. | NC WRC |
| **Bathymetry** | Depth (m) in Pamlico Sound. | Exclusion | Excluded if depth of entire 1km$^2$ cell was < 2m, which is required for navigational clearance. | - | NOAA Estuarine Bathymetry |
| **Substrate** | Substrate types in Pamlico Sound. Substrates types included: sand, muddy sand, sandy mud, mud, and soft mud. | Exclusion | Excluded cells with soft substrate (e.g., soft mud and mud), which is necessary to prevent subsidence of heavy material used for reef restoration. | - | NC DMF Estuarine Benthic Habitat Mapping and Trawl Survey Programs |

Appendix Table 1 Continued

| | | | | | |
|---|---|---|---|---|---|
| **SAV** | Location of SAV in Pamlico Sound. | Exclusion | Excluded if a cell contained SAV because reef restoration is not permitted in the presence of SAV. | - | NC DMF Estuarine Benthic Habitat Mapping Program |
| **Shellfish Leases** | Location of private shellfish leases in Pamlico Sound. | Exclusion | Excluded if a cell contained leased area to prevent user conflicts. | - | NC DMF Estuarine Benthic Habitat Mapping Program |
| **Nursery Areas** | Location of primary and special secondary nursery areas in Pamlico Sound, which serve as critical habitat for juvenile fishes. | Exclusion | Excluded if a cell contained primary or special secondary nursery areas because reef restoration is not permitted in the presence of nursery areas. | - | NC DMF |
| **Military Zones** | Location of military exclusion zones used for practice missions. | Exclusion | Excluded if a cell contained military protected area because habitat enhancement is not permitted in military zones due to the possibility of unexploded ordnance. | - | NC DEQ |
| **Navigational Channels** | Location of major navigational channels including the Intracoastal Waterway and Ferry routes. | Exclusion | Excluded if a cell contained the Intracoastal Waterway or Ferry routes to prevent navigational hazards to large vessels. | - | USGS |

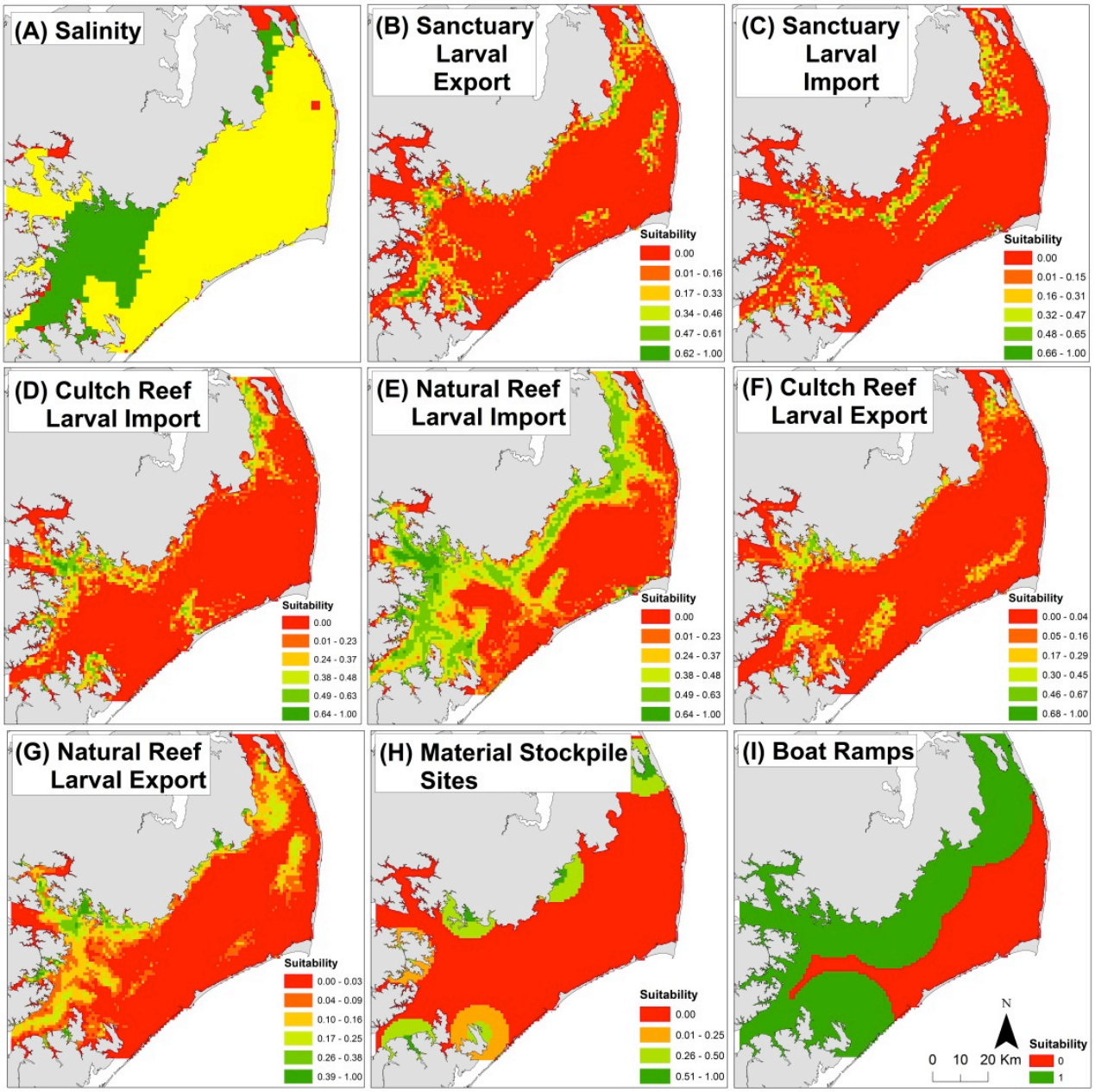


Appendix 2: Threshold layers used to compute habitat suitability for oyster restoration within the three HSI scenarios. A) Salinity. B) Sanctuary larval export. C) Sanctuary larval import. D) Cultch reef larval import. E) Natural reef larval import. F) Cultch reef larval export. G) Natural reef larval export. H) Material stockpile sites. I) Boat ramps. Suitability increases from low (red) to high (green) for each layer.

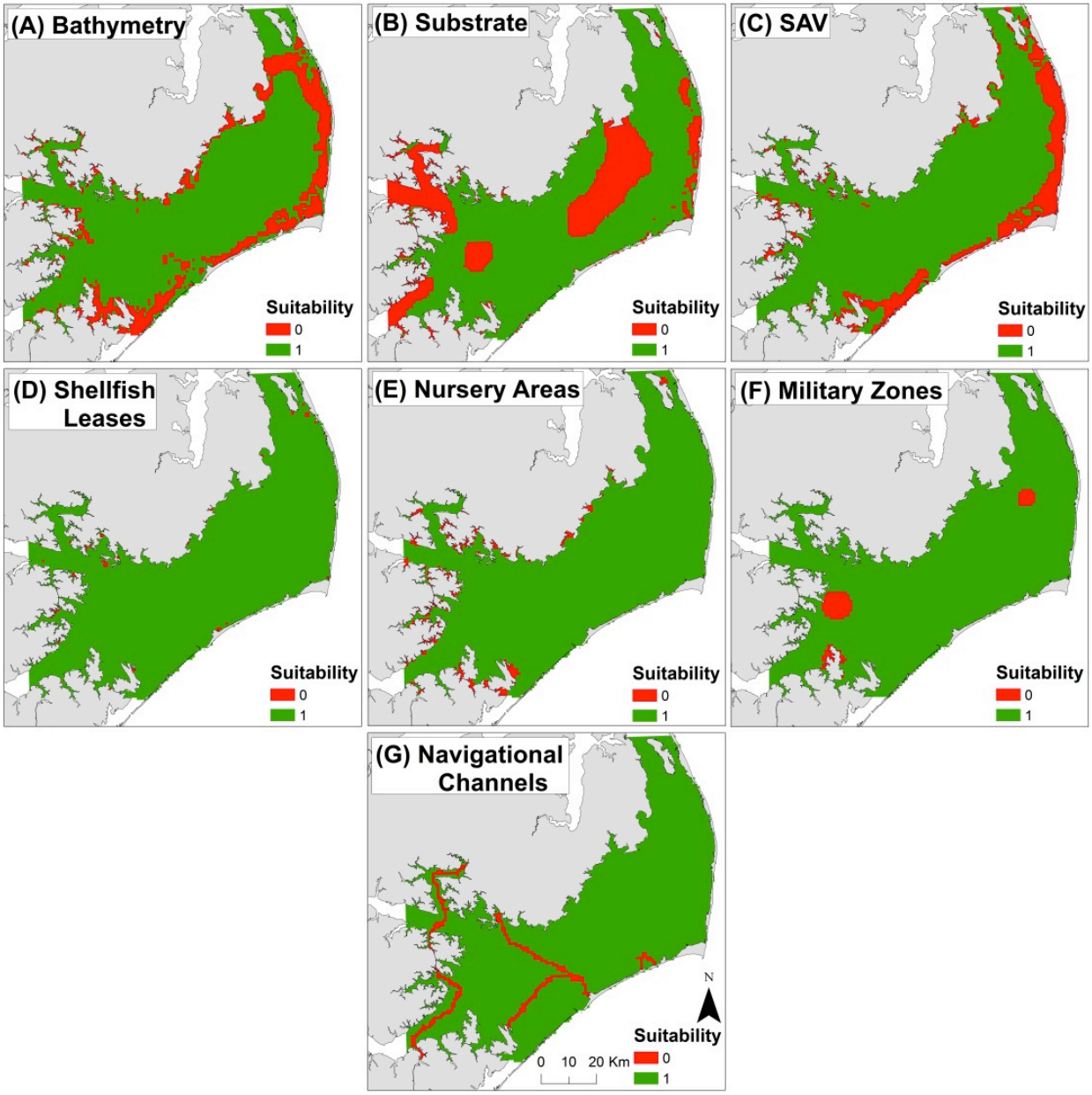


Appendix 3: Exclusion layers used to compute habitat suitability for oyster restoration within the three HSI scenarios. A) Bathymetry. B) Substrate. C) SAV. D) Shellfish leases. E) Nursery areas. F) Military zones. G) Navigational channels. Suitability increases from unsuitable (red) to optimal (green) for each layer.

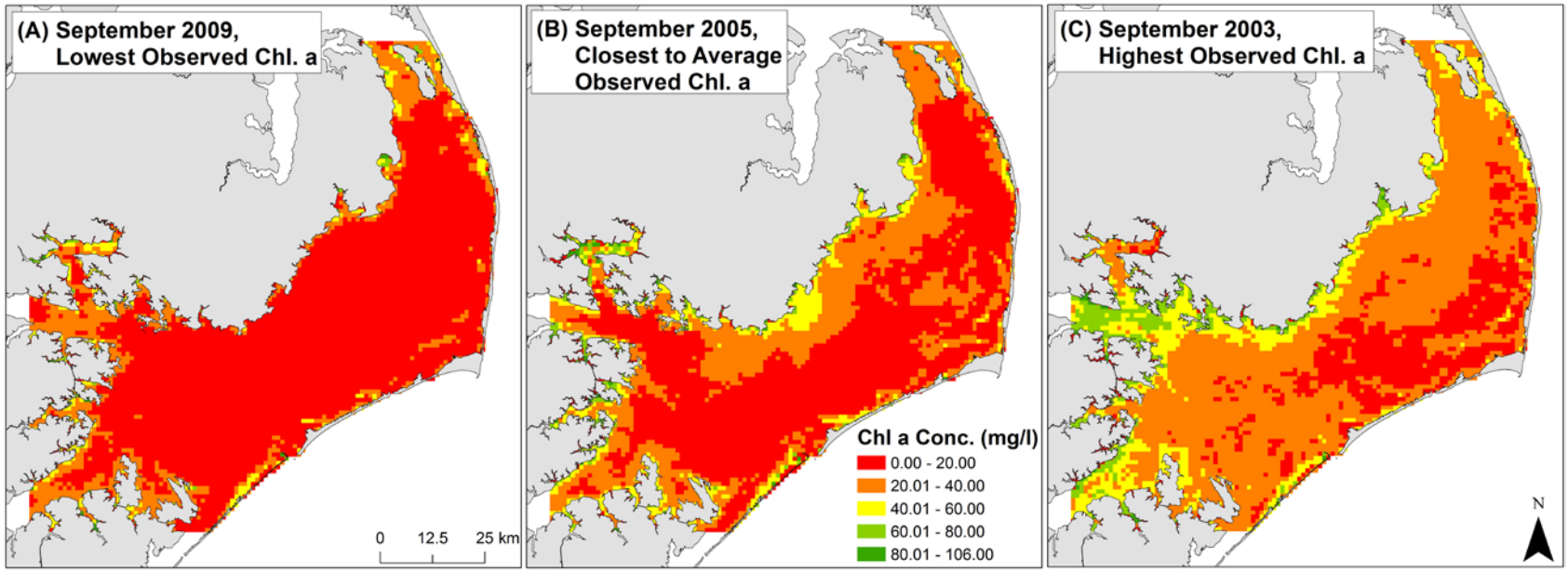


Appendix 4: Monthly-averaged (i.e., averaging across all days within the month) chlorophyll *a* concentrations (microgram $l^{-1}$) in Pamlico Sound corresponding with the (A) lowest overall, (B) closest to average, and (C) highest overall observed chlorophyll a concentrations as compared to all Septembers between 2003-2011.

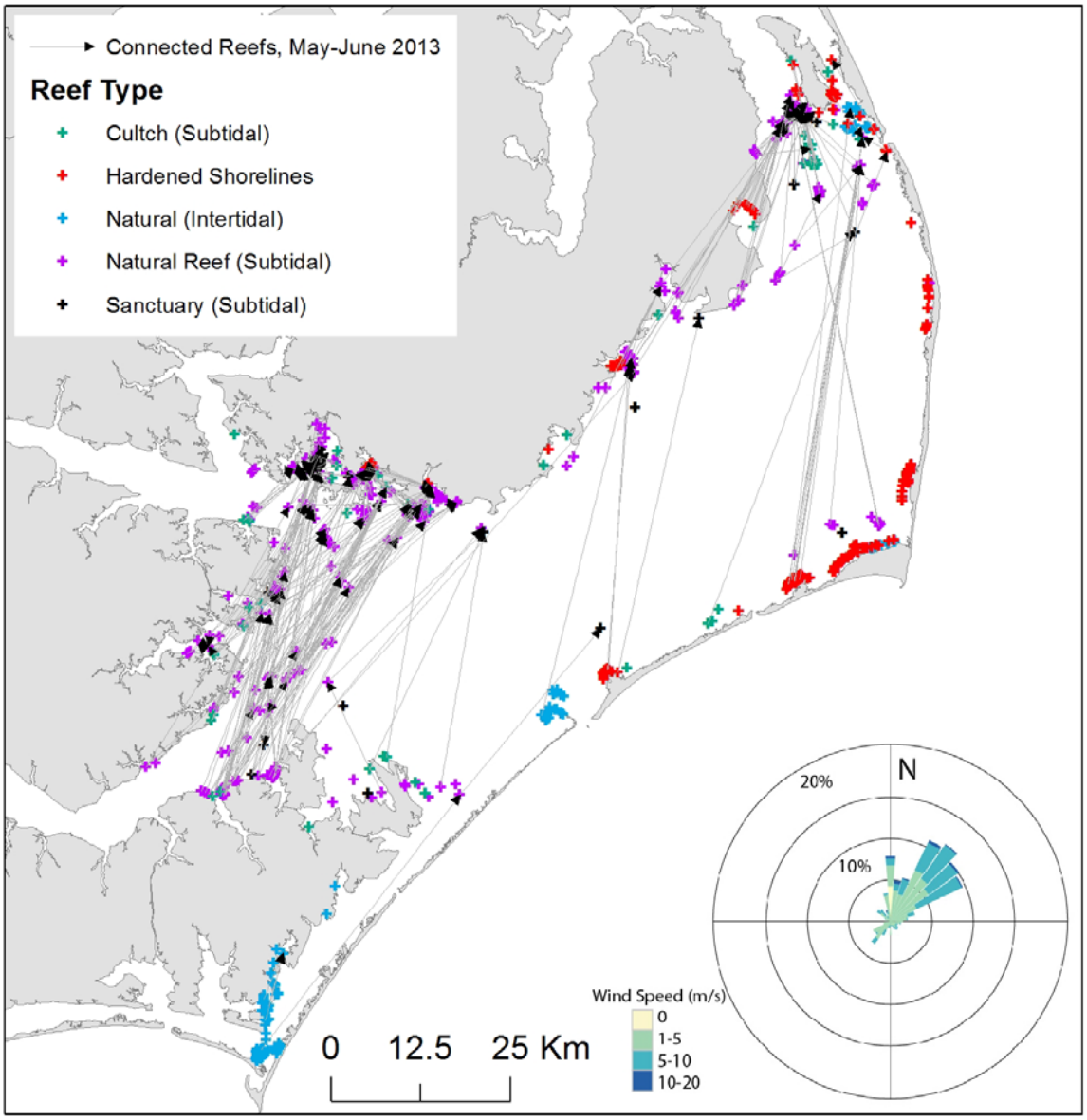


Appendix 5: Map depicting larval dispersal patterns during May–June of 2013. Lines depict connections between natal and settled reef locations (arrowheads point towards settled reef locations). Note that lines depict the least-cost path between reefs and not the actual dispersal path, and only a random subset (5%) of all connections are shown for illustrative purposes.

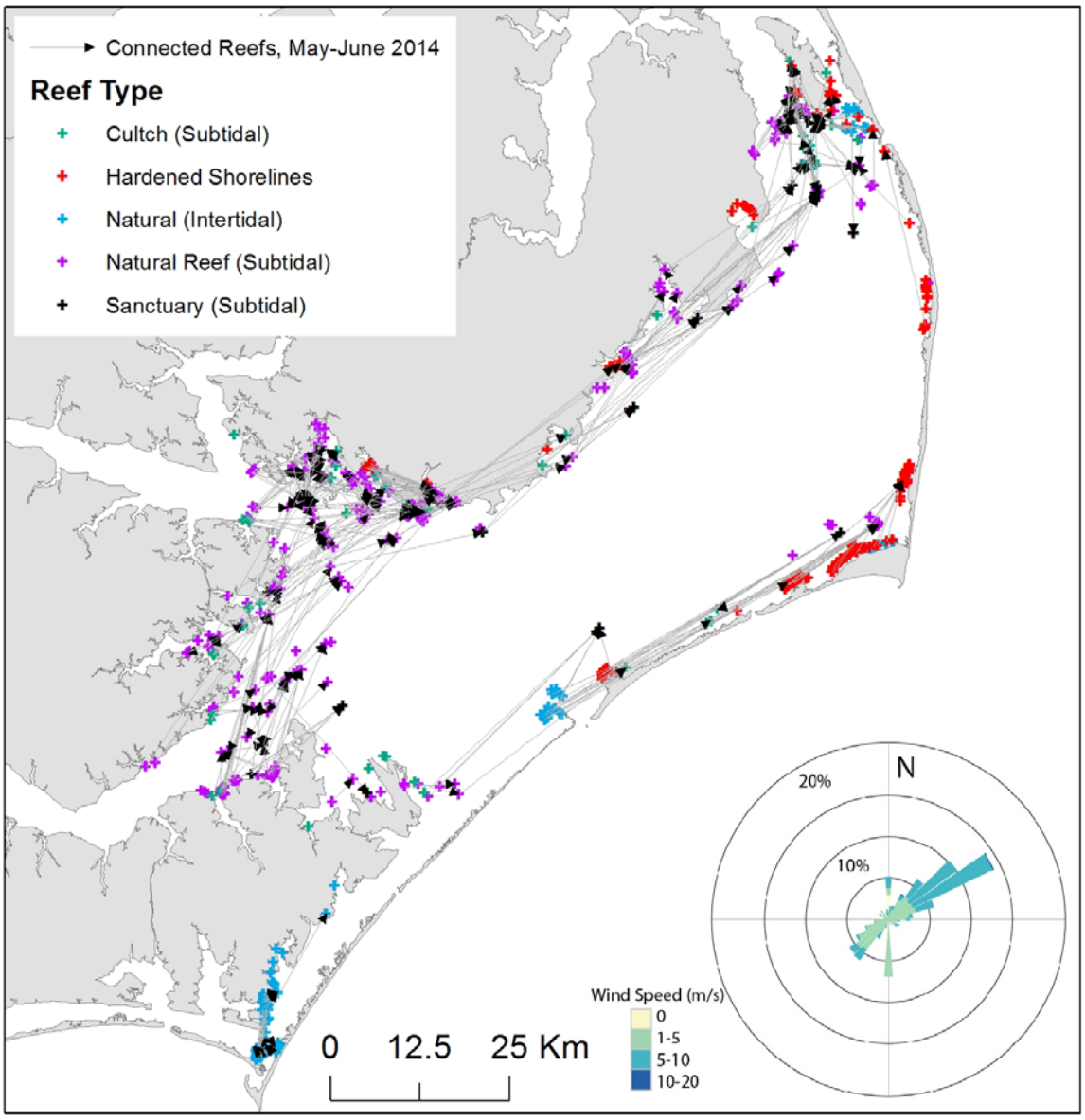


Appendix 6: Map depicting larval dispersal patterns during May–June of 2014. Lines depict connections between natal and settled reef locations (arrowheads point towards settled reef locations). Note that lines depict the least-cost path between reefs and not the actual dispersal path, and only a random subset (5%) of all connections are shown for illustrative purposes.

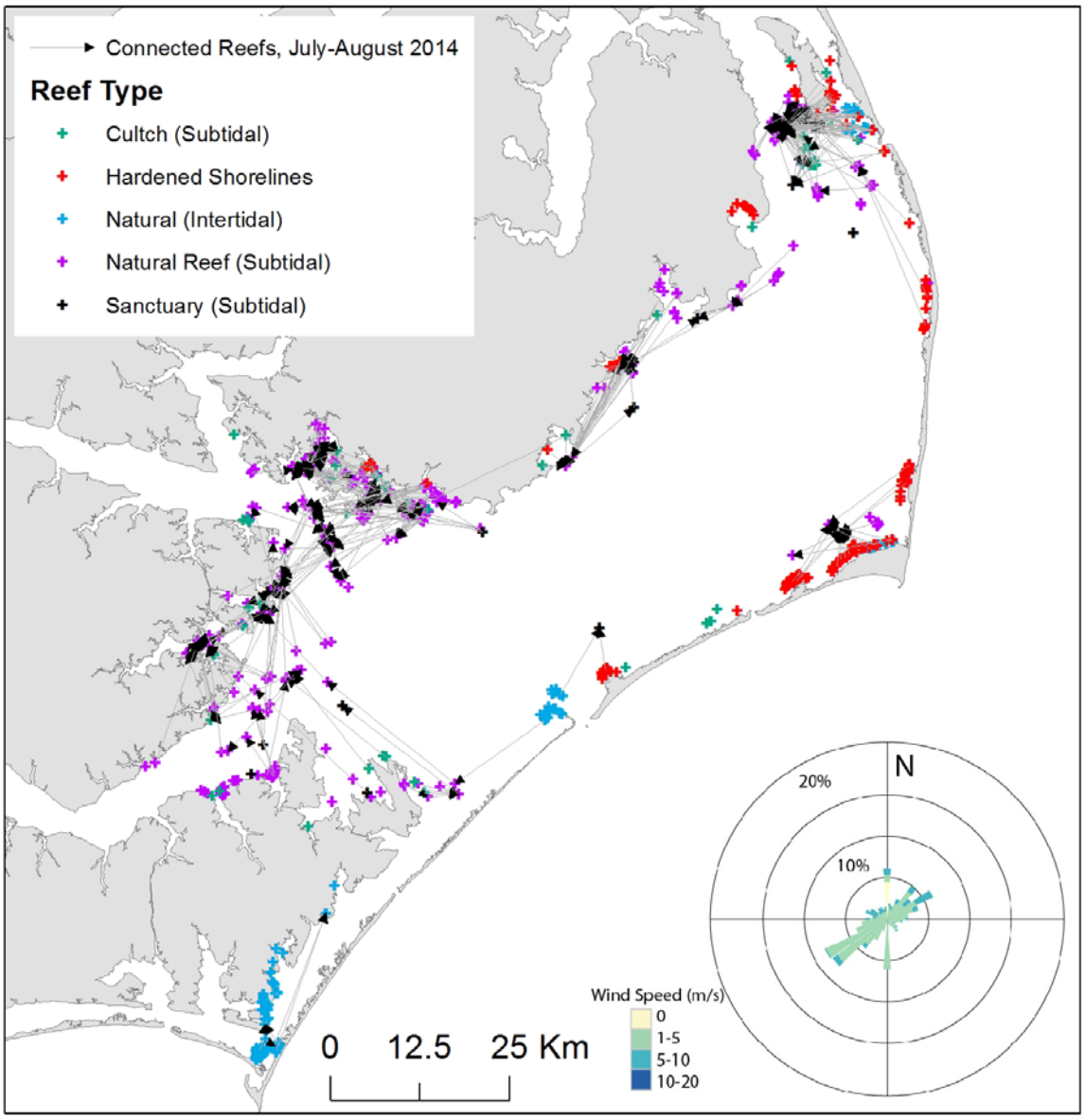


Appendix 7: Map depicting larval dispersal patterns during July–August of 2014. Lines depict connections between natal and settled reef locations (arrowheads point towards settled reef locations). Note that lines depict the least-cost path between reefs and not the actual dispersal path, and only a random subset (5%) of all connections are shown for illustrative purposes.

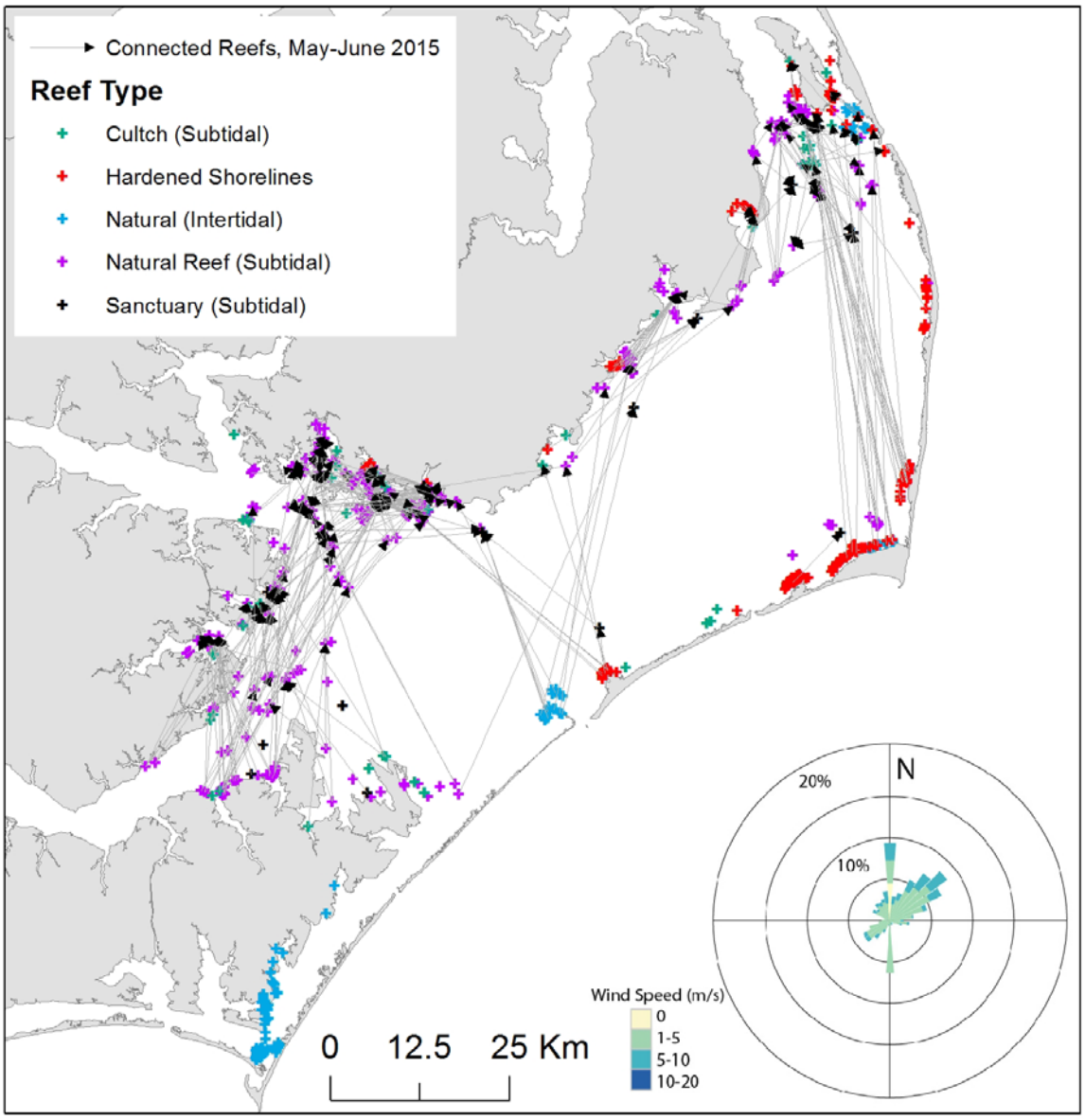


Appendix 8: Map depicting larval dispersal patterns during May–June of 2015. Lines depict connections between natal and settled reef locations (arrowheads point towards settled reef locations). Note that lines depict the least-cost path between reefs and not the actual dispersal path, and only a random subset (5%) of all connections are shown for illustrative purposes.

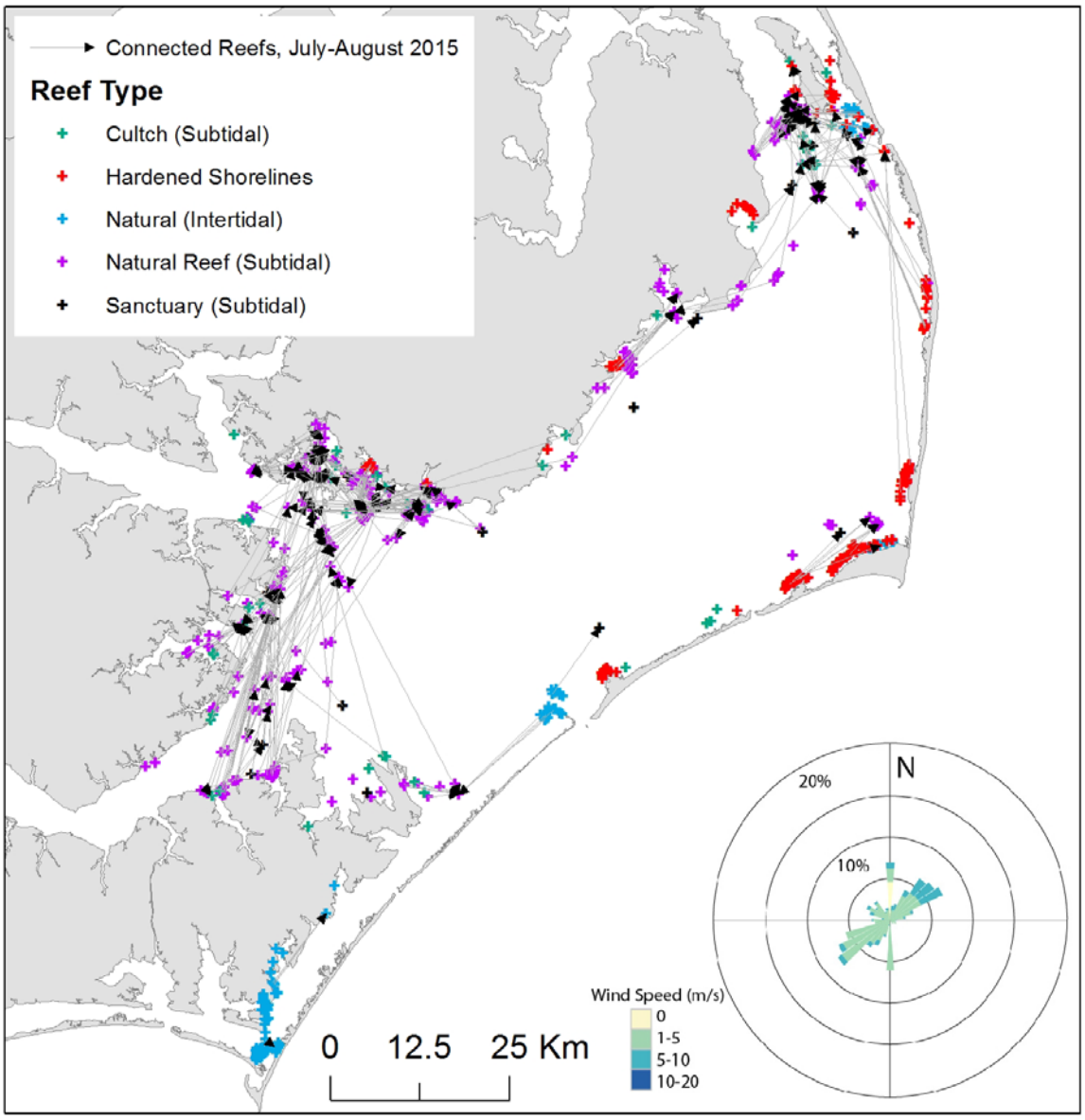


Appendix 9: Map depicting larval dispersal patterns during July–August of 2015. Lines depict connections between natal and settled reef locations (arrowheads point towards settled reef locations). Note that lines depict the least-cost path between reefs and not the actual dispersal path, and only a random subset (5%) of all connections are shown for illustrative purposes.

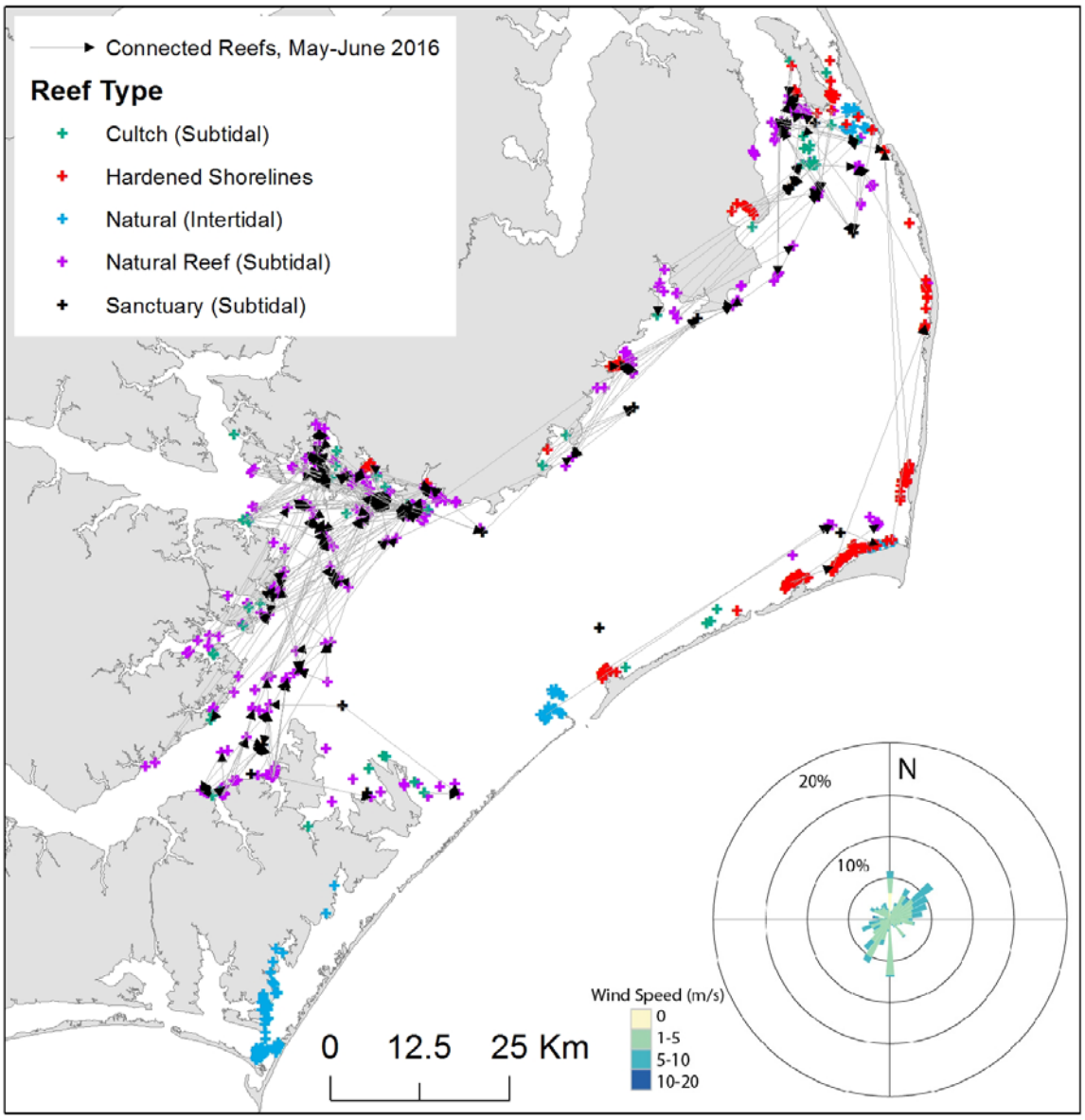


Appendix 10: Map depicting larval dispersal patterns during May–June of 2016. Lines depict connections between natal and settled reef locations (arrowheads point towards settled reef locations). Note that lines depict the least-cost path between reefs and not the actual dispersal path, and only a random subset (5%) of all connections are shown for illustrative purposes.

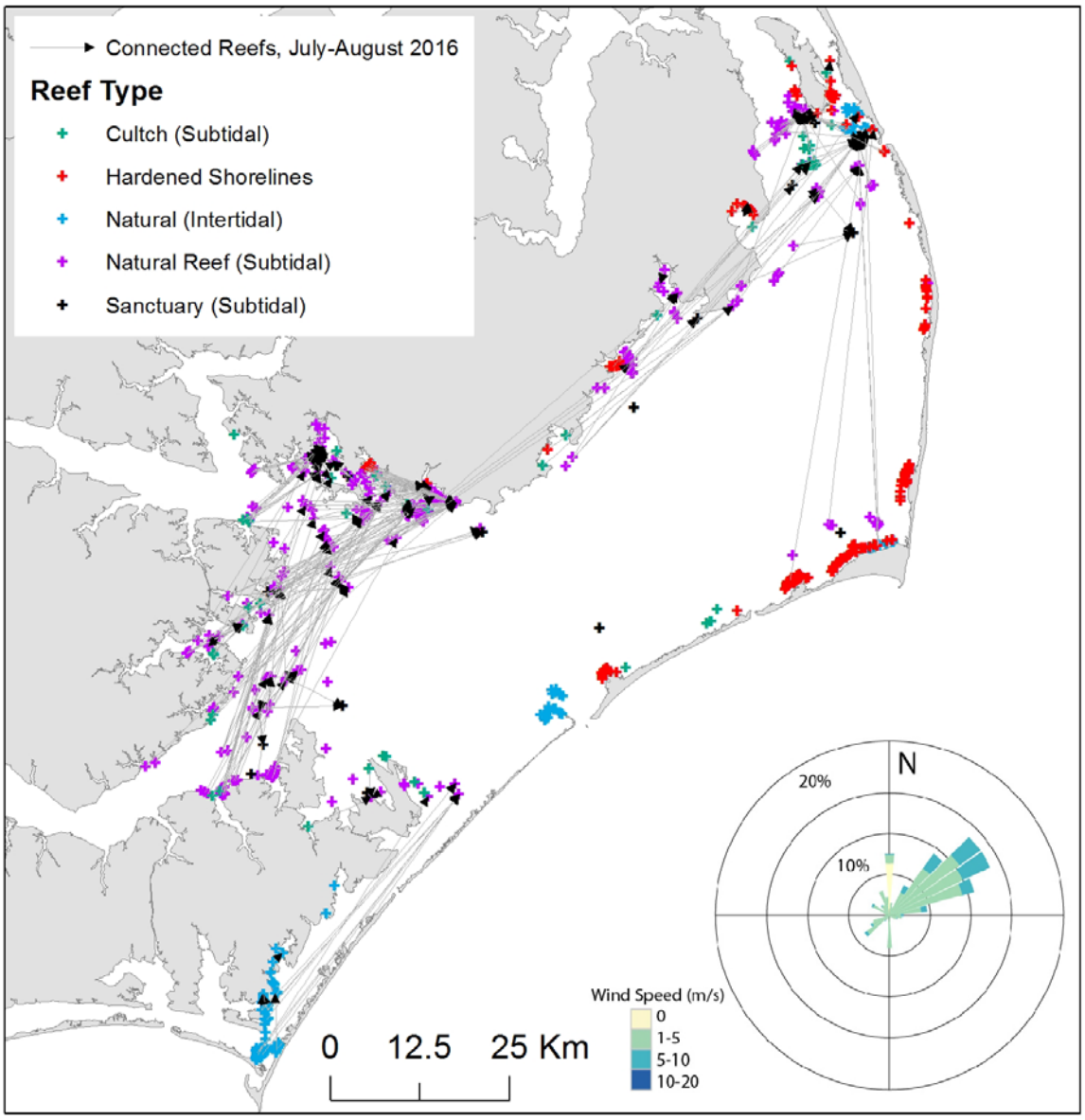


Appendix 11: Map depicting larval dispersal patterns during July–August of 2016. Lines depict connections between natal and settled reef locations (arrowheads point towards settled reef locations). Note that lines depict the least-cost path between reefs and not the actual dispersal path, and only a random subset (5%) of all connections are shown for illustrative purposes.

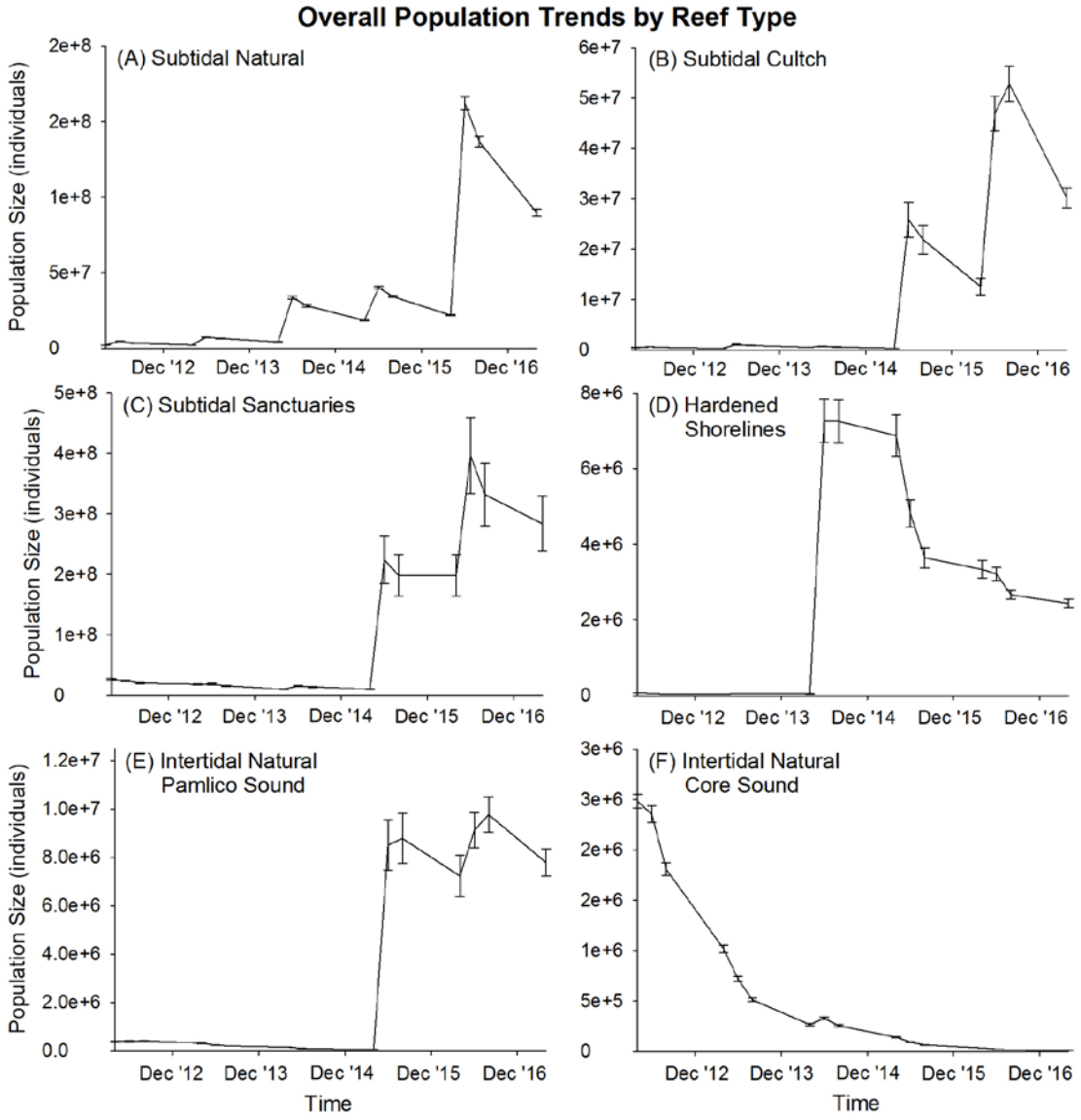


Appendix 12: Overall population trends (i.e., inclusive of all size classes) by reef type across the five-year model timeframe under the 7.5% larval mortality day$^{-1}$ scenario. Points represent the average population size on a given reef type at a given time step; error bars represent standard error of the mean.

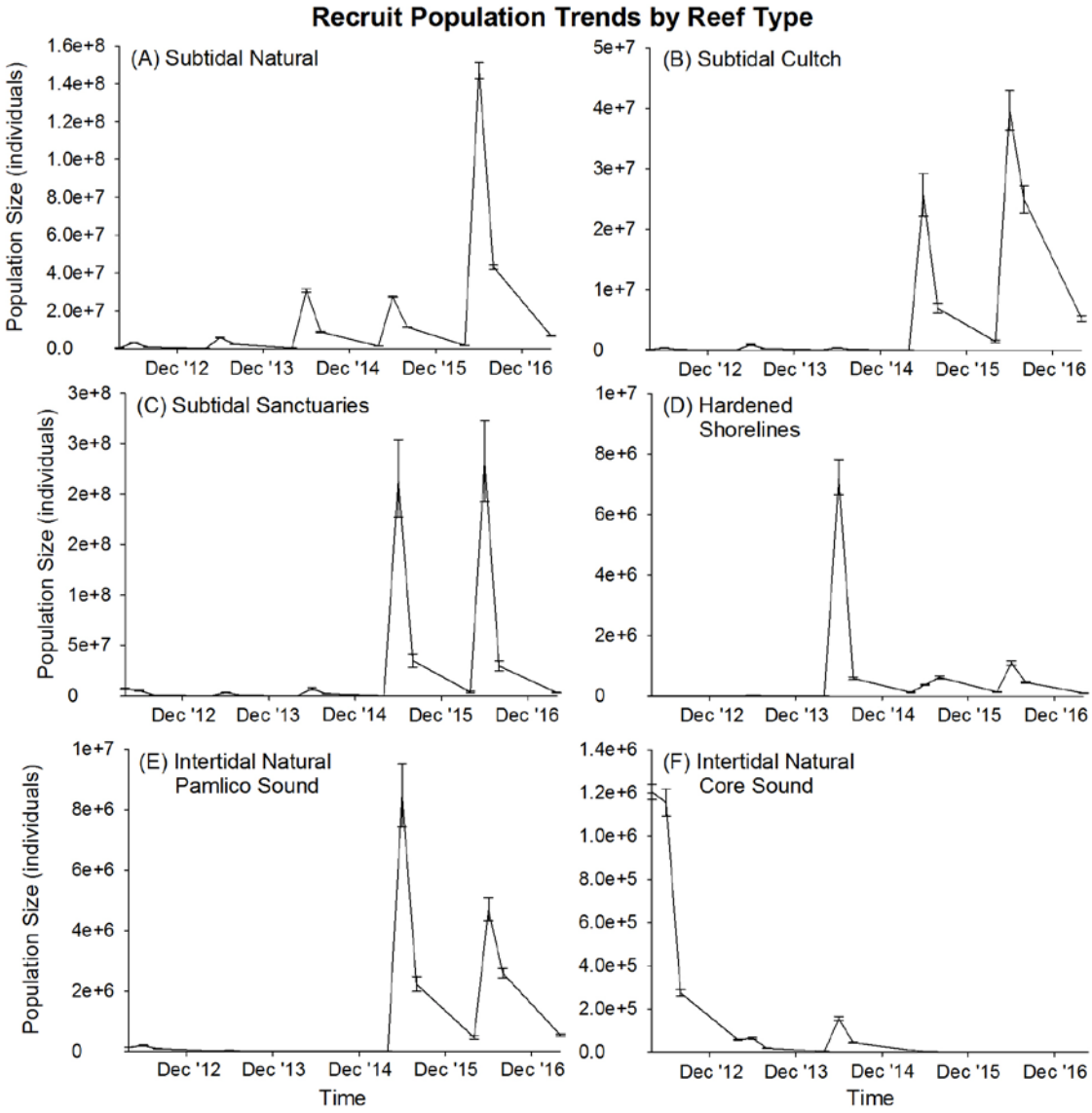


Appendix 13: Recruit size class population trends by reef type across the five-year model timeframe under the 7.5% larval mortality day$^{-1}$ scenario. Points represent the average recruit population size on a given reef type at a given time step; error bars represent standard error of the mean.

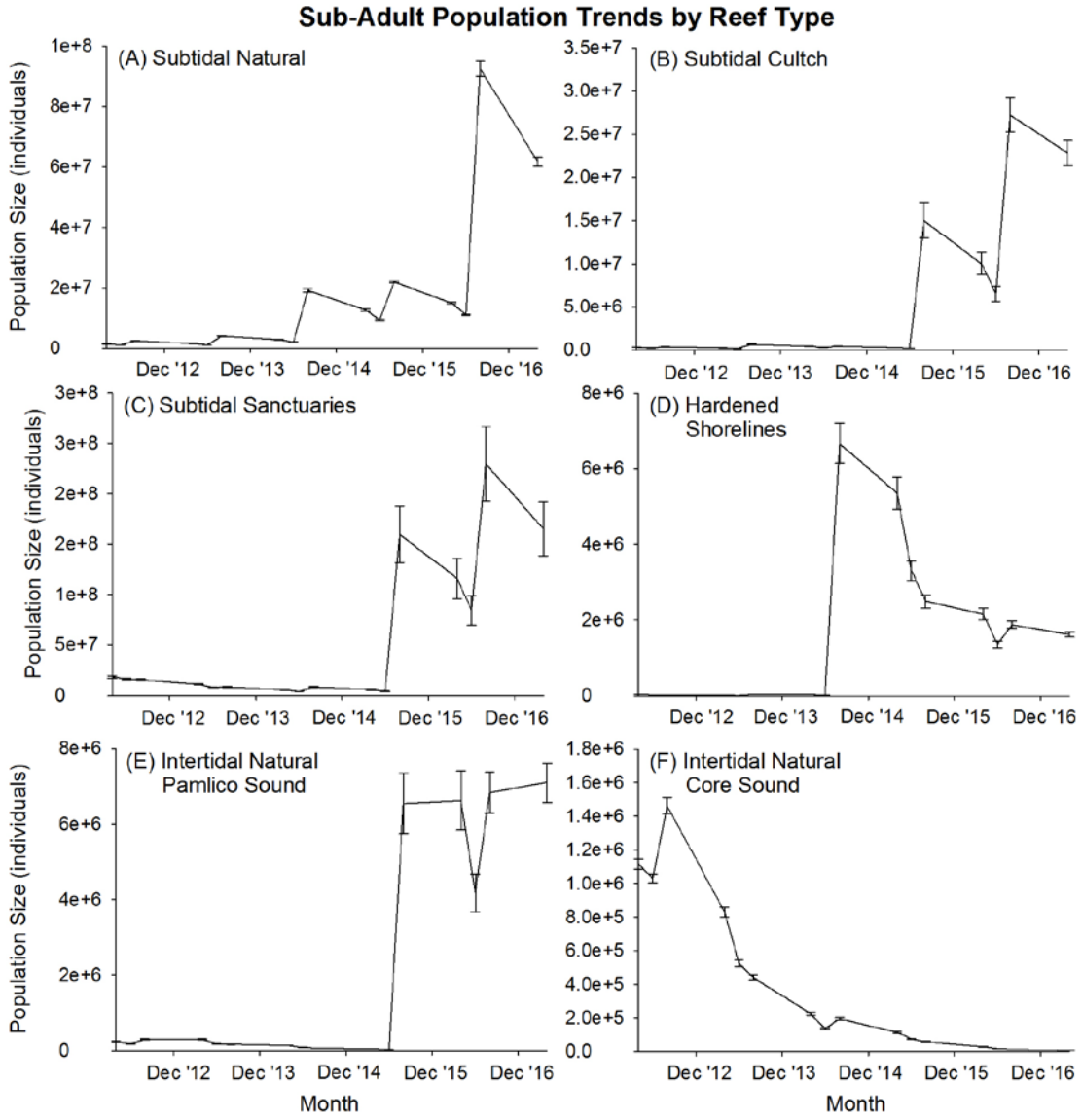


Appendix 14: Sub-adult size class population trends by reef type across the five-year model timeframe under the 7.5% larval mortality day$^{-1}$ scenario. Points represent the average sub-adult population size on a given reef type at a given time step; error bars represent standard error of the mean.

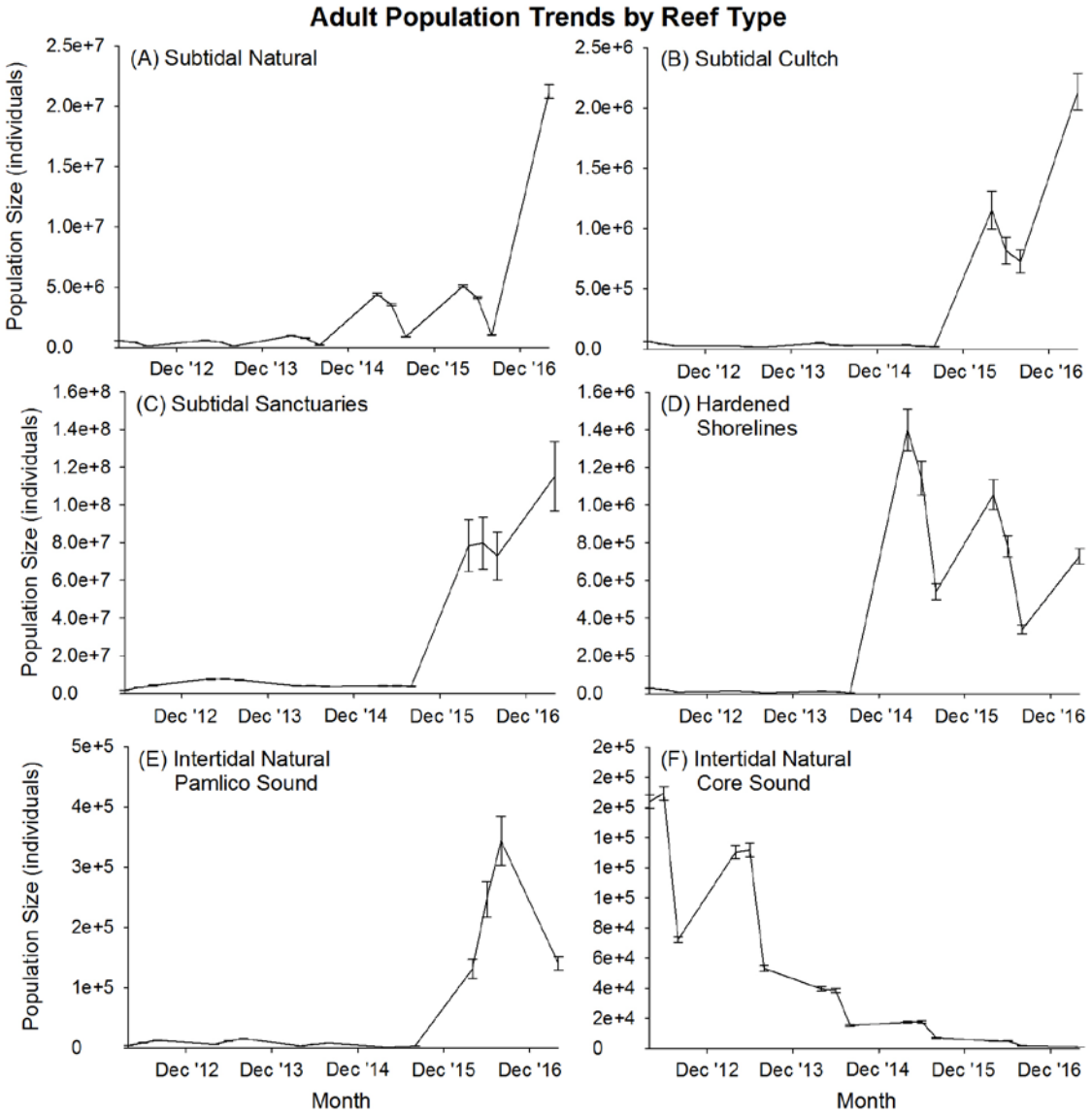


Appendix 15: Adult size class population trends by reef type across the five-year model timeframe under the 7.5% larval mortality day$^{-1}$ scenario. Points represent the average adult population size on a given reef type at a given time step; error bars represent standard error of the mean.

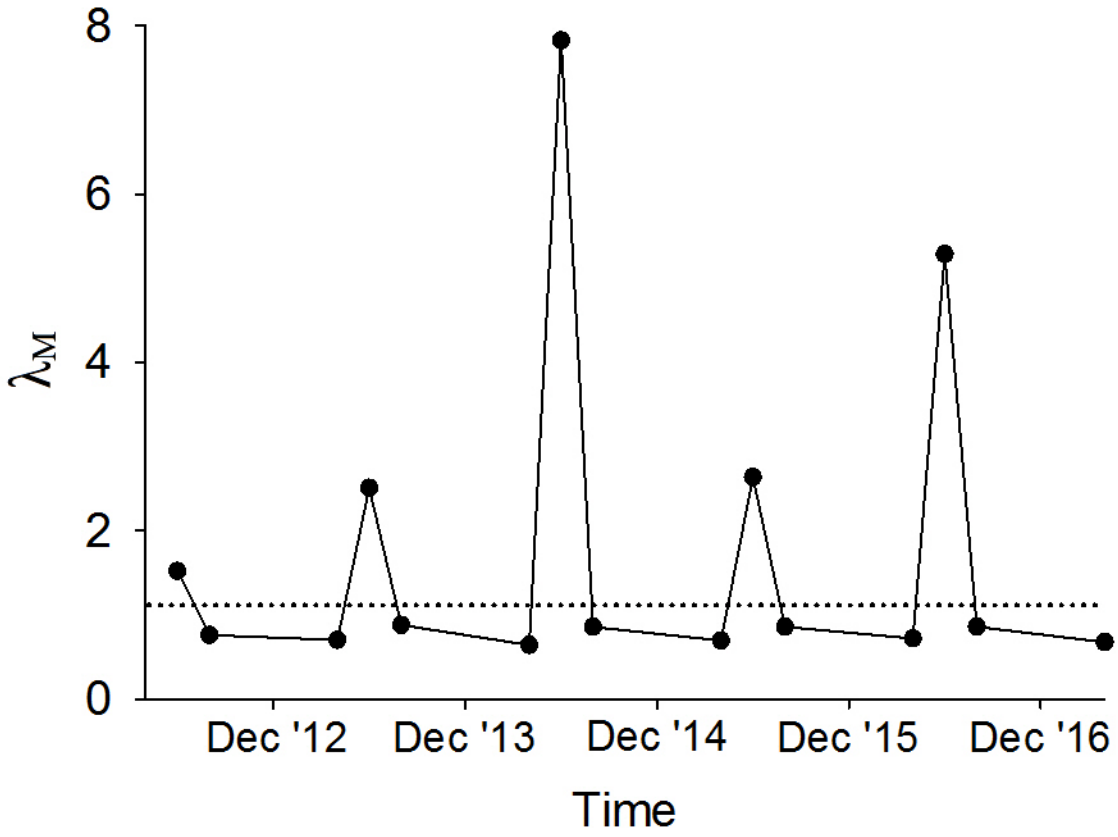


Appendix 16: Overall metapopulation growth ($\lambda_M$) across the five-year model timeframe under the 7.5% larval mortality day$^{-1}$ scenario. The dashed line indicates a $\lambda_M = 1$, above or equal to which a metapopulation is persistent during time *t*, and below which a metapopulation is non-persistent during time *t*.

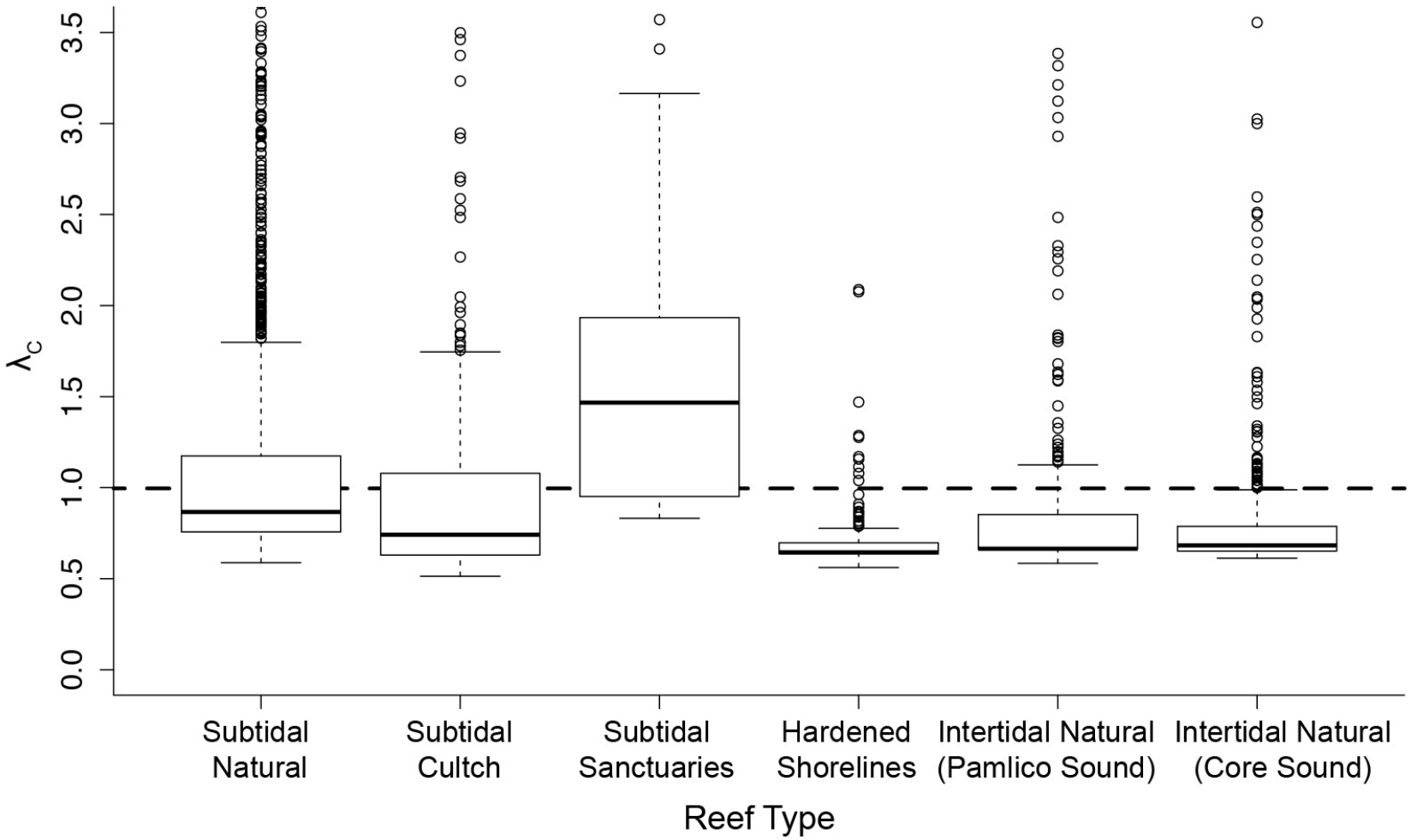


Appendix 17: Source-sink status ($\lambda_c$) of each reef (by reef type) during each May-June time step between 2012-2016 under the 7.5% larval mortality day$^{-1}$ scenario. $\lambda_c \geq 1$ indicates a given reef functioned as a source during time *t*, and $\lambda_c < 1$ indicates a given reef functioned as a sink during time *t*.

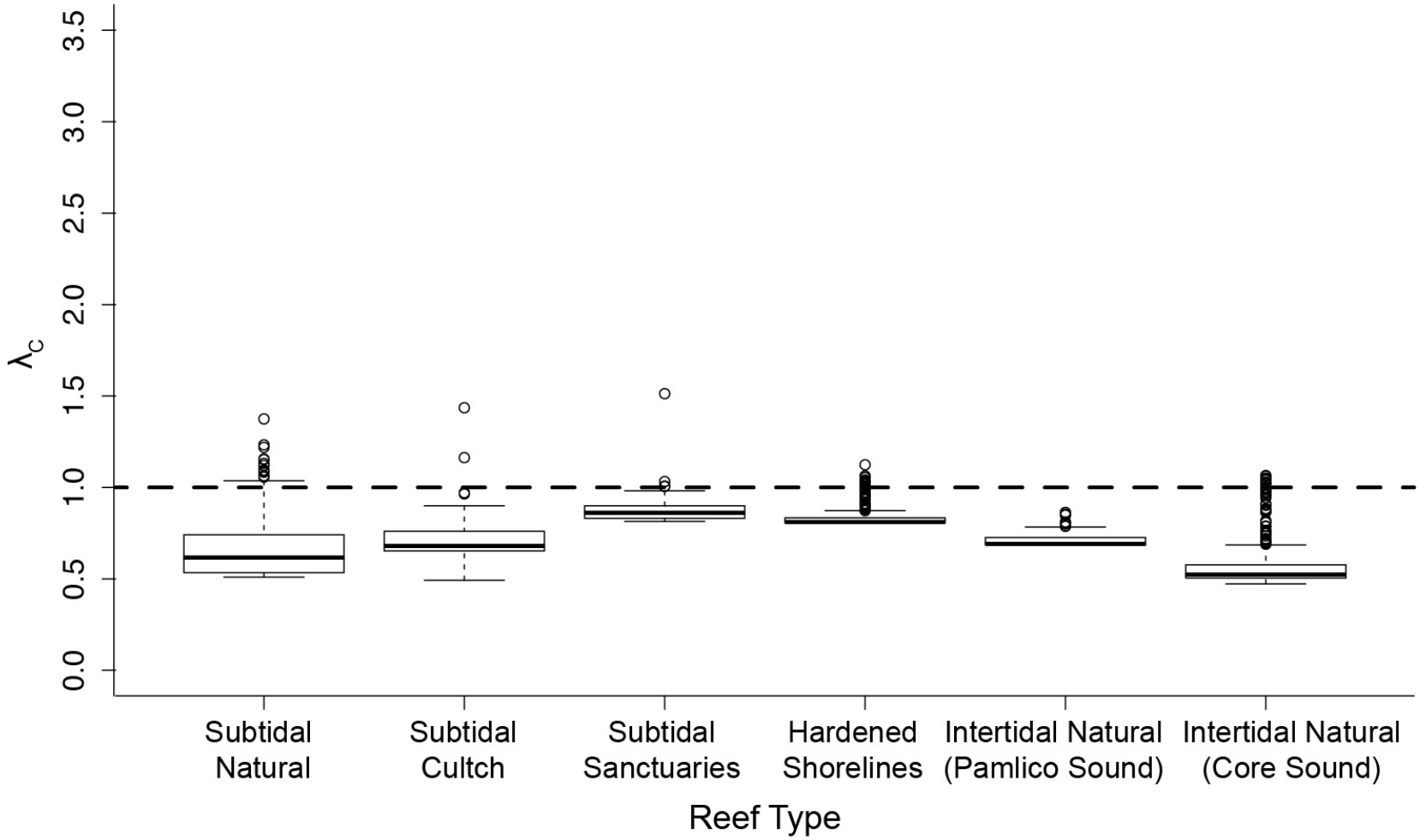


Appendix 18: Source-sink status ($\lambda_c$) of each reef (by reef type) during each July-August time step between 2012-2016 under the 7.5% larval mortality day$^{-1}$ scenario. $\lambda_c \geq 1$ indicates a given reef functioned as a source during time *t*, and $\lambda_c < 1$ indicates a given reef functioned as a sink during time *t*.

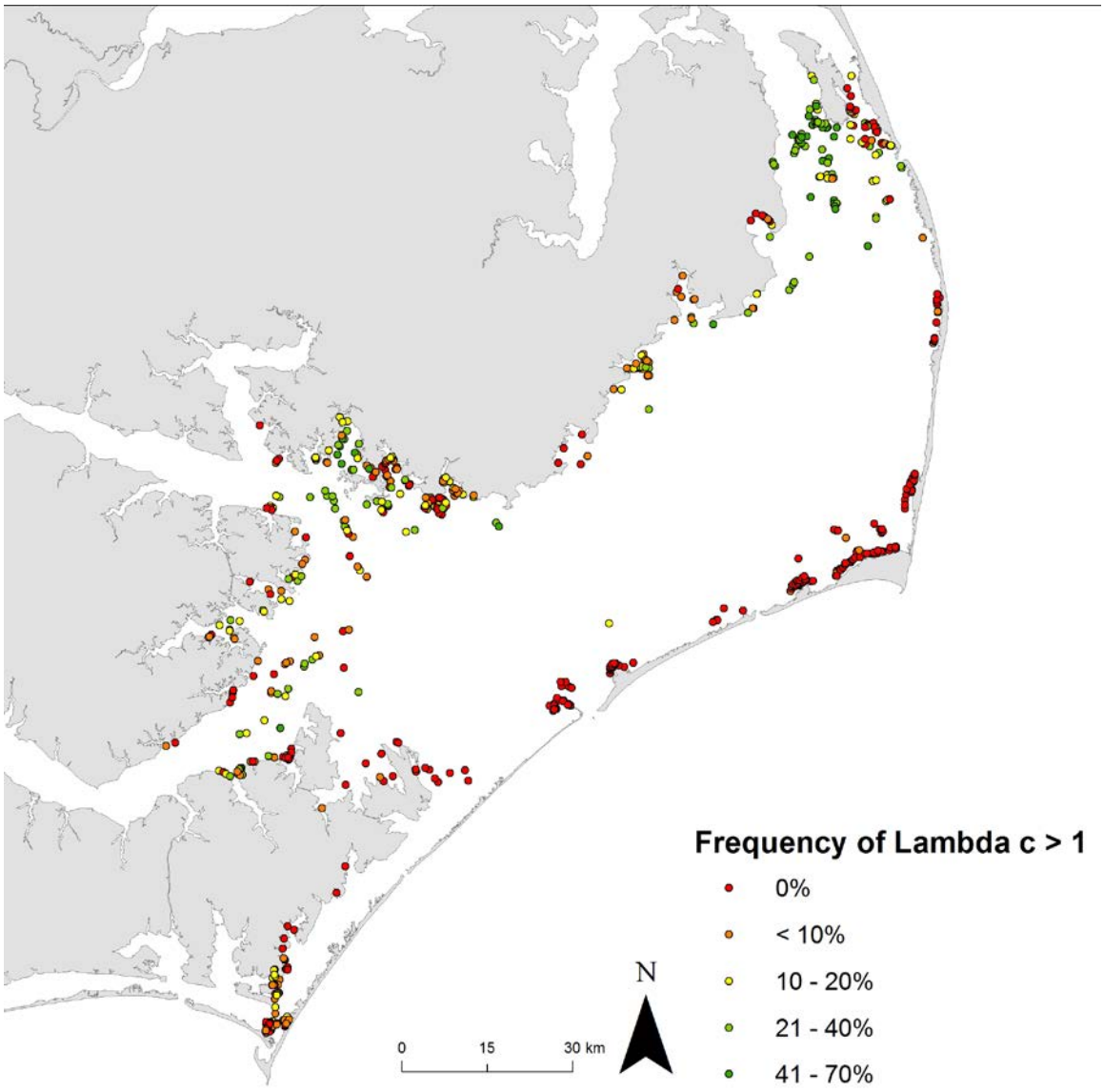


Appendix 19: Frequency of $\lambda_c \geq 1$ at all reefs across the five-year model timeframe under the 7.5% larval mortality day$^{-1}$ scenario. $\lambda_c \geq 1$ indicates a given reef functioned as a source during time *t*, and $\lambda_c < 1$ indicates a given reef functioned as a sink during time *t*. Green dots represent frequent 'source' reefs (i.e., $\lambda_c \geq 1$ 31-50% of the time), red dots represent 'sink' reefs (i.e, $\lambda_c \geq 1$ 0% of the time).

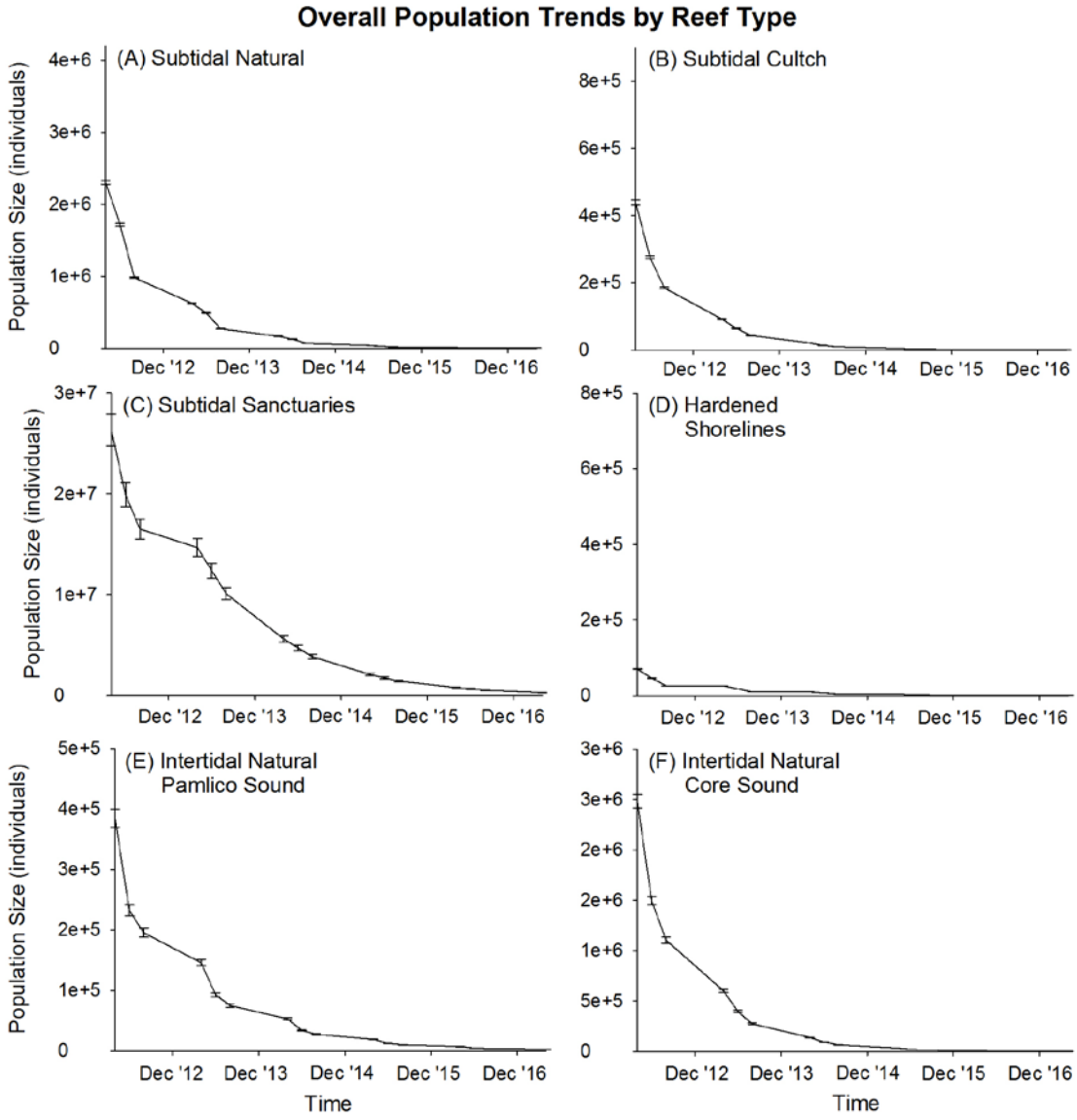


Appendix 20: Overall population trends (i.e., inclusive of all size classes) by reef type across the five-year model timeframe under the 20% larval mortality day$^{-1}$ scenario. Points represent the average population size on a given reef type at a given time step; error bars represent standard error of the mean.

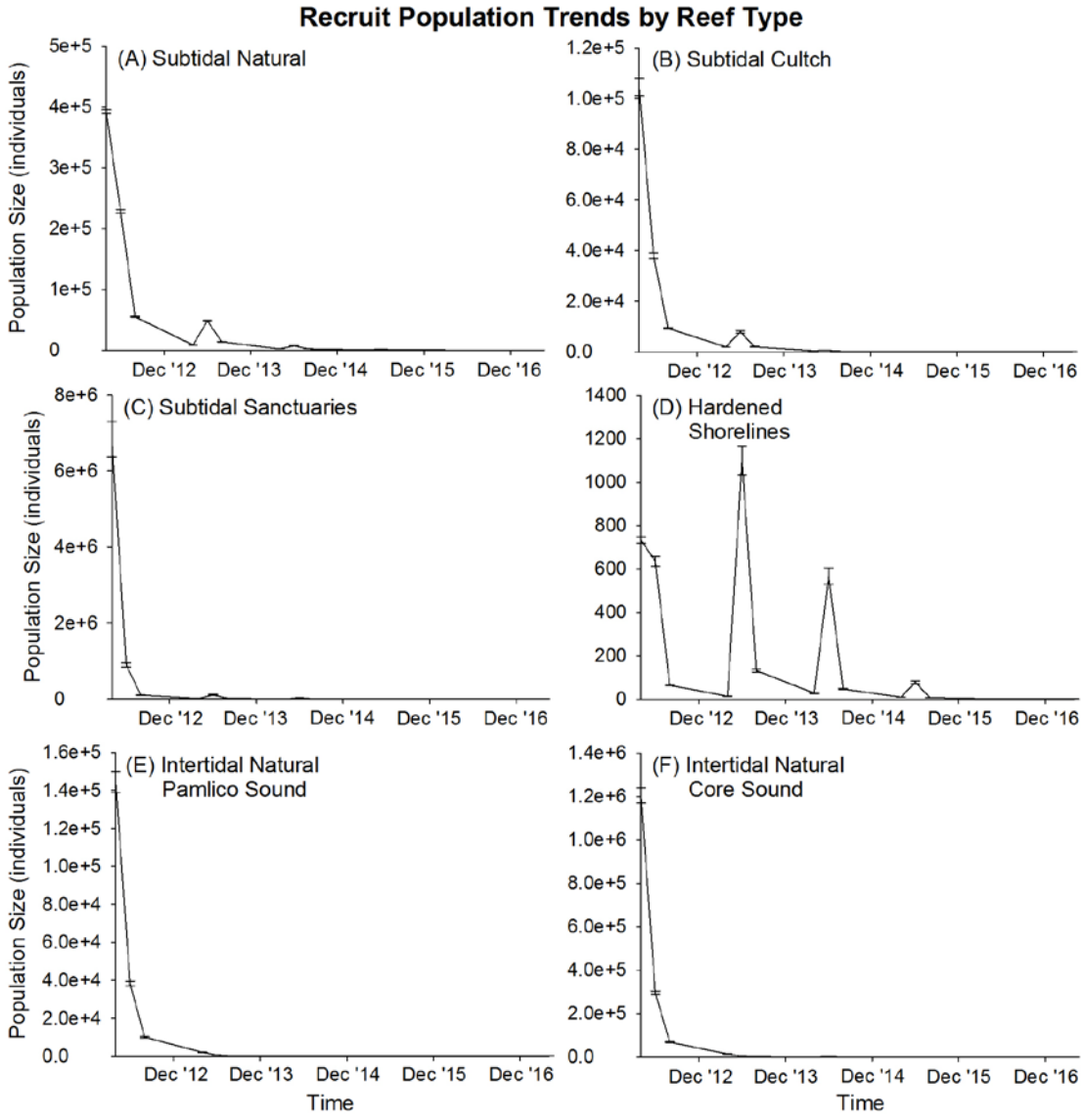


Appendix 21: Recruit size class population trends by reef type across the five-year model timeframe under the 20% larval mortality day$^{-1}$ scenario. Points represent the average recruit population size on a given reef type at a given time step; error bars represent standard error of the mean.

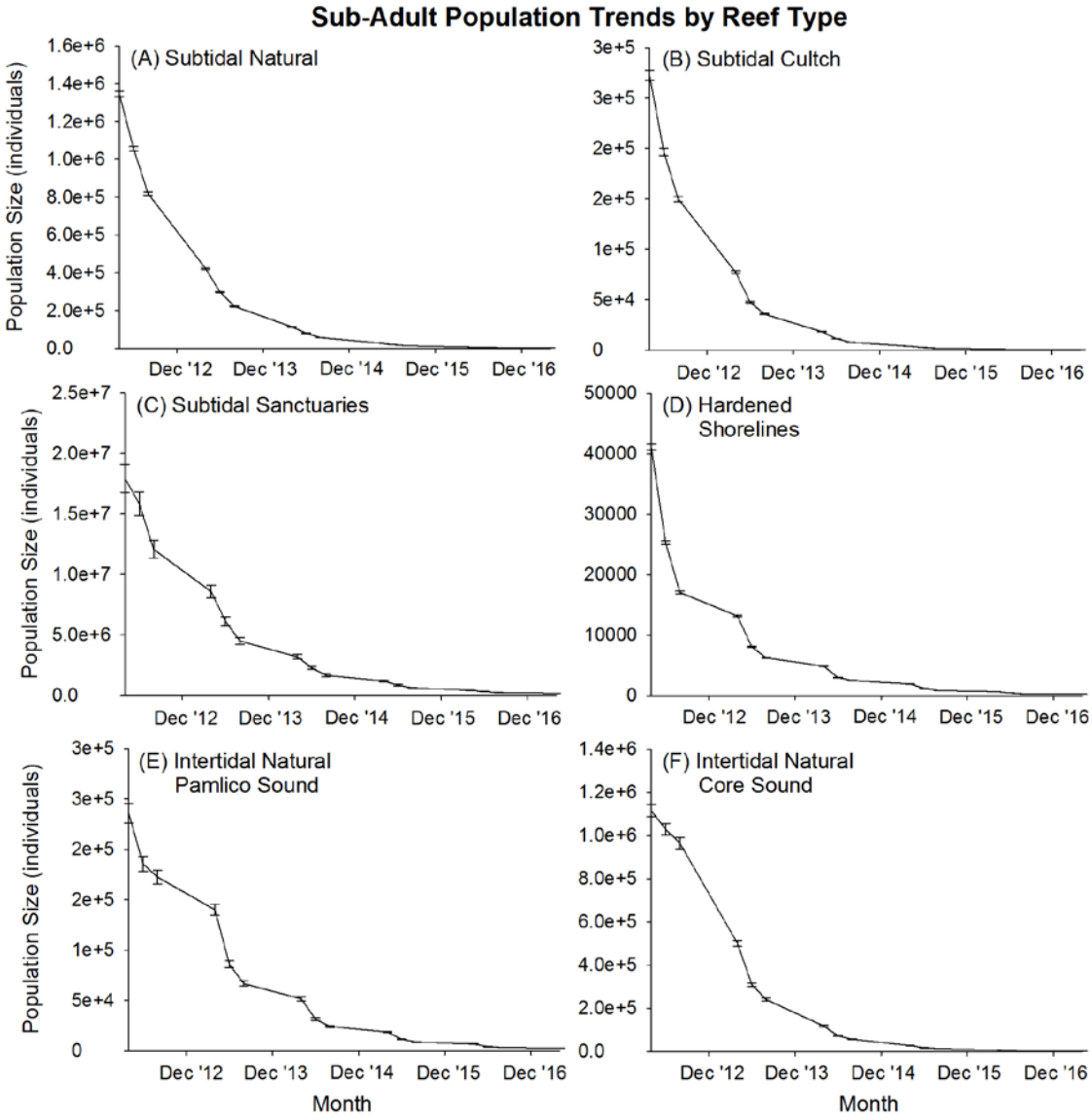


Appendix 22: Sub-adult size class population trends by reef type across the five-year model timeframe under the 20% larval mortality day$^{-1}$ scenario. Points represent the average sub-adult population size on a given reef type at a given time step; error bars represent standard error of the mean.

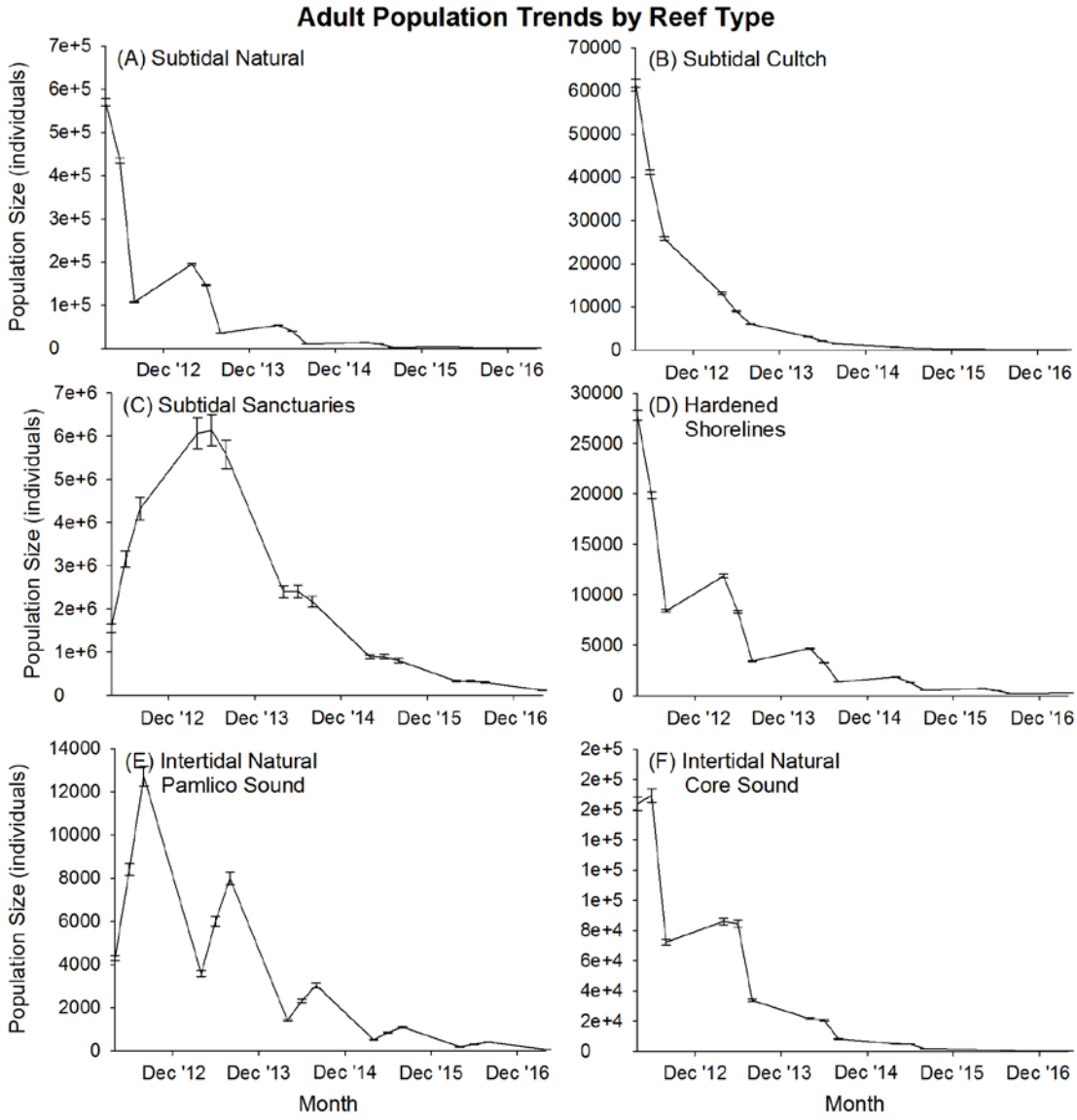


Appendix 23: Adult size class population trends by reef type across the five-year model timeframe under the 20% larval mortality day$^{-1}$ scenario. Points represent the average adult population size on a given reef type at a given time step; error bars represent standard error of the mean.

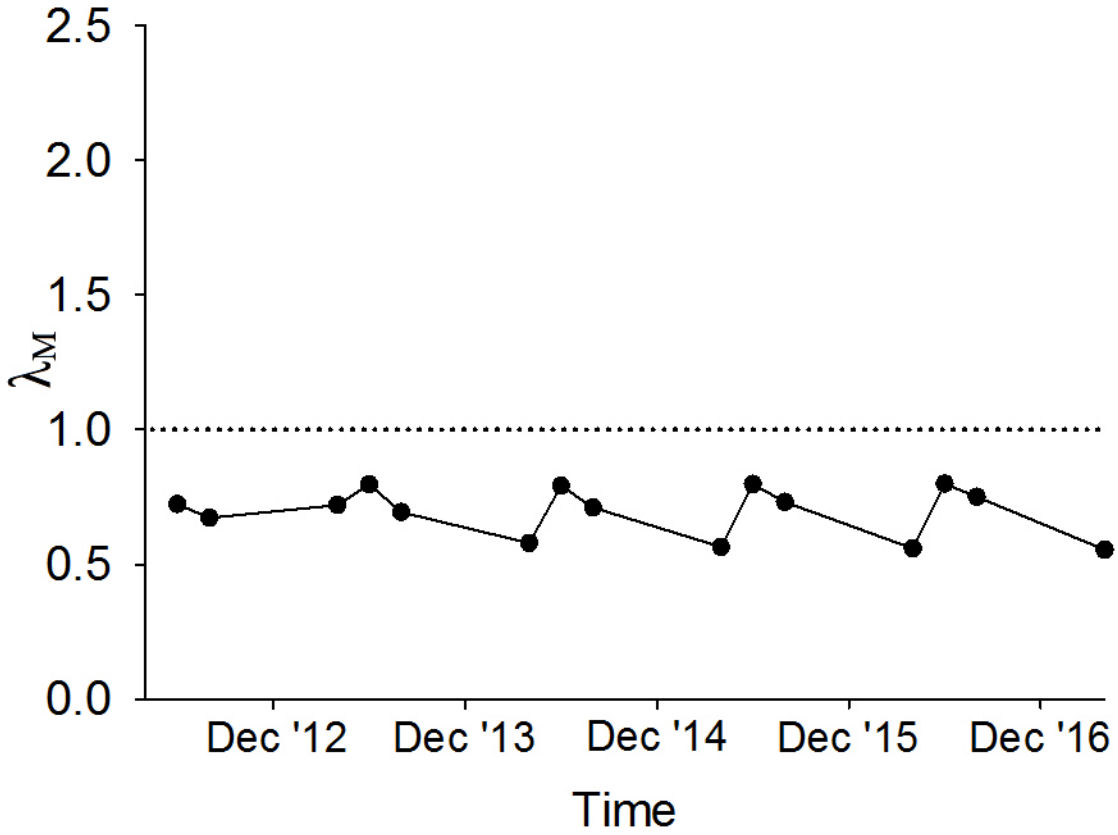


Appendix 24: Overall metapopulation growth ($\lambda_M$) across the five-year model timeframe under the 20% larval mortality day$^{-1}$ scenario. The dashed line indicates a $\lambda_M = 1$, above or equal to which a metapopulation is persistent during time *t*, and below which a metapopulation is non-persistent during time *t*.

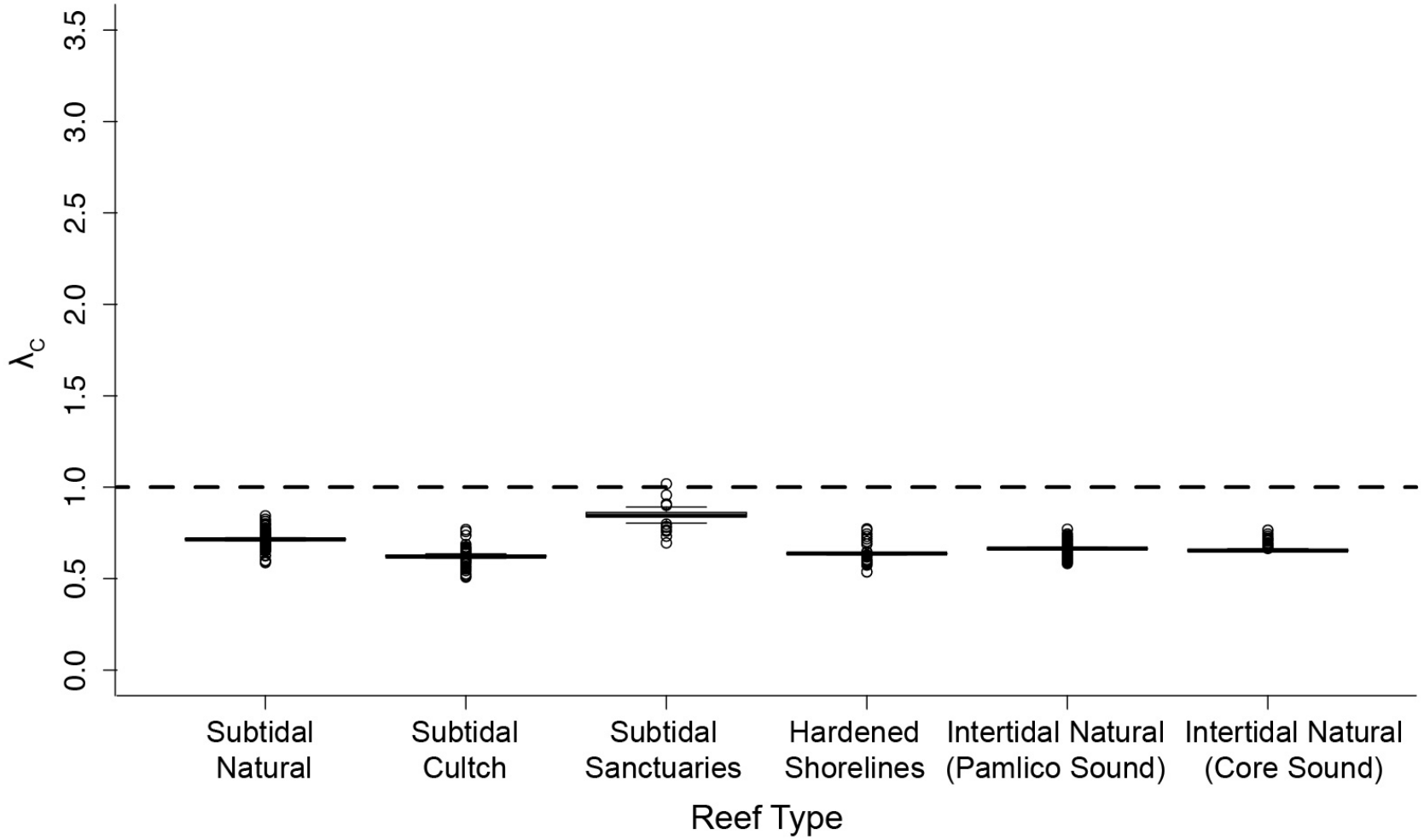


Appendix 25: Source-sink status ($\lambda_c$) of each reef (by reef type) during each May-June time step between 2012-2016 under the 20% larval mortality day$^{-1}$ scenario. $\lambda_c \geq 1$ indicates a given reef functioned as a source during time *t*, and $\lambda_c < 1$ indicates a given reef functioned as a sink during time *t*.